

GRAHAM COOP

POPULATION AND QUANTITATIVE GENETICS

Author: Graham Coop

Author address: Department of Evolution and Ecology & Center for Population Biology,
University of California, Davis.

To whom correspondence should be addressed: gmccoop@ucdavis.edu

This work is licensed under a Creative Commons Attribution 3.0 Unported License.

<http://creativecommons.org/licenses/by/3.0/>

i.e. you are free to reuse and remix this work, but please include an attribution to the original.

Typeset using L^AT_EX and the TUFTE-LATEX book style.

The L^AT_EX code and R code for this book are kept here <https://github.com/cooplab/popgen-notes/> and again are
under a Creative Commons Attribution 3.0 Unported License.

Updated on January 2020

Dedicated to my parents, partner, and children. Thank you for teaching me the true joy of descent with modification.

This book was developed from my set of notes for the Population Biology graduate group core class (PBG200A) and Undergraduate Population and Quantitative Genetics class (EVE102) at UC Davis. Thanks to the many students who've read these notes and suggested improvements. Thanks to Simon Aeschbacher, Vince Buffalo, and Erin Calfee who read and extensively edited earlier drafts of these notes. To illustrate these notes I've used old scientific and natural history illustrations, in part because they are out of copyright but mainly because they bring me joy. Many of the old images come from Biodiversity Heritage Library a consortium of natural history institutions that are digitizing their collections and make them freely available online. If you enjoy the images consider donating to the BHL. Many of the data and simulation graphics in the book were prepared in R (2018), the code for each is linked to from the caption of each figure. In many cases data were extracted from old figures using the WebPlotDigitizer tool, as such I advise re-extracting the data if you wish to use it for research purposes.

Contents

1	<i>Introduction</i>	7
2	<i>Allele and Genotype Frequencies</i>	11
3	<i>Population Structure and Correlations Among Loci.</i>	31
4	<i>Genetic Drift and Neutral Diversity</i>	49
5	<i>The Population Genetics of Divergence and Molecular Substitution.</i>	75
6	<i>Neutral Diversity and Population Structure.</i>	89
7	<i>Phenotypic Variation and the Resemblance Between Relatives</i>	99
8	<i>The Response to Phenotypic Selection</i>	121
9	<i>The Response of Multiple Traits to Selection.</i>	135
10	<i>One-Locus Models of Selection</i>	147
11	<i>The Interaction of Selection, Mutation, and Migration.</i>	183

12	<i>The Impact of Genetic Drift on Selected Alleles</i>	199
13	<i>The Effects of Linked Selection.</i>	211
14	<i>Interaction of Multiple Selected Loci</i>	227
A.	<i>An Introduction to Mathematical Concepts</i>	245
	<i>Bibliography</i>	259

1

Introduction

BIOLOGICAL EVOLUTION IS THE CHANGE OVER TIME IN THE GENETIC COMPOSITION OF A POPULATION.¹ Our population is made up of a set of interbreeding individuals, the genetic composition of which is made up of the genomes that each individual carries. The genetic composition of the population alters due to the death of individuals or the migration of individuals in or out of the population. If our individuals vary in the number of children they have, this also alters the genetic composition of the population in the next generation. Every new individual born into the population subtly changes the genetic composition of the population. Their genome is a unique combination of their parents' genomes, having been shuffled by segregation and recombination during meioses, and possibly changed by mutation. These individual events seem minor at the level of the population, but it is the accumulation of small changes in aggregate across individuals and generations that is the stuff of evolution. It is the compounding of these small changes over tens, hundreds, and millions of generations that drives the amazing diversity of life that has emerged on this earth.

Population genetics is the study of the genetic composition of natural populations and its evolutionary causes and consequences. Quantitative genetics is the study of the genetic basis of phenotypic variation and how phenotypic changes evolve over time. Both fields are closely conceptually aligned as we'll see throughout these notes. They seek to describe how the genetic and phenotypic composition of populations can be changed over time by the forces of mutation, recombination, selection, migration, and genetic drift. To understand how these forces interact, it is helpful to develop simple theoretical models to help our intuition. In these notes we will work through these models and summarize the major areas of population- and quantitative-genetic theory.

While the models we will develop will seem naïve, and indeed they are, they are nonetheless incredibly useful and powerful. Throughout

¹ DOBZHANSKY, T., 1951 *Genetics and the Origin of Species* (3rd Ed. ed.), pp. 16

"All models are wrong but some are useful" - Box (1979).

the course we will see that these simple models often yield accurate predictions, such that much of our understanding of the process of evolution is built on these models. We will also see how these models are incredibly useful for understanding real patterns we see in the evolution of phenotypes and genomes, such that much of our analysis of evolution, in a range of areas from human medical genetics to conservation, is based on these models. Therefore, population and quantitative genetics are key to understanding various applied questions, from how medical genetics identifies the genes involved in disease to how we preserve species from extinction.

Population genetics emerged from early efforts to reconcile Mendelian genetics with Darwinian thought. Part of the power of population genetics comes from the fact that the basic rules of transmission genetics are simple and nearly universal. One of the truly remarkable things about population genetics is that many of the important ideas and mathematical models emerged before the 1940s, long before the mechanistic-basis of inheritance (DNA) was discovered, and yet the usefulness of these models has not diminished. This is a testament to the fact that the models are established on a very solid foundation, building from the basic rules of genetic transmission combined with simple mathematical and statistical models.

Much of this early work traces to the ideas of R.A. Fisher, Sewall Wright, and J.B.S. Haldane, who, along with many others, described the early principals and mathematical models underlying our understanding of the evolution of populations. Building on this conceptual fusion of genetics and evolution, there followed a flourishing of evolutionary thought, the modern evolutionary synthesis, combining these ideas with those from the study of speciation, biodiversity, and paleontology. In total this work showed that both short-term evolutionary change and the long-term evolution of biodiversity could be well understood through the gradual accumulation of evolutionary change within and among populations. This evolutionary synthesis continues to this day, combining new insights from genomics, phylogenetics, ecology, and developmental biology.

Population and quantitative genetics are a necessary but not sufficient description of evolution; it is only by combining the insights of many fields that a rich and comprehensive picture of evolution emerges. We certainly do not need to know the genes underlying the displays of the birds of paradise to study how the divergence of these displays, due to sexual selection, may drive speciation. Indeed, as we'll see in our discussion of quantitative genetics, we can predict how populations respond to selection, including sexual selection and assortative mating, without any knowledge of the loci involved. Nor do we need to know the precise selection pressures and the ordering of genetic

See PROVINE (2001) for a history of early population genetics.

PROVINE, W. B., 2001 *The origins of theoretical population genetics: with a new afterword.* University of Chicago Press

“DOBZHANSKY (1951)
once defined evolution as ‘a
change in the genetic com-
position of the populations’
an epigram that should not
be mistaken for the claim
that everything worth saying
about evolution is contained
in statements about genes”

– LEWONTIN (2001)

changes to study the emergence of the tetrapod body plan. We do not necessarily need to know all the genetic details to appreciate the beauty of these, and many other, evolutionary case studies. However, every student of biology gains from understanding the basics of population and quantitative genetics, allowing them to base their studies on a solid bedrock of understanding of the processes that underpin all evolutionary change.

2

Allele and Genotype Frequencies

In this chapter we will work through how the basics of Mendelian genetics play out at the population level in sexually reproducing organisms.

Loci and alleles are the basic currency of population genetics—and indeed of genetics. A locus may be an entire gene, or a single nucleotide base pair such as A-T. At each locus, there may be multiple genetic variants segregating in the population—these different genetic variants are known as *alleles*. If all individuals in the population carry the same allele, we say that the locus is *monomorphic*; at this locus there is no genetic variability in the population. If there are multiple alleles in the population at a locus, we say that this locus is *polymorphic* (this is sometimes referred to as a segregating site).

Table 2.1 shows a small stretch of orthologous sequence for the ADH locus from samples from *Drosophila melanogaster*, *D. simulans*, and *D. yakuba*. *D. melanogaster* and *D. simulans* are sister species and *D. yakuba* is a close outgroup to the two. Each column represents a single haplotype from an individual (the individuals are diploid but were inbred so they’re homozygous for their haplotype). Only sites that differ among individuals of the three species are shown. Site 834 is an example of a polymorphism; some *D. simulans* individuals carry a *C* allele while others have a *T*. *Fixed differences* are sites that differ between the species but are monomorphic within the species. Site 781 is an example of a fixed difference between *D. melanogaster* and the other two species.

We can also annotate the alleles and loci in various ways. For example, position 781 is a non-synonymous fixed difference. We call the less common allele at a polymorphism the *minor allele* and the common allele the *major allele*, e.g. at site 1068 the *T* allele is the minor allele in *D. melanogaster*. We call the more evolutionarily recent of the two alleles the *derived allele* and the older of the two the *ancestral allele*. We infer that the *T* allele at site 1068 is the derived allele because the *C* is found in both other species, suggesting that the *T* allele

A *locus* (plural: *loci*) is a specific spot in the genome. The term allele was coined by Edith Rebecca Saunders and William Bateson in 1902 in their paper “The facts of heredity in the light of Mendel’s discovery” .

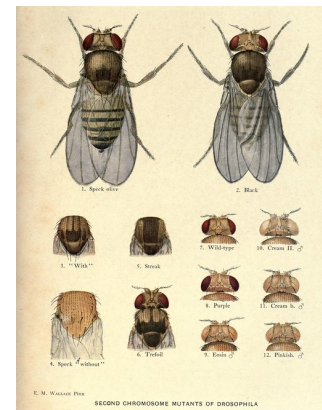


Figure 2.1: *Drosophila melanogaster* holds a special place in the history of genetics and population genetics. From Morgan’s fly room discovering the principals of genetics to Dobzhansky’s early work on natural genetic variation.

Contributions to the genetics of *Drosophila melanogaster* (1919). Morgan T.H., Bridges C.B., Sturtevant A. H. Image from the Biodiversity Heritage Library. Contributed by MBLWHOI Library. Not in copyright.

arose via a $C \rightarrow T$ mutation.

pos.	con.	a	b	c	d	e	f	g	h	i	j	k	l	a	b	c	d	e	f	g	h	i	j	k	l	NS/S	
781	G	T	T	T	T	T	T	T	T	T	T	T	-	-	-	-	-	-	-	-	-	-	-	-	NS		
789	T	-	-	-	-	-	-	-	-	-	-	-	-	-	-	-	-	-	-	C	C	C	C	C	C	C	S
808	A	-	-	-	-	-	-	-	-	-	-	-	-	-	-	-	-	-	-	G	G	G	G	G	G	NS	
816	G	T	T	T	T	-	-	-	-	T	T	T	T	-	-	-	-	-	-	G	G	G	G	G	G	S	
834	T	-	-	-	-	-	-	-	-	-	C	C	-	-	C	-	-	-	-	-	-	-	-	-	S		
859	C	-	-	-	-	-	-	-	-	-	-	-	-	-	-	-	-	-	-	G	G	G	G	G	G	NS	
867	C	-	-	-	-	-	-	-	-	-	-	-	-	-	-	-	-	-	-	G	G	G	G	G	G	S	
870	C	T	T	T	T	T	T	T	T	T	T	T	-	-	-	-	-	-	-	-	-	-	-	-	S		
950	G	-	-	-	-	-	-	-	-	-	-	-	A	-	-	-	-	-	-	-	-	-	-	-	S		
974	G	-	-	-	-	-	-	-	-	-	T	T	T	T	T	-	-	-	-	-	-	-	-	-	S		
983	T	-	-	-	-	-	-	-	-	-	-	-	-	-	C	C	C	C	C	C	C	C	C	C	S		
1019	C	-	-	-	-	-	-	-	-	-	-	-	-	-	-	-	-	-	-	A	-	-	-	-	S		
1031	C	-	-	-	-	-	-	-	-	-	-	-	-	-	-	-	-	-	-	-	A	-	-	-	S		
1034	T	-	-	-	-	-	-	-	-	-	-	-	-	-	C	C	C	C	C	C	C	C	C	C	S		
1043	C	-	-	-	-	-	-	-	-	-	-	-	-	-	-	-	-	-	-	A	-	-	-	-	S		
1068	C	T	T	-	-	-	-	-	-	-	-	-	-	-	-	-	-	-	-	-	-	-	-	-	S		
1089	C	-	-	-	-	-	-	-	-	-	A	A	A	A	A	A	A	A	A	A	A	A	A	A	NS		
1101	G	-	-	-	-	-	-	-	-	-	-	-	-	-	A	A	A	A	A	A	A	A	A	A	A	NS	
1127	T	-	-	-	-	-	-	-	-	-	-	-	-	-	C	C	C	C	C	C	C	C	C	C	S		
1131	C	-	-	-	-	-	-	-	-	-	-	-	-	-	-	T	-	-	-	-	-	-	-	-	S		
1160	T	-	-	-	-	-	-	-	-	-	-	-	-	-	C	C	C	C	C	C	C	C	C	C	S		

Table 2.1: Variable sites in exons 2 and 3 of the ADH gene in *Drosophila* McDONALD and KREITMAN (1991). The first column (pos.) gives the position in the gene; exon 2 begins at position 778 and we've truncated the dataset at site 1175. The second column gives the consensus nucleotide (con.), i.e. the most common base at that position; individuals with nucleotides that match the consensus are marked with a dash. The first columns of sequence (a-l) are from *D. melanogaster*; the next columns (a-f) give sequences from *D. simulans*, and the final set of columns (a-l) from *D. yakuba*. The last column shows whether the difference is a non-synonymous (N) or synonymous (S) change.

Question 1. A) How many segregating sites does the sample from *D. simulans* have in the ADH gene?

B) How many fixed differences are there between *D. melanogaster* and *D. yakuba*?

2.1 Allele frequencies

Allele frequencies are a central unit of population genetics analysis, but from diploid individuals we only get to observe genotype counts. Our first task then is to calculate allele frequencies from genotype counts. Consider a diploid autosomal locus segregating for two alleles (A_1 and A_2). We'll use these arbitrary labels for our alleles, merely to keep this general. Let N_{11} and N_{12} be the number of A_1A_1 homozygotes and A_1A_2 heterozygotes, respectively. Moreover, let N be the total number of diploid individuals in the population. We can then define the relative frequencies of A_1A_1 and A_1A_2 genotypes as $f_{11} = N_{11}/N$ and $f_{12} = N_{12}/N$, respectively. The frequency of allele A_1 in the population is then given by

$$p = \frac{2N_{11} + N_{12}}{2N} = f_{11} + \frac{1}{2}f_{12}. \quad (2.1)$$

Note that this follows directly from how we count alleles given individuals' genotypes, and holds independently of Hardy–Weinberg proportions and equilibrium (discussed below). The frequency of the alternate allele (A_2) is then just $q = 1 - p$.

2.1.1 Measures of genetic variability

Nucleotide diversity (π) One common measure of genetic diversity is the average number of single nucleotide differences between haplotypes chosen at random from a sample. This is called *nucleotide diversity*

and is often denoted by π . For example, we can calculate π for our ADH locus from Table 2.1 above: we have 6 sequences from *D. simulans* (a-f), there's a total of 15 ways of pairing these sequences, and

$$\pi = \frac{1}{15} ((2+1+1+1+0)+(3+3+3+2)+(0+0+1)+(0+1)+(1)) = 1.2\bar{6} \quad (2.2)$$

where the first bracketed term gives the pairwise differences between a and b-f, the second bracketed term the differences between b and c-f and so on.

Our π measure will depend on the length of sequence it is calculated for. Therefore, π is usually normalized by the length of sequence, to be a per site (or per base) measure. For example, our ADH sequence covers 397bp of DNA and so $\pi = 1.2\bar{6}/397 = 0.0032$ per site in *D. simulans* for this region. Note that we could also calculate π per synonymous site (or non-synonymous). For synonymous site π , we would count up number of synonymous differences between our pairs of sequences, and then divide by the total number of sites where a synonymous change could have occurred.¹

Number of segregating sites. Another measure of genetic variability is the total number of sites that are polymorphic (segregating) in our sample. One issue is that the number of segregating sites will grow as we sequence more individuals (unlike π). Later in the course, we'll talk about how to standardize the number of segregating sites for the number of individuals sequenced (see eqn (4.39)).

The frequency spectrum. We also often want to compile information about the frequency of alleles across sites. We call alleles that are found once in a sample *singletons*, alleles that are found twice in a sample *doubletons*, and so on. We count up the number of loci where an allele is found i times out of n , e.g. how many singletons are there in the sample, and this is called the *frequency spectrum*. We'll want to do this in some consistent manner, such as calculating the frequency spectrum of the minor allele or the derived allele.

Question 2. How many minor-allele singletons are there in *D. simulans* in the ADH region? [Defining minor allele just within *D. simulans*.]

Levels of genetic variability across species. Two observations have puzzled population geneticists since the inception of molecular population genetics. The first is the relatively high level of genetic variation observed in most obligately sexual species. This first observation,

¹ Technically we would need to divide by the total number of possible point mutations that would result in a synonymous change; this is because some mutational changes at a particular nucleotide will result in a non-synonymous or synonymous change depending on the base-pair change.

in part, drove the development of the Neutral theory of molecular evolution, the idea that much of this molecular polymorphism may simply reflect a balance between genetic drift and mutation. The second observation is the relatively narrow range of polymorphism across species with vastly different census sizes. This observation represented a puzzle as the Neutral theory predicts that levels of genetic diversity should scale with population size. Much effort in theoretical and empirical population genetics has been devoted to trying to reconcile models with these various observations. We'll return to discuss these ideas throughout our course.

The first observations of molecular genetic diversity within natural populations were made from surveys of allozyme data, but we can revisit these general patterns with modern data.

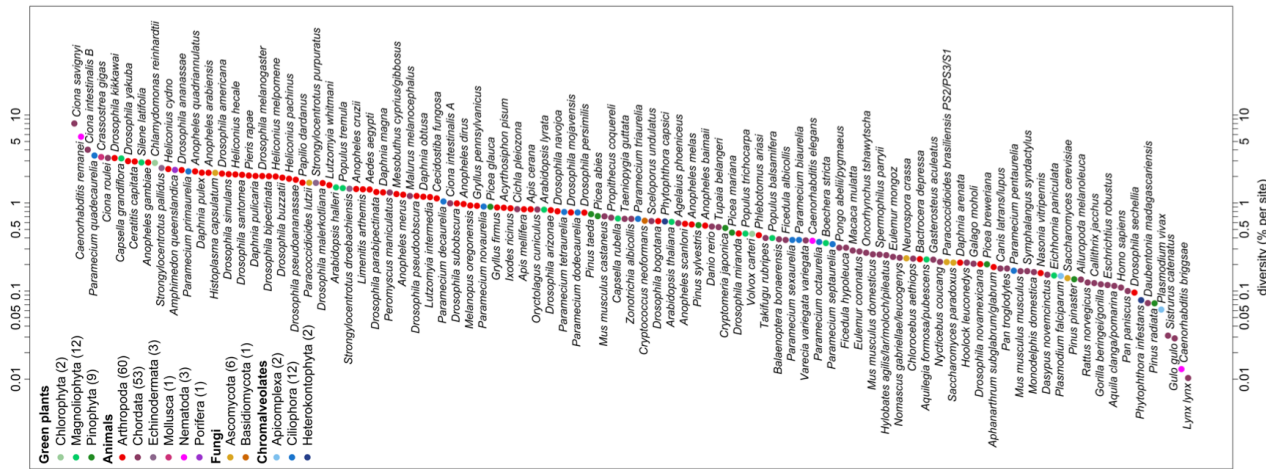


Figure 2.2: Sea Squirt (*Ciona intestinalis*).

Einleitung in die vergleichende gehirnphysiologie und vergleichende psychologie. Loeb, J. 1899. Image from the Biodiversity Heritage Library. Contributed by MBLWHOI Library. No known copyright restrictions.

For example, LEFFLER *et al.* (2012) compiled data on levels of within-population, autosomal nucleotide diversity (π) for 167 species across 14 phyla from non-coding and synonymous sites (Figure 2.3). The species with the lowest levels of π in their survey was Lynx, with $\pi = 0.01\%$, i.e. only 1/10000 bases differed between two sequences. In contrast, some of the highest levels of diversity were found in *Ciona savignyi*, Sea Squirts, where a remarkable 1/12 bases differ between pairs of sequences. This 800-fold range of diversity seems impressive, but census population sizes have a much larger range.

2.1.2 Hardy–Weinberg proportions

Imagine a population mating at random with respect to genotypes, i.e. no inbreeding, no assortative mating, no population structure, and no sex differences in allele frequencies. The frequency of allele A_1 in the population at the time of reproduction is p . An A_1A_1 genotype is

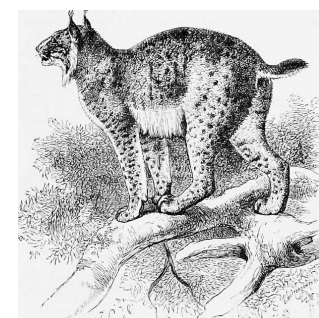
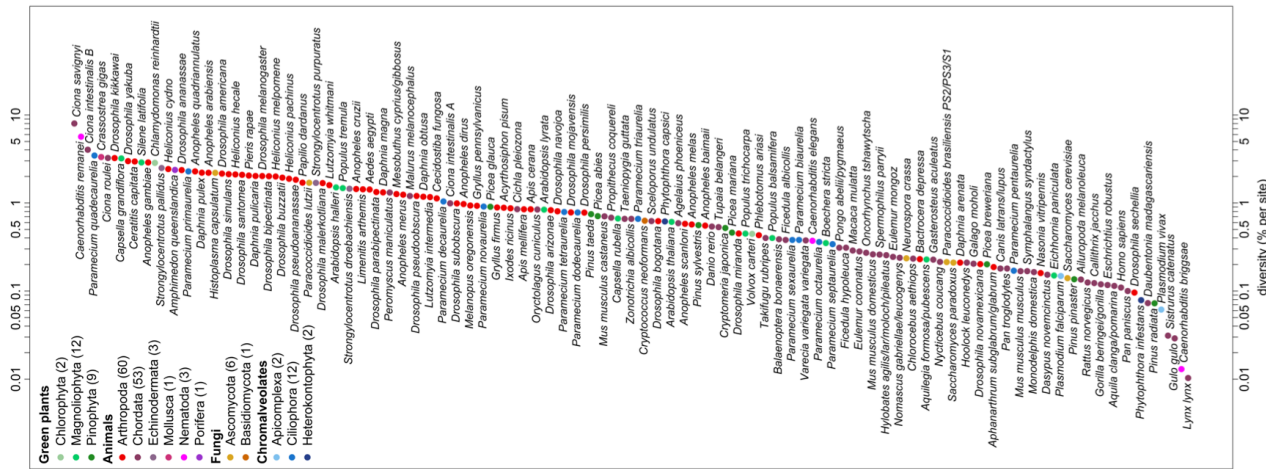


Figure 2.4: Eurasian Lynx (*Lynx lynx*).

An introduction to the study of mammals living and extinct. Flower, W.H. and Lydekker, R. 1891. Image from the Biodiversity Heritage Library. Contributed by Cornell University Library. No known copyright restrictions.



made by reaching out into our population and independently drawing two A_1 allele gametes to form a zygote. Therefore, the probability that an individual is an A_1A_1 homozygote is p^2 . This probability is also the expected frequencies of the A_1A_1 homozygote in the population. The expected frequency of the three possible genotypes are

$$\begin{array}{ccc} f_{11} & f_{12} & f_{22} \\ \hline p^2 & 2pq & q^2 \end{array}$$

Note that we only need to assume random mating with respect to our focal allele in order for these expected frequencies to hold in the zygotes forming the next generation. Evolutionary forces, such as selection, change allele frequencies within generations, but do not change this expectation for new zygotes, as long as p is the frequency of the A_1 allele in the population at the time when gametes fuse.

Question 3. On the coastal islands of British Columbia there is a subspecies of black bear (*Ursus americanus kermodei*, Kermode's bear). Many members of this black bear subspecies are white; they're sometimes called spirit bears. These bears aren't hybrids with polar bears, nor are they albinos. They are homozygotes for a recessive change at the MC1R gene. Individuals who are *GG* at this SNP are white while *AA* and *AG* individuals are black.

Below are the genotype counts for the MC1R polymorphism in a sample of bears from British Columbia's island populations from RITLAND *et al.* (2001).

<i>AA</i>	<i>AG</i>	<i>GG</i>
42	24	21

What are the expected frequencies of the three genotypes under HWE?

See Figure 2.6 for a nice empirical demonstration of Hardy–Weinberg proportions. The mean frequency of each genotype closely matches its HW expectations, and much of the scatter of the dots around the expected line is due to our small sample size (~ 60 individuals). While HW often seems like a silly model, it often holds remarkably well within populations. This is because individuals don't mate at random, but they do mate at random with respect to their genotype at most of the loci in the genome.

Question 4. You are investigating a locus with three alleles, A, B, and C, with allele frequencies p_A , p_B , and p_C . What fraction of the population is expected to be homozygotes under Hardy–Weinberg?

Microsatellites are regions of the genome where individuals vary for the number of copies of some short DNA repeat that they carry.

Throughout this chapter we'll be making use of the basic rules of probability to find the probabilities of combinations of events, e.g. the alleles found in an individual, see Appendix A.2.2 for a refresher.

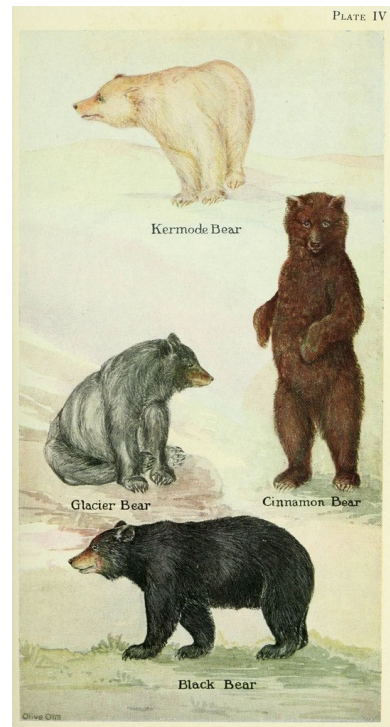


Figure 2.5: Kermode's bear (*Ursus americanus kermodei*). It's possible that this morph is favoured as the salmon these bears eat have a harder time seeing the light morph (KLINKA and REIMCHEN, 2009). The adaptive value of tasting like cinnamon is unknown.

Field book of North American mammals; descriptions of every mammal known north of the Rio Grande. Anthony, (1928) H. E. Image from the Biodiversity Heritage Library. Contributed by MBLWHOI Library. No known copyright restrictions.

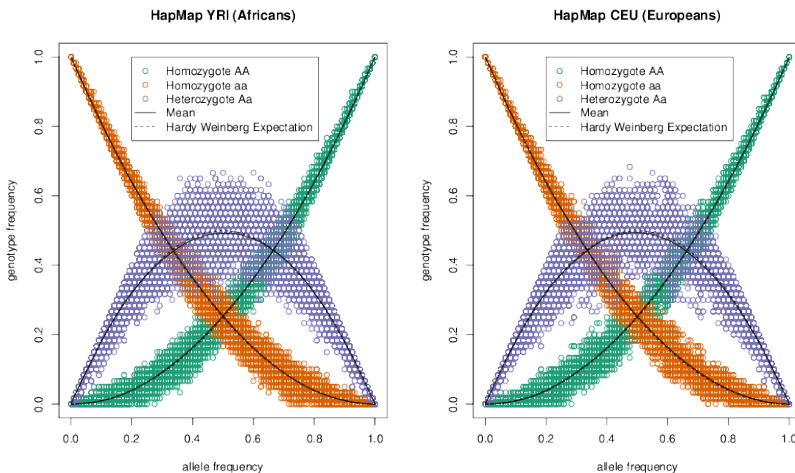


Figure 2.6: Demonstrating Hardy–Weinberg proportions using 10,000 SNPs from the HapMap European (CEU) and African (YRI) populations. Within each of these populations the allele frequency against the frequency of the 3 genotypes; each SNP is represented by 3 different coloured points. The solid lines show the mean genotype frequency. The dashed lines show the predicted genotype frequency from Hardy–Weinberg equilibrium. [Code here](#). [Blog post on figure here](#).

These regions are often highly variable across individuals, making them a suitable way to identify individuals from a DNA sample. This so-called DNA fingerprinting has a range of applications from establishing paternity and identifying human remains to matching individuals to DNA samples from a crime scene. The FBI make use of the CODIS database². The CODIS database contains the genotypes of over 13 million people, most of whom have been convicted of a crime. Most of the profiles record genotypes at 13 microsatellite loci that are tetranucleotide repeats (since 2017, 20 sites have been genotyped).

The allele counts for two loci (D16S539 and TH01) are shown in table 2.2 and 2.3 for a sample of 155 people of European ancestry. You can assume these two loci are on different chromosomes.

allele name	80	90	100	110	120	121	130	140	150
allele count	3	34	13	102	97	1	44	13	3

allele name	60	70	80	90	93	100	110
allele counts	84	42	37	67	77	1	2

Question 5. You extract a DNA sample from a crime scene. The genotype is 100/80 at the D16S539 locus and 70/93 at TH01.

A) You have a suspect in custody. Assuming this suspect is innocent and of European ancestry, what is the probability that their genotype would match this profile by chance (a false-match probability)?

² CODIS: Combined DNA Index System

Table 2.2: Data for 155 Europeans at the D16S539 microsatellite from CODIS from ALGEE-HEWITT *et al.* (2016). The top row gives the number of tetranucleotide repeats for each allele, the bottom row gives the sample counts.

Table 2.3: Same as 2.2 but for the TH01 microsatellite.

B) The FBI uses ≥ 13 markers. Why is this higher number necessary to make the match statement convincing evidence in court?

C) An early case that triggered debate among forensic geneticists was a crime among the Abenaki, a Native American community in Vermont (see LEWONTIN, 1994, for discussion). There was a DNA sample from the crime scene, and the perpetrator was thought likely to be a member of the Abenaki community. Given that allele frequencies vary among populations, why would people be concerned about using data from a non-Abenaki population to compute a false match probability?

2.2 Allele sharing among related individuals and Identity by Descent

All of the individuals in a population are related to each other by a giant pedigree (family tree). For most pairs of individuals in a population these relationships are very distant (e.g. distant cousins), while some individuals will be more closely related (e.g. sibling/first cousins). All individuals are related to one another by varying levels of relatedness, or *kinship*. Related individuals can share alleles that have both descended from the shared common ancestor. To be shared, these alleles must be inherited through all meioses connecting the two individuals (e.g. surviving the $1/2$ probability of segregation each meiosis). As closer relatives are separated by fewer meioses, closer relatives share more alleles. In Figure 2.7 we show the sharing of chromosomal regions between two cousins. As we'll see, many population and quantitative genetic concepts rely on how closely related individuals are, and thus we need some way to quantify the degree of kinship among individuals.

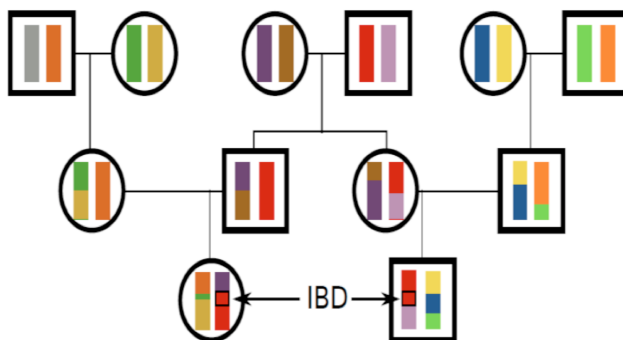


Figure 2.7: First cousins sharing a stretch of chromosome identical by descent. The different grandparental diploid chromosomes are coloured so we can track them and recombinations between them across the generations. Notice that the identity by descent between the cousins persists for a long stretch of chromosome due to the limited number of generations for recombination. The squares represent males and circles females.

We will define two alleles to be identical by descent (IBD) if they are identical due to transmission from a common ancestor in the past

few generations³. For the moment, we ignore mutation, and we will be more precise about what we mean by ‘past few generations’ later on. For example, parent and child share exactly one allele identical by descent at a locus, assuming that the two parents of the child are randomly mated individuals from the population. In Figure 2.13, I show a pedigree demonstrating some configurations of IBD.

One summary of how related two individuals are is the probability that our pair of individuals share 0, 1, or 2 alleles identical by descent (see Figure 2.8). We denote these identity-by-descent probabilities by r_0 , r_1 , and r_2 respectively. See Table 2.4 for some examples. We can also interpret these probabilities as genome-wide averages. For example, on average, at a quarter of all their autosomal loci full-sibs share zero alleles identical by descent.

One summary of relatedness that will be important is the probability that two alleles (I & J) picked at random, one from each of the two different individuals i and j , are identical by descent ($P(I\&J \text{ IBD})$). We call this quantity the *coefficient of kinship* of individuals i and j , and denote it by F_{ij} . It is calculated as

$$F_{ij} = P(\text{I&J IBD}) \quad (2.3)$$

$$\begin{aligned} &= P(\text{I&J IBD} | i\&j 0 \text{ IBD})P(i\&j 0 \text{ IBD}) \\ &\quad + P(\text{I&J IBD} | i\&j 1 \text{ IBD})P(i\&j 1 \text{ IBD}) \\ &\quad + P(\text{I&J IBD} | i\&j 2 \text{ IBD})P(i\&j 2 \text{ IBD}) \quad (2.4) \\ &= 0 \times r_0 + \frac{1}{4}r_1 + \frac{1}{2}r_2. \quad (2.5) \end{aligned}$$

In the above step, eqn(2.4), we’re summing the conditional probability of alleles I & J being IBD over whether our individuals i & j share 0, 1, or 2 alleles IBD, an example of using the Law of Total Probability (see Appendix eqn (A.12)). We’ve then, in eqn 2.5, used the fact that we can calculate our condition probabilities of I & J being IBD using the rules of Mendelian transmission. Consider the probability $P(\text{I&J IBD} | i\&j 1 \text{ IBD})$, i.e. that our pair of alleles (I & J) drawn from individuals i and j are IBD given that i and j share one allele IBD, this is a $1/4$ as we need to draw the allele that is IBD from both i and j , i.e. drawing both black alleles in the middle panel of Figure 2.8, which happens with probability $1/2 \times 1/2$. The coefficient of kinship will appear multiple times, in both our discussion of inbreeding and in the context of phenotypic resemblance between relatives.

Question 6. What are r_0 , r_1 , and r_2 for $1/2$ sibs? ($1/2$ sibs share one parent but not the other).

Question 7. Explain in words why $P(\text{I&J IBD} | i\&j 2 \text{ IBD}) = 1/2$.

³ COTTERMAN, C. W., 1940 A calculus for statistico-genetics. Ph. D. thesis, The Ohio State University; and MALÉCOT, G., 1948 Les mathématiques de l’hérédité

Here we’ll focus on IBD of outbred individuals. Dealing with sharing between inbred individuals requires 6 more identity-by-descent r coefficients, which honestly makes my head spin.

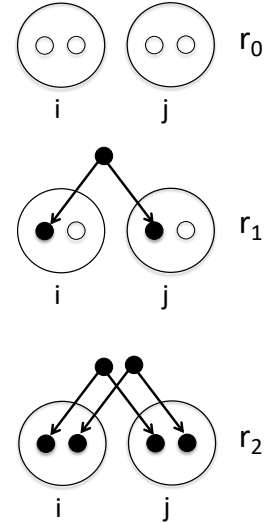


Figure 2.8: A pair of diploid individuals (i and j) sharing 0, 1, or 2 alleles IBD where lines show the sharing of alleles by descent (e.g. from a shared ancestor).

Relationship (i,j)*	$P(i\&j \text{ 0 IBD})$	$P(i\&j \text{ 1 IBD})$	$P(i\&j \text{ 2 IBD})$	$P(I\&J \text{ IBD})$
Relationship (i,j)*	r_0	r_1	r_2	F_{ij}
parent-child	0	1	0	$\frac{1}{4}$
full siblings	$\frac{1}{4}$	$\frac{1}{2}$	$\frac{1}{4}$	$\frac{1}{4}$
Monozygotic twins	0	0	1	$\frac{1}{2}$
1 st cousins	$\frac{3}{4}$	$\frac{1}{4}$	0	$\frac{1}{16}$

Table 2.4: Probability that two individuals of a given relationship share 0, 1, or 2 alleles identical by descent on the autosomes. *Assuming that our individuals are outbred and that this is the only close relationship the pair shares.

Genotypic sharing between pairs of individuals. Our r coefficients are going to have various uses. For example, they allow us to calculate the probability of the genotypes of a pair of relatives. Consider a biallelic locus where allele A_1 is at frequency p , and two individuals who have IBD allele sharing probabilities r_0 , r_1 , r_2 . What is the overall probability that these two individuals are both homozygous for allele 1?

Well that's

$$\begin{aligned} P(A_1A_1) = & P(A_1A_1|0 \text{ alleles IBD})P(0 \text{ alleles IBD}) \\ & + P(A_1A_1|1 \text{ allele IBD})P(1 \text{ allele IBD}) \\ & + P(A_1A_1|2 \text{ alleles IBD})P(2 \text{ alleles IBD}) \end{aligned} \quad (2.6)$$

Or, in our r_0 , r_1 , r_2 notation:

$$\begin{aligned} P(A_1A_1) = & P(A_1A_1|0 \text{ alleles IBD})r_0 \\ & + P(A_1A_1|1 \text{ alleles IBD})r_1 \\ & + P(A_1A_1|2 \text{ alleles IBD})r_2 \end{aligned} \quad (2.7)$$

If our pair of relatives share 0 alleles IBD, then the probability that they are both homozygous is $P(A_1A_1|0 \text{ alleles IBD}) = p^2 \times p^2$, as all four alleles represent independent draws from the population. If they share 1 allele IBD, then the shared allele is of type A_1 with probability p , and then the other non-IBD allele, in both relatives, also needs to be A_1 which happens with probability p^2 , so $P(A_1A_1|1 \text{ allele IBD}) = p \times p^2$. Finally, our pair of relatives can share two alleles IBD, in which case $P(A_1A_1|2 \text{ alleles IBD}) = p^2$, because if one of our individuals is homozygous for the A_1 allele, both individuals will be. Putting this all together our equation (2.7) becomes

$$P(A_1A_1) = p^4r_0 + p^3r_1 + p^2r_2 \quad (2.8)$$

Note that for specific cases we could also calculate this by summing over all the possible genotypes their shared ancestor(s) had; however, that would be much more involved and not as general as the form we have derived here.

We can write out terms like eq (2.8) for all of the possible configurations of genotype sharing/non-sharing between a pair of individuals. Based on this we can write down the expected number of polymorphic sites where our individuals are observed to share 0, 1, or 2 alleles.

Question 8. Trickier question. The genotype of our suspect in Question 5 turns out to be 100/80 for D16S539 and 70/80 at TH01. The suspect is not a match to the DNA from the crime scene; however, they could be a sibling.

Calculate the joint probability of observing the genotype from the crime and our suspect:

- A) Assuming that they share no close relationship.
- B) Assuming that they are full sibs.
- C) Briefly explain your findings.

There's a variety of ways to estimate the relationships among individuals using genetic data. An example of using allele sharing to identify relatives is offered by the work of Nancy Chen (in collaboration with Stepfanie Aguilera, see CHEN *et al.*, 2016; AGUILERA *et al.*, 2017). CHEN *et al.* has collected genotyping data from thousands of Florida Scrub Jays at over ten thousand loci. These Jays live at the Archbold field site, and have been carefully monitored for many decades allowing the pedigree of many of the birds to be known. Using these data she estimates allele frequencies at each locus. Then by equating the observed number of times that a pair of individuals share 0, 1, or 2 alleles to the theoretical expectation, she estimates the probability of r_0 , r_1 , and r_2 for each pair of birds. A plot of these are shown in Figure 2.10, showing how well the estimates match those known from the pedigree.

Sharing of genomic blocks among relatives. We can more directly see the sharing of the genome among close relatives using high-density SNP genotyping arrays. In Figure 2.11 we show a simulation of you and your first cousin's genomic material that you both inherited from your shared grandmother. Colored purple are regions where you and your cousin will have matching genomic material, due to having inherited it IBD from your shared grandmother.

You and your first cousin will share at least one allele of your genotype at all of the polymorphic loci in these purple regions. There's a range of methods to detect such sharing. One way is to look for unusually long stretches of the genome where two individuals are never homozygous for different alleles. By identifying pairs of individuals who share an unusually large number of such putative IBD blocks, we can hope to identify unknown relatives in genotyping datasets. In fact, companies like 23&me and Ancestry.com use signals of IBD to help



Figure 2.9: Florida Scrub-Jays (*Aphelocoma coerulescens*).
The birds of America : from drawings made in the United States and their territories. 1880.
Audubon J.J. Image from the Biodiversity Heritage Library. Contributed by Smithsonian Libraries. Licensed under CC BY-2.0.

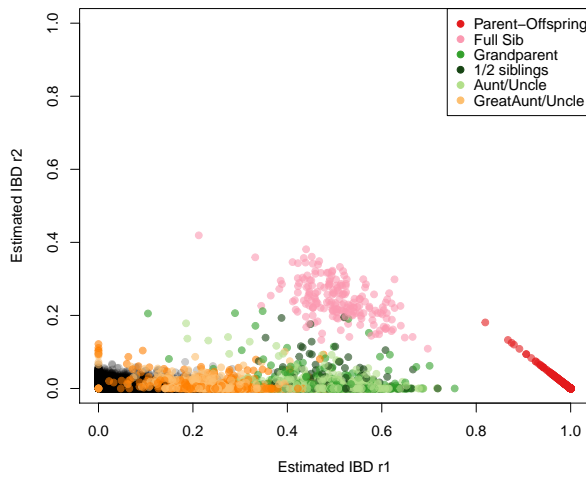


Figure 2.10: Estimated coefficient of kinship from Florida Scrub Jays. Each point is a pair of individuals, plotted by their estimated IBD (r_1 and r_2) from their genetic data. The points are coloured by their known pedigree relationships. Note that most pairs have low kinship, and no recent genealogical relationship, and so appear as black points in the lower left corner. Thanks to Nancy Chen for supplying the data. Code here.

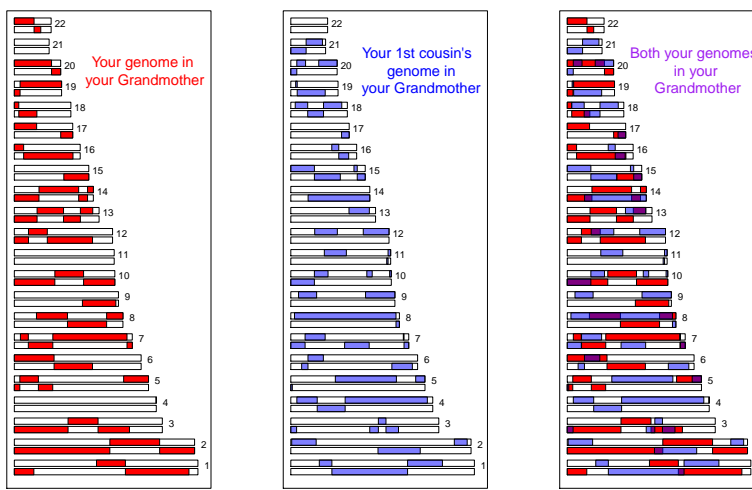


Figure 2.11: A simulation of sharing between first cousins. The regions of your grandmother's 22 autosomes that you inherited are coloured red, those that your cousins inherited are coloured blue. In the third panel we show the overlapping genomic regions in purple, these regions will be IBD in you and your cousin. If you are full first cousins, you will also have shared genomic regions from your shared grandfather, not shown here. Details about how we made these simulations here.

identify family ties.

As another example, consider the case of third cousins. You share one of eight sets of great-great grandparents with each of your (likely many) third cousins. On average, you and each of your third cousins each inherit one-sixteenth of your genome from each of those two great-great grandparents. This turns out to imply that on average, a little less than one percent of your and your third cousin's genomes ($2 \times (1/16)^2 = 0.78\%$) will be identical by virtue of descent from those shared ancestors. A simulated example where third cousins share blocks of their genome (on chromosome 16 and 2) due to their great, great grandmother is shown in Figure 2.12.

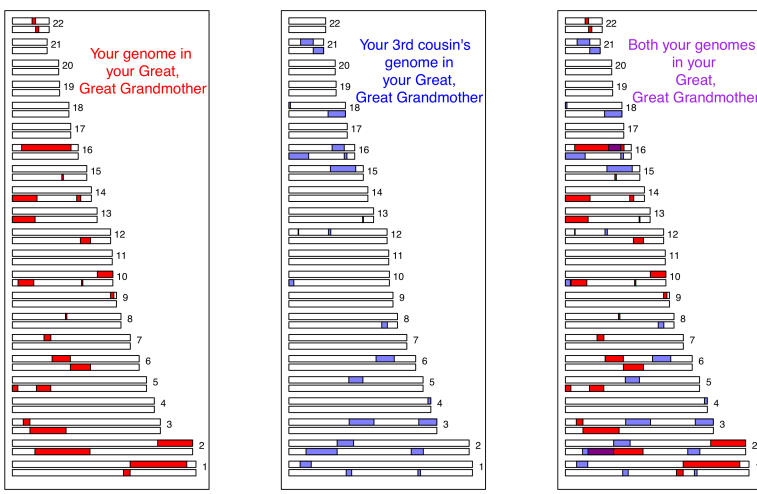


Figure 2.12: A simulation of sharing between third cousins, the details are the same as in Figure 2.11.

Note how if you compare Figure 2.12 and Figure 2.11, individuals inherit less IBD from a shared great, great grandmother than from a shared grandmother, as they inherit from more total ancestors further back. Also notice how the sharing occurs in shorter genomic blocks, as it has passed through more generations of recombination during meiosis. These blocks are still detectable, and so third cousins can be detected using high-density genotyping chips, allowing more distant relatives to be identified than single marker methods alone.⁴ More distant relations than third cousins, e.g. fourth cousins, start to have a significant probability of sharing none of their genome IBD. But you have many fourth cousins, so you will share some of your genome IBD with some of them; however, it gets increasingly hard to identify the degree of relatedness from genetic data the deeper in the family tree this sharing goes.

⁴ Indeed the suspect in case of the Golden State Killer was identified through identifying third cousins that genetically matched a DNA sample from an old crime scene (see a [here](#) for more details).

2.2.1 Inbreeding

We can define an inbred individual as an individual whose parents are more closely related to each other than two random individuals drawn from some reference population.

When two related individuals produce an offspring, that individual can receive two alleles that are identical by descent, i.e. they can be homozygous by descent (sometimes termed autozygous), due to the fact that they have two copies of an allele through different paths through the pedigree. This increased likelihood of being homozygous relative to an outbred individual is the most obvious effect of inbreeding. It is also the one that will be of most interest to us, as it underlies a lot of our ideas about inbreeding depression and population structure. For example, in Figure 2.13 our offspring of first cousins is homozygous by descent having received the same IBD allele via two different routes around an inbreeding loop.

As the offspring receives a random allele from each parent (i and j), the probability that those two alleles are identical by descent is equal to the kinship coefficient F_{ij} of the two parents (Eqn. 2.5). This follows from the fact that the genotype of the offspring is made by sampling an allele at random from each of our parents.

f_{11}	f_{12}	f_{22}
$(1 - F)p^2 + Fp$	$(1 - F)2pq$	$(1 - F)q^2 + Fq$

The only way the offspring can be heterozygous (A_1A_2) is if their two alleles at a locus are not IBD (otherwise they would necessarily be homozygous). Therefore, the probability that they are heterozygous is

$$(1 - F)2pq, \quad (2.9)$$

where we have dropped the indices i and j for simplicity. The offspring can be homozygous for the A_1 allele in two different ways. They can have two non-IBD alleles that are not IBD but happen to be of the allelic type A_1 , or their two alleles can be IBD, such that they inherited allele A_1 by two different routes from the same ancestor. Thus, the probability that an offspring is homozygous for A_1 is

$$(1 - F)p^2 + Fp. \quad (2.10)$$

Therefore, the frequencies of the three possible genotypes can be written as given in Table 2.5, which provides a generalization of the Hardy–Weinberg proportions.

Question 9. The frequency of the A_1 allele is p at a biallelic locus. Assume that our population is randomly mating and that the

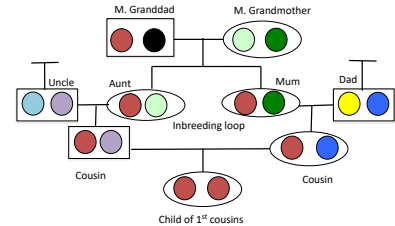


Figure 2.13: Alleles being transmitted through an inbred pedigree. The two sisters (mum and aunt) share two alleles identical by descent (IBD). The cousins share one allele IBD. The offspring of first cousins is homozygous by descent at this locus.

Table 2.5: Generalized Hardy–Weinberg

genotype frequencies in the population follow from HW. We select two individuals at random to mate from this population. We then mate the children from this cross. What is the probability that the child from this full sib-mating is homozygous?

Multiple inbreeding loops in a pedigree. Up to this point we have assumed that there is at most one inbreeding loop in the recent family history of our individuals, i.e. the parents of our inbred individual have at most one recent genealogical connection. However, an individual who has multiple inbreeding loops in their pedigree can be homozygous by descent thanks to receiving IBD alleles via multiple different different loops. To calculate inbreeding in pedigrees of arbitrary complexity, we can extend beyond our original relatedness coefficients r_0 , r_1 , and r_2 to account for higher order sharing of alleles IBD among relatives. For example, we can ask, what is the probability that *both* of the alleles in the first individual are shared IBD with one allele in the second individual? There are nine possible relatedness coefficients in total to completely describe kinship between two diploid individuals, and we won't go in to them here as it's a lot to keep track of. However, we will show how we can calculate the inbreeding coefficient of an individual with multiple inbreeding loops more directly.

Let's say the parents of our inbred individual (B and C) have K shared ancestors, i.e. individuals who appear in both B and C's recent family trees. We denote these shared ancestors by A_1, \dots, A_K , and we denote by n the total number of individuals in the chain from B to C via ancestor A_i , including B, C, and A_i . For example, if B is C's aunt, then B and C share two ancestors, which are B's parents and, equivalently, C's grandparents. In this case, there are $n=4$ individuals from B to C through each of these two shared ancestor. In the general case, the kinship coefficient of B and C, i.e. the inbreeding coefficient of their child, is

$$F = \sum_{i=1}^K \frac{1}{2^{n_i}} (1 + f_{A_i}) \quad (2.11)$$

where f_{A_i} is the inbreeding coefficient of the ancestor A_i . What's happening here is that we sum over all the mutually-exclusive paths in the pedigree through which B and C can share an allele IBD. With probability $1/2^{n_i}$, a pair of alleles picked at random from B and C is descended from the same ancestral allele in individual A_i , in which case the alleles are IBD.⁵ However, even if B inherits the maternal allele and C inherits the paternal allele of shared ancestor A_i , if A_i was themselves inbred, with probability f_{A_i} those two alleles are themselves IBD. Thus a shared *inbred* ancestor further increases the kinship of B and C.

⁵ For example, in the case of our aunt-nephew case, assuming that the aunt's two parents are their only recent shared ancestors, then $F = 1/2^4 + 1/2^4 = 1/8$, in agreement with the answer we would obtain from eqn (2.5).

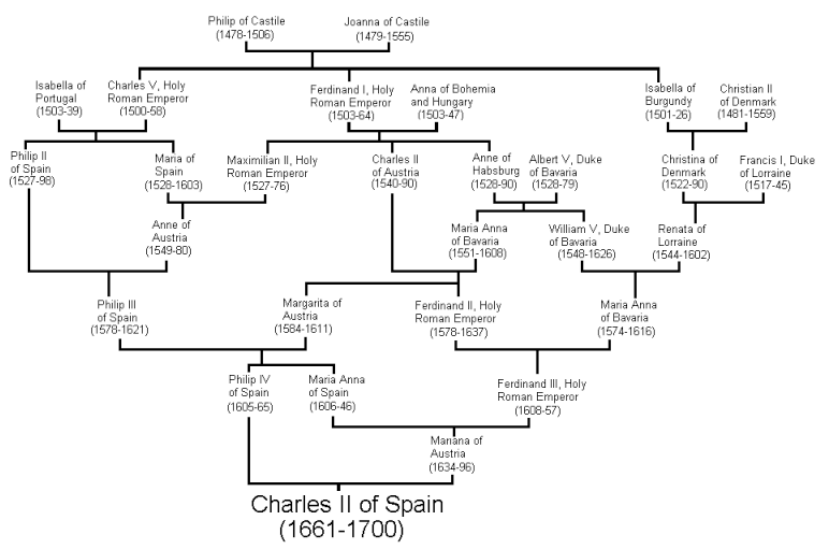


Figure 2.14: The pedigree of King Charles II of Spain. Pedigree from wikimedia drawn by Lec CRP1, public domain.

Multiple inbreeding loops increase the probability that a child is homozygous by descent at a locus, which can be calculated simply by plugging in F , the child's inbreeding coefficient, into our generalized HW equation.

As one extreme example of the impact of multiple inbreeding loops in an individual's pedigree, let's consider king Charles II of Spain, the last of the Spanish Habsburgs. Charles was the son of Philip IV of Spain and Mariana of Austria, who were uncle and niece. If this were the only inbreeding loop, then Charles would have had an inbreeding coefficient of $1/8$. Unfortunately for Charles, the Spanish Habsburgs had long kept wealth and power within their family by arranging marriages between close kin. The pedigree of Charles II is shown in Figure 2.14, and multiple inbreeding loops are apparent. For example, Phillip III, Charles II's grandfather and great-grandfather, was himself a child of an uncle-niece marriage.

ALVAREZ *et al.* (2009) calculated that Charles II had an inbreeding coefficient of 0.254, equivalent to a full-sib mating, thanks to all of the inbreeding loops in his pedigree. Therefore, he is expected to have been homozygous by descent for a full quarter of his genome. As we'll talk about later in these notes, this means that Charles may have been homozygous for a number of recessive disease alleles, and indeed he was a very sickly man who left no descendants due to his infertility.⁶ Thus plausibly the end of one of the great European dynasties came



Figure 2.15: Charles II of Spain (by Juan Carreño de Miranda, 1685). Public Domain.

⁶ Pedro Gargantilla, who performed Charles's autopsy, stated that his body "did not contain a single drop of blood; his heart was the size of a peppercorn; his lungs corroded; his intestines rotten and gangrenous; he had a single testicle, black as coal, and his head was full of water." While some of this description may refer to actual medical conditions, some of these details seem a little unlikely. See here.

about through inbreeding.

2.2.2 Calculating inbreeding coefficients from genetic data

If the observed heterozygosity in a population is H_O , and we assume that the generalized Hardy–Weinberg proportions hold, we can set H_O equal to f_{12} , and solve Eq. (2.9) for F to obtain an estimate of the inbreeding coefficient as

$$\hat{F} = 1 - \frac{f_{12}}{2pq} = \frac{2pq - f_{12}}{2pq}. \quad (2.12)$$

As before, p is the frequency of allele A_1 in the population. This can be rewritten in terms of the observed heterozygosity (H_O) and the heterozygosity expected in the absence of inbreeding, $H_E = 2pq$, as

$$\hat{F} = \frac{H_E - H_O}{H_E} = 1 - \frac{H_O}{H_E}. \quad (2.13)$$

Hence, \hat{F} quantifies the deviation due to inbreeding of the observed heterozygosity from the one expected under random mating, relative to the latter.

Question 10. Suppose the following genotype frequencies were observed for an esterase locus in a population of *Drosophila* (A denotes the “fast” allele and B denotes the “slow” allele):

AA	AB	BB
0.6	0.2	0.2

What is the estimate of the inbreeding coefficient at the esterase locus?

If we have multiple loci, we can replace H_O and H_E by their means over loci, \bar{H}_O and \bar{H}_E , respectively. Note that, in principle, we could also calculate F for each individual locus first, and then take the average across loci. However, this procedure is more prone to introducing a bias if sample sizes vary across loci, which is not unlikely when we are dealing with real data.

Genetic markers are commonly used to estimate inbreeding for wild and/or captive populations of conservation concern. As an example of this, consider the case of the Mexican wolf (*Canis lupus baileyi*), a sub-species of gray wolf.

They were extirpated in the wild during the mid-1900s due to hunting, and the remaining five Mexican wolves in the wild were captured to start a breeding program. vonHOLDT *et al.* (2011) estimated the current-day, average expected heterozygosity to be 0.18, based on allele frequencies at over forty thousand SNPs. However, the average Mexican wolf individual was only observed to be heterozygous at 12%



Figure 2.16: Grey wolf (*Canis lupus*). Dogs, jackals, wolves, and foxes: a monograph of the Canidae. 1890. y J.G. Keulemans. Image from the Biodiversity Heritage Library. Contributed by University of Toronto - Gerstein Science Information Centre. Not in copyright.

of these SNPs. Therefore, the average inbreeding coefficient for the Mexican wolf is $F = 1 - 0.12/0.18$, i.e. $\sim 33\%$ of a lobo's genome is homozygous due to recent inbreeding in their pedigree.

Genomic blocks of homozygosity due to inbreeding. As we saw above, close relatives are expected to share alleles IBD in large genomic blocks. Thus, when related individuals mate and transmit alleles to an inbred offspring, they transmit these alleles in big blocks through meiosis. An example, lets return to the case of our hypothetical first cousins from Figure 2.7. If this pair of individuals had a child, one possible pattern of genetic transmission is shown in Figure 2.17. The child has inherited the red stretch of chromosome via two different routes through their pedigree from the grandparents. This is an example of an autozygous segment, where the child is homozygous by descent at all of the loci in this red region. The inbreeding coefficient

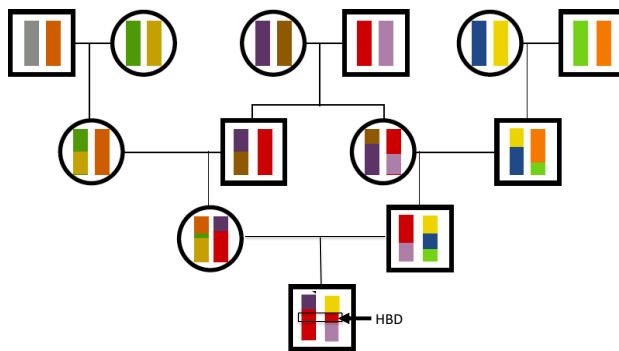


Figure 2.17: A pedigree showing the offspring of first cousins. The chromosomes of their great-grandparents are coloured different colours so their transmission can be tracked. The child is homozygous by descent (HBD) for a section of the red chromosome.

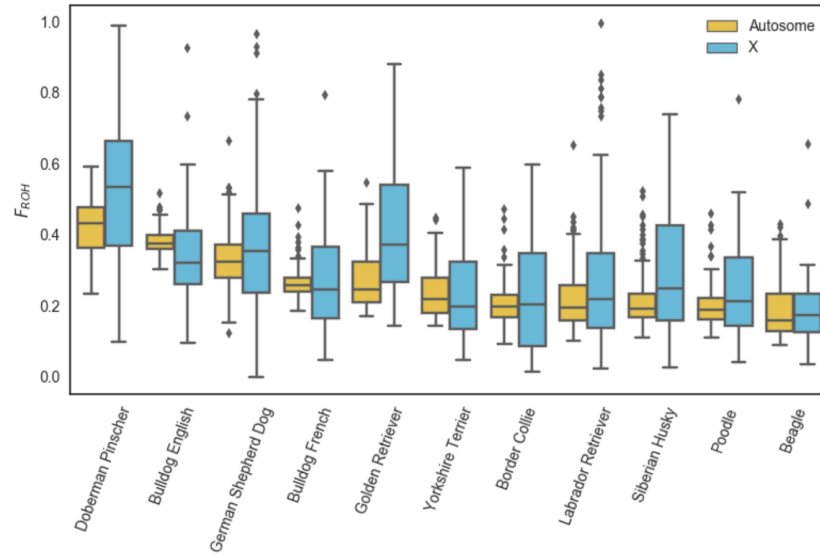
of the child sets the proportion of their genome that will be in these autozygous segments. For example, a child of first full cousins is expected to have $1/16$ of their genome in these segments. The more distant the loop in the pedigree, the more meioses that chromosomes have been through and the shorter individual blocks will be. A child of first cousins will have longer blocks than a child of second cousins, for example.

Individuals with multiple inbreeding loops in their family tree can have a high inbreeding coefficient due to the combined effect of many small blocks of autozygosity. For example, Charles II had an inbreeding coefficient that is equivalent to that of the child of full-sibs, with a quarter of his genome expected to homozygous by descent, but this would be made up of many shorter blocks.

We can hope to detect these blocks by looking for unusually long genomic runs of homozygosity (ROH) sites in an individual's genome. One way to estimate an individual's inbreeding coefficient is then to total up the proportion of an individual's genome that falls in such

ROH regions. This estimate is called F_{ROH} .

An example of using F_{ROH} to study inbreeding comes from the work of SAMS and BOYKO (2018b), who identified runs of homozygosity in 2,500 dogs, ranging from 500kb up to many megabases. Fig-



ure 2.18 shows the distribution of F_{ROH} of individuals in each dog breed for the X and autosome. In Figure 2.20 this is broken down by the length of ROH segments.

Dog breeds have been subject to intense breeding that has resulted in high levels of inbreeding. Of the population samples examined, Doberman Pinschers have the highest levels of their genome in runs of homozygosity (F_{ROH}), somewhat higher than English bulldogs. In 2.20 we can see that English bulldogs have more short ROH than Doberman Pinschers, but that Doberman Pinschers have more of their genome in very large ROH ($> 16Mb$). This suggests that English bulldogs have had long history of inbreeding but that Doberman Pinschers have a lot of recent inbreeding in their history.

Figure 2.18: The distribution of F_{ROH} of individuals from various dog breeds from SAMS and BOYKO (2018a), licensed under CC BY 4.0.

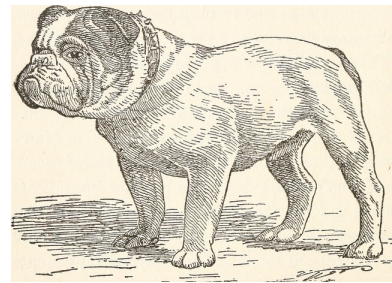


Figure 2.19: English bulldog. The dogs of Boytowm. 1918. Dyer, W. A.

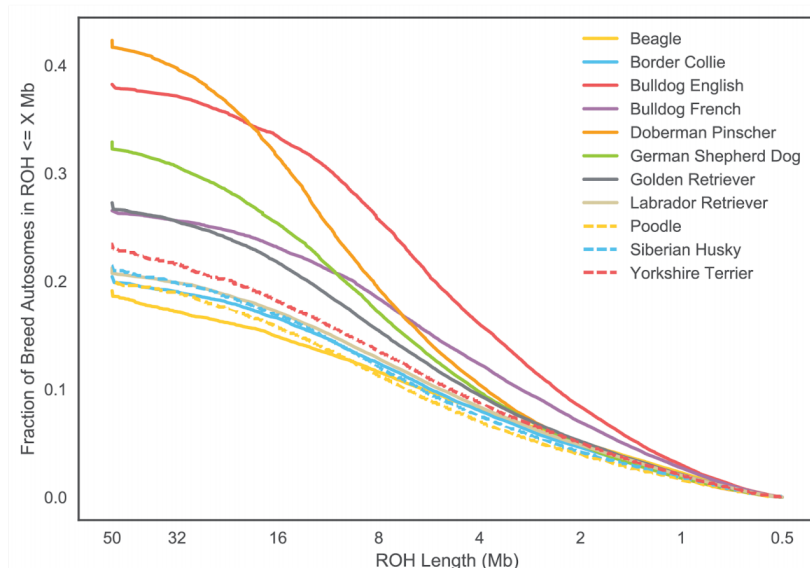


Figure 2.20: Cumulative density of ROH length, measured in megabases (Mb) from SAMS and BOYKO (2018a) for various dog breeds (licensed under CC BY 4.0). Note that longer lengths of ROH are on the left of the plot.

3

Population Structure and Correlations Among Loci.

INDIVIDUALS RARELY MATE COMPLETELY AT RANDOM; your parents weren't two Bilateria plucked at random from the tree of life. Even within species, there's often geographically-restricted mating among individuals. Individuals tend to mate with individuals from the same, or closely related sets of populations. This form of non-random mating is called population structure and can have profound effects on the distribution of genetic variation within and among natural populations.

Populations can often differ in their allele frequencies, either due to genetic drift or selection driving differentiation among populations. In this chapter we'll talk through some ways to summarize and visualize population genetic structure. Population differentiation is also a major driver of correlations in allelic state among loci, and we'll start our discussion of these correlations at the end of this chapter. One reason for talking about population structure so early in the book is that summarizing population structure is often a key initial stage in population genomic analyses. Thus you'll often encounter summaries and visualizations of population structure when we read research papers, so it's good to have some understanding of what they represent.

3.0.1 Inbreeding as a summary of population structure.

Our statements about inbreeding, and inbreeding coefficients, represent one natural way to summarize population structure. In the previous chapter, we defined inbreeding as having parents that are more closely related to each other than two individuals drawn at random from some reference population. The question that naturally arises is: Which reference population should we use? While I might not look inbred in comparison to allele frequencies in the United Kingdom (UK), where I am from, my parents certainly are not two individuals drawn at random from the world-wide population. If we estimated my in-

breeding coefficient F using allele frequencies within the UK, it would be close to zero, but would likely be larger if we used world-wide frequencies. This is because there is a somewhat lower level of expected heterozygosity within the UK than in the human population across the world as a whole.

WRIGHT¹ developed a set of ‘F-statistics’ (also called ‘fixation indices’) that formalize the idea of inbreeding with respect to different levels of population structure. See Figure 3.1 for a schematic diagram. Wright defined F_{XY} as the correlation between random gametes, drawn from the same level X , relative to level Y . We will return to why F -statistics are statements about correlations between alleles in just a moment. One commonly used F -statistic is F_{IS} , which is the inbreeding coefficient between an individual (I) and the subpopulation (S). Consider a single locus, where in a subpopulation (S) a fraction $H_I = f_{12}$ of individuals are heterozygous. In this subpopulation, let the frequency of allele A_1 be p_S , such that the expected heterozygosity under random mating is $H_S = 2p_S(1 - p_S)$. We will write F_{IS} as

$$F_{IS} = 1 - \frac{H_I}{H_S} = 1 - \frac{f_{12}}{2p_S q_S}, \quad (3.1)$$

a direct analog of eqn. 2.12. Hence, F_{IS} is the relative difference between observed and expected heterozygosity due to a deviation from random mating within the subpopulation. We could also compare the observed heterozygosity in individuals (H_I) to that expected in the total population, H_T . If the frequency of allele A_1 in the total population is p_T , then we can write F_{IT} as

$$F_{IT} = 1 - \frac{H_I}{H_T} = 1 - \frac{f_{12}}{2p_T q_T}, \quad (3.2)$$

which compares heterozygosity in individuals to that expected in the total population. As a simple extension of this, we could imagine comparing the expected heterozygosity in the subpopulation (H_S) to that expected in the total population H_T , via F_{ST} :

$$F_{ST} = 1 - \frac{H_S}{H_T} = 1 - \frac{2p_S q_S}{2p_T q_T}. \quad (3.3)$$

We can relate the three F -statistics to each other as

$$(1 - F_{IT}) = \frac{H_I}{H_S} \frac{H_S}{H_T} = (1 - F_{IS})(1 - F_{ST}). \quad (3.4)$$

Hence, the reduction in heterozygosity within individuals compared to that expected in the total population can be decomposed to the reduction in heterozygosity of individuals compared to the subpopulation, and the reduction in heterozygosity from the total population to that in the subpopulation.

¹ WRIGHT, S., 1943 Isolation by Distance. *Genetics* 28(2): 114–138; and WRIGHT, S., 1949 The Genetical Structure of Populations. *Annals of Eugenics* 15(1): 323–354

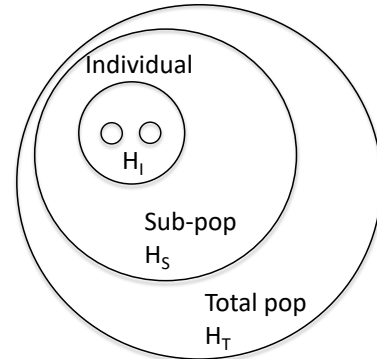


Figure 3.1: The hierarchical nature of F-statistics. The two dots within an individual represent the two alleles at a locus for an individual I . We can compare the heterozygosity in individuals (H_I), to that found by randomly drawing alleles from the sub-population (S), to that found in the total population (T).

If we want a summary of population structure across multiple sub-populations, we can average H_I and/or H_S across populations, and use a p_T calculated by averaging p_S across subpopulations (or our samples from sub-populations). For example, the average F_{ST} across K subpopulations (sampled with equal effort) is

$$F_{ST} = 1 - \frac{\bar{H}_S}{H_T}, \quad (3.5)$$

where $\bar{H}_S = 1/K \sum_{i=1}^K H_S^{(i)}$, and $H_S^{(i)} = 2p_i q_i$ is the expected heterozygosity in subpopulation i . It follows that the average heterozygosity of the sub-populations $\bar{H}_S \leq H_T$, and so $F_{ST} \geq 0$ and $F_{IS} \leq F_{IT}$. This observation that the average heterozygosity of the sub-populations must be less than or equal to that of the total population is called the Wahlund effect. Furthermore, if we have multiple sites, we can replace H_I , H_S , and H_T with their averages across loci (as above). ²

As an example of comparing a genome-wide estimate of F_{ST} to that at individual loci we can look at some data from blue- and golden-winged warblers (*Vermivora cyanoptera* and *V. chrysoptera* 1-2 & 5-6 in Figure 3.2).

These two species are spread across eastern Northern America, with the golden-winged warbler having a smaller, more northerly range. They're quite different in terms of plumage, but have long been known to have similar songs and ecologies. The two species hybridize readily in the wild; in fact two other previously-recognized species, Brewster's and Lawrence's warbler (4 & 3 in 3.2), are actually found to just be hybrids between these two species. The golden-winged warbler is listed as 'threatened' under the Canadian endangered species act as its habitat is under pressure from human activity and due to increasing hybridization with the blue-winged warbler, which is moving north into its range. TOEWS *et al.* (2016) investigated the population genomics of these warblers, sequencing ten golden- and ten blue-winged warblers. They found very low divergence among these species, with a genome-wide $F_{ST} = 0.0045$. In Figure 3.3, per SNP F_{ST} is averaged in 2000bp windows moving along the genome. The average is very low, but some regions of very high F_{ST} stand out. Nearly all of these regions correspond to large allele frequency differences at loci in, or close, to genes known to be involved in plumage colouration differences in other birds. To illustrate these frequency differences TOEWS *et al.* (2016) genotyped a SNP in each of these high- F_{ST} regions. Here's their genotyping counts from the SNP, segregating for an allele 1 and 2, in the *Wnt* region, a key regulatory gene involved in feather development:

² Averaging heterozygosity across loci first, then calculating F_{ST} , rather than calculating F_{ST} for each locus individually and then taking the average, has better statistical properties as statistical noise in the denominator is averaged out.



Figure 3.2: Blue-, golden-winged, and Lawrence's warblers (*Vermivora*). The warblers of North America. Chapman, F.M. 1907. Image from the Biodiversity Heritage Library. Contributed by American Museum of Natural History Library. Not in copyright.

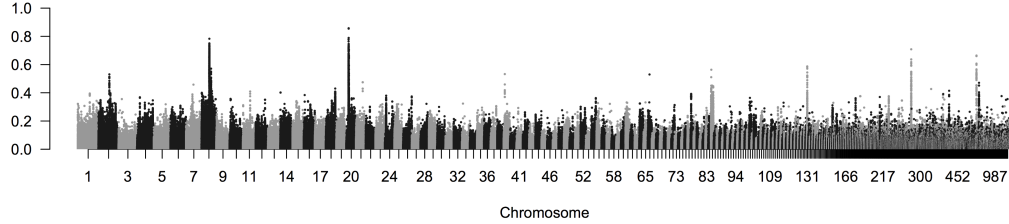


Figure 3.3: F_{ST} between blue- and golden-winged warbler population samples at SNPs across the genome. Each dot is a SNP, and SNPs are coloured alternating by scaffold. Thanks to David Toews for the figure.

Species	11	12	22
Blue-winged	2	21	31
Golden-winged	48	12	1

Question 1. With reference to the table of *Wnt*-allele counts:

- A) Calculate F_{IS} in blue-winged warblers.
- B) Calculate F_{ST} for the sub-population of blue-winged warblers compared to the combined sample.
- C) Calculate mean F_{ST} across both sub-populations.

Interpretations of F -statistics Let us now return to Wright's definition of the F -statistics as correlations between random gametes, drawn from the same level X , relative to level Y . Without loss of generality, we may think about X as individuals and S as the subpopulation.

Rewriting F_{IS} in terms of the observed homozygote frequencies (f_{11} , f_{22}) and expected homozygosities (p_S^2 , q_S^2) we find

$$F_{IS} = \frac{2psq_S - f_{12}}{2psq_S} = \frac{f_{11} + f_{22} - p_S^2 - q_S^2}{2psq_S}, \quad (3.6)$$

using the fact that $p^2 + 2pq + q^2 = 1$, and $f_{12} = 1 - f_{11} - f_{22}$.

The form of eqn. (3.6) reveals that F_{IS} is the covariance between pairs of alleles found in an individual, divided by the expected variance under binomial sampling. Thus, F -statistics can be understood as the correlation between alleles drawn from a population (or an individual) above that expected by chance (i.e. drawing alleles sampled at random from some broader population).³

We can also interpret F -statistics as proportions of variance explained by different levels of population structure. To see this, let us think about F_{ST} averaged over K subpopulations, whose frequencies are p_1, \dots, p_K . The frequency in the total population is

³ To see why the numerator of eqn (3.6) is the covariance of a discrete random variable see Appendix eqn. (A.40), where we imagine that the random variable is 1 if the alleles drawn from the population are the same and 0 if not. The denominator is the binomial variance of a sample of two, and so our eqn is a covariance divided by a variance and so interpretable as a correlation (see eqn (A.42))

$p_T = \bar{p} = 1/K \sum_{i=1}^K p_i$. Then, we can write

$$F_{\text{ST}} = \frac{2\bar{p}\bar{q} - \frac{1}{K} \sum_{i=1}^K 2p_i q_i}{2\bar{p}\bar{q}} = \frac{\left(\frac{1}{K} \sum_{i=1}^K p_i^2 + \frac{1}{K} \sum_{i=1}^K q_i^2 \right) - \bar{p}^2 - \bar{q}^2}{2\bar{p}\bar{q}} \quad (3.7)$$

$$= \frac{\text{Var}(p_1, \dots, p_K)}{\text{Var}(\bar{p})}, \quad (3.8)$$

which shows that F_{ST} is the proportion of the variance explained by the subpopulation labels.⁴

3.0.2 Other approaches to population structure

There is a broad spectrum of methods to describe patterns of population structure in population genetic datasets. We'll briefly discuss two broad-classes of methods that appear often in the literature: assignment methods and principal components analysis.

3.0.3 Assignment Methods

Here we'll describe a simple probabilistic assignment to find the probability that an individual of unknown population comes from one of K predefined populations. For example, there are three broad populations of common chimpanzee (*Pan troglodytes*) in Africa: western, central, and eastern. Imagine that we have a chimpanzee whose population of origin is unknown (e.g. it's from an illegal private collection). If we have genotyped a set of unlinked markers from a panel of individuals representative of these populations, we can calculate the probability that our chimp comes from each of these populations.

We'll then briefly explain how to extend this idea to cluster a set of individuals into K initially unknown populations. This method is a simplified version of what population genetics clustering algorithms such as STRUCTURE and ADMIXTURE do.⁵

A simple assignment method We have genotype data from unlinked S biallelic loci for K populations. The allele frequency of allele A_1 at locus l in population k is denoted by $p_{k,l}$, so that the allele frequencies in population 1 are $p_{1,1}, \dots, p_{1,L}$ and population 2 are $p_{2,1}, \dots, p_{2,L}$ and so on.

You genotype a new individual from an unknown population at these L loci. This individual's genotype at locus l is g_l , where g_l denotes the number of copies of allele A_1 this individual carries at this locus ($g_l = 0, 1, 2$).

The probability of this individual's genotype at locus l conditional on coming from population k , i.e. their alleles being a random HW

⁴ This follows because the numerator, in step eqn (3.7), is the averaged squared frequency minus the squared frequency, i.e. the variance (see Appendix eqn A.23).

⁵ PRITCHARD, J. K., M. STEPHENS, and P. DONNELLY, 2000 Inference of population structure using multilocus genotype data. *Genetics* 155(2): 945–959; and ALEXANDER, D. H., J. NOVEMBRE, and K. LANGE, 2009 Fast model-based estimation of ancestry in unrelated individuals. *Genome research* 19(9): 1655–1664

draw from population k , is

$$P(g_l | \text{pop } k) = \begin{cases} (1 - p_{k,l})^2 & g_l = 0 \\ 2p_{k,l}(1 - p_{k,l}) & g_l = 1 \\ p_{k,l}^2 & g_l = 2 \end{cases} \quad (3.9)$$

Assuming that the loci are independent, the probability of the individual's genotype across all S loci, conditional on the individual coming from population k , is

$$P(\text{ind.} | \text{pop } k) = \prod_{l=1}^S P(g_l | \text{pop } k) \quad (3.10)$$

We wish to know the probability that this new individual comes from population k , i.e. $P(\text{pop } k | \text{ind.})$. We can obtain this through Bayes' rule

$$P(\text{pop } k | \text{ind.}) = \frac{P(\text{ind.} | \text{pop } k)P(\text{pop } k)}{P(\text{ind.})} \quad (3.11)$$

where

$$P(\text{ind.}) = \sum_{k=1}^K P(\text{ind.} | \text{pop } k)P(\text{pop } k) \quad (3.12)$$

is the normalizing constant.⁶ We can interpret $P(\text{pop } k)$ as the prior probability of the individual coming from population k , and unless we have some other prior knowledge we will assume that the new individual has an equal probability of coming from each population $P(\text{pop } k) = 1/K$.

We interpret

$$P(\text{pop } k | \text{ind.}) \quad (3.13)$$

as the posterior probability that our new individual comes from each of our $1, \dots, K$ populations.

More sophisticated versions of this are now used to allow for hybrids, e.g. we can have a proportion q_k of our individual's genome come from population k and estimate the set of q_k 's.

Question 2.

Returning to our chimp example, imagine that we have genotyped a set of individuals from the Western and Eastern populations at two SNPs (we'll ignore the central population to keep things simpler). The frequency of the capital allele at two SNPs (A/a and B/b) is given by

Population	locus A	locus B
Western	0.1	0.85
Eastern	0.95	0.2

⁶ See the Appendix (A.16) for more on Bayes' Rule

A) Our individual, whose origin is unknown, has the genotype AA at the first locus and bb at the second. What is the posterior probability that our individual comes from the Western population versus Eastern chimp population?

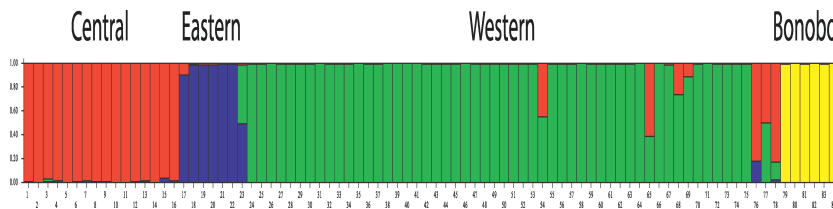
B) (Trickier) Lets assume that our individual from part A is a hybrid (not necessarily an F1). At each locus, with probability q_W our individual draws an allele from the Western population and with probability $q_E = 1 - q_W$ they draw an allele from the Eastern population. What is the probability of our individual's genotype given q_W ?

Optional You could plot this probability as a function of q_W . How does your plot change if our individual is heterozygous at both loci?

Clustering based on assignment methods While it is great to be able to assign our individuals to a particular population, these ideas can be pushed to learn about how best to describe our genotype data in terms of discrete populations without assigning any of our individuals to populations *a priori*. We wish to cluster our individuals into K unknown populations. We begin by assigning our individuals at random to these K populations.

1. Given these assignments we estimate the allele frequencies at all of our loci in each population.
2. Given these allele frequencies we chose to reassign each individual to a population k with a probability given by eqn. (3.10).

We iterate steps 1 and 2 for many iterations (technically, this approach is known as *Gibbs Sampling*). If the data is sufficiently informative, the assignments and allele frequencies will quickly converge on a set of likely population assignments and allele frequencies for these populations.



To do this in a full Bayesian scheme we need to place priors on the allele frequencies (for example, one could use a beta distribution prior). Technically we are using the joint posterior of our allele frequencies and assignments. Programs like STRUCTURE, use this type of algorithm to cluster the individuals in an “unsupervised” manner

Figure 3.4: BECQUET *et al.* (2007) genotyped 78 common chimpanzee and 6 bonobo at over 300 polymorphic markers (in this case microsatellites). They ran STRUCTURE to cluster the individuals using these data into $K = 4$ populations. In BECQUET *et al.* (2007) above figure they show each individual as a vertical bar divided into four colours depicting the estimate of the fraction of ancestry that each individual draws from each of the four estimated populations (licensed under CC BY 4.0). We can see that these four colours/populations correspond to: Red, central; blue, eastern; green, western; yellow, bonobo.

(i.e. they work out how to assign individuals to an unknown set of populations). See Figure 3.4 for an example of BECQUET *et al.* using STRUCTURE to determine the population structure of chimpanzees.

STRUCTURE-like methods have proven incredible popular and useful in examining population structure within species. However, the results of these methods are open to misinterpretation; see LAWSON *et al.* (2018) for a recent discussion. Two common mistakes are 1) taking the results of STRUCTURE-like approaches for some particular value of K and taking this to represent the best way to describe population-genetic variation. 2) Thinking that these clusters represent ‘pure’ ancestral populations.

There is no right choice of K, the number of clusters to partition into. There are methods of judging the ‘best’ K by some statistical measure given some particular dataset, but that is not the same as saying this is the most meaningful level on which to summarize population structure in data. For example, running STRUCTURE on world-wide human populations for low value of K will result in population clusters that roughly align with continental populations (ROSENBERG *et al.*, 2002). However, that does not tell us that assigning ancestry at the level of continents is a particularly meaningful way of partitioning individuals. Running the same data for higher value of K, or within continental regions, will result in much finer-scale partitioning of continental groups (ROSENBERG *et al.*, 2002; LI *et al.*, 2008). No one of these layers of population structure identified is privileged as being more meaningful than another.

It is tempting to think of these clusters as representing ancestral populations, which themselves are not the result of admixture. However, that is not the case, for example, running STRUCTURE on world-wide human data identifies a cluster that contains many European individuals, however, on the basis of ancient DNA we know that modern Europeans are a mixture of distinct ancestral groups.

3.0.4 Principal components analysis

Principal component analysis (PCA) is a common statistical approach to visualize high dimensional data, and used by many fields. The idea of PCA is to give a location to each individual data-point on each of a small number principal component axes. These PC axes are chosen to reflect major axes of variation in the data, with the first PC being that which explains largest variance, the second the second most, and so on. The use of PCA in population genetics was pioneered by Cavalli-Sforza and colleagues and now with large genotyping datasets, PCA has made a comeback.⁷

Consider a dataset consisting of N individuals at S biallelic SNPs.

⁷ MENOZZI, P., A. PIAZZA, and L. CAVALLI-SFORZA, 1978 Synthetic maps of human gene frequencies in Europeans. *Science* 201(4358): 786–792; and PATTERSON, N., A. L. PRICE, and D. REICH, 2006 Population structure and eigenanalysis. *PLoS genetics* 2(12): e190

The i^{th} individual's genotype data at locus ℓ takes a value $g_{i,\ell} = 0, 1$, or 2 (corresponding to the number of copies of allele A_1 an individual carries at this SNP). We can think of this as a $N \times S$ matrix (where usually $N \ll S$).

Denoting the sample mean allele frequency at SNP ℓ by p_ℓ , it's common to standardize the genotype in the following way

$$\frac{g_{i,\ell} - 2p_\ell}{\sqrt{2p_\ell(1 - p_\ell)}} \quad (3.14)$$

i.e. at each SNP we center the genotypes by subtracting the mean genotype ($2p_\ell$) and divide through by the square root of the expected variance assuming that alleles are sampled binomially from the mean frequency ($\sqrt{2p_\ell(1 - p_\ell)}$). Doing this to all of our genotypes, we form a data matrix (of dimension $N \times S$). We can then perform principal component analysis of this data matrix to uncover the major axes of genotype variance in our sample. Figure 3.5 shows a PCA from BECQUET *et al.* (2007) using the same chimpanzee data as in Figure 3.4.

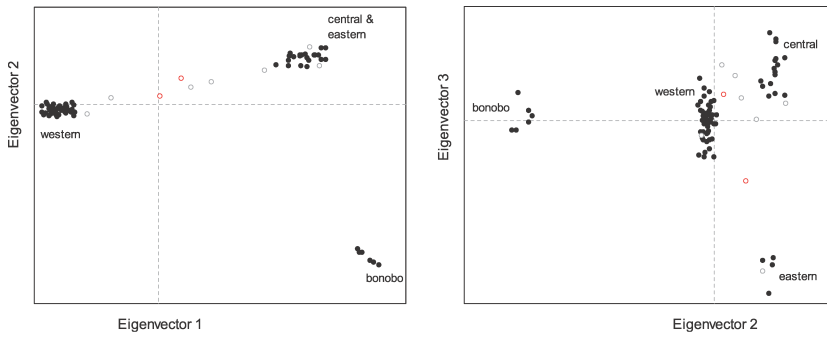


Figure 3.5: Principal Component Analysis by BECQUET *et al.* (2007) using the same chimpanzee data as in Figure 3.4. Here BECQUET *et al.* (2007) plot the location of each individual on the first two principal components (called eigenvectors) in the left panel, and on the second and third principal components (eigenvectors) in the right panel (licensed under CC BY 4.0). In the PCA, individuals identified as all of one ancestry by STRUCTURE cluster together by population (solid circles). While the nine individuals identified by STRUCTURE as hybrids (open circles) for the most part fall at intermediate locations in the PCA. There are two individuals (red open circles) reported as being of a particular population but that but appear to be hybrids.

It is worth taking a moment to delve further into what we are doing here. There's a number of equivalent ways of thinking about what PCA is doing. One of these ways is to think that when we do PCA we are building the individual by individual covariance matrix and performing an eigenvalue decomposition of this matrix (with the eigenvectors being the PCs). This individual by individual covariance matrix has entries $[i, j]$ given by

$$\frac{1}{S-1} \sum_{\ell=1}^S \frac{(g_{i,\ell} - 2p_\ell)(g_{j,\ell} - 2p_\ell)}{2p_\ell(1 - p_\ell)} \quad (3.15)$$

Note that this is the sample covariance, and is very similar to those we encountered in discussing F -statistics as correlations (equation (3.6)), except now we are asking about the covariance between two individuals above that expected if they were both drawn from the total sample at random (rather than the covariance of alleles within a

single individual). So by performing PCA on the data we are learning about the major (orthogonal) axes of the kinship matrix.

As an example of the application of PCA, let's consider the case of the putative ring species in the Greenish warbler (*Phylloscopus trochiloides*) species complex. This set of subspecies exists in a ring around the edge of the Himalayan plateau. ALCAIDE *et al.* (2014) collected 95 Greenish warbler samples from 22 sites around the ring, and the sampling locations are shown in Figure 3.6.

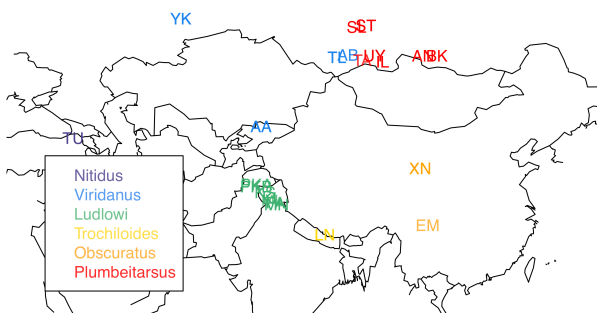


Figure 3.6: The sampling locations of 22 populations of Greenish warblers from ALCAIDE *et al.* (2014). The samples are coloured by the subspecies. Code here.

It is thought that these warblers spread from the south, northward in two different directions around the inhospitable Himalayan plateau, establishing populations along the western edge (green and blue populations) and the eastern edge (yellow and red populations). When they came into secondary contact in Siberia, they were reproductively isolated from one another, having evolved different songs and accumulated other reproductive barriers from each other as they spread independently north around the plateau, such that *P. t. viridanus* (blue) and *P. t. plumbeitarsus* (red) populations presently form a stable hybrid zone.

ALCAIDE *et al.* (2014) obtained sequence data for their samples at 2,334 snps. In Figure 3.8 you can see the matrix of kinship coefficients, using (3.15), between all pairs of samples. You can already see a lot about population structure in this matrix. Note how the red and yellow samples, thought to be derived from the Eastern route around the Himalayas, have higher kinship with each other, and blue and the (majority) of the green samples, from the Western route, form a similarly close group in terms of their higher kinship.

We can then perform PCA on this kinship matrix to identify the major axes of variation in the dataset. Figure 3.9 shows the samples plotted on the first two PCs. The two major routes of expansion clearly occupy different parts of PC space. The first principal com-



Figure 3.7: Greenish warbler, subspp. viridanus (*Phylloscopus trochiloides viridanus*). Coloured figures of the birds of the British Islands. 1885. Lilford T. L. P.. Image from the Biodiversity Heritage Library. Contributed by American Museum of Natural History Library. Not in copyright. (Greenish warblers are rare visitors to the UK.)

Montagu Beauvois, 1808
Phylloscopus viridanus. A. Gmel.
53

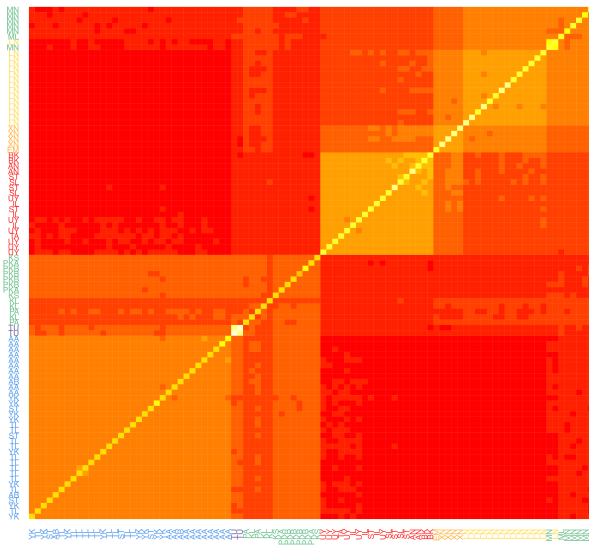


Figure 3.8: The matrix of kinship coefficients calculated for the 95 samples of Greenish warblers. Each cell in the matrix gives the pairwise kinship coefficient calculated for a particular pair. Hotter colours indicating higher kinship. The x and y labels of individuals are the population labels from Figure 3.6, and coloured by subspecies label as in that figure. The rows and columns have been organized to cluster individuals with high kinship. [Code here.](#)

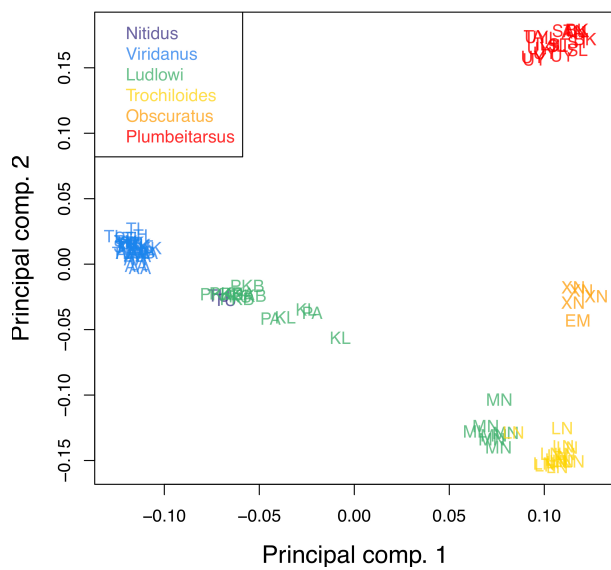


Figure 3.9: The 95 greenish warbler samples plotted on their locations on the first two principal components. The labels of individuals are the population labels from Figure 3.6, and coloured by subspecies label as in that figure. [Code here.](#)

ponent distinguishes populations running North to South along the western route of expansion, while the second principal component distinguishes among populations running North to South along the Eastern route of expansion. Thus genetic data supports the hypothesis that the Greenish warblers speciated as they moved around the Himalayan plateau. However, as noted by ALCAIDE *et al.* (2014), it also suggests additional complications to the traditional view of these warblers as an unbroken ring species, a case of speciation by continuous geographic isolation. The *Ludlowi* subspecies shows a significant genetic break, with the southern most MN samples clustering with the *Trochilooides* subspecies, in both the PCA and kinship matrix (Figures 3.9 and 3.8), despite being much more geographically close to the other *Ludlowi* samples. This suggests that genetic isolation is not just a result of geographic distance, and other biogeographic barriers must be considered in the case of this broken ring species.

Finally, while PCA is a wonderful tool for visualizing genetic data, care must be taken in its interpretation. The U-like shape in the case of the Greenish warbler PC might be consistent with some low level of gene flow between the red and the blue populations, pulling them genetically closer together and helping to form a genetic ring as well as a geographic ring. However, U-like shapes are expected to appear in PCAs even if our populations are just arrayed along a line, and more complex geometric arrangements of populations in PC space can result under simple geographic models (NOVEMBRE and STEPHENS, 2008). Inferring the geographical and population-genetic history of species requires the application of a range of tools; see ALCAIDE *et al.* (2014) and BRADBURD *et al.* (2016) for more discussion of the Greenish warblers.

3.0.5 Correlations between loci, linkage disequilibrium, and recombination

Up to now we have been interested in correlations between alleles at the same locus, e.g. correlations within individuals (inbreeding) or between individuals (relatedness). We have seen how relatedness between parents affects the extent to which their offspring is inbred. We now turn to correlations between alleles at different loci.

Recombination To understand correlations between loci we need to understand recombination a bit more carefully. Let us consider a heterozygous individual, containing AB and ab haplotypes. If no recombination occurs between our two loci in this individual, then these two haplotypes will be transmitted intact to the next generation. While if a recombination (i.e. an odd number of crossing over events) occurs between the two parental haplotypes, then $1/2$ the time the child receives an Ab haplotype and $1/2$ the time the child receives an aB haplotype. Effectively, recombination breaks up the association between loci. We'll define the recombination fraction (r) to be the probability of an odd number of crossing over events between our loci in a single meiosis. In practice we'll often be interested in relatively short regions such that recombination is relatively rare, and so we might think that $r = r_{BP}L \ll \frac{1}{2}$, where r_{BP} is the average recombination rate (in Morgans) per base pair (typically $\sim 10^{-8}$) and L is the number of base pairs separating our two loci.

Linkage disequilibrium The (horrible) phrase linkage disequilibrium (LD) refers to the statistical non-independence (i.e. a correlation) of alleles in a population at different loci. It's an awful name for a fantastically useful concept; LD is key to our understanding of diverse topics, from sexual selection and speciation to the limits of genome-wide association studies.

Our two biallelic loci, which segregate alleles A/a and B/b , have allele frequencies of p_A and p_B respectively. The frequency of the two locus haplotype AB is p_{AB} , and likewise for our other three combinations. If our loci were statistically independent then $p_{AB} = p_A p_B$, otherwise $p_{AB} \neq p_A p_B$. We can define a covariance between the A and B alleles at our two loci⁸ as

$$D_{AB} = p_{AB} - p_A p_B \quad (3.16)$$

and likewise for our other combinations at our two loci (D_{Ab} , D_{aB} , D_{ab}). Gametes with two similar case alleles (e.g. A and B, or a and b) are known as *coupling* gametes, and those with different case alleles are known as *repulsion* gametes (e.g. a and B, or A and b). Then,

⁸ Here again we are making use of a covariance of discrete random variables, see Appendix eqn (A.40), where the first variable is drawing haplotype with an A at the first locus, and the second is drawing a B allele at the other locus.

we can think of D as measuring the *excess* of coupling to repulsion gametes. These D statistics are all closely related to each other as $D_{AB} = -D_{Ab}$ and so on. Thus we only need to specify one D_{AB} to know them all, so we'll drop the subscript and just refer to D . Also a handy result is that we can rewrite our haplotype frequency p_{AB} as

$$p_{AB} = p_A p_B + D. \quad (3.17)$$

If $D = 0$ we'll say the two loci are in linkage equilibrium, while if $D > 0$ or $D < 0$ we'll say that the loci are in linkage disequilibrium (we'll perhaps want to test whether D is statistically different from 0 before making this choice). You should be careful to keep the concepts of linkage and linkage disequilibrium separate in your mind. Genetic linkage refers to the linkage of multiple loci due to the fact that they are transmitted through meiosis together (most often because the loci are on the same chromosome). Linkage disequilibrium merely refers to the covariance between the alleles at different loci; this may in part be due to the genetic linkage of these loci but does not necessarily imply this (e.g. genetically unlinked loci can be in LD due to population structure).

i

Question 3. You genotype 2 bi-allelic loci (A & B) segregating in two mouse subspecies (1 & 2) which mate randomly among themselves, but have not historically interbreed since they speciated. On the basis of previous work you estimate that the two loci are separated by a recombination fraction of 0.1. The frequencies of haplotypes in each population are:

Pop	p_{AB}	p_{Ab}	p_{aB}	p_{ab}
1	.02	.18	.08	.72
2	.72	.18	.08	.02

- A)** How much LD is there within species? (i.e. estimate D)
B) If we mixed individuals from the two species together in equal proportions, we could form a new population with p_{AB} equal to the average frequency of p_{AB} across species 1 and 2. What value would D take in this new population before any mating has had the chance to occur?

Our linkage disequilibrium statistic D depends strongly on the allele frequencies of the two loci involved. One common way to partially remove this dependence, and make it more comparable across loci, is to divide D through by its maximum possible value given the frequency of the loci. This normalized statistic is called D' and varies between +1 and -1. In Figure 3.10 there's an example of LD across the TAP2 region in human and chimp. Notice how physically close SNPs,

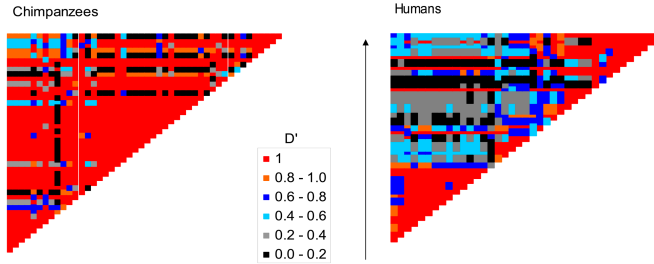


Figure 3.10: LD across the TAP2 gene region in a sample of Humans and Chimps, from PTAK *et al.* (2004), licensed under CC BY 4.0. The rows and columns are consecutive SNPs, with each cell giving the absolute D' value between a pair of SNPs. Note that these are different sets of SNPs in the two species, as shared polymorphisms are very rare.

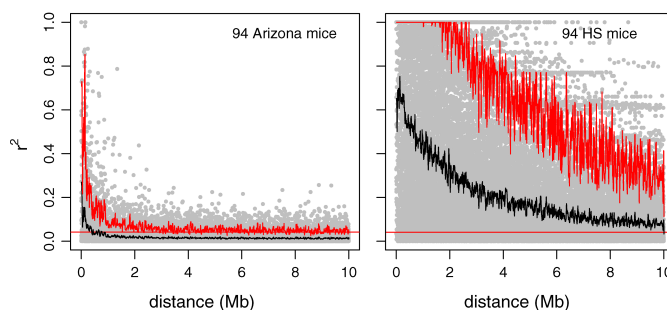
i.e. those close to the diagonal, have higher absolute values of D' as closely linked alleles are separated by recombination less often allowing high levels of LD to accumulate. Over large physical distances, away from the diagonal, there is lower D' . This is especially notable in humans as there is an intense, human-specific recombination hotspot in this region, which is breaking down LD between opposite sides of this region.

Another common statistic for summarizing LD is r^2 which we write as

$$r^2 = \frac{D^2}{p_A(1-p_A)p_B(1-p_B)} \quad (3.18)$$

As D is a covariance, and $p_A(1-p_A)$ is the variance of an allele drawn at random from locus A , r^2 is the squared correlation coefficient.⁹ Note that this r in r^2 is NOT the recombination fraction.

Figure 3.12 shows r^2 for pairs of SNPs at various physical distances in two population samples of *Mus musculus domesticus*. Again LD is highest between physically close markers as LD is being generated faster than it can decay via recombination; more distant markers have much lower LD as here recombination is winning out. Note the decay of LD is much slower in the advanced-generation cross population than in the natural wild-caught population. This persistence of LD across megabases is due to the limited number of generations for recombination since the cross was created.



⁹ See Appendix eqn (A.42) for the definition of a correlation coefficient.

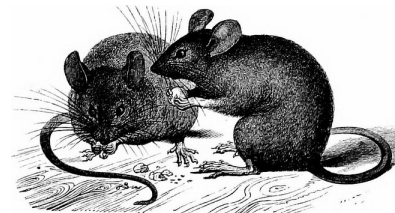


Figure 3.11: *Mus musculus*. A history of British quadrupeds, including the Cetacea. 1874. Bell T., Tomes, R. F m Alston E. R. Image from the Biodiversity Heritage Library. Contributed by Cornell University Library. No known copyright restrictions.

Figure 3.12: The decay of LD for autosomal SNPs in *Mus musculus domesticus*, as measured by r^2 , in a wild-caught mouse population from Arizona and a set of advanced-generation crosses between inbred lines of lab mice. Each dot gives the r^2 for a pair of SNPs a given physical distance apart, for a total of ~ 3000 SNPs. The solid black line gives the mean, the jagged red line the 95th percentile, and the flat red line a cutoff for significant LD. From LAURIE *et al.* (2007), licensed under CC BY 4.0.

The generation of LD. Various population genetic forces can generate LD. Selection can generate LD by favouring particular combinations of alleles. Genetic drift will also generate LD, not because particular combinations of alleles are favoured, but simply because at random particular haplotypes can by chance drift up in frequency. Mixing between divergent populations can also generate LD, as we saw in the mouse question above.

The decay of LD due to recombination We will now examine what happens to LD over the generations if, in a very large population (i.e. no genetic drift and frequencies of our loci thus follow their expectations), we only allow recombination to occur. To do so, consider the frequency of our AB haplotype in the next generation, p'_{AB} . We lose a fraction r of our AB haplotypes to recombination ripping our alleles apart but gain a fraction $rp_{AP}p_B$ per generation from other haplotypes recombining together to form AB haplotypes. Thus in the next generation

$$p'_{AB} = (1 - r)p_{AB} + rp_{AP}p_B \quad (3.19)$$

The last term above, in eqn 3.19, is $r(p_{AB} + p_{Ab})(p_{AB} + p_{aB})$ simplified, which is the probability of recombination in the different diploid genotypes that could generate a p_{AB} haplotype.

We can then write the change in the frequency of the p_{AB} haplotype as

$$\Delta p_{AB} = p'_{AB} - p_{AB} = -rp_{AB} + rp_{AP}p_B = -rD \quad (3.20)$$

So recombination will cause a decrease in the frequency of p_{AB} if there is an excess of AB haplotypes within the population ($D > 0$), and an increase if there is a deficit of AB haplotypes within the population ($D < 0$). Our LD in the next generation is

$$\begin{aligned} D' &= p'_{AB} - p'_{AP}p'_B \\ &= (p_{AB} + \Delta p_{AB}) - (p_A + \Delta p_A)(p_B + \Delta p_B) \\ &= p_{AB} + \Delta p_{AB} - p_{AP}p_B \\ &= (1 - r)D \end{aligned} \quad (3.21)$$

where we can cancel out Δp_A and Δp_B above because recombination only changes haplotype, not allele, frequencies. So if the level of LD in generation 0 is D_0 , the level t generations later (D_t) is

$$D_t = (1 - r)^t D_0 \quad (3.22)$$

Recombination is acting to decrease LD, and it does so geometrically at a rate given by $(1 - r)$. If $r \ll 1$ then we can approximate this by an exponential and say that

$$D_t \approx D_0 e^{-rt} \quad (3.23)$$

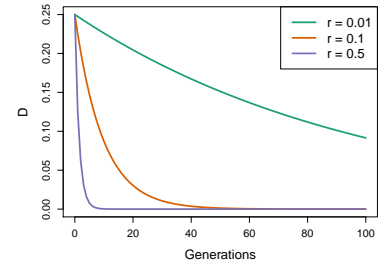


Figure 3.13: The decay of LD from an initial value of $D_0 = 0.25$ over time (Generations) for a pair of loci a recombination fraction r apart. Code here.

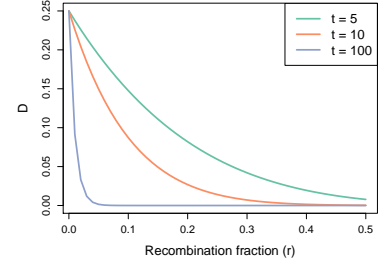
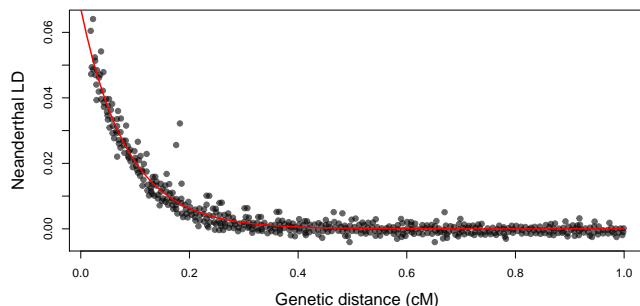


Figure 3.14: The decay of LD from an initial value of $D_0 = 0.25$ due to recombination over t generations, plotted across possible recombination fractions (r) between our pair of loci. Code here.

Question 4. You find a hybrid population between the two mouse subspecies described in the question above, which appears to be comprised of equal proportions of ancestry from the two subspecies. You estimate LD between the two markers to be 0.0723. Assuming that this hybrid population is large and was formed by a single mixture event, can you estimate how long ago this population formed?

A particularly striking example of the decay of LD generated by the mixing of populations is offered by the LD created by the interbreeding between humans and Neanderthals. Neanderthals and modern Humans diverged from each other likely over half a million years ago, allowing time for allele frequency differences to accumulate between the Neanderthal and modern human populations. The two populations spread back into secondary contact when humans moved out of Africa over the past hundred thousand years or so. One of the most exciting findings from the sequencing of the Neanderthal genome was that modern-day people with Eurasian ancestry carry a few percent of their genome derived from the Neanderthal genome, via interbreeding during this secondary contact. To date the timing of this interbreeding, SANKARARAMAN *et al.* (2012) looked at the LD in modern humans between pairs of alleles found to be derived from the Neanderthal genome (and nearly absent from African populations). In Figure 3.16 we show the average LD between these loci as a function of the genetic distance (r) between them, from the work of SANKARARAMAN *et al.*.



Assuming a recombination rate r , we can fit the exponential decay of LD predicted by eqn. (3.23) to the data points in this figure; the fit is shown as a red line. Doing this we estimate $t = 1200$ generations, or about 35 thousand years (using a human generation time of 29 years). Thus the LD in modern Eurasians, between alleles derived from the interbreeding with Neanderthals, represents over thirty thousand years of recombination slowly breaking down these old associations.¹⁰

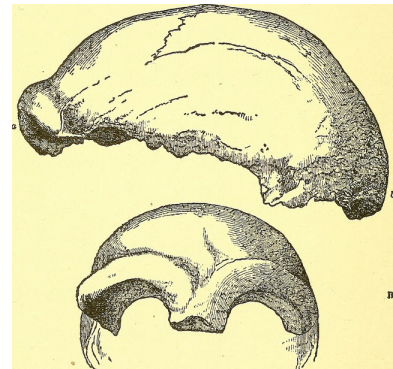


Figure 3.15: The earliest discovered fossil of a Neanderthal, fragments of skull found in a cave in the Neander Valley in Germany.
Man's place in nature. 1890. Huxley, T. H.
Image from the Internet Archive. Contributed by The Library of Congress. No known copyright restrictions.

Figure 3.16: The LD between putative-Neanderthal alleles in a modern European population (the CEU sample from the 1000 Genomes Project). Each point represents the average D statistic between a pair of alleles at a given genetic distance apart (as given on the x-axis and measured in centiMorgans (cM)). The putative Neanderthal alleles are alleles where the Neanderthal genome has a derived allele that is at very low frequency in a modern-human West African population sample (thought to have little admixture from Neanderthals). The red line is the fit of an exponential decay of LD, using non-linear least squared (nls in R).

¹⁰ The calculation done by SANKARARAMAN *et al.* (2012) is actually a bit more involved as they account for inhomogeneity in recombination rates and arrive at a date of 47,334 – 63,146 years.

4

Genetic Drift and Neutral Diversity

RANDOMNESS IS INHERENT TO EVOLUTION, from the lucky birds blown of course to colonize some new oceanic island, to which mutations arise first in the HIV strain infecting an individual taking anti-retroviral drugs. One major source of stochasticity in evolutionary biology is genetic drift. Genetic drift occurs because more or less copies of an allele by chance can be transmitted to the next generation. This can occur because, by chance, the individuals carrying a particular allele can leave more or less offspring in the next generation. In a sexual population, genetic drift also occurs because Mendelian transmission means that only one of the two alleles in an individual, chosen at random at a locus, is transmitted to the offspring.

Genetic drift can play a role in the dynamics of all alleles in all populations, but it will play the biggest role for neutral alleles. A neutral polymorphism occurs when the segregating alleles at a polymorphic site have no discernible differences in their effect on fitness. We'll make clear what we mean by "discernible" later, but for the moment think of this as "no effect" on fitness.

The neutral theory of molecular evolution. The role of genetic drift in molecular evolution has been hotly debated since the 60s when the Neutral theory of molecular evolution was proposed (see OHTA and GILLESPIE, 1996, for a history)¹. The central premise of Neutral theory theory is that patterns of molecular polymorphism within species and substitution between species can be well understood by supposing that the vast majority of these molecular polymorphisms and substitutions were neutral alleles, whose dynamics were just subject to the vagaries of genetic drift and mutation. Early proponents of this view suggested that the vast majority of new mutations are either neutral or highly deleterious (e.g. mutations that disrupt important protein functions). This latter class of mutations are too deleterious to contribute much to common polymorphisms or substitutions be-

¹ KIMURA, M., 1968 Evolutionary rate at the molecular level. *Nature* *217*(5129): 624–626; KING, J. L. and T. H. JUKES, 1969 Non-darwinian evolution. *Science* *164*(3881): 788–798; and KIMURA, M., 1983 *The neutral theory of molecular evolution*. Cambridge University Press

tween species, because they are quickly weeded out of the population by selection.

Neutral theory can sound strange given that much of the time our first brush with evolution often focuses on adaptation and phenotypic evolution. However, proponents of this world-view didn't deny the existence of advantageous mutations, they simply thought that beneficial mutations are rare enough that their contribution to the bulk of polymorphism or divergence can be largely ignored. They also often thought that much of phenotypic evolution may well be adaptive, but again the loci responsible for these phenotypes are a small fraction of all the molecular change that occur. The neutral theory of molecular evolution was originally proposed to explain protein polymorphism. However, we can apply it more broadly to think about neutral evolution genome-wide. With that in mind, what types of molecular changes could be neutral? Perhaps:

1. Changes in non-coding DNA that don't disrupt regulatory sequences. For example, in the human genome only about 2% of the genome codes for proteins. The rest is mostly made up of old transposable element and retrovirus insertions, repeats, pseudo-genes, and general genomic clutter. Current estimates suggest that, even counting conserved, functional, non-coding regions, less than 10% of our genome is subject to evolutionary constraint (RANDS *et al.*, 2014).
2. Synonymous changes in coding regions, i.e. those that don't change the amino-acid encoded by a codon.
3. Non-synonymous changes that don't have a strong effect on the functional properties of the amino acid encoded, e.g. changes that don't change the size, charge, or hydrophobic properties of the amino acid too much.
4. An amino-acid change with phenotypic consequences, but little relevance to fitness, e.g. a mutation that causes your ears to be a slightly different shape, or that prevents an organism from living past 50 in a species where most individuals reproduce and die by their 20s.

There are counter examples to all of these ideas, e.g. synonymous changes can affect the translation speed and accuracy of proteins and so are subject to selection. However, the list above hopefully convinces you that the general thinking that some portion of molecular change may not be subject to selection isn't as daft as it may have initially sounded.

Various features of molecular polymorphism and divergence have been viewed as consistent with the neutral theory of molecular evo-

lution. The two we'll focus on in this chapter are the high level of molecular polymorphism in many species (see for example Figure 2.3) and the molecular clock. We'll see that various aspects of the original neutral theory have merit in describing some features and types of molecular change, but we'll also see that it is demonstrably wrong in some cases. We'll also see the primary utility of the neutral theory isn't whether it is right or wrong, but that it serves as a simple null model that can be tested and in some cases rejected, and subsequently built on. The broader debate currently in the field of molecular evolution is the balance of neutral, adaptive, and deleterious changes that drive different types of evolutionary change.

4.1 Loss of heterozygosity due to drift.

Genetic drift will, in the absence of new mutations, slowly purge our population of neutral genetic diversity, as alleles slowly drift to high or low frequencies and are lost or fixed over time.

Imagine a randomly mating population of a constant size N diploid individuals, and that we are examining a locus segregating for two alleles that are neutral with respect to each other. This population is randomly mating with respect to the alleles at this locus. See Figures 4.1 and 4.2 to see how genetic drift proceeds, by tracking alleles within a small population.

In generation t our current level of heterozygosity is H_t , i.e. the probability that two randomly sampled alleles in generation t are non-identical is H_t . Assuming that the mutation rate is zero (or vanishingly small), what is our level of heterozygosity in generation $t + 1$?

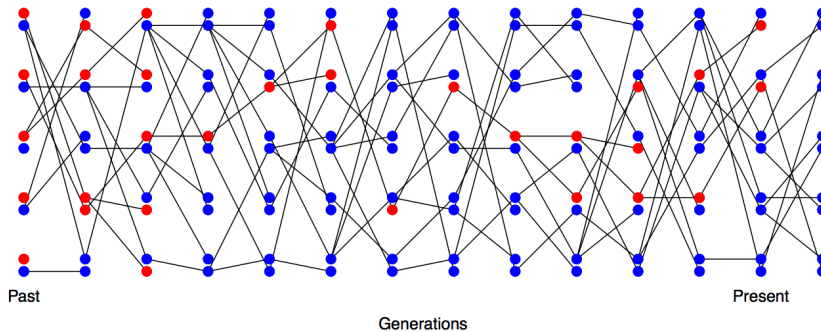


Figure 4.1: Loss of heterozygosity over time, in the absence of new mutations. A diploid population of 5 individuals over the generations, with lines showing transmission. In the first generation every individual is a heterozygote. Code here.

In the next generation ($t + 1$) we are looking at the alleles in the offspring of generation t . If we randomly sample two alleles in generation $t + 1$ which had different parental alleles in generation t , that is just like drawing two random alleles from generation t . So the probability that these two alleles in generation $t + 1$, that have different parental

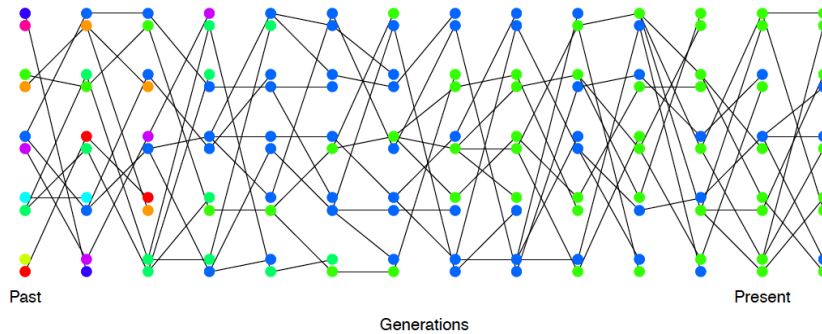


Figure 4.2: Loss of heterozygosity over time, in the absence of new mutations. A diploid population of 5 individuals. In the first generation I colour every allele a different colour so we can track their descendants. Code here.

alleles in generation t , are non-identical is H_t .

Conversely, if the two alleles in our pair had the same parental allele in the proceeding generation (i.e. the alleles are identical by descent one generation back) then these two alleles must be identical (as we are not allowing for any mutation).

In a diploid population of size N individuals there are $2N$ alleles. The probability that our two alleles have the same parental allele in the proceeding generation is $1/(2N)$ and the probability that they have different parental alleles is $1 - 1/(2N)$. So by the above argument, the expected heterozygosity in generation $t + 1$ is

$$H_{t+1} = \frac{1}{2N} \times 0 + \left(1 - \frac{1}{2N}\right) H_t \quad (4.1)$$

Thus, if the heterozygosity in generation 0 is H_0 , our expected heterozygosity in generation t is

$$H_t = \left(1 - \frac{1}{2N}\right)^t H_0 \quad (4.2)$$

i.e. the expected heterozygosity within our population is decaying geometrically with each passing generation. If we assume that $1/(2N) \ll 1$ then we can approximate this geometric decay by an exponential decay (see Question 2 below), such that

$$H_t = H_0 e^{-t/(2N)} \quad (4.3)$$

i.e. heterozygosity decays exponentially at a rate $1/(2N)$.

In Figure 4.3 we show trajectories through time for 40 independently simulated loci drifting in a population of 50 individuals. Each population was started from a frequency of 30%. Some drift up and some drift down, eventually being lost or fixed from the population, but, on average across simulations, the allele frequency doesn't change. We also track heterozygosity, you can see that heterozygosity sometimes goes up, and sometimes goes down, but on average we are losing heterozygosity, and this rate of loss is well predicted by eqn. (4.2).

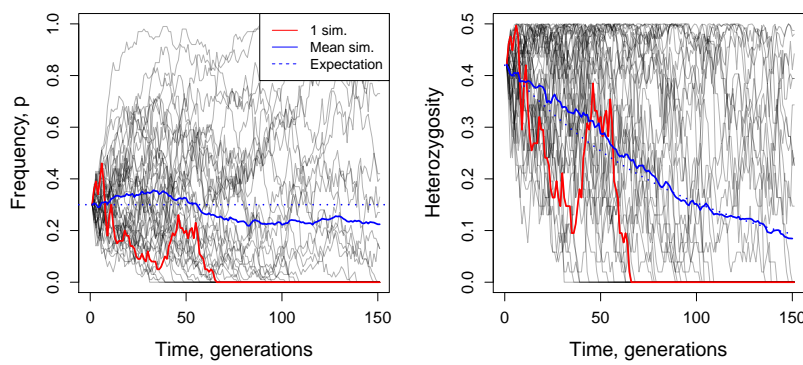


Figure 4.3: Change in allele frequency and loss of heterozygosity over time for 40 replicates. Simulations of genetic drift in a diploid population of 50 individuals, in the absence of new mutations. We start 40 independent, biallelic loci each with an initial allele at 30% frequency. The left panel shows the allele frequency over time and the right panel shows the heterozygosity over time, with the mean decay matching eqn. (4.2). Code here.

Question 1. You are in charge of maintaining a population of delta smelt in the Sacramento river delta. Using a large set of microsatellites you estimate that the mean level of heterozygosity in this population is 0.005. You set yourself a goal of maintaining a level of heterozygosity of at least 0.0049 for the next two hundred years. Assuming that the smelt have a generation time of 3 years, and that only genetic drift affects these loci, what is the smallest fully outbreeding population that you would need to maintain to meet this goal?

Note how this picture of decreasing heterozygosity stands in contrast to the consistency of Hardy-Weinberg equilibrium from the previous chapter. However, our Hardy-Weinberg *proportions* still hold in forming each new generation. As the offspring genotypes in the next generation ($t + 1$) represent a random draw from the previous generation (t), if the parental frequency is p_t , we *expect* a proportion $2p_t(1 - p_t)$ of our offspring to be heterozygotes (and HW proportions for our homozygotes). However, because population size is finite, the observed genotype frequencies in the offspring will (likely) not match exactly with our expectations. As our genotype frequencies likely change slightly due to sampling, biologically this reflects random variation in family size and Mendelian segregation, the allele frequency will change. Therefore, while each generation represents a sample from Hardy-Weinberg proportions based on the generation before, our genotype proportions are not at an equilibrium (an unchanging state) as the underlying allele frequency changes over the generations. We'll develop some mathematical models for these allele frequency changes later on. For now, we'll simply note that under our simple model of drift (formally the Wright-Fisher model), our allele count in the $t + 1^{th}$ generation represents a binomial sample (of size $2N$) from the popu-

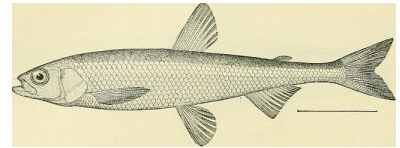


Figure 4.4: Pond smelt (*Hypomesus olidus*), a close relative of delta smelt. Bulletin of the United States Fish Commission, 1906. Image from the Biodiversity Heritage Library. Contributed by Smithsonian Libraries. Not in copyright.

lation frequency p_t in the previous generation. If you've read to here, please email Prof Coop a picture of JBS Haldane in a striped suit with the title "I'm reading the chapter 3 notes". (It's well worth googling JBS Haldane and to read more about his life; he's a true character and one of the last great polymaths.)

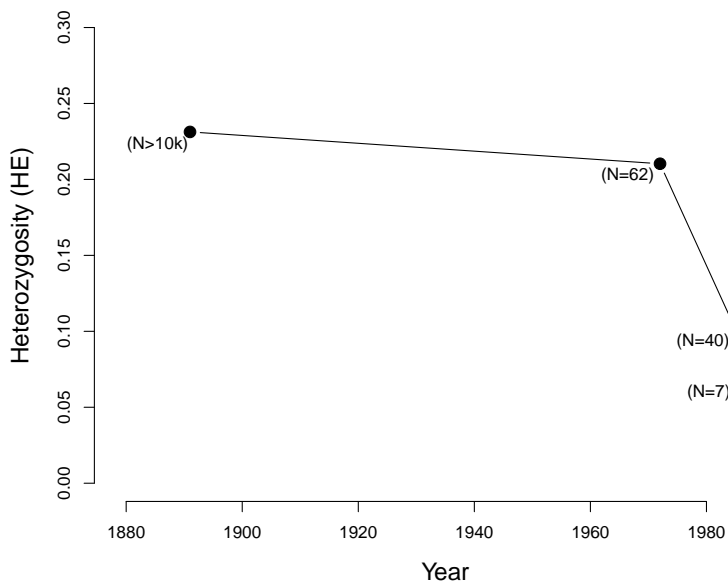


Figure 4.6: Loss of heterozygosity in the Black-footed Ferrets in their declining population. Numbers in brackets give estimated number of individuals alive at that time. Data from WISELY *et al.* (2002). Code here.



Figure 4.5: The black-footed ferret (*M. nigripes*).
Wild animals of North America. The National geographical society, 1918. Image from the Biodiversity Heritage Library. Contributed by American Museum of Natural History Library. Not in copyright.

To see how a decline in population size can affect levels of heterozygosity, let's consider the case of black-footed ferrets (*Mustela nigripes*). The black-footed ferret population has declined dramatically through the twentieth century due to destruction of their habitat. In 1979, when the last known black-footed ferret died in captivity, they were thought to be extinct. In 1981, a very small wild population was rediscovered (40 individuals), but in 1985 this population suffered a number of disease outbreaks. All of the 18 remaining wild individuals were brought into captivity, 7 of which reproduced. Thanks to intense captive breeding efforts and conservation work, a wild population of over 300 individuals has been established since. However, because all of these individuals are descended from those 7 individuals who survived the bottleneck, diversity levels remain low. WISELY *et al.* measured heterozygosity at a number of microsatellites in individuals from museum collections, showing the sharp drop in diversity as population sizes crashed (see Figure 4.6).

Question 2. In mathematical population genetics, a commonly used approximation is $(1 - x) \approx e^{-x}$ for $x \ll 1$ (formally, this

follows from the Taylor series expansion of $\exp(-x)$, ignoring second order and higher terms of x). This approximation is especially useful for approximating a geometric decay process by an exponential decay process, e.g. $(1 - x)^t \approx e^{-xt}$. Using your calculator, or R, check how good of an approximation this is compared to the exact expression for two values of x , $x = 0.1$, and 0.01 , across two different values of t , $t = 5$ and $t = 50$. Briefly comment on your results.

4.1.1 Levels of diversity maintained by a balance between mutation and drift

Next we're going to consider the amount of neutral polymorphism that can be maintained in a population as a balance between genetic drift removing variation and mutation introducing new neutral variation, see Figure 4.7 for an example. Note in our example, how no single allele is maintained at a stable equilibrium, rather an equilibrium level of polymorphism is maintained by a constantly shifting set of alleles.

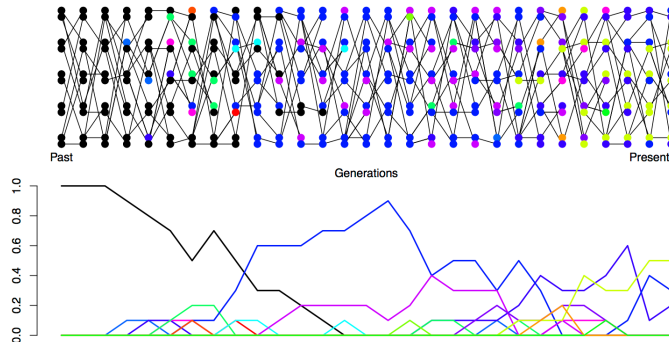


Figure 4.7: Mutation-drift balance. A diploid population of 5 individuals. In the first generation everyone has the same allele (black). Each generation the transmitted allele can mutate and we generate a new colour. In the bottom plot, I trace the frequency of alleles in our population over time. The mutation rate we use is very high, simply to maintain diversity in this small population. Code here.

The neutral mutation rate. We'll first want to consider the rate at which neutral mutations arise in the population. Thinking back to our discussion of the neutral theory of molecular evolution, let's suppose that there are only two classes of mutation that can arise in our genomic region of interest: neutral mutations and highly deleterious mutations. The total mutation rate at our locus is μ per generation, i.e. per transmission from parent to child. A fraction C of our mutations are new alleles that are highly deleterious and so quickly removed from the population. We'll call this C parameter the constraint, and it will differ according to the genomic region we consider. The remaining fraction $(1 - C)$ are our neutral mutations, such that our neutral mutation rate is $(1 - C)\mu$. This is the per generation rate.

Question 3. It's worth taking a minute to get familiar with both how rare, and how common, mutation is. The per base pair mutation

rate in humans is around 1.5×10^{-8} per generation. That means, on average, we have to monitor a site for ~ 66.6 million transmissions from parent to child to see a mutation. Yet populations and genomes are big places, so mutations are common at these levels.

A) Your autosomal genome is ~ 3 billion base pairs long (3×10^9). You have two copies, the one you received from your mum and one from your dad. What is the average (i.e. the expected) number of mutations that occurred in the transmission from your mum and your dad to you?

B) The current human population size is ~ 7 billion individuals. How many times, at the level of the entire human population, is a single base-pair mutated in the transmission from one generation to the next?

Levels of heterozygosity maintained as a balance between mutation and drift. Looking backwards in time from one generation to the previous generation, we are going to say that two alleles which have the same parental allele (i.e. find their common ancestor) in the preceding generation have *coalesced*, and refer to this event as a *coalescent event*.

The probability that our pair of randomly sampled alleles have coalesced in the preceding generation is $1/(2N)$, and the probability that our pair of alleles fail to coalesce is $1 - 1/(2N)$.

The probability that a mutation changes the identity of the transmitted allele is μ per generation. So the probability of no mutation occurring is $(1 - \mu)$. We'll assume that when a mutation occurs it creates some new allelic type which is not present in the population. This assumption (commonly called the infinitely-many-alleles model) makes the math slightly cleaner, and also is not too bad an assumption biologically. See Figure 4.7 for a depiction of mutation-drift balance in this model over the generations.

This model lets us calculate when our two alleles last shared a common ancestor and whether these alleles are identical as a result of failing to mutate since this shared ancestor. For example, we can work out the probability that our two randomly sampled alleles coalesce 2 generations in the past (i.e. they fail to coalesce in generation 1 and then coalesce in generation 2), and that they are identical as

$$\left(1 - \frac{1}{2N}\right) \frac{1}{2N} (1 - \mu)^4 \quad (4.4)$$

Note the power of 4 is because our two alleles have to have failed to mutate through 2 meioses each.

More generally, the probability that our alleles coalesce in generation $t + 1$ (counting backwards in time) and are identical due to no

mutation to either allele in the subsequent generations is

$$P(\text{coal. in } t+1 \& \text{ no mutations}) = \frac{1}{2N} \left(1 - \frac{1}{2N}\right)^t (1 - \mu)^{2(t+1)} \quad (4.5)$$

To make this slightly easier on ourselves let's further assume that $t \approx t + 1$ and so rewrite this as:

$$P(\text{coal. in } t+1 \& \text{ no mutations}) \approx \frac{1}{2N} \left(1 - \frac{1}{2N}\right)^t (1 - \mu)^{2t} \quad (4.6)$$

This gives us the approximate probability that two alleles will coalesce in the $(t + 1)^{\text{th}}$ generation. In general, we may not know when two alleles may coalesce: they could coalesce in generation $t = 1, t = 2, \dots$, and so on. Thus, to calculate the probability that two alleles coalesce in *any* generation before mutating, we can write:

$$\begin{aligned} P(\text{coal. in any generation} \& \text{ no mutations}) &\approx P(\text{coal. in } t = 1 \& \text{ no mutations}) + \\ &\quad P(\text{coal. in } t = 2 \& \text{ no mutations}) + \dots \\ &= \sum_{t=1}^{\infty} P(\text{coal. in } t \text{ generations} \& \text{ no mutation}) \end{aligned} \quad (4.7)$$

an example of using the Law of Total Probability, see Appendix eqn (A.12), combined with the fact that coalescing in a particular generation is mutually exclusive with coalescing in a different generation.

While we could calculate a value for this sum given N and μ , it's difficult to get a sense of what's going on with such a complicated expression. Here, we turn to a common approximation in population genetics (and all applied mathematics), where we assume that $1/(2N) \ll 1$ and $\mu \ll 1$. This allows us to approximate the geometric decay as an exponential decay (see Appendix eqn (A.2)). Then, the probability two alleles coalesce in generation $t + 1$ and don't mutate can be written as:

$$P(\text{coal. in } t+1 \& \text{ no mutations}) \approx \frac{1}{2N} \left(1 - \frac{1}{2N}\right)^t (1 - \mu)^{2t} \quad (4.8)$$

$$\approx \frac{1}{2N} e^{-t/(2N)} e^{-2\mu t} \quad (4.9)$$

$$= \frac{1}{2N} e^{-t(2\mu+1/(2N))} \quad (4.10)$$

Then we can approximate the summation by an integral, giving us:

$$\frac{1}{2N} \int_0^{\infty} e^{-t(2\mu+1/(2N))} dt = \frac{1/(2N)}{1/(2N) + 2\mu} = \frac{1}{1 + 4N\mu} \quad (4.11)$$

The equation above gives us the probability that our two alleles coalesce at some point in time, and do not mutate before reaching

their common ancestor. Equivalently, this can be thought of as the probability our two alleles coalesce *before* mutating, i.e. that they are homozygous.

Then, the complementary probability that our pair of alleles are non-identical (or heterozygous) is simply one minus this. The following equation gives the equilibrium heterozygosity in a population at equilibrium between mutation and drift:

$$H = \frac{4N\mu}{1 + 4N\mu} \quad (4.12)$$

The compound parameter $4N\mu$, the population-scaled mutation rate, will come up a number of times so we'll give it its own name:

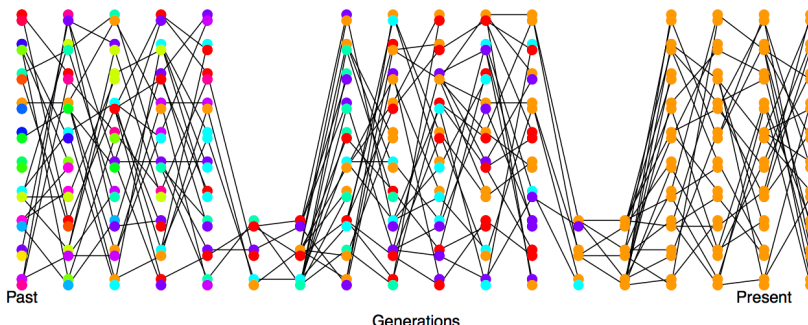
$$\theta = 4N\mu \quad (4.13)$$

So all else being equal, species with larger population sizes should have proportionally higher levels of neutral polymorphism.

Question 4. The sequence-level heterozygosity in *Capsella grandiflora* (grand shepherd's purse) is $\sim 2\%$ per base. Assuming a mutation rate of $10^{-9} bp^{-1}$ per generation, what is your estimate of the population size of *C. grandiflora*?

4.1.2 The effective population size

In practice, populations rarely conform to our assumptions of being constant in size with low variance in reproductive success. Real populations experience dramatic fluctuations in size, and there is often high variance in reproductive success. Thus rates of drift in natural populations are often a lot higher than the census population size would imply. See Figure 4.8 for a depiction of a repeatedly bottlenecked population losing diversity at a fast rate.



This result was derived by KIMURA and CROW (1964) and MALÉCOT (1948) (see MALÉCOT, 1969, for an English translation, the lack of earlier translation meant this result was missed). Technically we're assuming that every new mutation creates a new allele, the so-called "infinitely many alleles" model, otherwise our pair of sequences could be identical due to repeat or back mutation. See this GENETICS blog post and EWENS (2016) for a nice discussion of the history.

the effective population size (N_e) is the population size that would result in the same rate of drift in an idealized population of constant size (following our modeling assumptions) as that observed in our true population .

Figure 4.8: Loss of heterozygosity over time in a bottlenecking population. A diploid population of 10 individuals, that bottlenecks down to three individuals repeatedly. In the first generation, I colour every allele a different colour so we can track their descendants. There are no new mutations. Code here.

To cope with this discrepancy, population geneticists often invoke the concept of an *effective population size* (N_e). In many situations

(but not all), departures from model assumptions can be captured by substituting N_e for N .

If population sizes vary rapidly in size, we can (if certain conditions are met) replace our population size by the harmonic mean population size. Consider a diploid population of variable size, whose size is N_t t generations into the past. The probability our pairs of alleles have not coalesced by generation t is given by

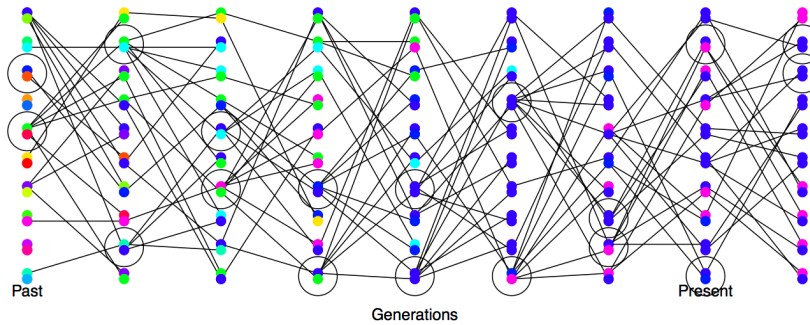
$$\prod_{i=1}^t \left(1 - \frac{1}{2N_i}\right) \quad (4.14)$$

Note that this simply collapses to our original expression $\left(1 - \frac{1}{2N}\right)^t$ if N_i is constant. Under this model, the rate of loss of heterozygosity in this population is equivalent to a population of effective size

$$N_e = \frac{1}{\frac{1}{t} \sum_{i=1}^t \frac{1}{N_i}}. \quad (4.15)$$

This is the harmonic mean of the varying population size.²

Thus our effective population size, the size of an idealized constant population which matches the rate of genetic drift, is the harmonic mean true population size over time. The harmonic mean is very strongly affected by small values, such that if our population size is one million 99% of the time but drops to 1000 every hundred or so generations, N_e will be much closer to 1000 than a million.



Variance in reproductive success will also affect our effective population size. Even if our population has a large constant size N individuals, if only small proportion of them get to reproduce, then the rate of drift will reflect this much smaller number of reproducing individuals. See Figure 4.9 for a depiction of the higher rate of drift in a population where there is high variance in reproductive success.

To see one example of this, consider the case where N_F of females get to reproduce and N_M males get reproduce. While every individual has a mother and a father, not every individual gets to be a parent. In

² To see this, note that if $1/(N_i)$ is small, then we can approximate (4.14) using the exponential approximation:

$$\prod_{i=1}^t \exp\left(-\frac{1}{2N_i}\right) = \exp\left(-\sum_{i=1}^t \frac{1}{2N_i}\right). \quad (4.16)$$

When we put the product inside the exponent, it becomes a sum. We can also write the probability of not coalescing by generation t in a population of constant size (N_e) as an exponential, so that it takes the same form as the expression above on the right. Comparing the exponent in the two cases, we see

$$\frac{t}{2N_e} = \sum_{i=1}^t 1/(2N_i) \quad (4.17)$$

So that if we want a constant effective population size (N_e) that has the same rate of loss of heterozygosity as our variable population, we need to rearrange and solve this equation to give (4.15).

Figure 4.9: High variance on reproductive success increases the rate of genetic drift. A diploid population of 10 individuals, where the circled individuals have much higher reproductive success. In the first generation I colour every allele a different colour so we can track their descendants, there are no new mutations. Code here.

practice, in many animal species far more females get to reproduce than males, i.e. $N_M < N_F$, as a few males get many mating opportunities and many males get no/few mating opportunities (see JANICKE *et al.*, 2016, for a broad analysis, and note that there are certainly many exceptions to this general pattern). When our two alleles pick an ancestor, 25% of the time our alleles were both in a female ancestor, in which case they are IBD with probability $1/(2N_F)$, and 25% of the time they are both in a male ancestor, in which case they coalesce with probability $1/(2N_M)$. The remaining 50% of the time, our alleles trace back to two individuals of different sexes in the prior generation and so cannot coalesce. Therefore, our probability of coalescence in the preceding generation is

$$\frac{1}{4} \left(\frac{1}{2N_M} \right) + \frac{1}{4} \left(\frac{1}{2N_F} \right) \quad (4.18)$$

i.e. the rate of coalescence is the harmonic mean of the two sexes' population sizes, equating this to $\frac{1}{2N_e}$ we find

$$N_e = \frac{4N_F N_M}{N_F + N_M} \quad (4.19)$$

Thus if reproductive success is very skewed in one sex (e.g. $N_M \ll N/2$), our effective population size will be much reduced as a result. For more on how different evolutionary forces affect the rate of genetic drift, and their impact on the effective population size, see CHARLESWORTH (2009).

Question 5. You are studying a population of 500 male and 500 female Hamadryas baboons. Assume that all of the females but only 1/10 of the males get to mate: **A)** What is the effective population size for the autosome?

B) Do you expect the *ratio* of X-chromosome to autosomal diversity to be higher or lower in this species compared to a species where the sexes have more similar variance in reproductive success? Explain the intuition behind your answer.

4.2 The Coalescent and patterns of neutral diversity

“Life can only be understood backwards; but it must be lived forwards” – Kierkegaard

Pairwise Coalescent time distribution and the number of pairwise differences. Thinking back to our calculations we made about the loss of neutral heterozygosity and equilibrium levels of diversity (in Sections 4.1 and 4.1.1), you’ll note that we could first specify which generation a pair of sequences coalesce in, and then calculate some

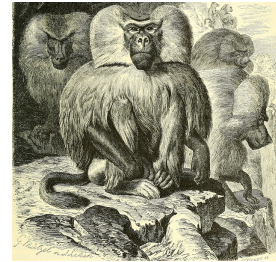
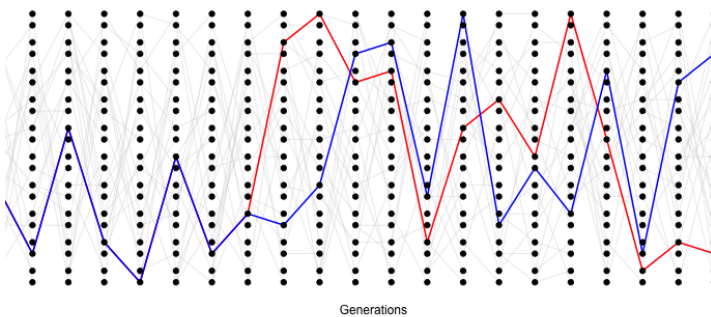


Figure 4.10: Male Hamadryas baboons. Up to ten females live in a harem with a single male. Brehm's Tierleben (Brehm's animal life). Brehm, A.E. 1893. Image from the Biodiversity Heritage Library. Contributed by University of Illinois Urbana-Champaign. Not in copyright.

properties of heterozygosity based on that. That's because neutral mutations do not affect the probability that an individual transmits an allele, and so don't affect the way in which we can trace ancestral lineages back through the generations.

As such, it will often be helpful to consider the time to the common ancestor of a pair of sequences, and then think of the impact of that time to coalescence on patterns of diversity. See Figure 4.11 for an example of this.



The probability that a pair of alleles have failed to coalesce in t generations and then coalesce in the $t + 1$ generation back is

$$P(T_2 = t + 1) = \frac{1}{2N} \left(1 - \frac{1}{2N}\right)^t \quad (4.20)$$

For example, the probability that a pair of sequences coalesce three generations back is the probability that they fail to coalesce in generation 1 and 2, which is $(1 - 1/2N) \times (1 - 1/2N)$, multiplied by the probability that they find a common ancestor, i.e. coalesce, in the third generation, which happens with probability $1/2N$.

From the form of eqn (4.20) we can see that the coalescent time of our pair of alleles is a Geometrically distributed random variable,³ where the probability of success is $p = 1/2N$. The waiting time for a pair of lineages to coalesce is like the number of tails thrown while waiting for a head on a coin with the probability of a head is $1/2N$, i.e. if the population is large we might be waiting for a long time for our pair to coalesce. We'll denote this geometric distribution by $T_2 \sim \text{Geo}(1/(2N))$. The expected (i.e. the mean over many replicates) coalescent time of a pair of alleles is then

$$\mathbb{E}(T_2) = 2N \quad (4.21)$$

generations. This form to the expectation follows from the fact that the mean of an geometric random variable is $1/p$.

In discussing the coalescent we'll be making use of random variables, e.g. number of generations back to the common ancestor of a pair of sequences is a random variable. We'll also use the expectation of random variables, e.g. the average number of generations back to the common ancestor of a pair of sequences. Have a look at sections A.2.1 and A.2.3.

Figure 4.11: A simple demonstration of the coalescent process. The simulation consists of a diploid population of 10 individuals (20 alleles). In each generation, each individual is equally likely to be the parent of an offspring (and the allele transmitted is indicated by a light grey line). We track a pair of alleles, chosen in the present day, back 14 generations until they find a common ancestor. [Code here.](#)

³ See Appendix eqn (A.29) and surrounding text for more on the Geometric distribution.

Conditional on a pair of alleles coalescing t generations ago, there are $2t$ generations in which a mutation could occur. See Figure 4.12 for an example. If the per generation mutation rate is μ , then the expected number of mutations between a pair of alleles coalescing t generations ago is $2t\mu$ (the alleles have gone through a total of $2t$ meioses since they last shared a common ancestor).

So we can write the expected number of mutations (S_2) separating two alleles drawn at random from the population as

$$\begin{aligned}\mathbb{E}(S_2) &= \sum_{t=0}^{\infty} \mathbb{E}(S_2|T_2 = t)P(T_2 = t) \\ &= \sum_{t=0}^{\infty} 2\mu t P(T_2 = t) \\ &= 2\mu \mathbb{E}(T_2) \\ &= 4\mu N\end{aligned}\tag{4.22}$$

this makes use of the law of total expectation (see Appendix eqn (A.27)) to average which generation our pair of sequences coalesce in. We'll assume that mutation is rare enough that it never happens at the same basepair twice, i.e. no multiple hits, such that we get to see all of the mutation events that separate our pair of sequences. This is assumption that repeat mutation is vanishingly rare at a basepair is called the infinitely-many-sites assumption, which should hold if $N\mu_{BP} \ll 1$, where μ_{BP} is the mutation rate per base pair. Thus the number of mutations between a pair of sites is the observed number of differences between a pair of sequences. In the previous chapter we denote the observed number of pairwise differences at putatively neutral sites separating a pair of sequences as π (we usually average this over a number of pairs of sequences for a region). Therefore, under our simple, neutral, constant population-size model we expect

$$\mathbb{E}(\pi) = 4N\mu = \theta\tag{4.23}$$

So we can get an empirical estimate of θ from π , let's call this $\hat{\theta}_\pi$, by setting $\hat{\theta}_\pi = \pi..$, i.e. our observed level of pairwise genetic diversity. If we have an independent estimate of μ , then from setting $\pi = \hat{\theta}_\pi = 4N\mu$ we can furthermore obtain an estimate of the population size N that is consistent with our levels of neutral polymorphism. If we estimate the population size this way, we should call it the effective coalescent population size (N_e). It's best to think about N_e estimated from neutral diversity as a long-term effective population size for the species, but there are many caveats that come along with that assumption. For example, past bottlenecks and population expansions are all subsumed into a single number and so this estimated N_e may not be very representative of the population size at any time. That

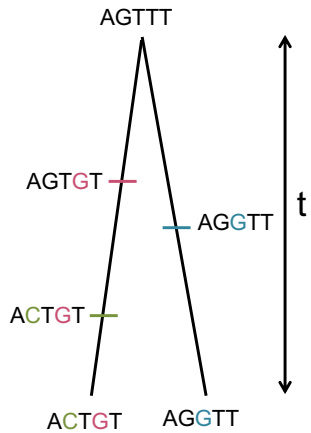


Figure 4.12: The ancestral lineages of a pair of sequences coalesce t generations in the past. There are $2t$ generations that mutations could occur in that would be differences between our sequences. Three mutations have occurred in this time changing the ancestral sequence (AGTTT) to the sequences at the bottom of the picture.

said, it's not a bad place to start when thinking about the rate of genetic drift for neutral diversity in our population over long time-periods.⁴

Lets take a moment to distinguish our expected heterozygosity (eqn. 4.12) from our expected number of pairwise differences (π). Our expected heterozygosity is the probability that two alleles at a locus, sampled from a population at random, are different from each other. If one or more mutations have occurred since a pair of alleles last shared a common ancestor, then our sequences will be different from each other. On the other hand, our π measure keeps track of the average total number of differences between our loci. As such, π is often a more useful measure, as it records the number of differences between the sequences, not just whether they are different from each other (however, for certain types of loci, e.g. microsatellites, heterozygosity is often used as we cannot usually count up the minimum number of mutations in a sensible way). In the case where our locus is a single basepair, the two measures will usually be close to one another, as $H \approx \theta$ for small values of θ . For example, comparing two sequences at random in humans, $\pi \approx 1/1000$ per basepair, and the probability that a specific base pair differs between two sequences is $\approx 1/1000$. However, these two quantities start to differ from each other when we consider regions with higher mutation rates. For example, if we consider a 10kb region, our mutation rate will 10,000 times larger than a single base pair. For this length of sequence the probability that two randomly chosen haplotypes differ is quite different from the number of mutational differences between them. (Try a mutation rate of 10^{-8} per base and a population size of 10,000 in our calculations of $E[\pi]$ and H to see this.)

Question 6. ROBINSON *et al.* (2016) found that the endangered Californian Channel Island fox on San Nicolas had very low levels of diversity ($\pi = 0.000014\text{bp}^{-1}$) compared to its close relative the California mainland gray fox (0.0012bp^{-1}).

A) Assuming a mutation rate of 2×10^{-8} per bp, what effective population sizes do you estimate for these two populations?

B) Why is the effective population size of the Channel Island fox so low? [Hint: quickly google Channel island foxes to read up on their history, also to see how ridiculously cute they are.]

Question 7. In your own words describe why the coalescent time of a pair of lineages scales linearly with the (effective) population size.

More details on the pairwise coalescent and the randomness of mutation. We found that our pairwise coalescent times followed a Geo-

⁴ Up to this point we've been describing only neutral processes, however, selection can also alter levels of polymorphism. For example, if some synonymous sites directly experience selection, then even if we use π calculated for synonymous changes we may underestimate the coalescent effective population size. As we'll see later in the notes, selection at linked sites can also impact neutral diversity. As such, if we can, we may want to use genomic sites subject to the weakest selective constraints, and also far from gene-dense or otherwise very constrained regions of the genome, to estimate N_e from π . But even then caution is warranted.



Figure 4.13: Gray Fox, *Urocyon cinereoargenteus*.
Diseases and enemies of poultry. Pearson and Warren. (1897) Image from the Biodiversity Heritage Library. Contributed by University of California Libraries. Not in copyright.

metric distribution, eqn (4.20). However, that assumes discrete generations and we'll often want to think about populations that lack discrete generations (i.e. individuals reproducing at random times with some mean generation time). Using our exponential approximation, we can see that is

$$\approx \frac{1}{2N} e^{-t/(2N)} \quad (4.24)$$

and so think of a continuous random variable, i.e. we could say that the coalescent time of a pair of sequences (T_2) is approximately exponentially distributed with a rate $1/(2N)$, i.e. $T_2 \sim \text{Exp}(1/(2N))$. Formally we can do this by taking the limit of the discrete process more carefully. See Appendix eqn (A.33) for more on exponential random variables.

We've derived the expected number of differences between a pair of sequences and talked about how variable the coalescent time is for a pair of sequences. The mutation process is also very variable; even if two sequences coalesce in the very distant past by chance, they may still be identical in the present if there was no mutation during that time.

Conditional on the coalescent time t , the probability that our pair of alleles are separated by S_2 mutations since they last shared a common ancestor is binomially distributed

$$P(S_2|T_2 = t) = \binom{2t}{j} \mu^j (1 - \mu)^{2t-j} \quad (4.25)$$

i.e. mutations happen in j generations and do not happen in $2t - j$ generations (with $\binom{2t}{j}$ ways this combination of events can possibly happen). See Appendix eqn (A.28) for discussion of the binomial distribution. Assuming that $\mu \ll 1$ and that $2t - j \approx 2t$, then we can approximate the probability that we have S_2 mutations as a Poisson distribution:

$$P(S_2|T_2 = t) = \frac{(2\mu t)^j e^{-2\mu t}}{j!} \quad (4.26)$$

i.e. a Poisson with mean $2\mu t$. This is an example of taking the binomial distribution to its Poisson distribution limit, see Appendix eqn (A.31) for more details. We'll not make much use of this result, but it is very useful in thinking about how to simulate the process of mutation.

4.3 The coalescent process of a sample of alleles.

Usually we are not just interested in pairs of alleles, or the average pairwise diversity. Generally we are interested in the properties of diversity in samples of a number of alleles drawn from the population. Instead of just following a pair of lineages back until they coalesce, we

can follow the history of a sample of alleles back through the population.

Consider first sampling three alleles at random from the population. The probability that all three alleles choose exactly the same ancestral allele one generation back is $1/(2N)^2$. If N is reasonably large, then this is a very small probability. As such, it is very unlikely that our three alleles coalesce all at once, and in a moment we'll see that it is safe to ignore such unlikely events.

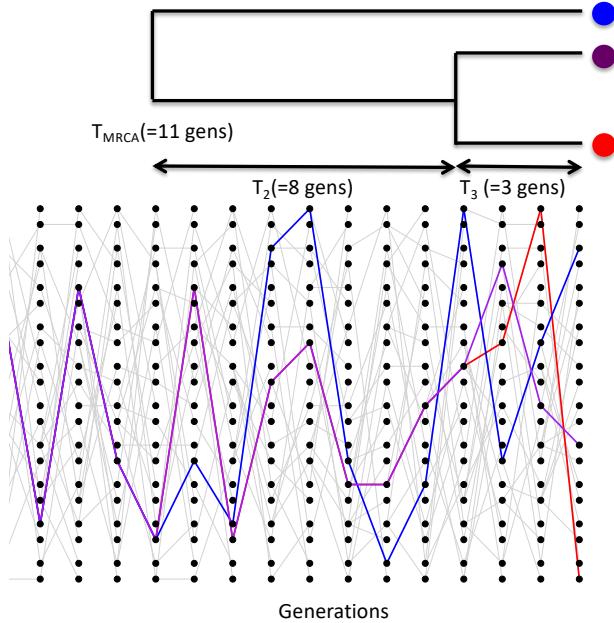


Figure 4.14: A simple simulation of the coalescent process for three lineages. We track the ancestry of three modern-day alleles, the first pair (blue and purple) coalesce four generations back, after which there are only two independent lineages we are tracking. This pair then coalesces twelve generations in the past. Note that different random realizations of this process will differ from each other a lot. The T_{MRCA} is $T_3 + T_2$. The total time in the tree is $T_{tot} = 3T_3 + 2T_2 = 25$ generations. Code here.

The probability that a specific pair of alleles find a common ancestor in the preceding generation is still $1/(2N)$. There are three possible pairs of alleles, so the probability that no pair finds a common ancestor in the preceding generation is

$$\left(1 - \frac{1}{2N}\right)^3 \approx \left(1 - \frac{3}{2N}\right) \quad (4.27)$$

In making this approximation we are multiplying out the right hand-side and ignoring terms of $1/N^2$ and higher (a Taylor approximation, see Appendix eqn (A.2)). See Figure 4.14 for a random realization of this process.

More generally, when we sample i alleles there are $\binom{i}{2}$ pairs,⁵ i.e. $i(i - 1)/2$ pairs. Thus, the probability that no pair of alleles in a sample of size i coalesces in the preceding generation is

$$\left(1 - \frac{1}{(2N)}\right)^{\binom{i}{2}} \approx \left(1 - \frac{\binom{i}{2}}{2N}\right) \quad (4.28)$$

⁵ said as “i choose 2”

while the probability any pair coalesces is $\approx \binom{i}{2}/2N$, again using eqn (A.2).

We can ignore the possibility that more than pairs of alleles (e.g. tripletons) simultaneously coalesce at once as terms of $1/N^2$ and higher can be ignored as they are vanishingly rare. Obviously in reasonable sample sizes there are many more triples ($\binom{i}{3}$) and higher order combinations than there are pairs ($\binom{i}{2}$), but if $i \ll N$ then we are safe to ignore these terms.

When there are i alleles, the probability that we wait until the $t + 1$ generation before any pair of alleles coalesces is

$$P(T_i = t + 1) = \frac{\binom{i}{2}}{2N} \left(1 - \frac{\binom{i}{2}}{2N}\right)^t \quad (4.29)$$

Thus the waiting time to the first coalescent event while there are i lineages is a geometrically distributed random variable⁶ with probability of success $p = \binom{i}{2}/2N$, which we denote by

$$T_i \sim \text{Geo} \left(\frac{\binom{i}{2}}{2N} \right). \quad (4.30)$$

The mean waiting time till any of pair within our sample coalesces is

$$\mathbb{E}(T_i) = \frac{2N}{\binom{i}{2}} \quad (4.31)$$

which again follows from the mean of a geometric random variable being $1/p$. After a pair of alleles first finds a common ancestral allele some number of generations back in the past, we only have to keep track of that common ancestral allele for the pair when looking further into the past. Thus when a pair of alleles in our sample of i alleles coalesces, we then switch to having to follow $i - 1$ alleles back in time. Then when a pair of these $i - 1$ alleles coalesce, we then only have to follow $i - 2$ alleles back. This process continues until we coalesce back to a sample of two, and from there to a single most recent common ancestor (MRCA).

Simulating a coalescent genealogy To simulate a coalescent genealogy at a locus for a sample of n alleles we therefore simply follow the following algorithm:

1. Set $i = n$.
2. Simulate a random variable to be the time T_i to the next coalescent event from $T_i \sim \text{Exp} \left(\frac{\binom{i}{2}}{2N} \right)$
3. Choose a pair of alleles to coalesce at random from all possible pairs.
4. Set $i = i - 1$

⁶ see Appendix eqn (A.29).

To see the continuous time version of this, note that (4.29) is

$$\approx \frac{\binom{i}{2}}{2N} \exp \left(-\frac{\binom{i}{2}}{2N} t \right) \quad (4.32)$$

The waiting time T_i to the first coalescent event in a sample of i alleles is thus exponentially distributed with rate $\binom{i}{2}/2N$, i.e. $T_i \sim \text{Exp} \left(\frac{\binom{i}{2}}{2N} \right)$.

5. Continue looping steps 2-4 until $i = 1$, i.e. the most recent common ancestor of the sample is found.

By following this algorithm we are generating realizations of the genealogy of our sample.

4.3.1 Expected properties of coalescent genealogies and mutations.

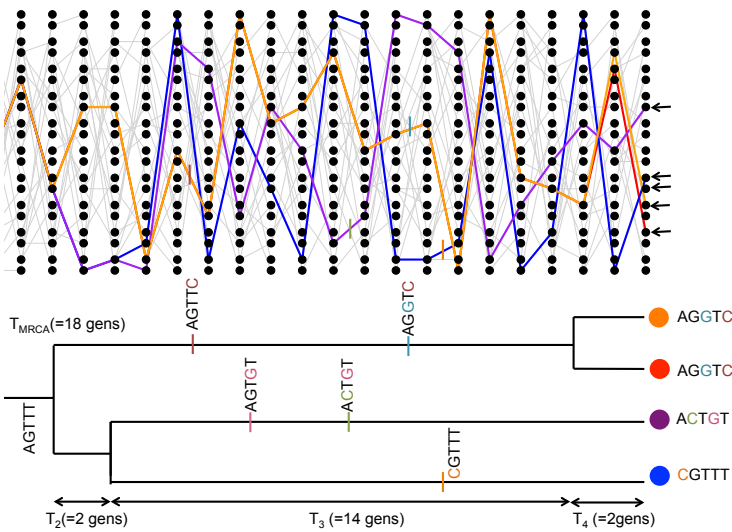


Figure 4.15: A simple coalescent tree from a single coalescent simulation, tracing the genealogy of 4 alleles with mutational changes marked with dashes showing transitions away from the MRCA sequence (AGTTT). The T_{MRCA} is $T_4 + T_3 + T_2$. The total time in the tree is $T_{tot} = 4T_4 + 3T_3 + 2T_2 = 54$ generations. [Code here](#).

The expected time to the most recent common ancestor. We will first consider the time to the most recent common ancestor of the entire sample (T_{MRCA}). This is

$$T_{MRCA} = \sum_{i=n}^2 T_i \quad (4.33)$$

generations back, where we are summing from $i = n$ alleles counting backwards to $i = 2$ alleles (see Figure 4.15 for example). As our coalescent times for different i are independent, the expected time to the most recent common ancestor is

$$\mathbb{E}(T_{MRCA}) = \sum_{i=n}^2 \mathbb{E}(T_i) = \sum_{i=n}^2 2N / \binom{i}{2} \quad (4.34)$$

Using the fact that $\frac{1}{i(i-1)} = \frac{1}{i-1} - \frac{1}{i}$ and a bit of rearrangement, we can rewrite this as

$$\mathbb{E}(T_{MRCA}) = 4N \left(1 - \frac{1}{n} \right) \quad (4.35)$$

So the average T_{MRCA} scales linearly with population size N . Interestingly, as we move to larger and larger samples (i.e. $n \gg 1$), the average time to the most recent common ancestor converges on $4N$. What's happening here is that in large samples our lineages typically coalesce rapidly at the start and very soon coalesce down to a much smaller number of lineages.

Question 8. Assume an autosomal effective population of 10,000 individuals (roughly the long-term human estimate) and a generation time of 30 years. What is the expected time to the most recent common ancestor of a sample of 20 people? What is this time for a sample of 500 people?

The expected total time in a genealogy and the number of segregating sites. Mutations fall on specific lineages of the coalescent genealogy and are transmitted to all descendants of their lineage. Furthermore, under the infinitely-many-sites assumption, each mutation creates a new segregating site. The mutation process is a *Poisson process*, and the longer a particular lineage, i.e. the more generations of meioses it represents, the more mutations that can accumulate on it. The total number of segregating sites in a sample is thus a function of the *total* amount of time in the genealogy of the sample, or the sum of all the branch lengths on the genealogical tree, T_{tot} . Our total amount of time in the genealogy is

$$T_{tot} = \sum_{i=n}^2 iT_i \quad (4.36)$$

as when there are i lineages, each contributes a time T_i to the total time (see Figure 4.15 for an example). Taking the expectation of the total time in the genealogy,

$$\mathbb{E}(T_{tot}) = \sum_{i=n}^2 i \frac{2N}{\binom{i}{2}} = \sum_{i=n}^2 \frac{4N}{i-1} = \sum_{i=n-1}^1 \frac{4N}{i} \quad (4.37)$$

we see that our expected total amount of time in the genealogy scales linearly with our population size N . Our expected total amount of time is also increasing with sample size n , but is doing so very slowly.

This again follows from the fact that in large samples, the initial coalescence usually happens very rapidly, so that extra samples add little to the total amount of time in the genealogical tree.

We saw above that the number of mutational differences between a pair of alleles that coalescence T_2 generations ago was Poisson with a mean of $2\mu T_2$, where $2T_2$ is the total branch length in this simple 2-sample genealogical tree. A mutation that occurs on any branch of our genealogy will cause a segregating polymorphism in the sample

To get a better sense of how T_{tot} grows with the sample size, we can approximate the sum 4.37 by an integral, which will work for large n . The result is $\int_1^{n-1} \frac{4N}{i} di = 4N \log(n - 1)$.

(meeting our infinitely-many-sites assumption). Thus, if the total time in the genealogy is T_{tot} , there are T_{tot} generations for mutations. So the total number of mutations segregating in our sample (S) is Poisson with mean μT_{tot} . Thus the expected number of segregating sites in a sample of size n is

$$\mathbb{E}(S) = \mu \mathbb{E}(T_{tot}) = \sum_{i=n-1}^1 \frac{4N\mu}{i} = \theta \sum_{i=n-1}^1 \frac{1}{i} \quad (4.38)$$

Note that this is growing with the sample size n , albeit very slowly (roughly at the rate of the log of the sample size). We can use this formula to derive another estimate of the population scaled mutation rate θ , by setting our observed number of segregating sites in a sample (S) equal to this expectation. We'll call this estimator $\hat{\theta}_W$:

$$\hat{\theta}_W = \frac{S}{\sum_{i=n-1}^1 1/i} \quad (4.39)$$

This estimator of θ was devised by WATTERSON (1975), hence the W .

The neutral site-frequency spectrum. We can use our coalescent process to find the expected number of derived alleles present i times out of a sample size n , e.g. how many singletons ($i = 1$) do we expect to find in our sample? For example, in Figure 4.15 in our sample of four sequences, there are 3 singletons and 2 doubletons. The number of sites with these different allele frequencies depends on the lengths of specific genealogical branches. A mutation that falls on a branch with i descendants will create a derived allele with frequency i . For example, in our example tree in Figure 4.15, the total number of generations where a mutation could arise and be a doubleton is $T_3 + 2T_2$, the total length of the branch ancestral to just the orange and red allele ($T_3 + T_2$) plus the branch ancestral to just the blue and purple allele (T_2).

To see how we could go about working this out, lets start by considering the simple coalescent tree, shown in Figure 4.16, for sample of 3 alleles drawn from a population. Mutations that fall on the branches coloured in black will be derived singletons, while mutations that fall along the orange branch will be doubletons in the sample. The total number of generations where a singleton mutation could arise is $3T_3 + T_2$. Note that we only count the time where there are two lineages (T_2) once. So our expected number of singletons, using eqn (4.31), is

$$\mathbb{E}(S_i) = \mu (3\mathbb{E}(T_3) + \mathbb{E}(T_2)) = \mu \left(3 \frac{2N}{3} + 2N \right) = \theta \quad (4.40)$$

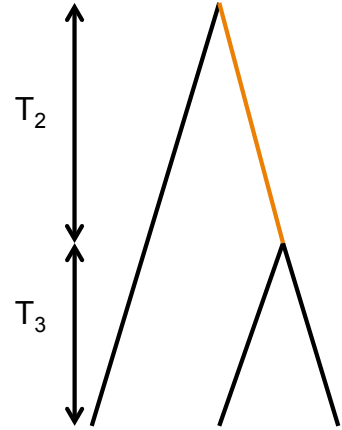


Figure 4.16: A tree for three samples; note that this is the only possible tree shape (treating the tips as unlabeled, i.e. I don't care which pair of sequences carry a doubleton, just that any two sequences carry a derived allele).

By similar logic, the time where doubletons could arise is T_2 and our expected number of doubletons is $\mathbb{E}(S_i) = \theta/2$. Thus, there are on average half as many doubletons as singletons.

Extending this logic to larger samples might be doable, but is tedious (I mean really tedious: for 10 alleles there are thousands of possible tree shapes and the task quickly gets impossible even computationally). A nice, relatively simple proof of the neutral site frequency spectrum is given by (HUDSON, 2015), but we won't give this here.

The general form is:

$$\mathbb{E}(S_i) = \frac{\theta}{i} \quad (4.41)$$

i.e. there are twice as many singletons as doubletons, three times as many singletons as tripletons, and so on. The other thing that will be helpful for us to know is that neutral alleles at intermediate frequency tend to be old, and those that are rare in the sample are young. We expect to see a lot more rare alleles in our sample than common alleles.

Question 9. There are two possible tree shapes that could relate four samples. Draw both of them and separately colour (or otherwise mark) the branches by where singletons, doubletons, and tripleton derived alleles could arise.

We can also ask the probability of observing a derived allele segregating at frequency i/n given that the site is polymorphic in our sample of size n (i.e. given that $0 < i < n$). We can obtain this probability by dividing the expected number of sites segregating for an allele at frequency i by the expected number segregating at all of the possible allele frequencies for polymorphisms in our sample

$$P(i|0 < i < n) = \frac{\mathbb{E}(S_i)}{\sum_{j=1}^{n-1} \mathbb{E}(S_j)} = \frac{1/i}{\sum_{j=1}^{n-1} 1/j}. \quad (4.42)$$

We can interpret this probability as the fraction of polymorphic sites we expect to find at a frequency i/n .

Tests based on the site frequency spectrum Population geneticists have proposed a variety of ways to test whether an observed site frequency spectrum conforms to its neutral, constant-size expectations. These tests are useful for detecting population size changes using data across many loci, or for detecting the signal of selection at individual loci. One of the first tests was proposed by (TAJIMA, 1989), and is called Tajima's D . Tajima's D is

$$D = \frac{\hat{\theta}_\pi - \hat{\theta}_W}{C} \quad (4.43)$$

where the numerator is the difference between the estimate of θ based on pairwise differences and that based on segregating sites. As these

two estimators both have expectation θ under the neutral, constant-size model, the expectation of D is zero. The denominator C is a positive constant; it's the square-root of an estimator of the variance of this difference under the constant population size, neutral model. This constant was chosen for D to have mean zero and variance 1 under the null model, so we can test for departures from this simple null model.

An excess of rare alleles compared to the constant-size, neutral model will result in a negative Tajima's D , because each additional rare allele increases the number of segregating sites by 1, but only has a small effect on the number of pairwise differences between samples. In contrast, a positive Tajima's D reflects an excess of intermediate frequency alleles relative to the constant-size, neutral expectation. Alleles at intermediate-frequency increase pairwise diversity more per segregating site than typical, thus increasing θ_π more than θ_W .

4.3.2 Demography and the coalescent

We've already seen how changes in population size can change the rate at which heterozygosity is lost from the population (see the discussion around eqn. (4.14)). If the population size in generation i is N_i , the probability that a pair of lineages coalesce is $1/(2N_i)$; this conforms to our intuition that if the population size is small, the rate at which pairs of lineages find their common ancestor is faster. We can potentially accommodate rapid random fluctuations in population size by simply using the effective population size N_e in place of N . However, longer term more systematic changes in population size will distort the coalescent genealogies, and hence patterns of diversity, in more systematic ways.

We can see how demography potentially distorts the observed frequency spectrum away from the neutral expectation in a very large sample of humans shown in Figure 4.17. For comparison, the neutral frequency spectrum, eqn (4.41), is shown as a red line. There are vastly more rare alleles than expected under our neutral, constant-size-size model, but the neutral prediction and reality agree somewhat more for alleles that are more common.

Why is this? Well, these patterns are likely the result of the very recent explosive growth in human populations. If the population has grown rapidly, then the pairwise-coalescent rate in the past may be much higher than the coalescent rate closer to the present. (see Figure 4.18).

One consequence of a recent population expansion is that there is much less genetic diversity in the population than you'd predict using the census population size. Humans are one example of this effect; there are 7 billion of us alive today, but this is due to very rapid

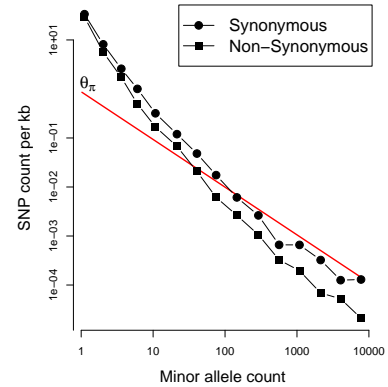
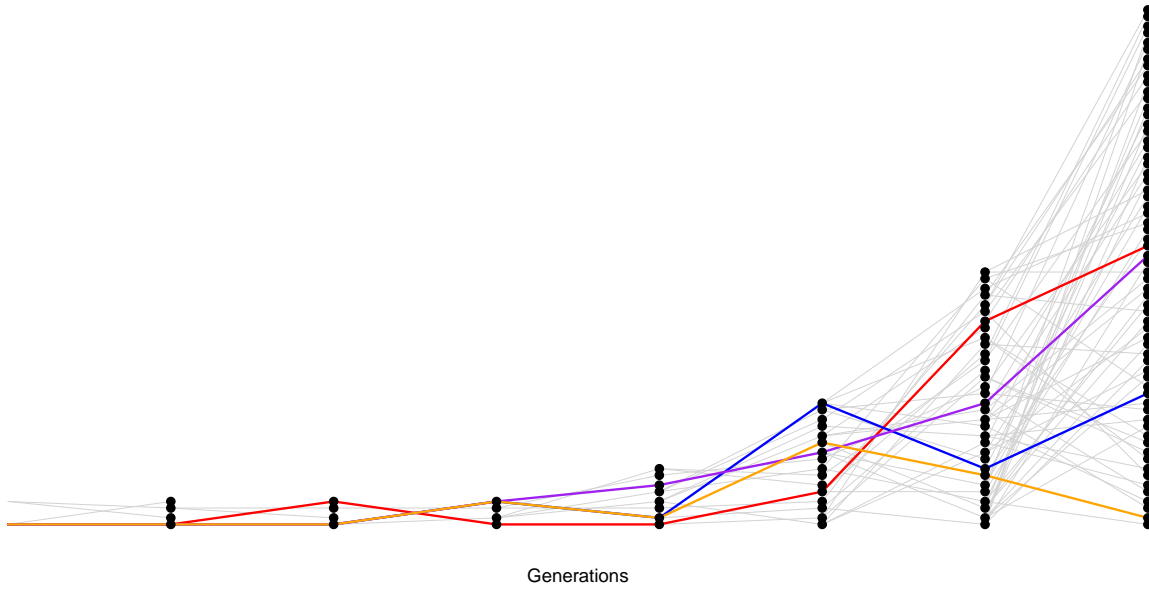


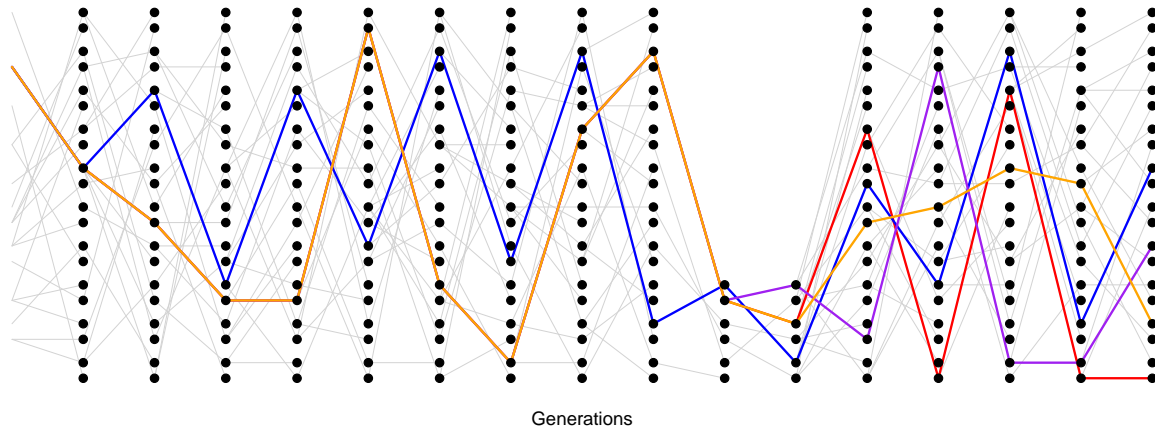
Figure 4.17: Data from 202 genes from 14002 people of European ancestry (28004 alleles). Note the double log-scale. The red line gives the neutral, constant population size estimate of the site frequency spectrum, our equation (4.41), using a θ estimated from π . Note how the non-synonymous changes are even more skewed towards rare alleles, likely due to selection against non-synonymous alleles preventing them from reaching high frequency. Data from NELSON *et al.* (2012). Code here.



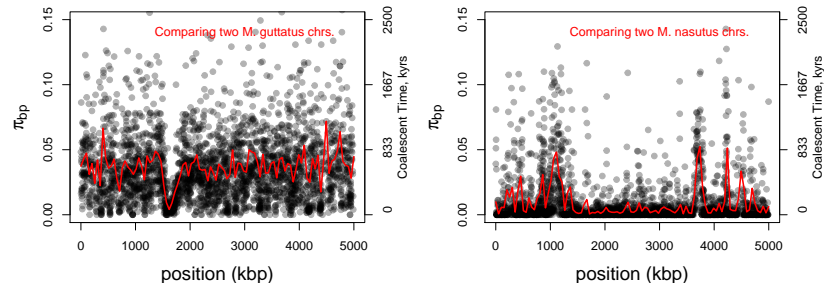
population growth over the past thousand to tens of thousands of years. Our level of genetic diversity is very much lower than you'd predict given our census size, reflecting our much smaller ancestral population. A second consequence of recent population expansion is that the deeper coalescent branches are much more squished together in time compared to those in a constant-sized population. Mutations on deeper branches are the source of alleles at more intermediate frequencies, and so there are even fewer intermediate-frequency alleles in growing populations. That's why there are so many rare alleles, especially singletons, in this large sample of Europeans.

Another common demographic scenario is a population bottleneck. In a bottleneck, the population size crashes dramatically, and subsequently recovers. For example, our population may have had size N_{Big} and crashed down to N_{Small} . One example of a bottleneck is shown in Figure 4.19. Looking at a sample of lineages drawn from the population today, if the bottleneck was somewhat recent ($\ll N_{\text{Big}}$ generations in the past) many of our lineages will not have coalesced before reaching the bottleneck, moving backward in time. But during the bottleneck our lineages coalesce at a much higher rate, such that many of our lineages will coalesce if the bottleneck lasts long enough ($\sim N_{\text{Small}}$ generations). If the bottleneck is very strong, then all of our lineages will coalesce during the bottleneck, and the resulting site frequency spectrum may look very much like our population growth model (i.e. an excess of rare alleles). However, if some pairs of lineages escape coalescing during the bottleneck, they will coalesce much more

Figure 4.18: A realization of the coalescent process in a growing population. The population underwent a period of doubling every generation. The initial population size of just two individuals, maintained for a number of generations, is obviously highly unrealistic but serves our purpose. [Code here.](#)



deeply in time (e.g. the blue and orange ancestral lineages in 4.19).



An example of this is shown Figure 4.20, data from BRANDVAIN *et al.*. *Mimulus nasutus* is a selfing species that arose recently from an out-crossing progenitor *M. guttatus*, and experienced a strong bottleneck. *M. guttatus* has very high levels of genetic diversity ($\pi = 4\%$ at synonymous sites), but *M. nasutus* has lost much of this diversity ($\pi = 1\%$). Looking along the genome, between a pair of *M. guttatus* chromosomes, levels of diversity are fairly uniformly high.

But in comparing two *M. nasutus* chromosomes, diversity is low because the pair of lineages generally coalesce recently. Yet in a few places we see levels of diversity comparable to *M. guttatus*; these regions correspond to genomic sites where our pair of lineages fail to coalesce during the bottleneck and subsequently coalesce much more deeply in the ancestral *M. guttatus* population.

Figure 4.19: A realization of the coalescent process in a bottlenecked population. Our population underwent a bottleneck eight generations in the past. Code here.

Figure 4.20: Diversity along a region of the *Mimulus* genome. Black dots give π in 1kb windows between chromosomes sampled from two individuals, the red line is a moving average (data from BRANDVAIN *et al.*). Pairwise coalescent times (t) estimated assuming $t = \pi/2\mu$ using $\mu_{BP} = 10^{-9}$. Code here.



Figure 4.21: Yellow Monkeyflower *M. guttatus*.
Choix des plus belles fleurs et des plus beaux fruits. Pierre-Joseph Redouté. (1833). Contributed to Flickr by Swallowtail Garden Seeds. Public Domain.

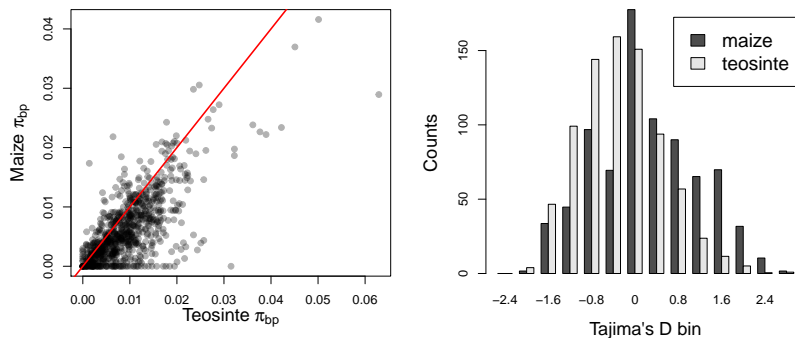


Figure 4.22: Data for polymorphism from Maize and Teosinte: 774 loci from WRIGHT *et al.* (2005). **Left)** Genetic diversity levels in maize and teosinte samples at each of these loci. Note how diversity levels are lower in maize than teosinte, i.e. most points are below the red $x = y$ line. **Right)** The distribution of Tajima's D in maize and teosinte, see how the maize distribution is shifted towards positive values. Code here.

Mutations that arise on deeper lineages will be at intermediate frequency in our sample, and so mild bottlenecks can lead to an excess of intermediate frequency alleles compared to the standard constant-size model. This can skew Tajima's D (see eqn 4.43) towards positive values and away from its expectation of zero. One example of this skew is shown in Figure 4.22. Maize (*Zea mays* subsp. *mays*) was domesticated from its wild progenitor teosinte (*Zea mays* subsp. *parviglumis*) roughly ten thousand years ago. We can see how the bottleneck associated with domestication has resulted in a loss of genetic diversity in maize compared to teosinte, and the polymorphism that remains is somewhat skewed towards intermediate frequencies resulting in more positive values of Tajima's D.

Question 10. VOIGHT *et al.* (2005) sequenced 40 autosomal regions from 15 diploid samples of Hausa people from Yaounde, Cameroon. The average length of locus they sequenced for each region was 2365bp. They found that the average number of segregating sites per locus was $S = 11.1$ and the average $\pi = 0.0011$ per base over the loci. Is Tajima's D positive or negative? Is a demographic model with a bottleneck or growth more consistent with this result?



Figure 4.23: Teosinte (*Zea mays* ssp. *mexicana*)
American grasses (1897). Scribner, FL Image from the Biodiversity Heritage Library. Contributed by Smithsonian Libraries. Not in copyright.

5

The Population Genetics of Divergence and Molecular Substitution.

“history is just one damn thing after another” -Arnold Toynbee

There are over 30 million base pair substitutions between human and chimpanzees, sites where humans carry one allele and chimps another at orthologous locations. These changes have occurred in the seven million years or so since human and chimp last shared a common ancestor. Other substitutions are shared between the sister species human and chimp to the exclusion of gorilla, yet others are shared between human, chimps and Gorilla but not Orangs. These substitutions represent changes at just a small percentage of sites genome-wide as we share the majority of our genome, our evolutionary history, and our biology with the other great apes. Each of the substitutions must have arisen as a single mutation in the population, spread through the population as a polymorphism before eventually reaching fixation. What forces drove the spread of these alleles?

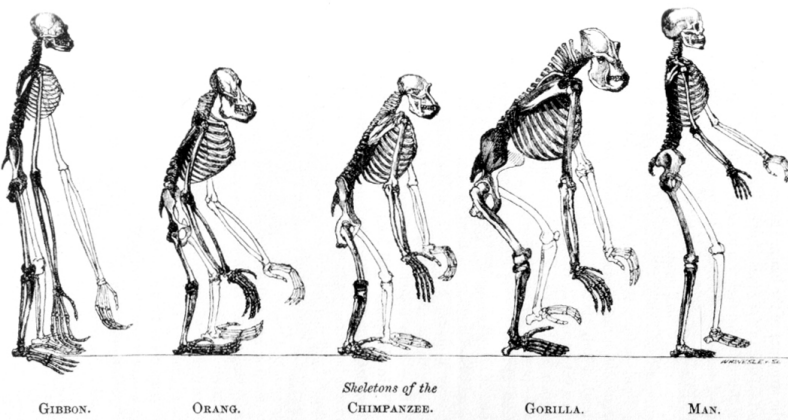
Human	accacagcattttagttactgccaagaaggcctgtatctgttagggtaaaatccctcgctgaagtgggttg
Chimpg.....c.....
Gorillacc.....
Orangutan	c.....c.....c.....
Gibbonc.....---
Crab-eating macaque	g.....gg...c.....c..t.t.....

Many substitutions were driven by selection, as there has undoubtedly been plenty of adaptive phenotypic adaptive evolution in great apes. However, these adaptive changes may be a small minority of all the substitutions, for a start many of these substitutions have occurred in non-coding DNA with no known functional effect. Thus it is reasonable initial position that the majority of substitutions genome-wide may well be neutral. How can we hope to identify regions undergoing adaptive divergence? How could we hope to address the claim that many amino-acid changing substitutions are also neutral, as posited

Table 5.1: Variable positions in a primate alignment of orthologous sequences of a 136bp region. This region starts at position 5242147 of chromosome 11, chosen pretty much at random from the UCSC browser. Dots indicate positions where the other sequences carry the same base as the human reference sequence.

Many of the topics covered in this chapter also fall within the field of ‘molecular evolution’, which shares many of its questions and tools with population genetics but often focuses on longer time-scales of evolution using phylogenetic approaches.

by the Neutral theory of molecular evolution. One way forward is to understand what neutral theory predicts for the rate of molecular substitution, and then develop ways to test these ideas.



Photographically reduced from Diagrams of the natural size (except that of the Gibbon, which was twice as large as nature), drawn by Mr. Waterhouse Hawkins from specimens in the Museum of the Royal College of Surgeons.

Figure 5.1: Illustration by Benjamin Waterhouse Hawkins from Huxley's Evidence as to Man's Place in Nature (1863).
Image from the wikimedia, public domain.

5.1 The Neutral Substitution process.

So how then do neutral substitutions occur? It is very unlikely that a rare neutral allele accidentally drifts up to fixation; more likely, such an allele will be eventually lost from the population. However, populations experience a large and constant influx of rare alleles due to mutation, so even if it is very unlikely that an individual allele fixes within the population, some neutral alleles will fix by chance. So we'll need to understand the probability that a neutral mutation fixes, and then how we can think about the rate of substitutions accumulate over time.

5.1.1 probability of the eventual fixation of a neutral allele

An allele which reaches fixation within a population is an ancestor to the entire population. In a particular generation there can only be a single allele that all other alleles at the locus in a later generation can claim as an ancestor (See Figure 5.2). At a neutral locus, the actual allele does not affect the number of descendants that the allele has (this follows from the definition of neutrality: neutral alleles don't leave more or less descendants on average than other neutral alleles). An equivalent way to state this is that the allele labels don't affect anything; thus the alleles are *exchangeable*. As a consequence of being exchangeable, any allele is equally likely to be the ancestor of the

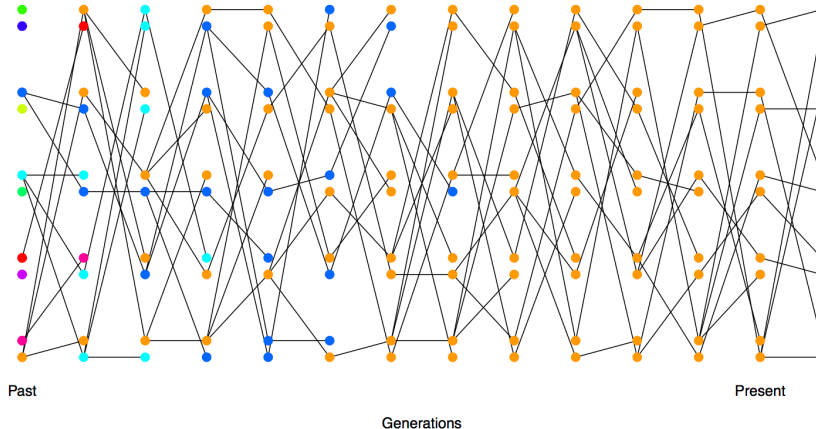


Figure 5.2: Each allele initially present in a small diploid population is given a different colour so we can track their descendants over time. By the 9th generation, all of the alleles present in the population can trace their ancestry back to the orange allele. [Code here.](#)

entire population. In a diploid population of size N , there are $2N$ alleles, all of which are equally likely to be the ancestor of the entire population at some later time point. So if our allele is present in a single copy, the chance that it is the ancestor to the entire population in some future generation is $1/(2N)$, i.e. the chance our neutral allele is eventually fixed is $1/(2N)$. In Figure 5.2, our orange allele in the first generation is one of 10 differently coloured alleles, and so has a $1/10$ chance of being the ancestor of the entire population at some later time point (and in this simulation it does become the common ancestor, by the 9th generation).

More generally, if our neutral allele is present in i copies in the population, of $2N$ alleles, the probability that this allele becomes fixed is $i/(2N)$, i.e. the probability that a neutral allele is eventually fixed is simply given by its frequency (p) in the population. (We can also derive this result by letting $N_s \rightarrow 0$ in eqn. (12.11), a result we'll encounter later.)

How long does it take on average for such an allele to fix within our population? Well, in developing equation (4.35) we've seen that it takes $4N$ generations for a large sample of alleles to all trace their ancestry back to a single most recent common ancestral allele. Any single-base pair change which arose as a single mutation at a locus, and fixed in the population, must have been present in the sequence transmitted by the most recent common ancestor of the population at that locus. Thus it must take roughly $4N$ generations for a neutral allele present in a single copy within the population to fix. This argument can be made more precise, but in general we would still find that it takes $\approx 4N$ generations for a neutral allele to go from its introduction to fixation with the population.

5.1.2 Rate of substitution of neutral alleles

A substitution between populations that do not exchange gene flow is simply a fixation event within one population. The rate of substitution is therefore the rate at which new alleles fix in the population, so that the long-term substitution rate is the rate at which mutations arise that will eventually become fixed within our population.

Lets assume, based on our discussion of the neutral theory of molecular evolution, that there are only two classes of mutational changes that can occur with a region, highly deleterious mutations and neutral mutations. A fraction C of all mutational changes are highly deleterious, and cannot possibly contribute to substitution nor polymorphism. The other $1 - C$ fraction of mutations are neutral. If our total mutation rate is μ per transmitted allele per generation, then a total of $2N\mu(1 - C)$ neutral mutations enter our population each generation.

Each of these neutral mutations has a $1/(2N)$ probability chance of eventually becoming fixed in the population. Therefore, the rate at which neutral mutations arise that eventually become fixed within our population is

$$2N\mu(1 - C) \frac{1}{2N} = \mu(1 - C) \quad (5.1)$$

Thus the rate of substitution, under a model where newly arising alleles are either highly deleterious or neutral, is simply given by the mutation rate of neutral alleles, i.e. $\mu(1 - C)$.

Consider a pair of species that have diverged for T generations, i.e. orthologous sequences shared between the species last shared a common ancestor T generations ago. If these species have maintained a constant μ over that time, they will have accumulated an average of

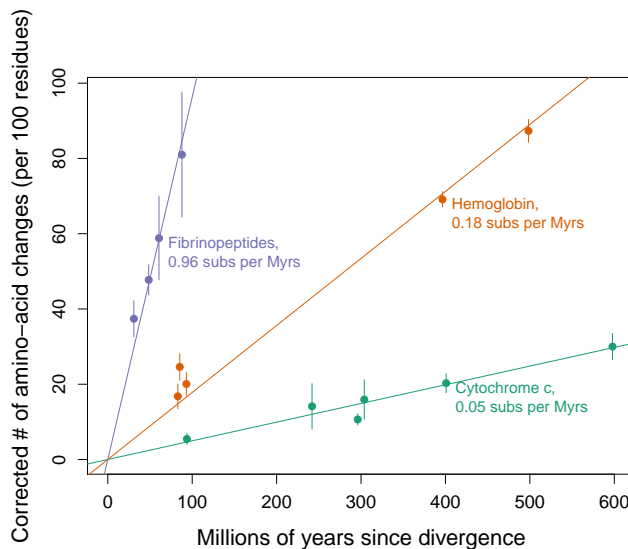
$$2\mu(1 - C)T \quad (5.2)$$

neutral substitutions. This assumes that T is a lot longer than the time it takes to fix a neutral allele, such that the total number of alleles introduced into the population that will eventually fix is the total number of substitutions.

This is a really pretty result as the population size has completely canceled out of the neutral substitution rate. However, there is another way to see this in a more straight forward way. If I look at a sequence in me compared to, say, a particular chimp, I'm looking at the mutations that have occurred in both of our germlines since they parted ways T generations ago. Since neutral alleles do not alter the probability of their transmission to the next generation, we are simply looking at the mutations that have occurred in $2T$ generations worth of transmissions. Thus the average number of neutral mutational differences separating our pair of species is simply $2\mu(1 - C)T$.

5.1.3 Implications for the Molecular Clock.

A number of observations follow under this model, from equation (5.2). The first is that a primary determinant of patterns of molecular evolution in a genomic region is the level of constraint (C). This pattern generally seems to hold empirically: non-coding regions often evolve more rapidly than coding regions, synonymous substitutions accumulate faster than nonsynonymous, and nonsynonymous substitutions accumulate faster in less vital proteins than ones that are absolutely necessary for early development. For example, Fibrinopeptides evolve in a less constrained manner than the Cytochrome c gene, see Figure 5.3. Note that this constraint prediction is not a unique prediction of the neutral model, e.g. less constrained regions may also be better able to evolve adaptively. However, it is a fantastically useful general insight, e.g. it allows us to spot putatively functional non-coding regions by looking for genomic regions that have very low levels of divergence among distantly related species.



The second important insight, and critical for the development of the neutral theory, is that equation (5.2) is seemingly consistent with ZUCKERKANDL and PAULING (1965)'s hypothesis of a surprisingly constant, protein molecular clock. The protein molecular clock is the observation that for some proteins there's a linear relationship between the number of non-synonymous (NS) substitutions and the time species last shared a common ancestor in the fossil record. DICKERSON (1971) provided an early example of this observation (Figure 5.3), by comparing various organisms whose molecular sequences were available to him. For example, he found that humans and rattlesnakes,

"functionally less important molecules or parts of a molecule evolve faster than more important ones."

— KIMURA and OHTA (1974)

Figure 5.3: The numbers of substitutions in three proteins, corrected for multiple hits, between various pairs of groups plotted against the time these groups shared a common ancestor in the fossil record. Data from DICKERSON (1971). The lines give the linear regression through the origin for each protein. The slope of the regression is given next to the protein name. See (ROBINSON *et al.*, 2016) who revisited this classic study and confirmed the conclusions.



Figure 5.4: Eastern diamondback rattlesnake (*Crotalus adamanteus*). North American herpetology. Holbrook, J. E. Image from the Biodiversity Heritage Library. Contributed by Smithsonian Libraries. Licensed under CC BY-2.0.

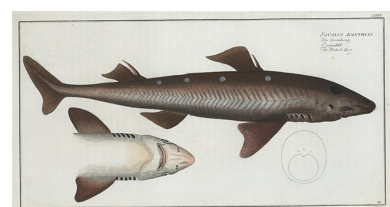


Figure 5.5: Spiny dogfish (*Squalus acanthias*). Rare Book Division, The New York Public Library. "Squalus Acanthias, The Picked-Dog" The New York Public Library Digital Collections. 1785. Public domain.

who last share a common ancestor in the fossil record around 300 million years, are separated by roughly 15 NS substitutions per 100 sites in the Cytochrome c protein. While, humans and dogfish, which diverged around 400 million years, are separated by 19 NS substitutions per 100 sites in this gene.

In equation (5.2), if we double the amount of time separating a pair of species T , we double the number of substitutions predicted. Note that for this to be true T must be measured in generations. To explain a protein molecular clock between species that clearly differed dramatically in generation time it was hypothesized that the mutation rate actually scaled with generation time, i.e. short-lived organisms introduced fewer mutations per generation, e.g. as they had fewer rounds of mitosis. This generation-time assumption meant that the mutation rate per year could be constant, such that μT would be a constant for pairs of species that had diverged for similar geological times, which are measured in years, even if the organisms differed in generation time. This assumption would allow neutral theory to be consistent with a protein molecular clock measured in years. We now know that this critical generation time assumption is false: organisms with shorter generation times have somewhat higher mutation rates per year so a strict neutral model is inconsistent with the protein molecular clock. We'll return to these ideas when we discuss the fate of very weakly selected mutations in Chapter 12 and OHTA (1973)'s Nearly Neutral theory. If you are still reading this send Graham a picture of Tomoko Ohta receiving the Crafoord Prize, an analog of the Nobel prize for biology, for her contributions to molecular evolution.

The contribution of ancestral polymorphism to divergence. If we are considering T to represent the divergence between long-separated species, then we can think of T as the time that the species split. However, for more recently diverged populations and species, we need to include the fact that the sorting of ancestral polymorphism contributes to divergence among species. In Figure 5.6, we see our two populations split T_s generations ago. However, the coalescence of our A and B lineage is necessarily deeper in time than T_s . The top mutation was polymorphic in the ancestral population but now contributes to the divergence between A and B. Assuming that our ancestral population had effective size N_A individuals, and that our populations split cleanly with no subsequent gene flow, then

$$T = T_s + 2N_A. \quad (5.3)$$

If our species split time is very large compared to $2N$ then we can think of T as the split time.

Question 1. For this, and the next question, assume that humans

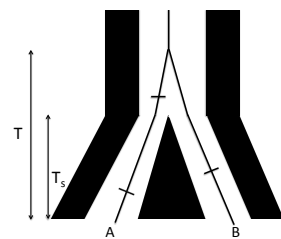


Figure 5.6: The genealogy of two alleles one sampled from population A and B. Mutations on the lineages are shown as dashes. The pair of alleles coalesces in the ancestral population of A and B. The two populations split T_s generations ago, with no subsequent gene flow, but the two lineages must coalesce deeper in time.

and chimps split around 5.5×10^6 years ago, have a generation time 20 years, that the speciation occurred instantaneously in allopatry with no subsequent gene flow, and the ancestral effective population size of the human and chimp common ancestor population was 10,000 individuals.

Nachman and Crowell sequenced 12 pseudogenes in humans and chimps and found substitutions at 1.3% of sites.

A) What is the mutation rate per site per generation at these genes?

B) All of the pseudogenes they sequenced are on the autosomes. What would your prediction be for pseudogenes on the X and Y chromosomes, given that there are fewer rounds of replication in the female germline than in the male germline.

5.2 Tests of molecular evolution.

One of the great appeals of neutral models is they offer a simple null for us to test real data against.

5.2.1 Comparing the rates of non-synonymous to synonymous substitutions d_N/d_S

One common tool in molecular evolution is to compare the estimated number (or rates) of substitutions in different classes of genomic sites, for example the ratio of the number of non-synonymous to synonymous substitutions in a given gene. The simplest way to calculate d_N is to count up the non-synonymous changes and divide by the total number of positions in the gene where a non-synonymous point mutation could occur. We can do likewise for synonymous changes d_S , and then take the ratio d_N/d_S .¹

For the vast majority of protein-coding genes in the genome we see that $d_N/d_S < 1$. This observation is consistent with the view that non-synonymous sites are much more constrained than synonymous sites, i.e. that most non-synonymous mutations are deleterious and quickly removed from the population. If we are willing to make the assumption that all synonymous changes are neutral, $d_S = 2T\mu$, then we can estimate the degree of constraint on non-synonymous sites. (Note that synonymous changes can sometimes be subject to both positive and negative selection, but this neutral assumption is a useful starting place.)

Assume that a fraction C of non-synonymous changes are too deleterious to contribute to polymorphism. Then, after T generations of divergence have elapsed between two populations, we'd expect d_N

¹ This ignores the fact that some changes are more likely to occur by mutation than others and also does not account for multiple hits (multiple mutations at the same bp position). Therefore, in practice the ratio d_N/d_S is more typically calculated by model-based likelihood and bayesian methods that can account for these features.

neutral non-synonymous substitutions, where

$$d_N = 2T(1 - C)\mu \quad (5.4)$$

Dividing by d_S , we find

$$d_N/d_S = (1 - C) \quad (5.5)$$

Therefore, if we assume that non-synonymous mutations can only be strongly deleterious or neutral, we estimate the fraction of mutational changes that are constrained by negative selection as $C = 1 - d_N/d_S$. C has the interpretations of being the fraction of non-synonymous mutations that are quickly weeded out of the population by selection, and so do not contribute to divergence among species.

We can test whether our gene is evolving in a constrained way at the protein level by estimating d_N/d_S and testing whether this is significantly less than 1. A d_N/d_S test can provide evolutionary evidence that a stretch of DNA proposed to be protein-coding is subject to selective constraint, and so likely does encode for a functional protein. We can also perform a d_N/d_S test on specific branches of a phylogeny for a gene, to test on which branches the gene is subject to constraint, or to test for changes in the level of constraint across the phylogeny.

Loss of constraint at pseudogenes. While most protein genes evolve under constraint, we can find examples of genes that are evolving in a less constrained manner. The simplest example of this is where the gene has lost function. Genes can lose function because of inactivating mutations that stop them being transcribed or translated into functional proteins. Such genes are called ‘pseudogenes’. When a gene completely loses function there is no longer selection against non-synonymous changes and so such mutations are just as free to accumulate as synonymous changes, and so $d_N/d_S = 1$. Pseudogenes are a wonderful example of the extension of Darwin’s ideas about vestigial traits (‘Rudimentary organs’) to the DNA level; we can still recognize a once useful word (gene) whose spelling is slowly degrading. Our genomes are filled with old pseudogenes whose original meanings (functional protein coding sequences) are slowly being eroded through the accumulation of neutral substitutions. One nice example of a gene that has repeatedly lost function, i.e. become repeatedly pseudogenized, is the Enamlin gene from the study of MEREDITH *et al.* (2009).

“Rudimentary organs may be compared with the letters in a word, still retained in the spelling, but become useless in the pronunciation, but which serve as a clue .. for its derivation.” – DARWIN (1859) pg. 455

	818	827	1239	1247	2501	2512	2533	2542	4028	4039	
<i>Sus</i>AAATCAACT..	TGTTTACTA..	ACATGGCATGAA..	TATGCCAATC..	GGGCACAGTT..						
<i>Hippopotamus</i>AAATCAACT..	TGTTTACTA..	ACATGGCATGAA..	CATGCCAATC..	GGGCACAGTT..						
<i>Eubalaena glacialis</i>AAATCAACT..	TGTTTACTA..	ATATGGCATGAA..	CATGCCAATC..	GGGCACAGTT..						
<i>Eubalaena australis</i>AAATCAACT..	TGTTTACTA..	ATATGGCATGAA..	CATGCCAATC..	GGGCACAGTT..						
<i>Megaptera</i>AAATCAACT..	TGTTTACTA..	AATACTGAA..	CATGCCAATC..	GGGCACAGTT..						
<i>Caperea</i>AAATCAACT..	TGTTTACTA..	AATACTGAA..	CATGCCAATC..	GGGCACAGTT..						
<i>Eschrichtius</i>AAATCAACT..	CGTTTACTA..	ATATGGCATGAA..	CATGCCAATC..	GGGCACAGTT..						
<i>Kogia sima</i>AAATCAACT..	TGTTTACTA..	ATATGGCATGAA..	CATGCCAATC..	GGGCACAGTT..						
<i>Kogia breviceps</i>AAATCAACT..	TGTTTACTA..	ATATGGCATGAA..	CATGCCAATC..	GGGCACAGTT..						
D	918	935	1584	1593	1614	1620	2499	2507	4017	4023	
<i>Sus</i>GGGA-GTCCAAAAGGCC..	ACCTTCCCTA..	AAAAACC..	CAACATGGC..	GCT-AGC..						
<i>Bradypterus</i>???????????????????	ACT- C CCA..	AAAAACC..	CAAATGGC..	GTT-AGC..						
<i>Choloepus didactylus</i>ATTCAGGAGCAGTC..	ATTCAGGAGCAGTC..	AAAAACC..	CAAATGGC..	GTT-AGC..						
<i>Choloepus hoffmanni</i>GTGA-TTCAGGAGAATC..	ATTCAGGAGAATC..	CAAATGGC..	CAAATGGC..	GTT-AGC..						
<i>Myrmecophaga</i>GAGAATTCAGGAGAATC..	ATTTTCACCA..	CAGAAC..	CAAATGGC..	GTT-AGC..						
<i>Tamandua</i>GAGAATTCAGGAGAATC..	ATTTTCACCA..	CAGAAC..	CAAATGGC..	GTT-AGC..						
<i>Cyclopes</i>GTGA-TTCAGGAGAATC..	ATTCAGGAGAATC..	CAAATGGC..	CAAATGGC..	GTT-AGC..						
<i>Dasyprocta</i>GAGAATTCAGGAGAATC..	ATTCAGGAGAATC..	CAAATGGC..	CAAATGGC..	GTT-AGC..						
<i>Tolypterus</i>GAGAATTCAGGAGAATC..	ATTCAGGAGAATC..	CAAATGGC..	CAAATGGC..	GTT-AGC..						
<i>Chaetophractus</i>GAGAATTCAGGAGAATC..	ATTCAGGAGAATC..	CAAATGGC..	CAAATGGC..	GTT-AGC..						
<i>Euphractus</i>GAGAATTCAGGAGAATC..	ATTCAGGAGAATC..	CAAATGGC..	CAAATGGC..	GTT-AGC..						
GAGAATTCAGGAGAATC..	ATTCAGGAGAATC..	CAAATGGC..	CAAATGGC..	GTT-AGC..						

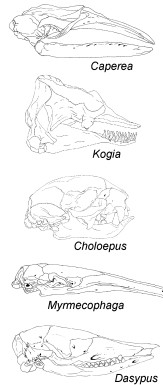


Figure 5.7: Examples of frameshift mutations (insertions blue, deletions red) and premature stop codons in Enamlin in Cetacea and Xenarthra. Figure from MEREDITH *et al.* (2009), licensed under CC BY 4.0.

The protein Enamlin is a key structural protein involved in the outer cap of enamel on teeth. Various mammals have secondarily evolved diets that do not require hard teeth, and so greatly reduced the selection pressure for hard enamel, or even teeth at all. For example, two-toed sloths (*Choloepus*), Pygmy sperm whales (*Kogia*), and aardvark (*Orycteropus*) all lack enamel on teeth. Other mammals have lost their teeth entirely, e.g. giant anteaters (*Myrmecophaga*) and Baleen whales. Due to this relaxation of constraint on the phenotype, the Enamlin gene has accumulated pseudogenizing substitutions such as premature stop codons and frameshift mutations (see Figure 5.7 for examples). MEREDITH *et al.* (2009) sequenced Enamlin across a range of species and found that none of the species with enamel have frameshift mutations in Enamlin, while 17/20 of species that lack enamel or teeth have frameshifts in Enamlin, and all of them carry premature stop codons.

MEREDITH *et al.* (2009) found that the branches of the Enamlin phylogeny with a functional Enamlin gene had an estimated $d_N/d_S = 0.51$, consistent with the protein evolving in a constrained manner. In contrast, the branches with a pseudogenized Enamlin had $d_N/d_S = 1.02$, consistent with the gene evolving a completely unconstrained way. The branches where the gene was likely transitioning from a functional to non-function state, i.e. pre-mutation and mixed, had intermediate values of $d_N/d_S = 0.83 - 0.98$, consistent with a transition from a constrained to unconstrained mode of protein evolution somewhere along these branches of the phylogeny.

Question 2. The Enamlin gene was pseudogenized somewhere along the branch leading to Aardvarks (*Orycteropus afer*), see Figure 5.9. MEREDITH *et al.* (2009) estimated that this branch has a $d_N/d_S = 0.75$

A) Calculate the average constraint against amino-acid changes on

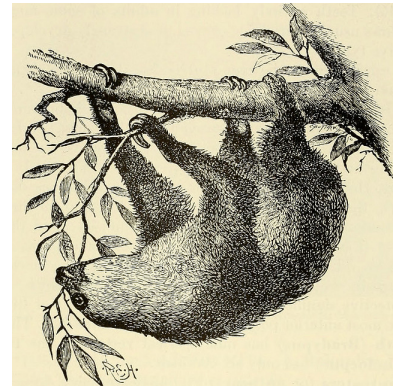


Figure 5.8: Two-toed sloth (*Choloepus hoffmanni*). An introduction to the study of mammals, living and extinct. 1891. Flower W. H. and Lydekker R. Image from the Biodiversity Heritage Library. Contributed by University of Toronto. Not in copyright.

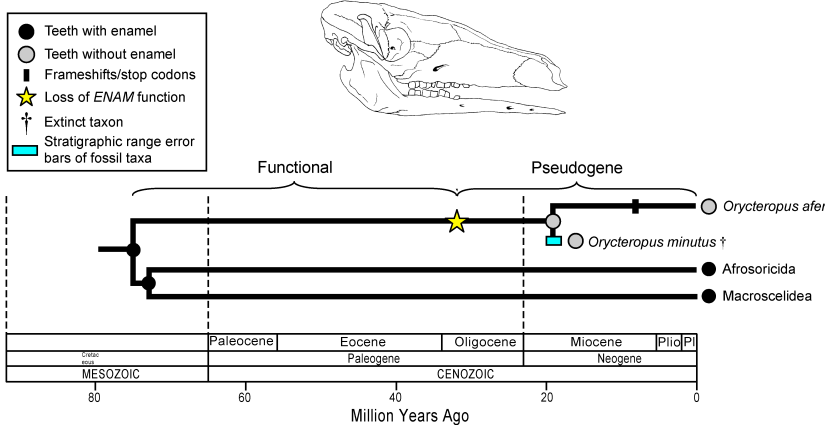


Figure 5.9: A synthetic interpretation of the history of enamel degeneration in *Tubulidentata* (the order of aardvarks) based on fossils, phylogenetics, molecular clocks, frameshift mutations, and d_N/d_S ratios. The oldest fossil aardvarks are *O. minutus* (19 mya) from the early Miocene of Kenya and also lack enamel. Figure & caption modified from MEREDITH *et al.* (2009), licensed under CC BY 4.0.

this branch.

B) Aardvarks last shared a common ancestor with *Afrosoricida* (golden moles, tenrecs) and *Macroselididae* (elephant shrews) around ~ 75.1 million years ago in the Cretaceous. Assume that for the portion of the branch while Enamlin was functional $d_N/d_S = 0.51$ and after it was pseudogenized there was no constraint (i.e. $d_N/d_S = 1$). Based on the branch's average $d_N/d_S = 0.75$, can you estimate the time at which Enamlin was pseudogenized? (I.e. when is the star in Figure 5.9?)

Adaptive evolution and d_N/d_S . Clearly genes are not only subject to neutral and deleterious mutations; beneficial mutations must also arise and fix from time to time. Let's assume that a fraction B of non-synonymous mutations that arise are beneficial such that $2N\mu B$ beneficial mutations arise per generation. Newly arisen beneficial alleles are not destined to fix in the population, as they may be lost to genetic drift when they are rare in the population (we'll discuss how to calculate the fixation probability for beneficial alleles in Chapter 12). A newly arisen beneficial allele reaches fixation in the population with probability f_B from its initial frequency of $1/2N$. This fixation probability may be much higher than that of neutral mutations, but still much less than 1. If $2T$ generations of divergence have elapsed between the two populations then a total of

$$dN = 2T(1 - C - B)\mu + 2T \times (2N\mu B) \times f_B \quad (5.6)$$

non-synonymous substitutions will have accumulated. Then

$$d_N/d_S = (1 - C - B) + 2NBf_B \quad (5.7)$$

assuming again that all synonymous mutations are neutral. Note that this means that our estimates of C using $1 - d_N/d_S$ will be a lower

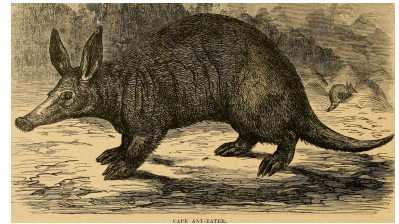


Figure 5.10: Aardvarks (Cape ant-eater, *Orycteropus afer*) Cassell's natural history (1896). Duncan, P. M. Image from the Biodiversity Heritage Library. Contributed by NCSU Libraries. Not in copyright.

bound on the true constraint if even a small fraction of mutations are beneficial. Those cases where the gene is evolving more rapidly at the protein level than at synonymous sites, i.e. $d_N/d_S > 1$, are potentially strong candidates for positive selection rapidly driving change at the protein level. We can identify genes that have d_N/d_S significantly greater than one, either on the complete gene phylogeny, or on particular branches. Note that is a very conservative test that few genes in the genome meet, as many genes that are fixing adaptive non-synonymous substitutions will have $d_N/d_S < 1$; even if adaptive mutations are common, genes may still evolve in a constrained way (i.e. $d_N/d_S < 1$) if the rapid fixation of beneficial mutations due to positive selection is outweighed by the loss of non-synonymous mutations to negative selection.

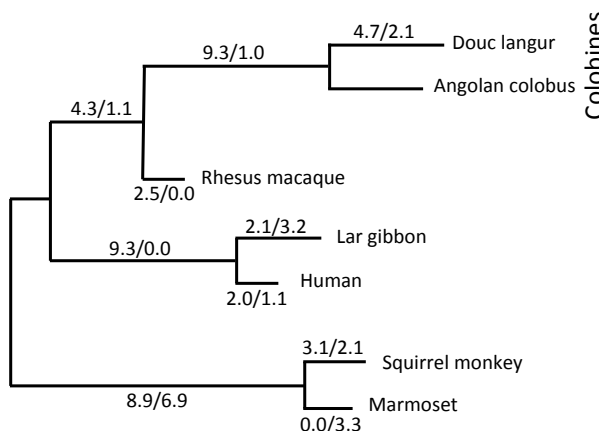


Figure 5.11: A phylogram for the primate lysozyme gene, data from YANG (1998). For each branch, the numbers give the estimated average number of non-synonymous to synonymous changes in the lysozyme protein.

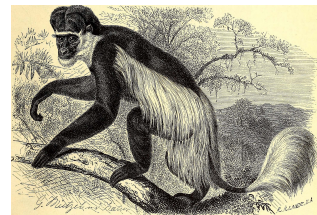


Figure 5.12: Abyssinian black-and-white colobus (*Colobus guereza*). A member of the leaf-eating Colobines. Brehm's Tierleben, Brehm, A.E. 1893. Image from the Biodiversity Heritage Library. Contributed by University of Illinois Urbana-Champaign. Not in copyright.



Figure 5.13: (Hoatzin (*Opisthocomus hoazin*)). A leaf-eating bird. A history of birds (1910) Pycraft, W.P. Image from the Biodiversity Heritage Library. Contributed by American Museum of Natural History Library. Not in copyright.

The McDonald-Kreitman test As noted above, a big issue with using d_N/d_S to detect adaptation is that it is very conservative. For a more powerful test of rapid divergence, what we need to do is adjust for the level of constraint a gene experiences at non-synonymous sites. One way to do this is to use polymorphism data as an internal control. If we see little non-synonymous polymorphism at a gene, but a lot of synonymous polymorphism, we now know that there is likely strong constraint on the gene (i.e. high C), thus we expect d_N/d_S to be low. McDONALD and KREITMAN (1991) devised a simple test of the neutral theory of molecular evolution at a gene based on this intuition (building on the conceptually similar HKA test HUDSON *et al.*, 1987). McDONALD and KREITMAN took the case where we have polymorphism data at a gene for one species and divergence to a closely related species. They partitioned polymorphism and fixed differences in their sample into non-synonymous and synonymous changes:

	Poly.	Fixed
Non-Syn.	P_N	D_N
Syn.	P_S	D_S
Ratio	P_N/P_S	D_N/D_S

Under neutral theory, we expect a smaller number of non-synonymous to synonymous fixed differences ($D_N/D_S < 1$) and exactly the same expectation holds for polymorphism (P_N/P_S). Let's consider a gene with L_S and L_N sites where synonymous and non-synonymous mutations could arise respectively. We can think of the underlying gene genealogy at our gene, see Figure 5.14, with the total time on the coalescent genealogy within the species as T_{tot} and the total time for fixed differences between our species as T'_{div} . Then under neutrality we expect $\mu L_N(1 - C)T_{tot}$ non-synonymous polymorphisms (i.e. our number of segregating sites), and $\mu L_N(1 - C)T'_{div}$ non-synonymous fixed differences. We can then fill out the rest of our table as follows:

	Poly.	Fixed
Non-Syn.	$\mu L_N(1 - C)T_{tot}$	$\mu L_N(1 - C)T'_{div}$
Syn.	$\mu L_S T_{tot}$	$\mu L_S T'_{div}$
Ratio	$L_N(1 - C)/(L_S)$	$L_N(1 - C)/(L_S)$

Therefore, we expect the ratio of non-synonymous to synonymous changes to be the same for polymorphism and divergence under a strict neutral model. We can test this expectation of equal ratios via the standard tests of a 2×2 table. If the ratio of N/S is significantly higher for divergence than polymorphism we have evidence that non-synonymous substitutions are accumulating more rapidly than we would predict given levels of constraint alone.

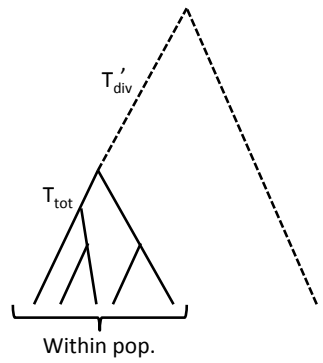


Figure 5.14: An example ogene genealogy for a set of alleles sampled within a population and a single allele sampled from a distantly-related species.

As example of a McDonald-Kreitman (MK) table consider the work of FRENTIU *et al.* (2007) on the molecular evolution of L Photopigment opsin in Admiral (*Limenitis*) butterflies, responsible for colour vision in the long-wavelength part of the visual spectrum. FRENTIU *et al.* found that the sensitivity of this opsin had shifted towards blue in its sensitivity in *L. archippus archippus* (viceroy) compared to *L. arthemis astyanax*. To test whether this molecular evolution reflected positive selection they sequenced 24 *L. arthemis astyanax* individuals and one *L. archippus archippus* sequence. They identified 11 polymorphic sites in *L. arthemis astyanax* and 16 fixed differences, which break down as follows:

	Poly.	Fixed
Non-Syn.	2	12
Syn.	9	4
Ratio	2/9	3/1

Note the strong excess of non-synonymous to synonymous divergence compared to polymorphism (p-value of 0.006, Fisher's exact test), which is consistent with the gene evolving in an adaptive manner among the two species. We would expect roughly only 3 non-synonymous substitutions out of 16 substitutions if the gene was evolving neutrally ($16 \times 2/11$).

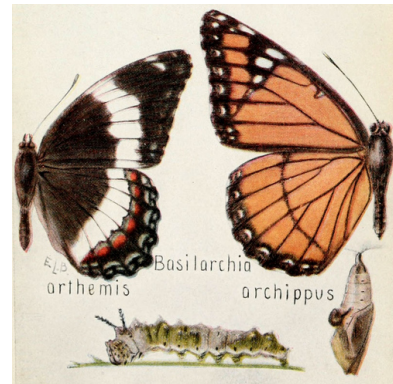


Figure 5.15: White admiral (*Limenitis arthemis*) and Viceroy (*Limenitis archippus*). *Basilarchia* is the old genus that these two species were originally placed in. Viceroy and Monarch butterflies are Müllerian mimics.

Field book of insects (1918). Lutz, F.E. . illustrations by Edna L. Beutenmüller. Image from the Biodiversity Heritage Library. Contributed by MBLWHOI Library. Not in copyright.

6

Neutral Diversity and Population Structure.

How does genetic differentiation build up between closely related populations? How does migration act to reduce differentiation? These questions are key to understand the conditions under which populations can start to genetically diverge from each other. To answer these questions we'll first consider this in the context of neutral alleles, and then return to think about selection and differentiation in later chapters. We've considered neutral alleles drawn from a randomly-mating population, and divergence among alleles drawn from two distantly-related populations. We'll now turn to consider divergence among more closely related populations. In thinking about the coalescent within populations we made the assumption that any pair of lineages is equally likely to coalesce with each other. However, when there is population structure this assumption is violated.

To develop models of about population structure we'll use the statistic F_{ST} , which we introduced in Section 3.0.1 of discussion of summarizing population structure in allele frequencies. We have previously written the measure of population structure F_{ST} as

$$F_{ST} = \frac{H_T - H_S}{H_T} \quad (6.1)$$

where H_S is the probability that two alleles sampled at random from a subpopulation differ, and H_T is the probability that two alleles sampled at random from the total population differ.

6.1 A simple population split model

Imagine a population of constant size of N_e diploid individuals that T generations in the past split into two daughter populations (subpopulations) each of size N_e individuals, which do not subsequently exchange migrants. In the current day we sample an equal number of alleles from both subpopulations.

Consider a pair of alleles sampled within one of our sub-populations and think about their per site heterozygosity. These alleles have expe-

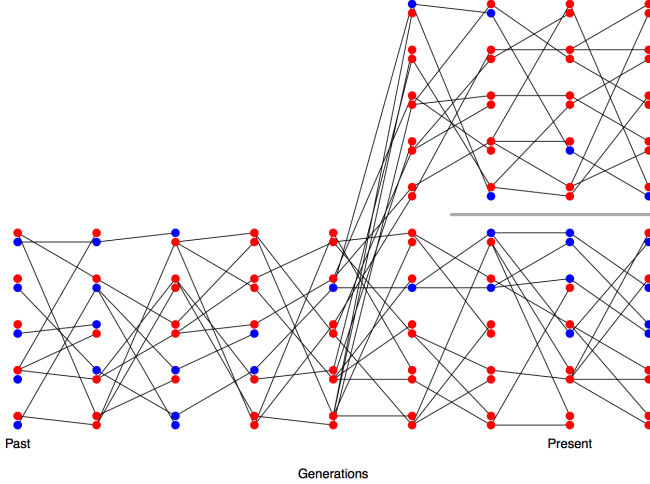


Figure 6.1: Change in allele frequencies following a population split. Code here.

rienced a population of size N_e and so the probability that they differ is $H_S \approx 4N_e\mu$ (assuming that $N_e\mu \ll 1$, using our equation 4.12 for heterozygosity within a population).

The heterozygosity in our total population is a little more tricky to calculate. Assuming that we equally sample both sub-populations, when we draw two alleles from our total sample, 50% of the time they are drawn from the same subpopulation and 50% of the time they are drawn from different subpopulations. Therefore, our total heterozygosity is given by

$$H_T = \frac{1}{2}H_S + \frac{1}{2}H_B \quad (6.2)$$

where H_B is the probability that a pair of alleles drawn from our two different sub-populations differ from each other. A pair of alleles from different sub-populations cannot find a common ancestor with each other for at least T generations into the past as they are in distinct populations (not connected by migration). Once our alleles find themselves back in the combined ancestral population it takes them on average $2N$ generations to coalesce. So the total opportunity for mutation between our pair of alleles sampled from different populations is $2(T + 2N)$ generations of meioses, such that the probability that our pairs of alleles is different is

$$H_B \approx 2\mu(T + 2N) \quad (6.3)$$

We can plug this into our expression for H_T , and then that in turn into F_{ST} . Doing so we find that

$$F_{ST} \approx \frac{\mu T}{\mu T + 4N_e\mu} = \frac{T}{T + 4N_e} \quad (6.4)$$

Note that μ cancels out of this equation. In this simple toy model, F_{ST} is increasing because the amount of between-population diversity increases with the divergence time of the two populations (initially linearly with T). F_{ST} grows at a rate given by $T/(4N_e)$ so that differentiation will be higher between populations separated by long divergence times or with small effective population sizes.

Question 1. The genome-wide F_{ST} between Bornean and Sumatran orangutan species samples (*Pongo pygmaeus* and *Pongo abelii*) is ≈ 0.37 (LOCKE *et al.*, 2011), representing a deep population split between the species (potentially with little subsequent gene flow). Within the populations the genome-wide average Watterson's θ is $\theta_W = 1.4\text{kb}^{-1}$, estimated from the number of segregating sites. Assume a generation time of 20 years, and a mutation rate of 2×10^{-8} per base per generation. How far in the past did the two populations diverge?

6.2 A simple model of migration between an island and the mainland.

We can also use the coalescent to think about patterns of differentiation under a simple model of migration-drift equilibrium. Let's consider a small island population that is relatively isolated from a large mainland population, where both of these populations are constant in size. We'll assume that the expected heterozygosity for a pair of alleles sampled on the mainland is H_M .

Our island has a population size N_I that is very small compared to our mainland population. Each generation some low fraction m of our individuals on the island have migrant parents from the mainland the generation before. Our island may also send migrants back to the mainland, but these are a drop in the ocean compared to the large population size on the mainland and their effect can be ignored.

If we sample an allele on the island and trace its ancestral lineage backward in time, each generation our ancestral allele has a low probability m of being descended from the mainland in the preceding generation (if we go back far enough the allele eventually has to be descended from an allele on the mainland). The probability that a pair of alleles sampled on the island are descended from a shared recent common ancestral allele on the island is the probability that our pair of alleles coalesces before either lineage migrates. For example, the probability that our pair of alleles coalesces $t + 1$ generations back on the island is

$$\frac{1}{2N_I}(1-m)^{2(t+1)} \left(1 - \frac{1}{2N_I}\right)^t \approx \frac{1}{2N_I} \exp\left(-t\left(\frac{1}{2N_I} + 2m\right)\right), \quad (6.5)$$

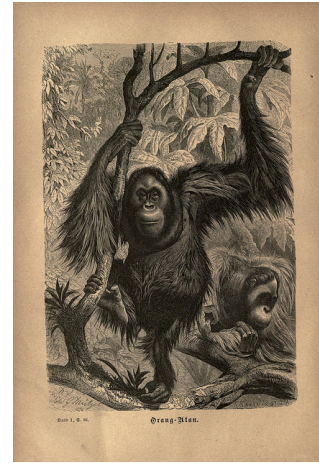


Figure 6.2: Orangutan (*Pongo*).
Brehms thierleben, allgemeine kunde des thierreichs. Brehm, A. E. Image from the Biodiversity Heritage Library. Contributed by MBLWHOI Library. Not in copyright.

with the approximation following from assuming that $m \ll 1$ & $\frac{1}{(2N_I)} \ll 1$ (note that this is very similar to our derivation of heterozygosity above). The probability that our alleles coalesce before either one of them migrates off the island, irrespective of the time, is

$$\int_0^\infty \frac{1}{2N_I} \exp\left(-t\left(\frac{1}{2N_I} + 2m\right)\right) dt = \frac{1/(2N_I)}{1/(2N_I) + 2m}. \quad (6.6)$$

Let's assume that the mutation rate is very low such that it is very unlikely that the pair of alleles mutate before they coalesce on the island. Therefore, the only way that the alleles can be different from each other is if one or other of them migrates to the mainland, which happens with probability

$$1 - \frac{1/(2N_I)}{1/(2N_I) + 2m} \quad (6.7)$$

Conditional on one or other of our alleles migrating to the mainland, both of our alleles represent independent draws from the mainland and so differ from each other with probability H_M . Therefore, the level of heterozygosity on the island is given by

$$H_I = \left(1 - \frac{1/(2N_I)}{1/(2N_I) + 2m}\right) H_M \quad (6.8)$$

So the reduction of heterozygosity on the island compared to the mainland is

$$F_{IM} = 1 - \frac{H_I}{H_M} = \frac{1/(2N_I)}{1/(2N_I) + 2m} = \frac{1}{1 + 4N_I m}. \quad (6.9)$$

The level of inbreeding on the island compared to the mainland will be high if the migration rate is low and the effective population size of the island is low, as allele frequencies on the island are drifting and diversity on the island is not being replenished by migration. The key parameter here is the number individuals on the island replaced by immigrants from the mainland each generation ($N_I m$).

We have framed this problem as being about the reduction in genetic diversity on the island compared to the mainland. However, if we consider collecting individuals on the island and mainland in proportion to their population sizes, the total level of heterozygosity would be $H_T = H_M$, as samples from our mainland would greatly outnumber those from our island. Therefore, considering the island as our sub-population, we have derived another simple model of F_{ST} .

Question 2. You are investigating a small river population of sticklebacks, which receives infrequent migrants from a very large marine population. At a set of putatively neutral biallelic markers the freshwater population has frequencies:

0.2, 0.7, 0.8

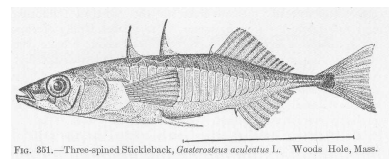


Figure 6.3: Three-spined stickleback (*Gasterosteus aculeatus*).
Jordan, David Starr (1907) Fishes, New York City, NY: Henry Holt and Company. Image from Wikimedia Commons Public domain.

at the same markers the marine population has frequencies:
0.4, 0.5 and 0.7.

From studying patterns of heterozygosity at a large collection of markers, you have estimated the long term effective size of your freshwater population is 2000 individuals.

What is your estimate of the migration rate from the marine populations into the river?

6.3 Incomplete Lineage Sorting

Finally we turn to the interaction of Because it can take a long time for an polymorphism to drift up or down in frequency, multiple population splits may occur during the time an allele is still segregating. This can lead to incongruence between the overall population tree and the information about relationships present at individual loci. In Figure 6.4 and 6.5 we show a simulation of three populations where the bottom population splits off from the other two first, followed by the subsequent splitting of the the top and the middle populations. We start both simulations with a newly introduced red allele being polymorphic in the combined ancestral population. The most likely fate of this allele is that it is quickly lost from the population, but sometimes the allele can drift up in frequency and be polymorphic when the populations split, as the allele in our two figures has done. If the allele is lost/fixed in the descendant populations before the next population split, our allele configuration will agree with the population tree, as it does in Figure 6.4, and so too the gene tree will agree with population tree (as shown in the left side of Figure 6.6). However, if the allele persists as a polymorphism in the ancestral population until the top and the middle populations split, then the allele could fix in one of these populations and not the other. Such an event leads to a substitution pattern that disagrees with the population tree, as in Figure 6.5. If we were to construct a phylogeny using the variation at this site we would see a disagreement between the gene tree and population tree. In Figure 6.5 an allele drawn from the top and the bottom populations are necessarily more closely related to each other than either is to an allele drawn from population 2; tracing our allelic lineages from the top and bottom populations back through time, they must coalesce with each other before we reach the point where the red mutation arose; in contrast, a lineage from the middle population cannot have coalesced with either other lineage until past the time the red mutation arose. An example of this ‘incomplete lineage sorting’ in terms of the underlying tree is shown on the right side of Figure 6.6.

A natural pedigree analogy to incomplete lineage sorting is the fact that while two biological siblings are more closely related to each other

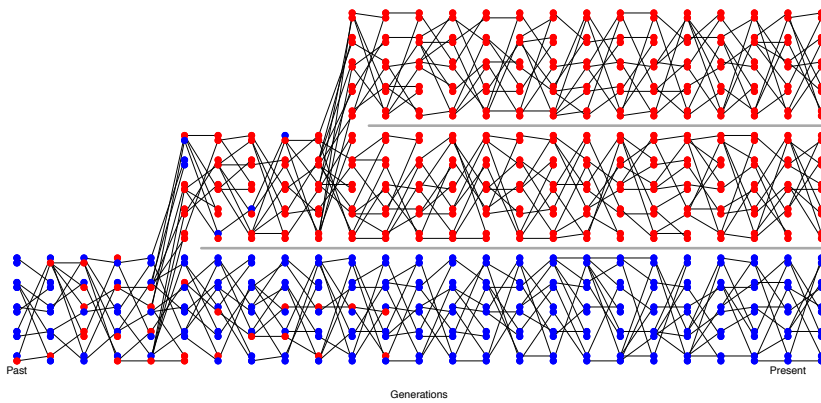


Figure 6.4: An example of alleles assorting among three populations such that there is no incomplete lineage sorting. [Code here.](#)

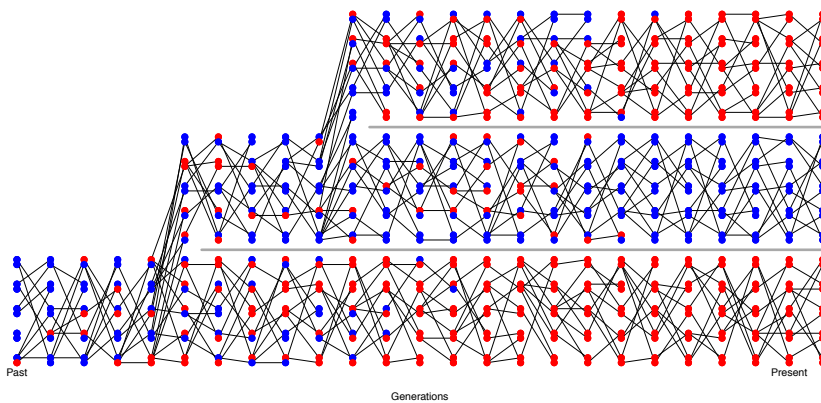


Figure 6.5: An example of alleles assorting among three populations leading to incomplete lineage sorting. [Code here.](#)



Figure 6.6: The population tree of three populations ((A, B), C) is shown blocked out with black shapes. Two different coalescent trees relating a single allele drawn from A, B, and C are shown with thinner lines.

genealogically than either is to their cousin, at any given locus one of the siblings can share an allele IBD with their cousin that they do not share with their own sibling, due to the randomness of Mendelian segregation down their pedigree. In these cases, the average relatedness of the individuals/populations disagrees with the patterns of relatedness at a particular locus.

As an empirical example of incomplete lineage sorting, let's consider the work of JENNINGS and EDWARDS (2005) who sequenced a single allele from three different species of Australian grass finches (*Poephila*): two sister species of long-tailed finches (*Poephila acuticauda* and *P. hecki*) and the black-throated finch (*Poephila cincta*, see Figure 6.7). They collected sequence data for 30 genes, and constructed phylogenetic gene trees at each of these loci, resulting in 28 well-resolved gene trees. 16 of the gene trees showed *P. acuticauda* and *P. hecki* as sisters with *P. cincta* (the tree ((A,H),C)), while for twelve genes the gene tree was discordant with the population tree: for seven of their genes *P. hecki* fell as an outgroup to the other two and at five *P. acuticauda* fell as an outgroup (the trees ((A,C),H) and ((H,C),A) respectively).

Let's use the coalescent to understand this discordance between gene trees and species trees. Let's assume that two sister populations (A & B) split t_1 generations in the past, with a deeper split from a third outgroup population (C) t_2 generations in the past. We'll assume that there's no gene flow among our populations after each split. We can trace back the ancestral lineages of our three alleles. The first opportunity for the A & B lineages to coalesce is t_1 generations ago. If they coalesce with each other in their shared ancestral population before t_2 in the past (left side of Figure 6.6) their gene tree will definitely agree with the population tree. So the only way for the gene tree to disagree with the population tree is for the A & B lineages to fail to coalesce in their shared ancestral population between t_1 and t_2 ; this happens with probability $(1 - 1/2N)^{t_2 - t_1}$. We'll get a discordant gene tree if A & B make it back to the shared ancestral population with C without coalescing, and then one or the other of them coalesces with the C lineage before they coalesce with each other. This happens with probability 2/3, as at the first pairwise-coalescent event there are three possible pairs of lineages that could coalesce, two of which (A & C and B & C) result in a discordant tree. So the probability that we get a coalescent tree that is discordant with the population tree is

$$\frac{2}{3} (1 - 1/2N)^{t_2 - t_1}. \quad (6.10)$$

This equation allows us to relate the fraction of loci showing incomplete lineage sorting to the population genetics parameters of the ancestral population.

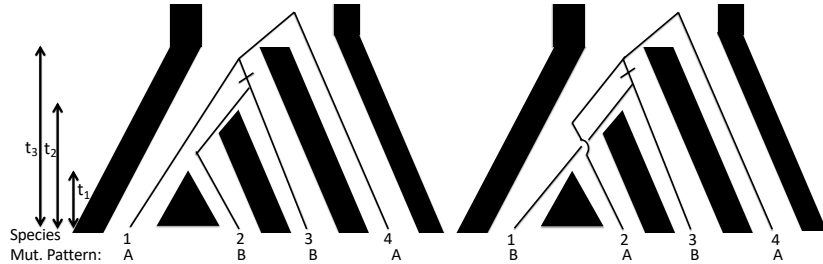


Figure 6.7: Banded Grass Finch (*P. cincta*). Illustration by Elizabeth Gould.
Birds of Australia Gould J. 1840. CC BY 4.0 uploaded to Flickr by rawpixel.com.

Question 3. Let's return to JENNINGS and EDWARDS's Australian grass finches example. They estimated that the ancestral population size of our two long-tailed finches was four hundred thousand. What is your best estimate of the inter-speciation time, i.e. $t_2 - t_1$?

The fraction of loci showing ILS, eqn (6.10), depends on the times between population splits ($t_2 - t_1$) Thus we should expect gene-tree population-tree discordance when populations split in rapid succession and/or population sizes are large.

Testing for gene flow. We often want to test whether gene flow has occurred between populations. For example, we might want to establish a case that interbreeding between humans and Neanderthals occurred or demonstrate that gene flow occurred after two populations began to speciate. A broad range of methods have been designed to test for gene flow and to estimate gene flow rates based on neutral expectations. Here we'll briefly just discuss one method based on some simple coalescent ideas. Above we assumed that gene-tree population-tree discordance was due to incomplete lineage sorting due to populations rapidly splitting. However, gene flow among populations can also lead to gene-tree discordance. While both ILS and gene flow can lead to discordance, under simplifying assumptions, ILS implies more symmetry in how these discordances manifest themselves.



Take a look at Figure 6.8. In both cases the lineages from A and B fail to coalesce in their initial shared ancestral population, and one or the other of them coalesces with the lineage from C before they coalesce with each other. Each option is equally likely; therefore the mutational patterns ABBA and BABA are equally likely to occur under ILS.¹

However, if gene flow occurs from population C into population B, in addition to ILS the lineage from B can more recently coalesce with the lineage from C, and so we should see more ABBAAs than BABAs. To test for this effect of gene flow, we can sample a sequence from each of our 4 populations and count up the number of sites that show the two mutational patterns consistent with the gene-tree discordance

Figure 6.8: In both the left and right trees ILS has occurred between our single lineages sampled from populations A, B, and C. Imagine that population D is a somewhat distant outgroup such that the lineages from A through C (nearly) always coalesce with each other before any coalescence with D. The small dash on the branch indicates the mutation A → B occurring, giving rise to the ABBA or BABA mutational pattern shown at the bottom.

¹ Here we have to assume no structure in the ancestral population.

n_{ABBA} and n_{BABA} and calculate

$$\frac{n_{ABBA} - n_{BABA}}{n_{ABBA} + n_{BABA}} \quad (6.11)$$

This statistic will have expectation zero if the gene-tree discordance is due to ILS and will be skewed negative if gene flow occurred from C into B (and skewed positive if gene flow occurred from C into A).

7

Phenotypic Variation and the Resemblance Between Relatives

THE DISTINCTION BETWEEN GENOTYPE AND PHENOTYPE is one of the most useful ideas in Biology.¹ The genotype of an individual (the genome), for most purposes, is decided when the gametes fuse to form a zygote (individual). The phenotype of an individual represents any measurable aspect of an organism.

Your height, to the amount of RNA transcribed from a given gene, to what you ate last Tuesday: all of these are phenotypes. Nearly any phenotype we can choose to measure about an organism represents the outcome of the information encoded by their genome played out through an incredibly complicated developmental, physiological and/or behavioural processes that in turn interact with a myriad of environmental and stochastic factors. Honestly it boggles the mind how organisms work as well as they do, let alone that I managed to eat lunch last Tuesday.

There are many different ways to think about studying the path from genotype through to phenotype. The one we will take here is to think about how phenotypic variation among individuals in a population arises as a result of genetic variation in the population. One simple way to measure this genotype-phenotype relationship is to calculate the phenotypic mean for each genotype at a locus. For example, WANG *et al.* (2018) explored the genetic basis of budset time in European aspen (*Populus tremula*); the effect of one specific SNP on that phenotype is shown in Figure 7.2. Budset timing is a key trait underlying local adaptation to varying growing season length. The associated SNP falls in a gene (*PtFT2*) that is known to play a strong role in flowering time regulation in other plants.

One way for us to assess the relationship between genotype and phenotype is to find the best fitting linear line through the data, i.e. fit a linear regression of phenotypes for our individuals on their geno-

¹ JOHANNSEN, W., 1911 The Genotype Conception of Heredity. *The American Naturalist* 45(531): 129–159



Figure 7.1: European aspen *P. tremula*. H. Schacht. 1860. BHL Image from the Biodiversity Heritage Library. Contributed by The Library of Congress. Not in copyright.

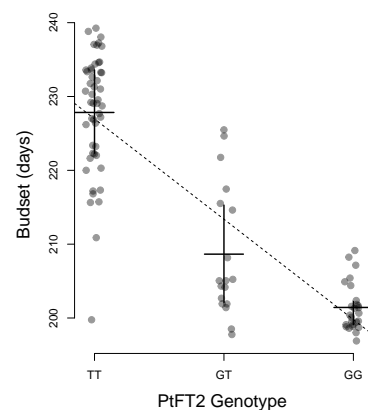


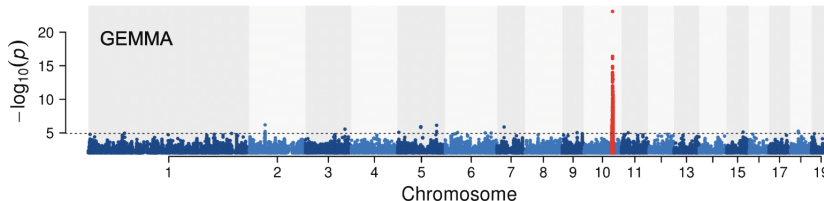
Figure 7.2: The effect of a flowering time gene (*PtFT2*) SNP on budset time in European aspen. Each dot gives the genotype-phenotype combination for an individual. The horizontal lines give the budset mean for each genotype and the vertical lines show the inter-quartile range. The dotted line gives the linear regression of phenotype on genotype. Thanks to Pär Ingvarsson for sharing these data from WANG *et al.* (2018).

types at a particular SNP (l):

$$X \sim \mu + a_l G_l \quad (7.1)$$

In the equation above, X is a vector of the phenotypes of a set of individuals and G_l is our vector of genotypes at locus l , with $G_{i,l}$ taking the value 0, 1, or 2 depending on whether our individual i is homozygote, heterozygote, or the alternate homozygote at our locus of interest. Here μ is our phenotypic mean. The slope of this regression line (a_l) has the interpretation of being the average effect of substituting a copy of allele 2 for a copy of allele 1. In our Aspen example the slope is -13.6 , i.e. swapping a single T for a G allele moves the budset forward by 13.6 days, such that the GG homozygote is predicted to set buds 27.2 days earlier than the TT homozygote.

As a measure of the significance of this genotype-phenotype relationship, we can calculate the p-value of our regression. To try and identify loci that are associated with our trait genome-wide, we can conduct this regression at each SNP we genotype in the genome. One common way to display the results of such an analysis (called a genome-wide association study or GWAS for short) is to plot the logarithm of the p-value for each SNP along genome (a so-called Manhattan plot). Here's one from WANG *et al.* (2018) for their Aspen budset phenotype



The SNP with the most significant p-value is the PtFT2 SNP. Note that other SNPs in the surrounding region also light up as showing a significant association with budset timing. This is because loci that are in LD with a functional locus may in turn show an association, not because they directly affect the phenotype, but simply because the genotypes at the two loci are themselves non-randomly associated. Below is a zoomed in version (Figure 2 in WANG *et al.* (2018)) with SNPs coloured by the strength of their LD with the putatively functional SNP. Note how SNPs in strong LD with the functional allele (redder points) have more significant p-values.

Variation in some traits seems to have a relatively simple genetic basis. In our Aspen example there is one clear large-effect locus, which explains 62% of the variation in budset. Note that even in this case, where we have an allele with a very strong effect on a phenotype, this

We'll encounter linear regressions at various points during the next few chapters, see the math appendix around eqn A.43 for more background details.

Figure 7.3: Manhattan plot of the p-value of the linear association between genotype and budset in Aspen. Each dot represents the test at a single SNP, plotted at its physical coordinate in the genome. Different chromosomes are plotted in alternating colours. The SNPs surrounding the PtFT2 gene are shown in red. From WANG *et al.* (2018), licensed under CC BY 4.0.

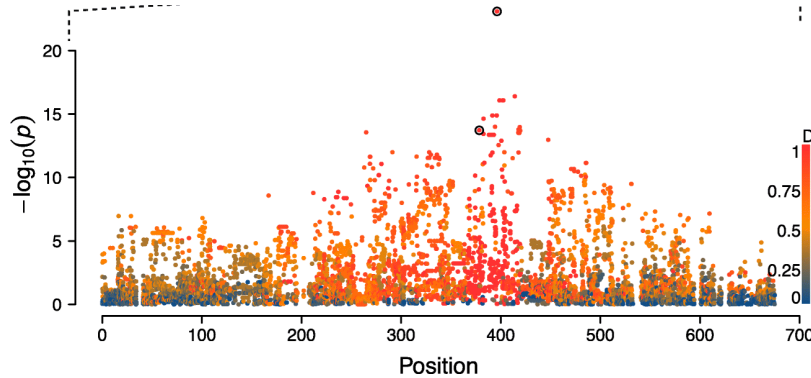


Figure 7.4: The Manhattan plot zoomed in on the top-hit (red SNPs from Figure 7.3). SNPs are now coloured by their D/t value with the most significant SNP. D/t is the LD covariance between a pair of loci (D , eqn (3.16)) normalized by the largest value D can take given the allele frequencies. Figure from WANG *et al.* (2018), licensed under CC BY 4.0.

is not an allele *for* budset, nor is PtFT2 a gene *for* budset. It is an allele that is associated with budset in the sampled environments and populations. In a different set of environments, this allele's effects may be far smaller, and a different set of alleles may contribute to phenotype variation. PtFT2, the gene our focal SNP falls close to, is just one of many genes and molecular pathways involved in budset. A mutant screen for budset may uncover many genes with larger effects; this gene is just a locus that happens to be polymorphic in this particular set of genotyped individuals.

While phenotypic variation for some phenotypes has a relatively simple genetic basis, many phenotypes are likely much more genetically complex, involving the functional effect of many alleles at hundreds or thousands of polymorphic loci. For example hundreds of small effect loci affecting human height have been mapped in European populations to date. Such genetically complex traits are called polygenic traits.

In this chapter, we will use our understanding of the sharing of alleles between relatives to understand the phenotypic resemblance between relatives in quantitative phenotypes. This will allow us to understand the contribution of genetic variation to phenotypic variation. In the next chapter, we will then use these results to understand the evolutionary change in quantitative phenotypes in response to selection.

7.0.1 A simple additive model of a trait

Let's imagine that the genetic component of the variation in our trait is controlled by L autosomal loci that act in an additive manner. The frequency of allele 1 at locus l is p_l , with each copy of allele 1 at this locus increasing your trait value by a_l above the population mean. The phenotype of an individual, let's call her i , is X_i . Her genotype at SNP l is $G_{i,l}$. Here $G_{i,l} = 0, 1$, or 2 , representing the number of

"All that we mean when we speak of a gene [allele] for pink eyes is, a gene which differentiates a pink eyed fly from a normal one —not a gene [allele] which produces pink eyes per se, for the character pink eyes is dependent on the action of many other genes." - STURTEVANT (1915)

copies of allele 1 she has at this SNP. Her expected phenotype, given her genotype at all L SNPs, is then

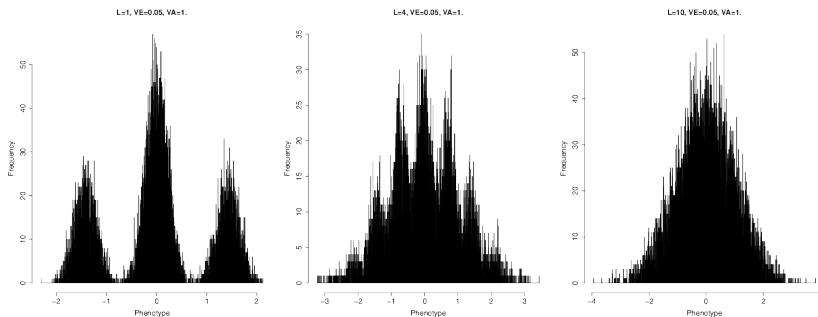
$$\mathbb{E}(X_i|G_{i,1}, \dots, G_{i,L}) = \mu + X_{A,i} = \mu + \sum_{l=1}^L G_{i,l}a_l \quad (7.2)$$

where μ is the mean phenotype in our population, and $X_{A,i}$ is the deviation away from the mean phenotype due to her genotype. Now in reality the phenotype is a function of the expression of those alleles in a particular environment. Therefore, we can think of this expected phenotype as being an average across a set of environments that occur in the population.

When we measure our individual's observed phenotype we see

$$X_i = \mu + X_{A,i} + X_{E,i} \quad (7.3)$$

where X_E is the deviation from the mean phenotype due to the environment. This X_E includes the systematic effects of the environment our individual finds herself in and all of the noise during development, growth, and the various random insults that life throws at our individual. If a reasonable number of loci contribute to variation in our trait then we can approximate the distribution of $X_{A,i}$ by a normal distribution due to the central limit theorem (see Figure 7.5).² Thus if we can approximate the distribution of the effect of environmental variation on our trait ($X_{E,i}$) also by a normal distribution, which is reasonable as there are many small environmental effects, then the distribution of phenotypes within the population (X_i) will be normally distributed (see Figure 7.5).



Note that as this is an additive model; we can decompose eqn. 7.3 into the effects of the two alleles at each locus and rewrite it as

$$X_i = \mu + X_{iM} + X_{iP} + X_{iE} \quad (7.4)$$

where X_{iM} and X_{iP} are the contribution to the phenotype of the alleles that our individual received from her mother (maternal alleles) and

² The central limit theory is discussed briefly in the math appendix section A.2.5.

Figure 7.5: The convergence of the phenotypic distribution to a normal distribution. Each of the three histograms shows the distribution of the phenotype in a large sample, for increasingly large numbers of loci ($L = 1, 4$, and 10 , with the proportion of variance explained held at $V_A = 1$). I have simulated each individual's phenotype following equations 7.2 and 7.3. Specifically, we've simulated each individual's biallelic genotype at L loci, assuming Hardy-Weinberg proportions and that the allele is at 50% frequency. We assume that all of the alleles have equal effects and combine them additively together. We then add an environmental contribution, which is normally distributed with variance 0.05. Note that in the left two pictures you can see peaks corresponding to different genotypes due to our low environmental noise (in practice we can rarely see such peaks for real quantitative phenotypes). Code here.

father (paternal alleles) respectively. This will come in handy in just a moment when we start thinking about the phenotypic covariance of relatives.

Now obviously this model seems silly at first sight as alleles don't only act in an additive manner, as they interact with alleles at the same loci (dominance) and at different loci (epistasis). Later we'll relax this assumption, however, we'll find that if we are interested in evolutionary change over short time-scales it is actually only the "additive component" of genetic variation that will (usually) concern us. We will define this more formally later on, but for the moment we can offer the intuition that parents only get to pass on a single allele at each locus on to the next generation. As such, it is the effect of these transmitted alleles, averaged over possible matings, that is an individual's average contribution to the next generation (i.e. the additive effect of the alleles that their genotype consists of).

7.0.2 Additive genetic variance and heritability

As we are talking about an additive genetic model, we'll talk about the additive genetic variance (V_A), the phenotypic variance due to the additive effects of segregating genetic variation. This is a subset of the total genetic variance if we allow for non-additive effects.

The variance of our phenotype across individuals (V) we can write as

$$V = \text{Var}(X_A) + \text{Var}(X_E) = V_A + V_E \quad (7.5)$$

In writing the phenotypic variance as a sum of the additive and environmental contributions, we are assuming that there is no covariance between $X_{G,i}$ and $X_{E,i}$ i.e. there is no covariance between genotype and environment.³

Our additive genetic variance can be written as

$$V_A = \sum_{l=1}^L \text{Var}(G_{i,l}a_l) \quad (7.6)$$

where $\text{Var}(G_{i,l}a_l)$ is the contribution of locus l to the additive variance among individuals. Assuming random mating, and that our loci are in linkage equilibrium, we can write our additive genetic variance as

$$V_A = \sum_{l=1}^L a_l^2 2p_l(1 - p_l) \quad (7.7)$$

where the $2p_l(1 - p_l)$ term follows from the binomial sampling of two alleles per individual at each locus.⁴

Question 1. You have two biallelic SNPs contributing to variance in human height. At the first SNP you have an allele with an additive

³ In this section we're making use of the properties of the variance of a random variable, see math appendix eqn (A.25)

⁴ These results follow from the properties of variance in math appendix eqn (A.25).

effect of 5cm which is found at a frequency of 1/10,000. At the second SNP you have an allele with an additive effect of -0.5cm segregating at 50% frequency. Which SNP contributes more to the additive genetic variance? Explain the intuition of your answer.

An example of the additive basis of variation using polygenic scores.

Now we don't usually get to see the individual loci contributing to highly polygenic traits. Instead, we only get to see the distribution of the trait in the population. However, with the advent of GWAS in human genetics we can see some of the underlying genetics using the many trait-associated loci identified to date. Using the estimated effect sizes at each locus, each one of which is tiny, we can calculate the weighted sum over an individual's genotype as in equation 7.2. This weighted sum is called the individual's polygenic score. To illustrate how polygenic scores work, we can take a set of 1700 SNPs⁵. The effects of these SNPs are tiny; the median, absolute additive effect size is 0.07cm. Figure 7.6 shows the distribution of a thousand individuals' polygenic scores calculated using these 1700 SNPs (simulated genotypes using the UKBB frequencies). The standard deviation of these polygenic scores $\sim 2\text{cm}$. The individuals with higher polygenic scores for height are predicted to be taller than the individuals with lower polygenic scores.

⁵ each chosen as the SNP with the strongest signal of association with height in 1700 roughly independent bins spaced across the genome

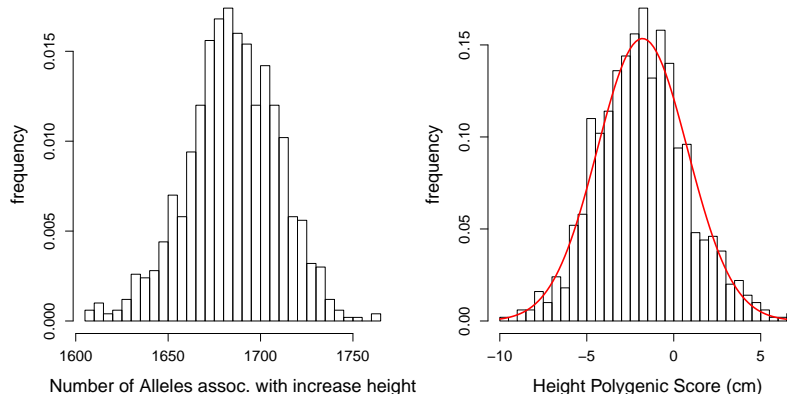


Figure 7.6: **Left)** The distribution of the number of height-increasing alleles that individuals carry at 1700 SNPs associated with height in the UK Biobank, for a sample of 1000 individuals. **right)** The distribution of the polygenic scores for these 1000 individuals. Plotted on top is a normal distribution with the same mean and variance. The empirical variance of these polygenic scores is 0.13, the additive genetic variance calculated by equation (7.7) is 0.135, so the two are in good agreement. Code here.

The narrow sense heritability We would like a way to think about what proportion of the variation in our phenotype across individuals is due to genetic differences as opposed to environmental differences. Such a quantity will be key in helping us think about the evolution of phenotypes. For example, if variation in our phenotype had no genetic

basis, then no matter how much selection changes the mean phenotype within a generation the trait will not change over generations.

We'll call the proportion of the variance that is genetic the *heritability*, and denote it by h^2 . We can then write heritability as

$$h^2 = \frac{Var(X_A)}{V} = \frac{V_A}{V} \quad (7.8)$$

Remember that we are thinking about a trait where all of the alleles act in a perfectly additive manner. In this case our heritability h^2 is referred to as the *narrow sense heritability*, the proportion of the variance explained by the additive effect of our loci. When we allow dominance and epistasis into our model, we'll also have to define the *broad sense heritability* (the total proportion of the phenotypic variance attributable to genetic variation).

The narrow sense heritability of a trait is a useful quantity; indeed we'll see shortly that it is exactly what we need to understand the evolutionary response to selection on a quantitative phenotype. We can calculate the narrow sense heritability by using the resemblance between relatives. For example, if the phenotypic differences between individuals in our population were solely determined by environmental differences experienced by these different individuals, we should not expect relatives to resemble each other any more than random individuals drawn from the population. Now the obvious caveat here is that relatives also share an environment, so may resemble each other due to shared environmental effects.

Note that the heritability is a property of a sample from the population in a particular set of environments at a particular time. Changes in the environment may change the phenotypic variance. Changes in the environment may also change how our genetic alleles are expressed through development and so change V_A . Thus estimates of heritability are not transferable across environments or populations.

7.0.3 The covariance between relatives

People have long been fascinated by the resemblance between relatives, particularly twins (see Figure 7.7). Families hold a special place in quantitative genetics, as remarkably we can use the resemblance between relatives to directly estimate the heritability and covariance of traits. To see this we can calculate the covariance in phenotype between two individuals (1 and 2) who have phenotypes X_1 and X_2 respectively.⁶ To think about imagine plotting the phenotypes of, say, sisters against each other. The x and y coordinates of each point will be the, say, heights of the pair of siblings. Do tall women tend to have tall sisters, do short women tend to have short sisters? How much do their phenotypes covary. If some of the variation in our phenotype is

⁶ We'll be dealing with covariance a lot this chapter, see math appendix section A.2.5 for more background.

genetic we expect identical twins to resemble each other more than full siblings, who in turn will resemble each other more than half-sibs and so on out (see Figure 7.8). Under our simple additive model of phenotypes we can write the covariance as

$$\text{Cov}(X_1, X_2) = \text{Cov}((X_{1M} + X_{1P} + X_{1E}), ((X_{2M} + X_{2P} + X_{2E})) \quad (7.9)$$

We can expand this out in terms of the covariance between the various components in these sums.



Figure 7.7: The Cholmondeley Ladies. Unknown British Painter, circa 1600. Inscription on bottom left of the painting “Two Ladies of the Cholmondeley Family, Who were born the same day, Married the same day, And brought to Bed the same day.” The ladies are thought to be twin sisters, but there’s a clue that they’re not identical twins. Can you spot it?

Image from Wikimedia, considered public domain in the United States, UK Tate ©Creative Commons CC-BY-NC-ND (3.0 Unported)

To make our task easier, we will make two commonly made assumptions:

1. We can ignore the covariance of the environments between individuals (i.e. $\text{Cov}(X_{1E}, X_{2E}) = 0$)
2. We can ignore the covariance between the environment of one individual and the genetic variation in another individual (i.e. $\text{Cov}(X_{1E}, (X_{2M} + X_{2P})) = 0$). (We can actually incorporate these effects in later if we choose too.)

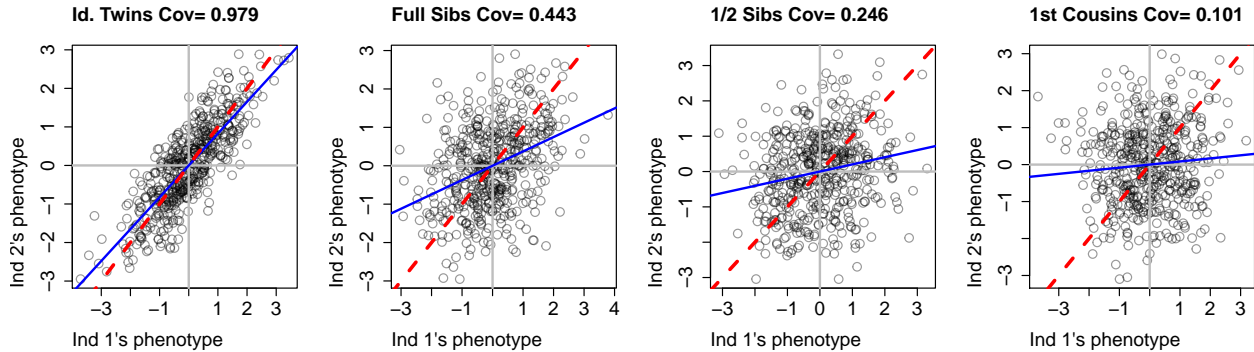
The failure of these assumptions to hold can undermine our estimates of heritability, but we’ll return to that later. Moving forward with these assumptions, we can simplify our original expression above and write our phenotypic covariance between our pair of individuals as

$$\text{Cov}(X_1, X_2) = \text{Cov}((X_{1M}, X_{2M}) + \text{Cov}(X_{1M}, X_{2P}) + \text{Cov}(X_{1P}, X_{2M}) + \text{Cov}(X_{1P}, X_{2P}) \quad (7.10)$$

This equation is saying that, under our simple additive model, we can see the covariance in phenotypes between individuals as the covariance between the maternal and paternal allelic effects in our individuals.

We can use our results about the sharing of alleles between relatives to

obtain these covariance terms. But before we write down the general case, let's quickly work through some examples.



The covariance between identical twins Let's first consider the case of a pair of identical twins, monozygotic twins, from two unrelated parents. Our pair of twins share their maternal and paternal allele identical by descent ($X_{1M} = X_{2M}$ and $X_{1P} = X_{2P}$). As their maternal and paternal alleles are not correlated draws from the population, i.e. have no probability of being *IBD* as we've said the parents are unrelated, the covariance between their effects on the phenotype is zero (i.e. $Cov(X_{1P}, X_{2M}) = Cov(X_{1M}, X_{2P}) = 0$). In that case, eqn. 7.10 is

$$Cov(X_1, X_2) = Cov((X_{1M}, X_{2M}) + Cov(X_{1P}, X_{2P}) = 2Var(X_{1M}) = V_A \quad (7.11)$$

To calculate the narrow sense heritability we could then in principal divide the covariance of our pairs of MZ twins (MZ_1 and MZ_2) by the trait variance to give

$$h^2 = \frac{Cov(MZ_1, MZ_2)}{V} = \rho_{MZ} \quad (7.12)$$

where ρ_{MZ} is the correlation of pairs of MZ twins (see Appendix eqn (A.42) for more on correlations). For example, we could estimate the heritability of a measure of body from the MZ correlation in Figure 7.9. In general, this simple estimator isn't great as the correlation of identical twins includes the effects of the shared family environment of the twins (i.e. $Cov(X_{1E}, X_{2E})$).

Moreover, it can be inflated by non-additive effects as identical twins don't just share alleles, they share their entire genotypes, and thus resemble each other in phenotype also because of shared dominance effects (we'll discuss non-additive effects in Section 7.1.1).

Figure 7.8: Covariance of phenotypes between pairs of individuals of a given relatedness. Each point gives the phenotypes of a different pair of individuals. The additive genetic variance is held constant at $V_A = 1$, such that the expected covariances ($2F_{1,2}V_A$) should be 1, 0.5, 0.25, and 0.125 respectively in good agreement with the empirical covariances reported in the title of each graph. The data were simulated as described in the caption of Figure 7.5. The blue line shows $x = y$ and the red line shows the best fitting linear regression line. Code here.

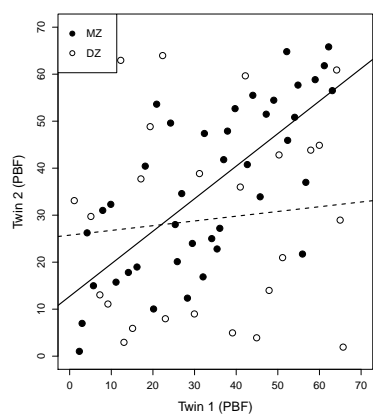
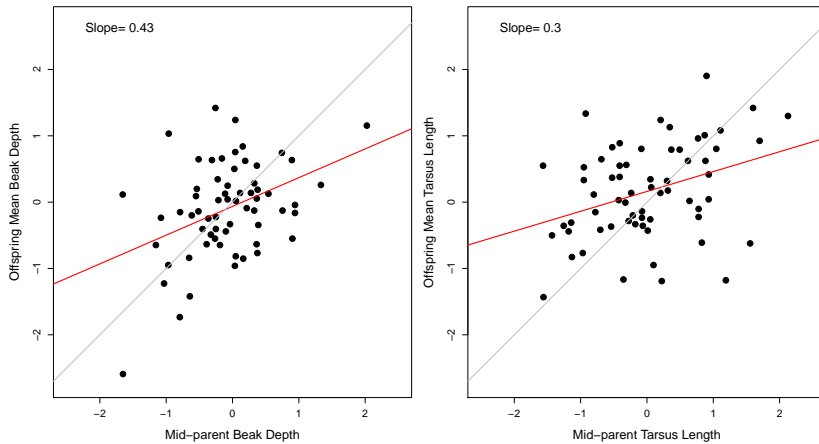


Figure 7.9: A measure of body fat in pairs of Monozygotic (MZ) and Dizygotic (DZ) twins. Our sample correlations are $\hat{\rho}_{MZ} = 0.72$ and $\hat{\rho}_{DZ} = 0.10$. Data from FAITH *et al.* (1999), Code here.

Better twin-based estimates of heritability are commonly used based on the comparison of MZ vs twins that bypass some of these issues.

The covariance in phenotype between parent and child Children resemble their biological parents because children inherit their genome from their parents (putting aside shared environments for the moment). If a mother and father are unrelated individuals, i.e. are two random draws from the population, then this mother and her child share one allele IBD at each locus (i.e. $r_1 = 1$ and $r_0 = r_2 = 0$). Lets assume that our mother (ind 1) transmits her paternal allele to the child (ind 2), in which case $X_{P1} = X_{M2}$, and so $Cov(X_{P1}, X_{M2}) = Var(X_{P1}) = \frac{1}{2}V_A$, and all the other covariances in eqn. 7.10 are zero. We'd also arrive at this result if instead we had thought of the mother transmitting her own maternal allele. Thus $Cov(X_1, X_2) = \frac{1}{2}V_A$, we can leverage this form of the covariance to directly estimate h^2 by regression.

We can estimate the narrow sense heritability through the regression of child's phenotype on the parental mid-point phenotype. The parental mid-point phenotype is simply the average of the mum and dad's phenotype. See Figure 7.11 for an example from Song sparrows.



We denote the child's phenotype by X_{kid} and mid-point phenotype by X_{mid} , so that if we take the regression $X_{kid} \sim X_{mid}$ this regression has slope $\beta = Cov(X_{kid}, X_{mid})/Var(X_{mid})$. The covariance of $Cov(X_{kid}, X_{mid}) = \frac{1}{2}V_A$, and $Var(X_{mid}) = \frac{1}{2}V$, as by taking the average of the parents we have halved the variance, such that the slope of the regression is

$$\beta_{mid,kid} = \frac{Cov(X_{kid}, X_{mid})}{Var(X_{mid})} = \frac{V_A}{V} = h^2 \quad (7.13)$$

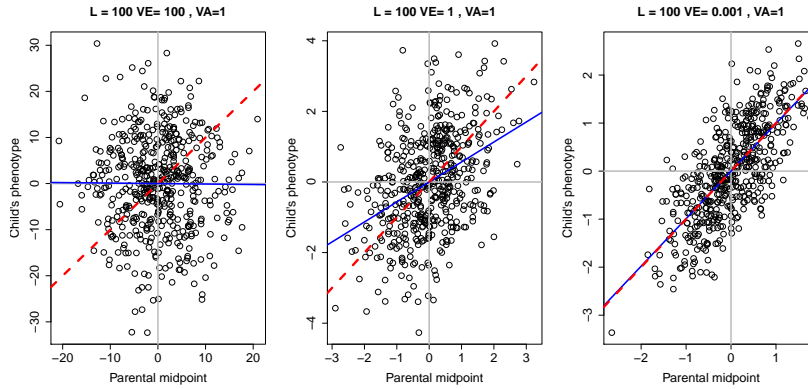
i.e. the regression of the child's phenotype on the parental midpoint



Figure 7.10: Song sparrow (*Melospiza melodia*). “He is the most incurable optimist of my acquaintance”. Bird biographies (1923). Ball, A.E. illustrations by Horsfall R.B. Image from the Biodiversity Heritage Library. Contributed by American Museum of Natural History Library. Not in copyright.

Figure 7.11: Parent-midpoint offspring regression for beak depth and tarsus length in song sparrows. The phenotypes have been standardized to have mean 0 and variance 1. The red line shows the best fitting slope, whose slope is reported on the graph. Note that SMITH and ZACH (1979) regressed the average offspring phenotype for each family on parental mid-point ($X_{avg, kid} \sim X_{mid}$), as they had multiple offspring per family. However, this doesn't change the slope of the regression from the form given by eqn (7.13). The grey line is the $x = y$ line. Data from SMITH and ZACH (1979), Code here.

phenotype is an estimate of the narrow sense heritability.⁷ If much of the phenotypic variation is due to the (additive) differences in genotypes among individuals ($h^2 \approx 1$), then children will closely resemble their parents. Conversely if much of the variation is environmental ($h^2 \approx 0$), and there is no shared environment between parent and child, children will not resemble their parents.



⁷ See math appendix eq (A.45) for more on regression slopes.

Applying this heritability estimate to the Song sparrow sample we find $h^2 = 0.43$ and $h^2 = 0.3$ for beak depth and tarsus length respectively from Figure 7.11. So in SMITH and ZACH (1979) analysis, for example, 30% of the variance in tarsus length is attributable to the additive effect of genetic differences among individuals. SMITH and ZACH (1979) also regressed the average offspring phenotype against their fathers or mothers against their offspring, giving a slope of $\beta_{\text{dad,avg. kid}}$ and $\beta_{\text{mum,kid}}$, and for tarsus length, for example, they found $\beta_{\text{dad,avg. kid}} = 0.19$ and $\beta_{\text{mum,avg. kid}} = 0.17$. Following a similar argument to that in eqn (7.13) we find that these slopes are $\beta_{\text{dad,kid}} = v_A/2/V = h^2/2$, and the same for mums. Thus the regression of offspring's phenotype on a particular parent is an estimate of half the narrow-sense heritability, in line with the reduced slopes found by SMITH and ZACH (1979), this halving of the slope is due to the fact that a single parent's phenotype is a noisier estimate of the parental mid-point and so less informative about the child's phenotype. These parent specific estimates of heritability are particularly useful as they allow us to investigate sex-specific inheritance and sexual dimorphism (we'll explore this in a later section).

Estimating heritability by these various parent-offspring regression have the issue of not controlling for environmental correlations between parent and offspring, which can inflate our estimates of heritability (as we will mistake environmentally mediated resemblance for genetics). Raising the organisms in the lab could remove much of the

Figure 7.12: Regression of child's phenotype of the parental mid-point phenotype. The three panels show decreasing levels of environmental variance (V_E) holding the additive genetic variance constant ($V_A = 1$). In these figures, we simulate 100 loci, as described in the caption of Figure 7.5. We simulate the genotypes and phenotypes of the two parents, and then simulate the child's genotype following mendelian transmission. The blue line shows $x = y$ and the red line shows the best fitting linear regression line. Code here.

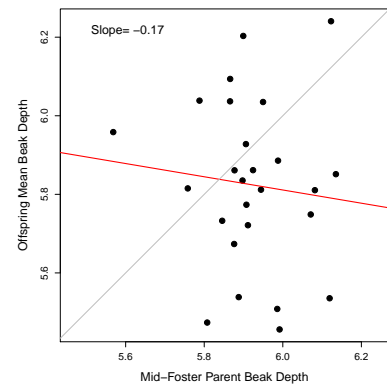


Figure 7.13: Foster Parent-midpoint offspring regression for beak depth and tarsus length in song sparrows. The red line shows the best fitting slope, whose slope is reported on the graph. The slope is not significant. The grey line is the $x = y$ line. Data from SMITH and DHONDT (1980), Code here.

potential for shared environment between parent and offspring, but it also removes much of the environmental variation and we (as evolutionary geneticists) are usually not primarily interested in knowing the heritability in the lab but rather in the field. In some organisms, notably plants, we can begin to sidestep these issues by raising offspring in a common set of randomized field conditions (a so called “common garden”). Another option is cross-foster animals, for example SMITH and DHONDT (1980) returned to the song sparrow population and swapped eggs between parents nests. They found that the covariance between biological parents and children was still high despite these children being raised in a different nest, but that there was no significant covariance between foster parents and their non-biological children (see Figure 7.13 for beak depth). This suggests that family environment is not confounder in estimating the heritability in this song sparrow sample. However, such manipulations are often impossible in many systems, and issues of shared environmental covariance due to maternal resources from egg (or seed) are still present.

Despite its issues, this measure of heritability provides useful intuition and is directly relevant to our discussion of the response to selection in the next chapter. That’s because our regression allows us to attempt to predict the phenotype of the child given the phenotypes of the parents; how well we can do this depends on the slope. See Figure 7.12 for examples. If the slope is close to zero then the parental phenotypes hold no information about the phenotype of the child, while if the slope is close to one then the parental mid-point is a good guess at the child’s phenotype. As we will see, natural selection will only efficiently drive evolution if children resemble their parents.

Thinking abour our prediction of child’s phenoptye more formally, the expected phenotype of the child given the parental phenotypes is

$$\mathbb{E}(X_{kid}|X_{mom}, X_{dad}) = \mu + \beta_{mid,kid}(X_{mid} - \mu) = \mu + h^2(X_{mid} - \mu) \quad (7.14)$$

which follows from the definition of linear regression. So to find the child’s predicted phenotype, we simply take the mean phenotype and add on the difference between our parental mid-point and the population mean, multiplied by our narrow sense heritability.

Question 2. Briefly explain what Galton meant by ‘regression towards mediocrity’, and why he observed this pattern in light of Mendelian inheritance.

The covariance between general pairs of relatives under an additive model The above examples above make clear that to understand the covariance between phenotypes of relatives, we simply need to think about the alleles they share IBD. Consider a pair of relatives (1

and 2) with a probability r_0 , r_1 , and r_2 of sharing zero, one, or two alleles IBD respectively. When they share zero alleles $Cov((X_{1M} + X_{1P}), (X_{2M} + X_{2P})) = 0$, when they share one allele $Cov((X_{1M} + X_{1P}), (X_{2M} + X_{2P})) = Var(X_{1M}) = \frac{1}{2}V_A$, and when they share two alleles $Cov((X_{1M} + X_{1P}), (X_{2M} + X_{2P})) = V_A$. Therefore, the general covariance between two relatives is

$$Cov(X_1, X_2) = r_0 \times 0 + r_1 \frac{1}{2}V_A + r_2 V_A = 2F_{1,2}V_A \quad (7.15)$$

So under a simple additive model of the genetic basis of a phenotype, to measure the narrow sense heritability we need to measure the covariance between pairs of relatives (assuming that we can remove the effect of shared environmental noise). From the covariance between relatives we can calculate V_A , and we can then divide this by the total phenotypic variance to get h^2 .

Question 3. **A)** In polygynous red-winged blackbird populations (i.e. males mate with several females), paternal half-sibs can be identified. Suppose that the covariance of tarsus lengths among half-sibs is 0.25 cm^2 and that the total phenotypic variance is 4 cm^2 . Use these data to estimate h^2 for tarsus length in this population.

B) Why might paternal half-sibs be preferable for measuring heritability than maternal half-sibs?

Estimating additive genetic variance across a variety of different relationships (The animal model). In many natural populations we may have access to individuals with a range of different relationships to each other (e.g. through monitoring of the paternity of individuals), but relatively few pairs of individuals for a specific relationship (e.g. sibs). We can try and use this information on various relatives as fully as possible in a mixed model framework. Building from equation 7.3, we can write an individual's phenotype X_i as

$$X_i = \mu + X_{A,i} + X_{E,i} \quad (7.16)$$

where $X_{E,i} \sim N(0, V_E)$ and $X_{A,i}$ is normally distributed across individuals with covariance matrix $V_A A$, where the entries for a pair of individuals i and j are $A_{ij} = 2F_{i,j}$ and $A_{ii} = 1$. Given the matrix A we can estimate V_A . We can also add fixed effects into this model to account for generation effects, additional mixed effects could also be included to account for shared environments between particular individuals (e.g. a shared nest). This approach is sometimes called the “animal model”, and is widely used to in modern quantitative genetics to estimate genetic variances and heritabilities.



Figure 7.14: Red-winged blackbird and Tricolored Red-winged blackbirds (*Agelaius phoeniceus* and *Agelaius tricolor*).
Bird-lore (1899). National Association of Audubon Societies for the Protection of Wild Birds and Animals. Image from the Biodiversity Heritage Library. Contributed by American Museum of Natural History Library. Not in copyright.

7.1 Multiple traits

Traits often covary with each other, both due to environmentally induced effects (e.g. due to the effects of diet on multiple traits) and due to the expression of underlying genetic covariance between traits. Genetic covariance, in turn, can reflect pleiotropy, a mechanistic effect of an allele on multiple traits (e.g. variants that affect skin pigmentation often affect hair color), the genetic linkage of loci independently affecting multiple traits, or the effects of assortative mating.

Consider two traits $X_{1,i}$ and $X_{2,i}$ in an individual i . These traits could be, say, the individual's leg length and nose length. As before, we can write these as

$$\begin{aligned} X_{1,i} &= \mu_1 + X_{1,A,i} + X_{1,E,i} \\ X_{2,i} &= \mu_2 + X_{2,A,i} + X_{2,E,i} \end{aligned} \tag{7.17}$$

As before we can talk about the total phenotypic variance (V_1, V_2), environmental variance ($V_{1,E}$ and $V_{2,E}$), and the additive genetic variance for trait one and two ($V_{1,A}, V_{2,A}$). But now we also have to consider the total covariance between trait one and trait two, $V_{1,2} = \text{Cov}(X_1, X_2)$, as well as the environmentally induced covariance ($V_{E,1,2} = \text{Cov}(X_{1,E}, X_{2,E})$) and the additive genetic covariance ($V_{A,1,2} = \text{Cov}(X_{1,A}, X_{2,A})$). To better understand the covariance arising due to pleiotropy, let's think about a set of L SNPs contributing to our two traits. If the additive effect of an allele at the i^{th} SNP is $\alpha_{i,1}$ and $\alpha_{i,2}$ on traits 1 and 2, then the additive covariance between our traits is

$$V_{A,1,2} = \sum_{i=1}^L 2\alpha_{i,1}\alpha_{i,2}p_i(1-p_i) \tag{7.18}$$

assuming our loci are in linkage disequilibrium. Thus a genetic correlation arises due to pleiotropy, because loci that tend to affect trait 1 also systematically affect trait 2. For example, alleles associated with later Age at Menarche (AAM) in European women also tend to be positively associated with height (see Figure 7.15), thereby creating a genetic correlation between AAM and height.

We can store our variance and covariance values in matrices, a way of gathering these terms that will be useful when we discuss selection:

$$\mathbf{V} = \begin{pmatrix} V_1 & V_{1,2} \\ V_{1,2} & V_2 \end{pmatrix} \tag{7.19}$$

and

$$\mathbf{G} = \begin{pmatrix} V_{1,A} & V_{A,1,2} \\ V_{A,1,2} & V_{2,A} \end{pmatrix} \tag{7.20}$$

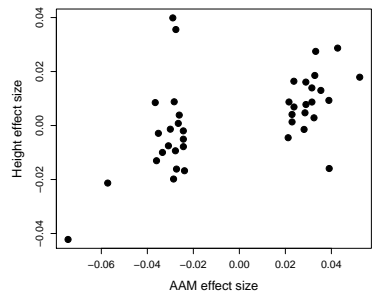


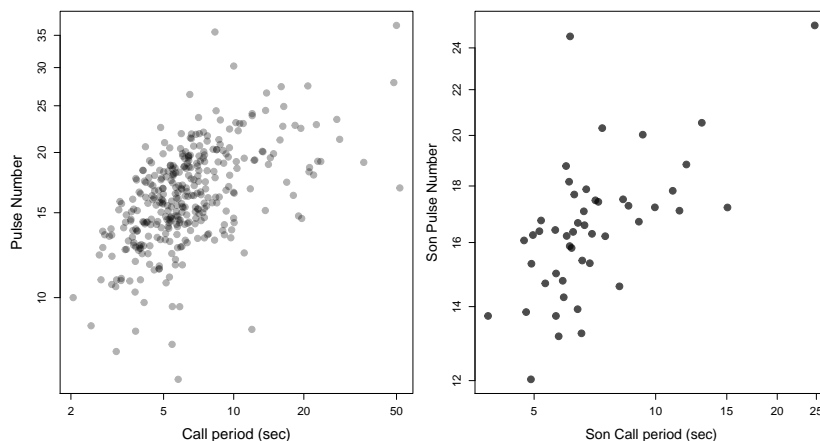
Figure 7.15: The additive effect sizes of loci associated with female Age at Menarche (AAM) and their effect size on Height in a European population. Data from PICKRELL *et al.* (2016). Code here.

Here we've shown the matrices for two traits, but we can generalize this to an arbitrary number of traits.

We can estimate these quantities, in a similar way as before, by studying the covariance in different traits between relatives:

$$\text{Cov}(X_{1,i}, X_{2,j}) = 2F_{i,j}V_{A,1,2} \quad (7.21)$$

An example of phenotype and genetic covariance are shown on the left and right of Figure 7.17 respectively. Gray treefrogs (*Hyla versicolor*) chorus to attract mates. Their call is made up of a trill, a note rapidly pulsed a number of times, that is then repeated after some period. Female frogs prefer males who make a lot of calls and where each of those calls have a large number of pulses. However, doing both is very energetic, and so there is potentially a tradeoff between these two aspects of a male frog's call. Indeed WELCH *et al.* (2014) found in lab-reared male frogs that the pulse number and the time period between calls were positively correlated, left side of Figure 7.17, i.e. individuals were investing their energy in making either few highly pulsed calls or many calls with few pulses. This phenotypic covariance reflects underlying a genetic covariance between these two frog call characteristics (right side Figure 7.17). Fathers whose sons have calls with highly pulsed calls also have sons whose calls are more spaced apart.



One useful summary of a genetic covariance is the genetic correlation between two phenotypes

$$r_g = \frac{V_{A,1,2}}{\sqrt{V_{A,1}V_{A,2}}} \quad (7.22)$$

where $V_{A,1}$ and $V_{A,2}$ are the additive genetic variance for trait 1 and 2 respectively. Here, r_g tells us to what extent the additive genetic variance in two traits is correlated.



Figure 7.16: Grey treefrog (*Hyla versicolor*)
Historia Natural, tomo V "Reptiles y peces"
(1874) Juan Vilanova y Piera, p. 156. Image
from wikipedia contributed by Dorieo.
Cropped. Public Domain

Figure 7.17: Phenotypic and Genetic correlations in male grey treefrog (*Hyla versicolor*) calls. On the left each male is shown as a dot, recording their inter-call period and the number of pulses in each call. On the right each dot corresponds to a father with the mean of sons for both phenotypes. Data from WELCH *et al.* (2014) downloaded from dryad, Code here.

Another important application of genetic covariances is in the study of sexually antagonistic selection and the evolution of sexual dimorphism, here we'll calculate the genetic covariance between male and female phenotypes. For example, below is the relationship between the forehead patch size for Pied fly-catcher fathers and their sons and daughters. The phenotype has been standardized to have mean 0 and variance 1 in each group. The phenotypic covariance of the sample of fathers and sons is 0.35, while the phenotypic covariance of fathers and daughter is 0.23.

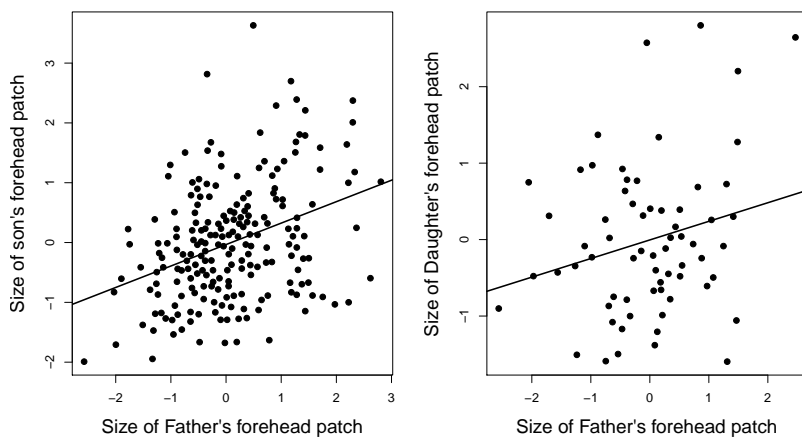


Figure 7.18: Relationship of standardized forehead patch size between fathers and sons and daughters in Pied fly-catchers. Data from POTTI and CANAL. Code here.



Figure 7.19: *Ficedula hypoleuca*, Pied fly-catcher.
Coloured illustrations of British birds, and
their eggs (1842-1850). London :G.W.
Nickisson. Image from the Biodiversity
Heritage Library. Contributed by Smithsonian
Libraries. Not in copyright.

Question 4. Assume we can ignore the effect of the shared environment in our Pied fly-catcher example.

- A) What is the additive genetic covariance between male and female patch size?
- B) What is the additive genetic correlation of male and female patch size? You can assume that the additive genetic variance is the same in males and females.

7.1.1 Non-additive variation.

Up to now we've assumed that our alleles contribute to our phenotype in an additive fashion. However, that does not have to be the case as there may be non-additivity among the alleles present at a locus (*dominance*) or among alleles at different loci (*epistasis*). We can accommodate these complications into our models. We do this by partitioning our total genetic variance into independent variance components.

Dominance. To understand the effect of dominance, let's consider how the allele that a parent transmits influences their offspring's phenotype. A parent transmits one of their two alleles at a locus to their offspring. Assuming that individuals mate at random, this allele is paired with another allele drawn at random from the population. For example, assume your mother transmitted an allele 1 to you: with probability p it would be paired with another allele 1, and you would be a homozygote; and with probability q it's paired with a 2 allele and you're a heterozygote.

Now consider an autosomal biallelic locus ℓ , with frequency p for allele 1, and genotypes 0, 1, and 2 corresponding to how many copies of allele 1 individuals carry. We'll denote the mean phenotype of an individual with genotype 0, 1, and 2 as $\bar{X}_{\ell,0}$, $\bar{X}_{\ell,1}$, $\bar{X}_{\ell,2}$ respectively. This mean is taking an average phenotype over all the environments and genetic backgrounds the alleles are present on. We'll mean center (MC) these phenotypic values, setting $\bar{X}'_{\ell,0} = \bar{X}_{\ell,0} - \mu$, and likewise for the other genotypes.

We can think about the average (marginal) MC phenotype of an individual who received an allele 1 from their parent as the average of the MC phenotype for heterozygotes and 11 homozygotes, weighted by the probability that the individual has these genotypes, i.e. the probability they receive an additional allele 1 or an allele 2 from their other parent:

$$a_{\ell,1} = p\bar{X}'_{\ell,2} + q\bar{X}'_{\ell,1}, \quad (7.23)$$

Similarly, if your parent transmitted an 2 allele to you, your average MC phenotype would be

$$a_{\ell,2} = p\bar{X}'_{\ell,1} + q\bar{X}'_{\ell,0} \quad (7.24)$$

Let's now consider the average phenotype of an offspring by how many copies of the allele 1 they carry

genotype:	0,	1,	2.
additive genetic value:	$a_{\ell,2} + a_{\ell,2}$,	$a_{\ell,1} + a_{\ell,2}$,	$a_{\ell,1} + a_{\ell,1}$

i.e. the mean phenotype of each genotypes' offspring averaged over all possible matings to other individuals in the population (assuming individuals mate at random). These are the additive MC genetic values (breeding values) of our genotypes. Here we are simply adding up the additive contributions of the alleles present in each genotype and ignoring any non-additive effects of genotype.

To illustrate this, in Figure 7.20 we plot two different cases of dominance relationships; in the top row an additive polymorphism and in the second row a fully dominant allele. The additive genetic values of the genotypes are shown as red dots. Note that the additive values of the genotypes line up with the observed MC phenotypic means in the

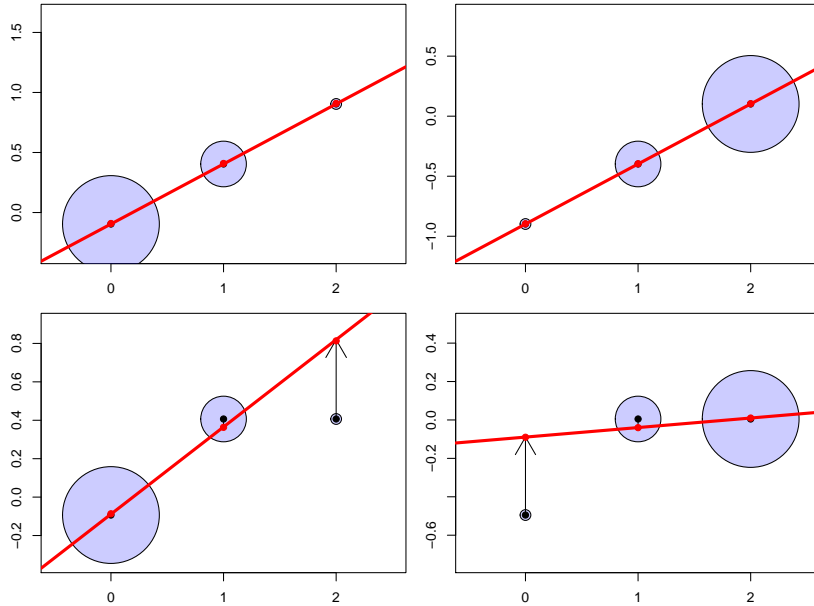


Figure 7.20: The average mean-centered (MC) phenotypes plotted against the number of allele 1 carried (from 0 for 22 to 2 for 11). **Top Row:** Additive relationship between genotype and phenotype. **Bottom Row:** Allele 1 is dominant over allele 2, such that the heterozygote has the same phenotype as the 11 genotype. The area of each circle is proportion to the fraction of the population in each genotypic class (p^2 , $2pq$, and q^2). One the left column $p = 0.1$ and the right column is $p = 0.9$. The additive genetic values of the genotypes are shown as red dots. The regression between phenotype and additive genotype is shown as a red line. The black vertical arrows show the difference between the average MC phenotype and additive genetic value for each genotype. Code here.

top row, when our alleles interact in a completely additive manner. Our additive genetic values always fall along a linear line (the red line in our figure). The additive values are falling along the best fitting line of linear regression for our population, when phenotype is regressed against the additive genotype (0, 1, 2 copies of allele 1) across all individuals in our population. Note in the dominant case the additive genetic values differ from the observed phenotypic means, and are closer to the observed values for the genotypes that are most common in the population.

The difference in the additive effect of the two alleles $a_{\ell,2} - a_{\ell,1}$ can be interpreted as an average effect of swapping an allele 1 for an allele 2; we'll call this difference $\alpha_\ell = a_{\ell,2} - a_{\ell,1}$. Our α_ℓ is also the slope of the regression of phenotype against genotype (the red line in Figure 7.20). Note that the slope of our regression of phenotype on genotype (α_ℓ) does not depend on the population allele frequency for our completely additive locus (top row of 7.20). In contrast, when there is dominance, the slope between genotype and phenotype (α_ℓ) is a function of allele frequency (bottom row of 7.20). When a dominant allele (1) is rare there is a strong slope of phenotype on genotype, bottom left Figure 7.20. This strong slope is because replacing a single copy of the 2 allele with a 1 allele in an individual has a big effect on average phenotype, as it will most likely move an individual from being a 22 homozygote to being a 12 heterozygote. In contrast, when the dominant allele (1) is common in the population, replacing a 2 allele by a 1 allele in an individual on average has little phenotypic effect,

leading to a weak slope bottom right Figure 7.20. This small effect is because as we are mainly turning heterozygotes into homozygotes (11), who have the same mean phenotype as each other.

As an example of how dominance and population allele frequencies can change the additive effect of an allele, let's consider the genetics of the age of sexual maturity in Atlantic Salmon. A single allele of large effect segregates in Atlantic Salmon that influences the sexual maturation rate in salmon (AYLLON *et al.*, 2015; BARSON *et al.*, 2015), and hence the timing of their return from the sea to spawn (sea age). The allele falls close to the autosomal gene VGLL3 (COUSMINER *et al.*, 2013, variation at this gene in humans also influences the timing of puberty). The left side of Figure 7.22 shows the age at sexual maturity in males. The L allele associated with slower sexual maturity is recessive in males. While the LL homozygotes mature on average a whole year later, the additive effect of the allele is weak while the L allele is rare in the population. The right panel shows the effect of the L allele in females. Note how the allele is much more dominant in females, and has a much more pronounced additive effect. The dominance of an allele is not a fixed property of the allele but rather a statement of the relationship of genotype to phenotype, such that the dominance relationship between alleles may vary across phenotypes and contexts (e.g. sexes).

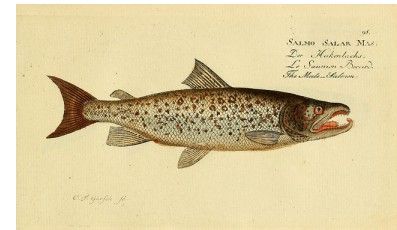
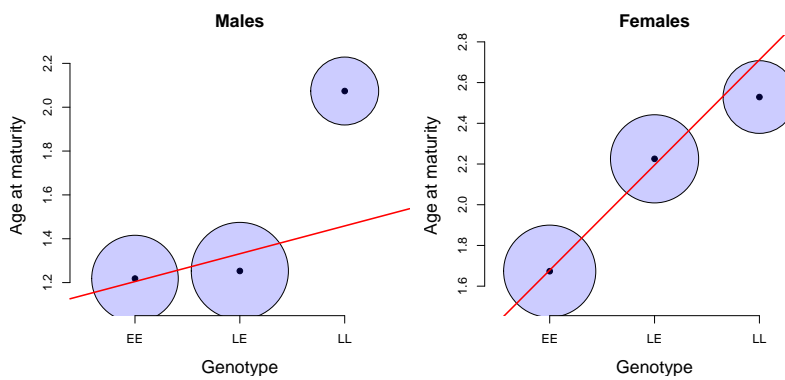


Figure 7.21: Atlantic Salmon (*Salmo salar*).
Histoire naturelle des poissons. 1796. Bloch, M. E. Image from the Biodiversity Heritage Library. Contributed by Ernst Mayr Library, Museum of Comparative Zoology. Not in copyright.

Figure 7.22: The average age at sexual maturity for each genotype, broken down by sex. The area of each circle is proportional to the fraction of the population in each genotypic class. The regression between phenotype and additive genotype is shown as a red line. Data from BARSON *et al.* (2015). Code here.

The variance in the population phenotype due to these additive breeding values at locus ℓ , assuming HW proportions, is

$$\begin{aligned}
 V_{A,\ell} &= p^2(2a_{\ell,2})^2 + 2pq(a_{\ell,1} + a_{\ell,1})^2 + q^2(2a_{\ell,0})^2 \\
 &= 2(pa_{\ell,1}^2 + qa_{\ell,2}^2) \\
 &= 2pq\alpha_{\ell}^2
 \end{aligned} \tag{7.25}$$

The total additive variance for the whole genotype can be found by

summing the individual additive genetic variances over loci

$$V_A = \sum_{\ell=1}^L V_{A,\ell} = \sum_{\ell=1}^L 2p_\ell q_\ell \alpha_\ell^2. \quad (7.26)$$

Having assigned the additive genetic variance to be the variance explained by the additive contribution of the alleles at a locus, we define the dominance variance as the population variance among genotypes at a locus due to their deviation from additivity. We can calculate how much each genotypic mean deviates away from its additive prediction at locus ℓ (the length of the arrows in Figure 7.20). For example, the heterozygote deviates

$$d_{\ell,1} = \bar{X}'_{\ell,1} - (a_{\ell,1} + a_{\ell,2}) \quad (7.27)$$

away from its additive genetic value, with similar expressions for each of the homozygotes ($d_{\ell,0}$ and $d_{\ell,2}$). We can then write the dominance variance at our locus as the genotype-frequency weighted sum of our squared dominance deviations

$$V_{D,\ell} = p^2 d_{\ell,0}^2 + 2pq d_{\ell,1}^2 + q^2 d_{\ell,2}^2. \quad (7.28)$$

Writing our total dominance variance as the sum across loci

$$V_D = \sum_{\ell=1}^L V_{D,\ell}. \quad (7.29)$$

Having now partitioned all of the genetic variance into additive and dominant terms, we can write our total genetic variance as

$$V_G = V_A + V_D. \quad (7.30)$$

We can do this because by construction the covariance between our additive and dominant deviations for the genotypes is zero. We can define the narrow sense heritability as before $h^2 = V_A/V_P = V_A/(V_G + V_E)$, which is the proportion of phenotypic variance due to additive genetic variance. We can also define the total proportion of the phenotypic variance due to genetic differences among individuals, as the broad-sense heritability $H^2 = V_G/(V_G + V_E)$.

Relationship (i,j)*	$Cov(X_i, X_j)$
parent-child	$1/2V_A$
full siblings	$1/2V_A + 1/4V_D$
identical (monozygotic) twins	$V_A + V_D$
1 st cousins	$1/8V_A$

Table 7.1: Phenotypic covariance between some pairs of relatives, include the dominance variation. * Assuming this is the only relationship the pair of individuals share (above that expected from randomly sampling individuals from the population).

When dominance is present in the loci influencing our trait ($V_D > 0$), we need to modify our phenotype covariance among relatives to

account for this non-additivity. Specifically, our equation for the covariance among a general pair of relatives (eqn. 7.15 for additive variation) becomes

$$Cov(X_1, X_2) = 2F_{1,2}V_A + r_2V_D \quad (7.31)$$

where r_2 is the probability that the pair of individuals share 2 alleles identical by descent, making the same assumptions (other than additivity) that we made in deriving eqn. 7.15. In table 7.1 we show the phenotypic covariance for some common pairs of relatives. The regression of offspring phenotype on parental midpoint still has a slope V_A/V_P .

Full sibs and parent-offspring have the same covariance if there is no dominance variance (as they have the same kinship coefficient $F_{1,2}$). However, when dominance is present ($V_D > 0$), full-sibs resemble each other more than parent-offspring pairs. That's because parents and offspring share precisely one allele, while full-sibs can share both alleles (i.e. the full genotype at a locus) identical by descent. We can attempt to estimate V_D by comparing different sets of relationships. For example, non-identical twins (full sibs born at same time) should have 1/2 the phenotypic covariance of identical twins if $V_D = 0$. Therefore, we can attempt to estimate V_D by looking at whether identical twins have more than twice the phenotypic covariance than non-identical twins.

The most important aspect of this discussion for thinking about evolutionary genetics is that the parent-offspring covariance is still only a function of V_A . This is because our parent (e.g. the mother) transmits only a single allele, at each locus, to its offspring. The other allele the offspring receives is random (assuming random mating), as it comes from the other unrelated parent (the father). Therefore, the average effect on the child's phenotype of an allele the child receives from their mother is averaged over all possible random alleles the child could receive from their father (weighted by their frequency in the population). Thus we only care about the additive effect of the allele, as parents transmit only alleles (not genotypes) to their offspring. This means that the short-term response to selection, as described by the breeder's equation, depends only on V_A and the additive effect of alleles. Therefore, if we can estimate the narrow-sense heritability we can predict the short-term response. However, if alleles display dominance, our value of V_A will change as alleles at our loci change in frequency, e.g. as dominant alleles become common in the population their contribution to V_A decreases. Therefore, if there is dominance our value of V_A will not be constant across generations.

Up to this point we have only considered dominance and not epistasis. However, we can include epistasis in a similar manner (for ex-

ample among pairs of loci). This gets a little tricky to think about, so we will only briefly explain it. We can first estimate the additive effect of the alleles by considering the effect of the alleles averaging over their possible genetic backgrounds (including the other interacting alleles they are possibly paired with), just as before. We can then calculate the additive genetic variance from this. We can estimate the dominance variance, by calculating the residual variance among genotypes at a locus unexplained by the additive effect of the loci. We can then estimate the epistatic variance by estimating the residual variance left unexplained among the two locus genotypes after accounting for the additive and dominant deviations calculated from each locus separately. In practice these high variance components are hard to estimate, and usually small as much of our variance is assigned to the additive effect. Again we would find that we mostly care about V_A for predicting short-term evolution, but that the contribution of loci to the additive genetic variance will depend on the epistatic relationships among loci.

Question 5. How could you use 1/2 sibs vs. full-sibs to estimate V_D ? Why might this be difficult in practice? Why are identical vs. non-identical twins better suited for this?

Question 6. Can you construct a case where $V_A = 0$ and $V_D > 0$? You need just describe it qualitatively; you don't need to work out the math. (tricker question).

8

The Response to Phenotypic Selection

Evolution by natural selection requires:

1. Variation in a phenotype
2. That survival is non-random with respect to this phenotypic variation.
3. That this variation is heritable.

Points 1 and 2 encapsulate our idea of Natural Selection, but evolution by natural selection will only occur if the 3rd condition is also met.

¹ It is the heritable nature of variation that couples change within a generation due to natural selection to change across generations (evolutionary change).

Let's start by thinking about the change within a generation due to directional selection, where selection acts to change the mean phenotype within a generation. For example, a decrease in mean height within a generation, due to taller organisms having a lower chance of surviving to reproduction than shorter organisms. Specifically, we'll denote our mean phenotype at reproduction by μ_S , i.e. after selection has acted, and our mean phenotype before selection acts by μ_{BS} . This second quantity may be hard to measure, as obviously selection acts throughout the life-cycle, so it might be easier to think of this as the mean phenotype if selection hadn't acted. So the change in mean phenotype within a generation is $\mu_S - \mu_{BS} = S$.

We are interested in predicting the distribution of phenotypes in the next generation. In particular, we are interested in the mean phenotype in the next generation to understand how directional selection has contributed to evolutionary change. We'll denote the mean phenotype in offspring, i.e. the mean phenotype in the next generation before selection acts, as μ_{NG} . The change across generations we'll call the response to selection R and put this equal to $\mu_{NG} - \mu_{BS}$.

The mean phenotype in the next generation is

$$\mu_{NG} = \mathbb{E}(\mathbb{E}(X_{kid}|X_{mom}, X_{dad})) \quad (8.1)$$

See LEWONTIN (1970). Note that these requirements are not specific to DNA, i.e. the concept of evolution by natural selection is substrate independent.

¹ Some people consider natural selection to only operate on heritable phenotype variation and so require all three conditions to say that natural selection occurs. This is mostly a semantic point, however, it is useful to be able to distinguish the action of selection from a possible response.

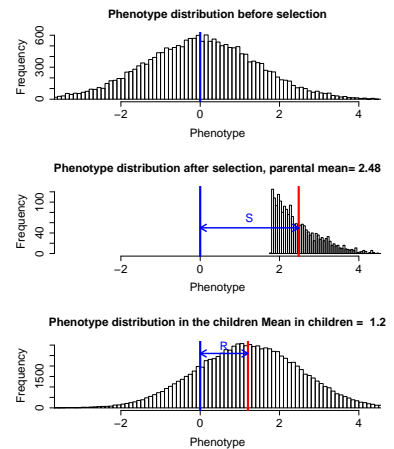


Figure 8.1: **Top.** Distribution of a phenotype in the parental population prior to selection, $V_A = V_E = 1$. **Middle.** Only individuals in the top 10% of the phenotypic distribution are selected to reproduce; the resulting shift in the phenotypic mean is S . **Bottom.** Phenotypic distribution of children of the selected parents; the shift in the mean phenotype is R . Code here.

where the outer expectation is over possible pairs of randomly mating individuals who survive to reproduce. We can use eqn. 7.14 to obtain an expression for this expectation:

$$\mu_{NG} = \mu_{BS} + \beta_{mid,kid}(\mathbb{E}(X_{mid}) - \mu_{BS}) \quad (8.2)$$

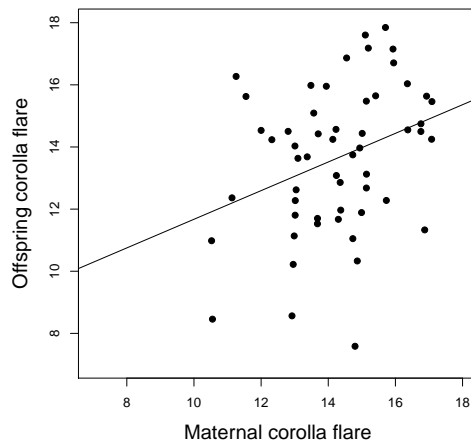
So to obtain μ_{NG} we need to compute $\mathbb{E}(X_{mid})$, the expected mid-point phenotype of pairs of individuals who survive to reproduce. Well this is just the expected phenotype in the individuals who survived to reproduce (μ_S), so

$$\mu_{NG} = \mu_{BS} + h^2(\mu_S - \mu_{BS}) \quad (8.3)$$

So we can write our response to selection as

$$R = \mu_{NG} - \mu_{BS} = h^2(\mu_S - \mu_{BS}) = h^2S \quad (8.4)$$

So our response to selection is proportional to our selection differential, and the constant of proportionality is the narrow sense heritability. This equation is sometimes termed the Breeder's equation. It is a statement that the evolutionary change across generations (R) is proportional to the change caused by directional selection within a generation (S), and that the strength of this relationship is determined by the narrow sense heritability (h^2).



Question 1. GALEN (1996) explored selection on flower shape in *Polemonium viscosum*. She found that plants with larger corolla flare had more bumblebee visits, which resulted in higher seed set and a 17% increase in corolla flare in the plants contributing to the next generation. Based on the data in the caption of Figure 8.3 what is the expected response in the next generation?

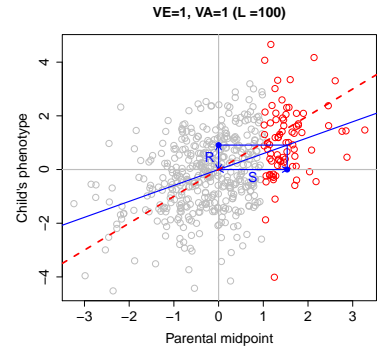


Figure 8.2: A visual representation of the Breeder's equation. Regression of child's phenotype on parental midpoint phenotype ($V_A = V_E = 1$). The parents and children of all families are shown as grey or red points. However, under truncation selection, only individuals with phenotypes > 1 (red) are bred. The use of the red families only results in a phenotypic shift S in the parental generation, which drives a shift R in the offspring generation. [Code here.](#)

Figure 8.3: The relationship between maternal and offspring corolla flare (flower width) in *P. viscosum*. From GALEN's data the covariance of mother and child is 1.3, while the variance of the mother is 2.8. Data from GALEN (1996). [Code here.](#)

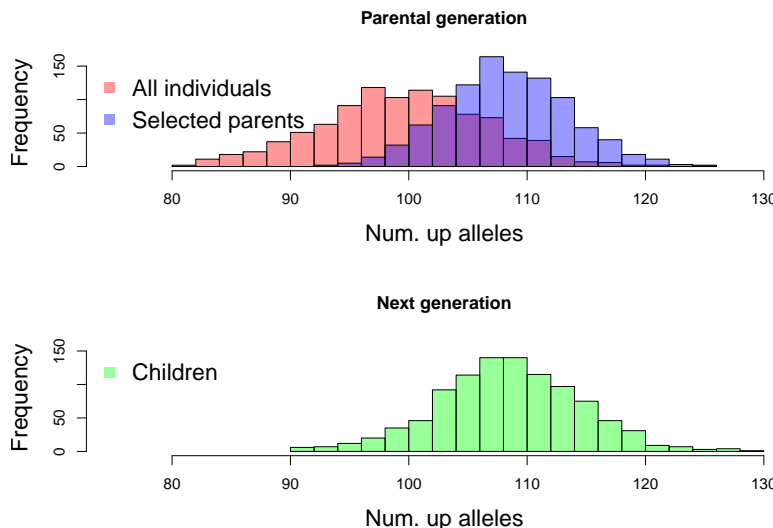


Figure 8.4: Sticky jacob's ladder (*Polemonium viscosum*). Flowers of Mountain and Plain (1920). Clements, E. Image from the Biodiversity Heritage Library. Contributed by New York Botanical Garden, Mertz Library. Not in copyright. Cropped from original.

If we know R and S we can estimate h^2 . Heritabilities estimated like this are called ‘realized heritability’. Estimates of the ‘realized heritability’ can readily be produced in artificial selection experiments:

Question 2. From the experiment shown in Figure 8.5, the mean corn oil content in 1897 was 4.78, among the 24 individuals chosen to breed to for the next generation the mean was 5.2. The offspring of these individuals had a mean kernel oil content of 5.1. What is the narrow sense realized heritability?

To understand the genetic basis of the response to selection take a look at Figure 8.6. The setup is the same as in our previous simulation figures. The individuals who are selected to form our next generation



carry more alleles that increase the phenotype in the current range of environments currently experienced by the population. The average individual before selection carried 100 of these ‘up’ alleles, while the average individual surviving selection carries 108 ‘up’ alleles.

As individuals faithfully transmit their alleles to the next generation the average child of the selected parents carries 108 up alleles. Note that the variance has changed little, the children have plenty of variation in their genotype, such that selection can readily drive evolution in future generations. The average frequency of an ‘up’ allele has changed from 50% to 54%. Gains due to selection will be stably inherited to future generations and can be compounded on generation after generation if selection pressures were to remain constant.

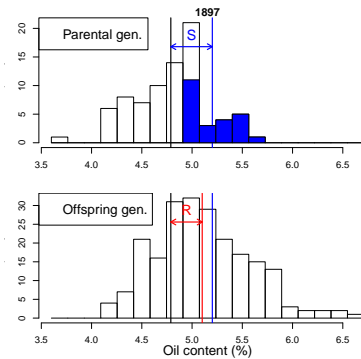


Figure 8.5: **Top.** Phenotypic distribution of oil content in corn in 1897, and the individuals who were selected to breed for the next generation are marked in blue. **Bottom.** The distribution in the next generation. Data from the Illinois selection experiment available here, [Code here](#).

Figure 8.6: **Top.** Distribution of the number of up alleles in the parental population prior to selection (red), for the selected individuals in the top 10% phenotypic tail of the population (blue) **Bottom.** The same distribution for the offspring of the selected parents in the next generation (green). [Code here](#).



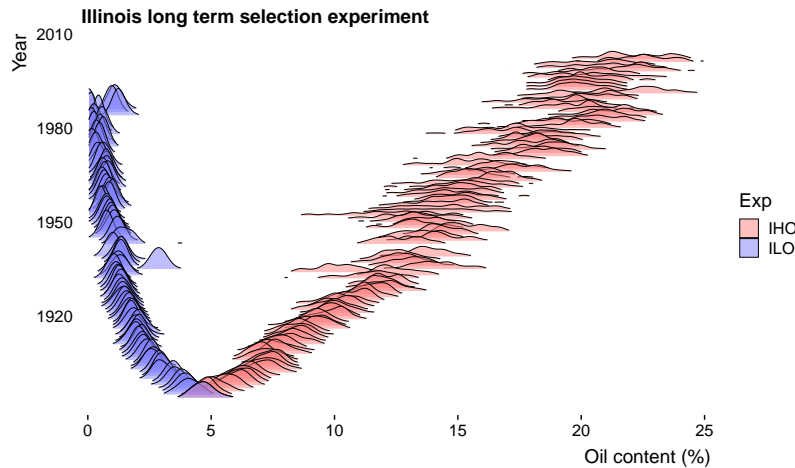
Figure 8.7: Maize (*Zea mays*). Prof. Dr. Thomé's Flora von Deutschland. 1886. Thomé, O. W. Image from the Biodiversity Heritage Library. Contributed by New York Botanical Garden. Not in copyright.

8.0.1 The Long-Term Response to Selection

If our selection pressure is sustained over many generations, we can use our breeder's equation to predict the response. If we are willing to assume that our heritability does not change and we maintain a constant selection differential (S), then after n generations our phenotype mean will have shifted

$$nh^2S \quad (8.5)$$

i.e. our population will keep up a linear response to selection. There-



fore, long-term, consistent selection can drive impressive evolutionary change. One example of this comes from a field experiment in Illinois, where plant breeders have systematically selected for higher and lower oil content in corn (see our previous Figure 8.5 for one generation of up selection). For over a century, they have taken seeds from the plants in the extremes of the distribution and using them to form the next generation. They have achieved impressive long-term responses, pushing the population distributions well beyond their initial range (Figure 8.9.. They've established two secondary populations where the selection differential was reversed. In the up-selection population they have maintained an impressively linear increase in oil content, shown by red line in Figure 8.8, but while the response is linear at first in the down line but they quickly reach very low oil content.

Question 3. A population of red deer were trapped on Jersey (an island off of England) during the last inter-glacial period. From the fossil record ² we can see that the population rapidly adapted to their new conditions, perhaps due to selection for shorter reproductive times in the absence of predation. Within 6,000 years they evolved from an estimated mean weight of the population of 200kg to an estimated

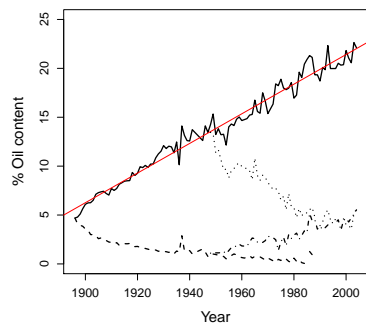


Figure 8.8: The mean oil content of corn in the Illinois long term selection experiment. Two populations were established in 1896 from the same initial population. Two secondary populations were established in 1948 where the direction of selection was reversed. Linear fit to the up experiment shown as a red line. Data available here, Code here.

Figure 8.9: Density plots showing the phenotypic distributions of the up- and down-selection populations of the Illinois long term selection experiment over time. Data available here, Code here.

² LISTER, A., 1989 Rapid dwarfing of red deer on Jersey in the last interglacial. Nature 342(6249): 539

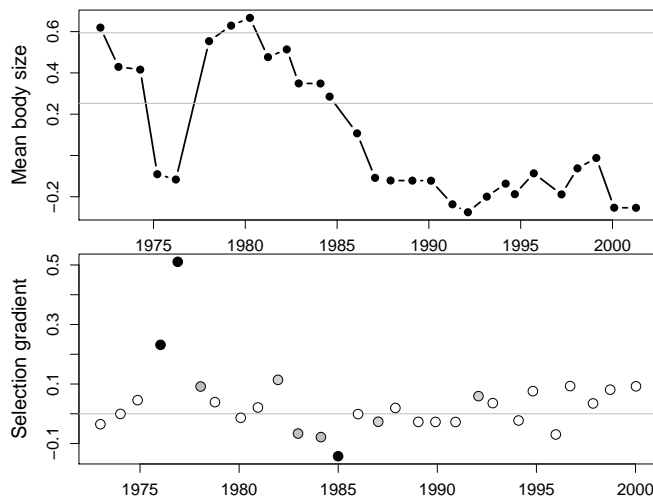
mean weight of 36kg (a 6 fold reduction)! You estimate that the generation time of red deer is 5 years and, from a current day population, that the narrow sense heritability of the phenotype is 0.5.

A) Estimate the mean change per generation in the mean body weight.

B) Estimate the change in mean body weight caused by selection within a generation. State your assumptions.

C) Assuming we only have fossils from the founding population and the population after 6000 years, should we assume that the calculations accurately reflect what actually occurred within our population?

In wild populations, selection pressures are likely rarely sustained for large numbers of generations. For example, the Grants' have measured phenotypic selection in Darwin's Finches over multiple decades on the island of Daphne Major. They have seen that selection pressures in the Medium ground-finch (*Geospiza fortis*) have reversed a number of times over the years (Figure 8.11).



Patterns of long-term phenotypic change in the wild. Looking across the diversity of plants and animals we see huge changes in size and form, can the strengths of selection we can observe over short time periods possibly explain these changes?

To compare phenotypic changes over various time periods we need some measure of the rate of phenotypic change. (HALDANE, 1949) proposed the rate of change from X_1 to X_2 in time interval Δt , mea-

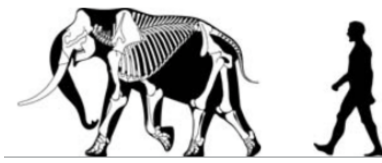


Figure 8.10: It's not just deer that evolve to be small on islands, pygmy mammoths and elephants have evolved from large mainland species on numerous islands. For example, the California Channel Islands were home to a dwarf mammoth until about 13,000 years ago.
Santa Rosa *Mammuthus exilis*. wikimedia, CC BY 3.0.

Figure 8.11: **Top)** Mean body size of the Medium ground-finch population measured each year. The 1973 95% confidence intervals are shown as horizontal bars. **Bottom)** Standardized selection differentials on body size. The statistical significance of the selection differentials is shown, black points are $p < 0.001$ and grey $p < 0.05$. Data from GRANT and GRANT (2002) Code here.



Figure 8.12: Medium ground-finch (*Geospiza fortis*).
The zoology of the voyage of H.M.S. Beagle. Birds Part 3. (1841) Gould G. Edited by Darwin, C. Illustration by Elizabeth Gould. Image from the Biodiversity Heritage Library. Contributed by Natural History Museum Library, London. Not in copyright.

sured in Millions of years, be quantified as

$$\frac{\log(X_2/X_1)}{\Delta t} = \frac{\log(X_2) - \log(X_1)}{\Delta t} \quad (8.6)$$

by expressing this the log of the ratio³, we are looking at the proportional fold change, which makes sense as a evolutionary change of 1cm in length is more impressive if you're a mouse than an elephant. By putting this on a log-scale we are looking at the fold relative change HALDANE called the units of this measure ‘the Darwin’, with a one Darwin change corresponding to a $e \approx 2.71$ fold change in a Million years, a two Darwin change corresponding to a $e^2 \approx 7.34$ fold change in a Million years and so on.

Question 4. Calculate the rate of change in body size in the Jersey red deer from Question 3 in Darwins. Do the same for the total change in corn oil content in the up lines in Figure 8.8.

GINGERICH (1983) examined the absolute rate of phenotypic change in field study data and the fossil record, a dataset considerably expanded by UYEDA *et al.* (2011). In Figure 8.14 each point is an observation of phenotype evolution. The x-axis shows the time period in years over which the evolutionary change was observed, the x-axis is plotted on a \log_{10} scale. The y-axis shows absolute rate of phenotypic change, measured in Darwins, again on a \log_{10} ,

³ Note that here, as elsewhere, log refers the natural logarithm, i.e. log base e . We'll make it clear if we using log in a different base, e.g. we'll use \log_{10} for log in base 10.

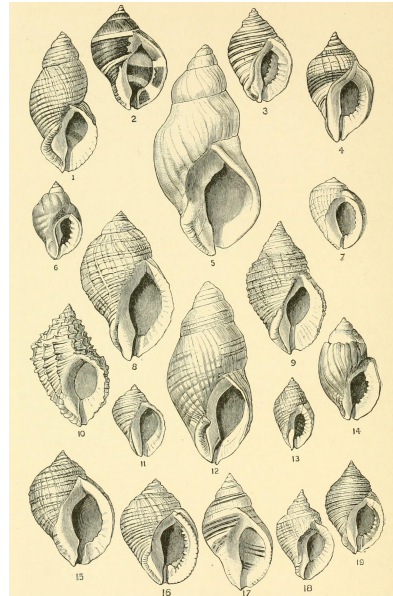
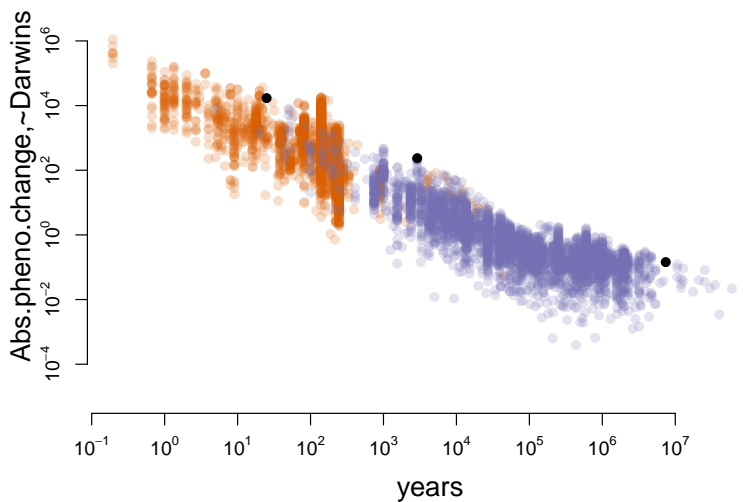


Figure 8.13: Variation in Atlantic dog whelks (*Nucella lapillus*, synonym *Purpura lapukkus*) along the coast of Great Britain.

The Cambridge natural history, Molluscs and Brachiopods (1895). Cooke AH, Shipley AE, Reed FRC. Image from the Biodiversity Heritage Library. Contributed by University of Toronto - Earth Sciences Library. Not in copyright.



Over short timescales we see incredibly rapid evolution, note the high rates on the left of Figure 8.14. For example, the first black dot

Figure 8.14: The absolute rate of phenotypic evolution, measured in Darwins, plotted against the time interval over which the evolution was observed. The orange points show direct observations of phenotypic change in historical and contemporary populations. The blue dots give changes observed in the fossil record. The three black dots left to right give examples from Dog whelks, our Red deer example, and *Triceratops*. Based on an original plot by GINGERICH (1983) using an expanded dataset from UYEDA *et al.* (2011). Code here.

from the left is a case of evolution over decades in dog whelks. The invasion the green crab (*Carcinus maenas*) drove the evolution of more robust shells in Atlantic dog whelk (*Nucella lapillus*) in response to predation along the North American coast (VERMEIJ, 1982). The shell lip thickness of dog whelks in the St. Andrews, New Brunswick population had changed from 0.94mm to 1.44mm in just 25 years. That's a 50% increase, and a rate of 17060 Darwins.

However, when we observe phenotypic evolution over longer time periods it is usually much slower. For example, the rightmost black dot in Figure 8.14 shows the phenotypic evolution along the lineage leading to *Triceratops*. *Triceratops* measured in an impressive 25.9–29.5 ft in length. They evolved from a close relative of *Protoceratops*, which was a bit bigger than a sheep at ~5.9 ft in about 7.5 million years (COLBERT, 1948). However, that's only a phenotypic change of 0.143 Darwins, its only a roughly four fold change in millions of years. These rates of change in Dinosaurs have nothing on our dog whelks, or many other examples of evolution on short time scales. Thus evolutionary changes we can observe over short timescales readily explain long term changes in quantitative phenotypes.

8.1 Fitness and the Breeder's Equation.

So directional evolution occurs as selection drives a change in the mean phenotype within a generation. But precisely how does this relate to the natural-selection requirement that organisms vary in their fitness? Some different ways of formulating the Breeder's equation give us insight into the conditions for directional selection and the relationship to fitness landscapes.

8.1.1 Directional selection as the covariance between fitness and phenotype.

To think more carefully about this change within a generation, let's think about a simple fitness model where our phenotype affects the viability of our organisms (i.e. the probability they survive to reproduce). The probability that an individual has a phenotype X before selection is $p(X = x)$, so that the mean phenotype before selection is

$$\mu_{BS} = \mathbb{E}[X] = \int_{-\infty}^{\infty} xp(x)dx \quad (8.7)$$

The probability that an organism with a phenotype X survives to reproduce is $w(X)$, and we'll think about this as the fitness of our organism. The probability distribution of phenotypes in those who do

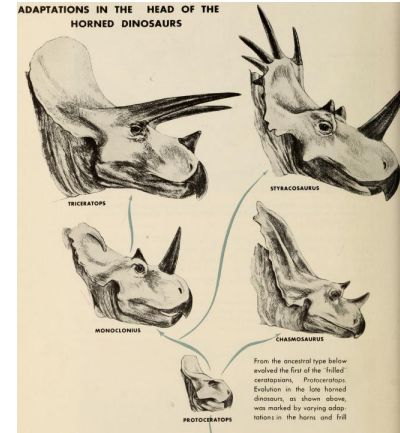


Figure 8.15: The evolution of *Triceratops* from *Protoceratops*, see here for a fun updated view of the *Coronosauria* phylogeny. See these figures from Holtz for an updated & fuller phylogeny.

The dinosaur book : the ruling reptiles and their relatives. (1951) Colbert, E.H. Image from the Internet Archive. Contributed by American Museum of Natural History Library. No known copyright restrictions.

survive to reproduce is

$$\mathbb{P}(X|\text{survive}) = \frac{p(x)w(x)}{\int_{-\infty}^{\infty} p(x)w(x)dx}. \quad (8.8)$$

where the denominator is a normalization constant which ensures that our phenotypic distribution integrates to one. The denominator also has the interpretation of being the mean fitness of the population, which we'll call \bar{w} , i.e.

$$\bar{w} = \int_{-\infty}^{\infty} p(x)w(x)dx. \quad (8.9)$$

Therefore, we can write the mean phenotype in those who survive to reproduce as

$$\mu_S = \frac{1}{\bar{w}} \int_{-\infty}^{\infty} xp(x)w(x)dx \quad (8.10)$$

If we mean center the distribution of phenotypes in our population, i.e. set the phenotype before selection to zero, then

$$S = \mu_S = \frac{1}{\bar{w}} \int_{-\infty}^{\infty} xp(x)w(x)dx = \frac{1}{\bar{w}} \mathbb{E}(Xw(X)) \quad (8.11)$$

where the final part follows from the fact that the integral is taking the mean of $Xw(X)$ over the population.

As our phenotype is mean centered ($\mathbb{E}(X) = 0$), we can see that S has the form of a covariance⁴ between our phenotype X and our relative fitness $w(X)/\bar{w}$.

$$S = \mathbb{E}(X^{w(X)/\bar{w}}) = \text{Cov}(X, {}^{w(X)/\bar{w}}) \quad (8.12)$$

Thus our change in mean phenotype is directly a measure of the covariance of our phenotype and our fitness. Rewriting our breeder's equation using this observation we see

$$R = \frac{V_A}{V} \text{Cov}(X, {}^{w(X)/\bar{w}}) \quad (8.13)$$

we see that the response to selection is due to the fact that our fitness (viability) of our organisms/parents covaries with our phenotype, and that our child's phenotype covaries with our parent's phenotype.

Fitness Gradients and linear regressions To understand this in more detail let imagine that we calculate the linear regression of an individual i 's mean-centered phenotype (X_i) on fitness (W_i), i.e.

$$W_i \sim \beta X_i + \bar{w} \quad (8.14)$$

The best fitting slope of this regression (β), see math appendix around eqn A.43 for more on linear regression, lets call it the ‘fitness gradient’, is given by

$$\beta = \text{Cov}(X, {}^{w(X)/\bar{w}})/V \quad (8.15)$$



Figure 8.16: Red deer (*Cervus elaphus*).

British mammals. Thorburn, A. (1920) Image from the Biodiversity Heritage Library.

Contributed by Field Museum of Natural History Library. Licensed under CC BY-2.0.

⁴ See our math appendix Equation A.39 for the definition of covariance.

i.e. the fitness gradient is the phenotype-fitness covariance divided by the phenotypic variance. Using this result we can rewrite the breeder's equation as

$$R = V_A \beta \quad (8.16)$$

i.e. we'll see a directional response to selection if there is a linear relationship of phenotype on fitness, and if there is additive genetic variance for the phenotype. As one example of a fitness gradient, in Figure 8.17 the lifetime reproductive success (LRS) of male Red Deer is plotted against the weight of their antlers. The red line gives the linear regression of fitness (LRS) on antler mass and the slope of this line is the fitness gradient (β).

Fisher's fundamental theorem of natural selection Finally how does the mean fitness of our population evolve? If we choose relative fitness to be our phenotype ($X = w(X)/\bar{w}$), then the response in fitness is

$$\begin{aligned} R &= \frac{V_A}{V} \text{Cov}(w(X)/\bar{w}, w(X)/\bar{w}) = \frac{V_A}{V} V \\ &= V_A \end{aligned} \quad (8.17)$$

i.e. the response to selection is equal to the additive genetic variance for relative fitness. Or as Fisher put it

"The rate of increase in fitness of any organism at any time is equal to its genetic variance in fitness at that time." -FISHER (1930) (pg 37)

Fisher called this 'the fundamental theorem of natural selection'. Our proof here is just a sketch, and more formal approaches are needed to show it in generality. There has been much gnashing of teeth over exactly how broadly this result holds, and exactly what Fisher meant (see EWENS, 2010, for a recent overview).

8.1.2 Directional Selection on Fitness Landscapes.

One common metaphor when we talk about evolution is that of a population exploring an adaptive landscape with natural selection pushing a population towards higher fitness states corresponding to peaks in this landscape (see e.g. Figure 8.18). LANDE (1976) found an evocative formulation of the Breeder's equation which aids our intuition of phenotypic fitness landscapes. LANDE showed that, if the phenotype is normally distributed, the response to selection (R) could be written in terms of the gradient (derivative) of the mean fitness (\bar{w}) of the population⁵ as a function of the mean phenotype:

$$R = \frac{V_A}{\bar{w}} \frac{\partial \bar{w}}{\partial \bar{x}} \quad (8.19)$$

What does this mean? Well V_A/\bar{w} is always positive, so the direction our population responds to selection is predicted by the sign of the

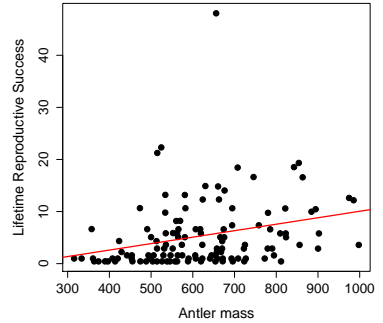
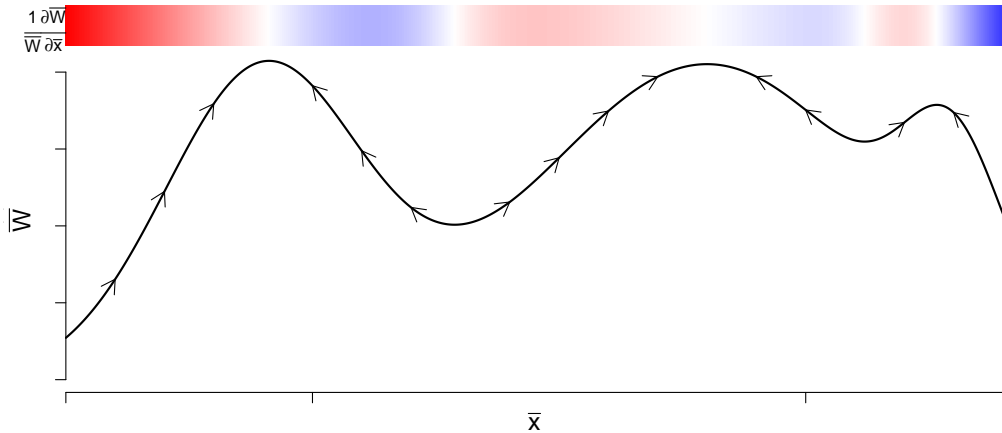


Figure 8.17: Lifetime reproductive success (LRS) of male Red Deer as a function of their antler mass. Data from KRUUK *et al.* (2002); see the paper for discussion of the complexities of equating this selection gradient with the evolutionary response. Code here..

⁵ This follows from the fact that we can then move the derivative inside the integral of \bar{w} , eqn (8.9), to write the new term in eqn (8.19) as

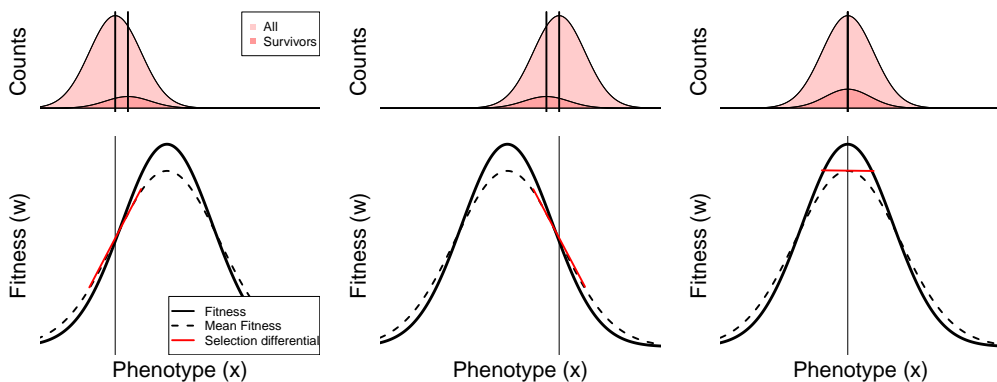
$$\begin{aligned} \frac{1}{\bar{w}} \frac{\partial \bar{w}}{\partial \bar{x}} &= \frac{1}{\bar{w}} \int_{-\infty}^{\infty} w(x) \frac{\partial p(x)}{\partial \bar{x}} dx \\ &= \int_{-\infty}^{\infty} \frac{w(x)}{\bar{w}} \frac{(x - \bar{x})}{V} dx \\ &= \frac{\text{cov}(w(x), x)}{\text{var}(x)} \end{aligned} \quad (8.18)$$

which is β , so that eqns (8.16) and (8.19) are equivalent. For this equivalence to hold, in the first line we assume that $w(x)$ is not a function of \bar{x} , while the middle line is true when $p(x)$ is the normal distribution.



derivative (see Appendix Section A.1 for more on derivatives). If increasing the mean phenotype of the population slightly would increase mean fitness ($\partial \bar{w} / \partial \bar{x} > 0$) our population will respond that generation by evolving toward higher values of the trait ($R > 0$), left panel of Figure 8.19. Conversely, if decreasing the population mean phenotype slightly would increase the mean fitness ($\partial \bar{w} / \partial \bar{x} < 0$) the population will that generation evolve towards lower values of the phenotype (middle panel of Figure 8.19). Thus, if selection pressures remain constant, we can think of the population as evolving on an adaptive landscape where the elevation is given by the population mean fitness. Natural selection operates on the basis of individual-level fitness, but as a result of this our population is increasing in its average fitness, i.e. our population is becoming better adapted. We'll discuss the caveats of this hill-climbing interpretation below.

Figure 8.18: An example of a fitness landscape, showing the mean fitness of the population (\bar{w}) as a function of the mean phenotype of the population (\bar{x}). The arrows show the expected direction of movement of our population on the fitness landscape, with natural selection moving our population toward local fitness optima. The coloured bar shows the derivative (slope) of the mean fitness with respect to mean phenotype (eqn. (8.19)). Red values are positive slopes corresponding to the population evolving towards the right of the page, blue is a negative slope with the population moving to the left.



What happens when it reaches the top of a peak? Well at the top of a peak $\partial \bar{w} / \partial \bar{x} = 0$, as it is a local maximum, and so $R = 0$. As-

Figure 8.19: A population evolving on a (guassian) fitness surface. The bottom panel shows the expected individual fitness ($w()$) and mean fitness as a function of phenotype. The red line shows the best fitting linear approximation to the relationship between phenotype and individual fitness, eqn (8.14), whose slope is β . The top panel shows the distribution of the phenotype before and after selection. Code here..

suming that the relationship between fitness and phenotype stays constant, our population will stay at the top of the fitness peak. This view of natural selection does not imply that the population is evolving to the best possible state. Our population is just marching up the hill of mean fitness (end panel Figure 8.19). However, this peak isn't necessarily the highest fitness peak but simply whichever peak was closest. So our population can become trapped on a local, but not global peak of fitness (see, for example Figure 8.18).

One dramatic example documenting adaptive evolution to a new fitness optimum is offered by a remarkable time-series of stickleback evolution from a fossil lake-bed in Nevada (BELL *et al.*, 2006). In this lake the layers of sediment are laid down each year allowing a very detailed time series with over five thousand fossils measured. The time-series documents the evolution towards a new set of optimum phenotypes in the fifteen thousand years after the initial invasion of the lake by a heavily armoured stickleback species. In Figure 8.20 the population mean number of touching pterygiophores, the bones supporting the dorsal spines, through the fossil record (Figure 8.21). Note how quickly the species evolves toward its new value, presumably a fitness optimum in their new environment, and the long subsequent time interval over which the population mean phenotype fluctuates about its new value.

HUNT *et al.* (2008) fitted a model of a population adapting to a fitness landscape, with a single peak, to these time-series data. Their fitted fitness surface is shown in the lower panel of Figure 8.20 . The arrows show the moves that the population mean phenotype is making on this inferred fitness surface. The population initially takes large steps up toward the peak of this surface and subsequently fluctuates around the peak. Under the interpretation that there is a single stationary peak these fluctuations represent genetic drift randomly knocking the population off its optimum, with selection acting to restore the population towards this local optimum.

Issues with the interpretation of fitness landscapes. In practice, fitness landscapes may not be constant. The environment may be constantly changing so our population is constantly forced to change to keep up with the fitness peak. Indeed our environment may change so quickly that our population cannot keep up with the peak. Our population is still trying to increase its mean fitness, to ‘adapt’, but the landscape itself is evolving. In the case of very rapid environmental change our population may slide further and further away the peak, and as a consequence its mean fitness decreases which may drive the population to extinction if our population drops below $\bar{w} < 1$ for long enough. The conditions for extinction are an active area of research

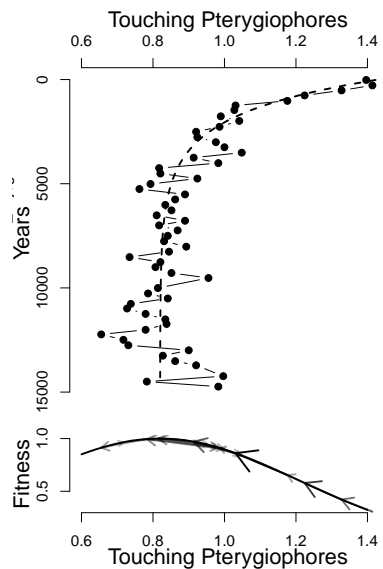


Figure 8.20: **Top)** A time series of stickleback phenotypic evolution from the fossil record. After a heavily armoured stickleback invades the lake it quickly evolves towards fewer touching pterygiophores (the bones supporting the dorsal spines). Fossil measurements means are calculated in 250 year bins. **Bottom)** How our population moves on the Inferred fitness landscape. The arrows show each move made by the population in the 250 intervals. Data from BELL *et al.* (2006) and HUNT *et al.* (2008) Code here.



Figure 8.21: Fossil stickleback. Photo by Peter J. Park from LOSOS *et al.* (2013), licensed under CC BY 4.0.

in the field of ‘Evolutionary rescue’. More generally, for our fitness landscape result (eqn (8.19)) to hold, and for us to be able to talk of our population attempting to evolve to higher mean fitness states, we need the fitness of our phenotypes to be independent of the frequency of other phenotypes in the population. (This independence allows us to assume that the fitness of individuals is not a function of the mean phenotype, as needed in eqn (8.18)). The assumption of frequency independence may not hold when there is competition between individuals, e.g. for resources or mates, as then the fitness of an individual depends on the strategies pursued by other individuals in the populations.

8.1.3 Stabilizing and Disruptive selection

Up to now we have just looked at directional selection, where selection acts to change the mean phenotype. However, we can also use quantitative genetic models to describe other modes of selection, extending from effects on the population mean the next natural step is to think about selection which acts on the population variance. Selection might act more strongly against individuals in the tails of the distribution, with those closer to the mean phenotype having higher fitness, which lowers the variance. Selection could also disfavour individuals close to the population mean, with individuals with extreme phenotypes having higher fitness, which acts to increase the variance of the population.

Directional selection occurs because of the covariance between our phenotype and fitness, eqn (8.12). Just as expressing directional selection as a covariance allowed us to characterize directional selection as the linear relationship between fitness and phenotype, β , we can summarize the variance reducing selection by including a quadratic term in the regression of fitness on phenotype

$$w_i \sim \beta x_i + 1/2\gamma x_i^2 + \bar{w} \quad (8.20)$$

This γ , the coefficient of the quadratic term in our model, is the quadratic selection gradient: the covariance of fitness and the squared deviation from the phenotypic mean (μ_{BS}), i.e.

$$\gamma = \frac{\text{Cov}(w(X), (X - \mu_{BS})^2)}{V^2} \quad (8.21)$$

Our γ describes the curvature of the fitness surface around the mean.

Values of $\gamma < 0$ are consistent with stabilizing selection, reducing the variance. While values of $\gamma > 0$ are consistent with disruptive selection, increasing the variance.

Under stabilizing selection the individuals with extreme phenotypes in either tail have lower fitness, the result of which is to reduce the

Just like how β could be interpreted as the mean gradient of the fitness surface, our γ is the mean curvature of the fitness surface

$$\gamma = \mathbb{E} [\partial^2 w(x)/\partial x^2] = \int \partial^2 w(x)/\partial x^2 p(x) dx \quad (8.22)$$

see Appendix Section A.1 for more on 2nd derivatives.

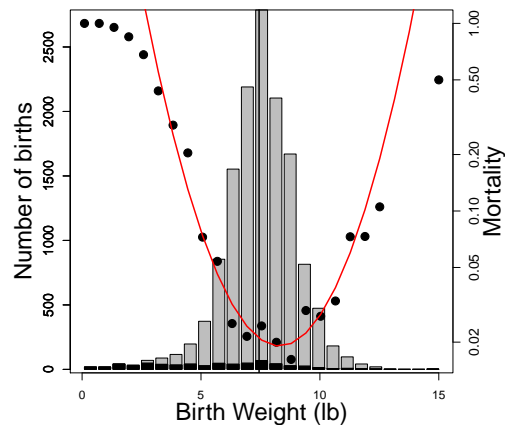


Figure 8.22: Bars show the total number of births with different birth weights (left axis) Dots show the mortality probability for different birth-weight bins (right axis), the red line shows a fitted quadratic model to mortality. Data from KARN and PENROSE (1951) Table 2, collapsing male and female births, Code here.

phenotypic variance within a generation. A classic case of stabilizing selection is birth weight in humans (KARN and PENROSE, 1951). Mary Karn collected data for nearly fourteen thousand pregnancies from 1935-46 for birth weight and mortality. These data are replotted in Figure 8.22. The variance of all births is 1.575lb^2 , while in live births this was reduced to 1.26lb^2 , a 20% reduction in variance due to stabilizing selection. It is worth noting that this selection pressure has been greatly reduced over the decades in societies with access to good prenatal care (ULIZZI and TERRENATO, 1992).

In Central Africa, Black-bellied seedcrackers (*Pyrenestes ostrinus*) show disruptive selection on a remarkable beak-size polymorphism (Figure 8.24). The small-beaked individuals feed on soft seeds from one species of marsh sedge while the big-beaked individuals feed on hard seeds from another sedge, which requires ten times the force to crack. SMITH (1993) recorded the fates of hundreds of juveniles, and found that individuals with intermediate beak sizes survived at much lower rates (Figure 8.24) because they were not well adapted to either seed resource. Break length is subject to disruptive selection, as can also be seen by the significant negative quadratic term in the regression of survival probability on break length. The variance of mandible length in the total sample of individuals was 0.5mm^2 in the survivors this variance increased by a factor of 2.5 to 1.3mm^2 .

To illustrate how directional selection and quadratic terms play off during adaptation, lets consider the goldenrod gall fly (*Eurosta solidaginis*), aka the goldenrod ball gallmaker. See Figure 8.26. As it's wonderful name implies this insect lays its eggs in Goldenrod plants, and the larvae release chemicals forcing the plant to form a gall that forms a home for the larvae as they develop. While this seems like a pretty sweet deal for the larvae, it is not without its perils.



Figure 8.23: Lesser seedcracker *Pyrenestes minor* a close relative of the Black-bellied seedcracker, whose beak is about the same size as the smallest Black-bellied individuals.
The birds of Africa, comprising all the species which occur in the Ethiopian region. (1986) Sclater, W. L Plate by H. Grönvold Image from the Biodiversity Heritage Library. Contributed by Smithsonian Libraries. Not in copyright.

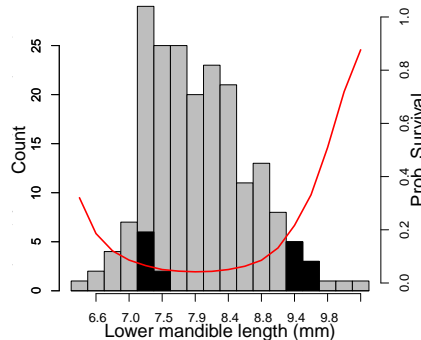
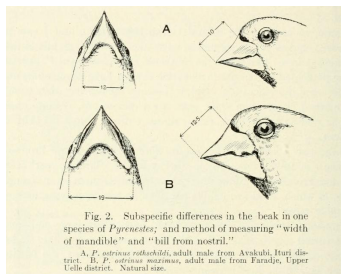


Figure 8.24: **Left** An illustration of the remarkable variation in beak size within Black-bellied seedcrackers (*P. ostrinus*). **Right** A histogram of a beak size measurement in Black-bellied seedcrackers. All juveniles are shown in grey, while the black bars show the survivors. The red curve shows the best fitting linear and quadratic model to the probability of survival, fitted using a binomial generalized linear model with a logit link function.

Left illustration from: Size variation in *Pyrenestes* by Chapin J.P. in the Bulletin of the American Museum of Natural History (Vol. XLIX 1923) Image from the Biodiversity Heritage Library. Contributed by Toronto Library. Not in copyright.

When the small, ball galls fall risk of parasitism from parasitoid wasps. When all the ball galls are small in the population selection drives strong positive directional selection on gall size, with little stabilizing selection. Notice in the left panel of Figure 8.26 the good agreement between the linear selection gradient and the fit including a linear and quadratic term. However, bigger galls fall under the pall of predation from downy woodpeckers and black-capped chickadees, who seek out the tasty larvae. Thus intermediate size galls are favoured, a fitness peak that the population quickly reaches. Once on this peak, as shown in the right panel of Figure 8.26 there is no directional selection, i.e. no linear slope, but there is strong stabilizing selection, i.e. a quadratic term. Thus the population will be maintained at this fitness peak indefinitely if the environment remains unchanged.

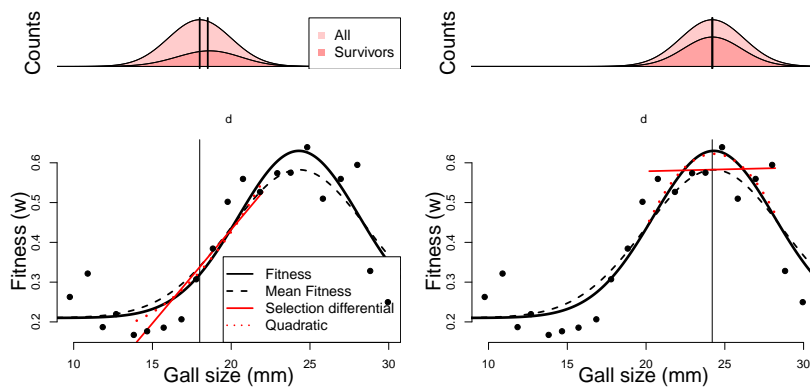


Figure 8.25: The gall formed by the goldenrod ball gallmaker (*Eurosta solidaginis*) in a goldenrod plant. The one on the right is cut to show a partial cross-section.

Annual report of the New York State Museum (1917) Image from the Biodiversity Heritage Library. Contributed by The LuEsther T Mertz Library, the New York Botanical Garden. Not in copyright.

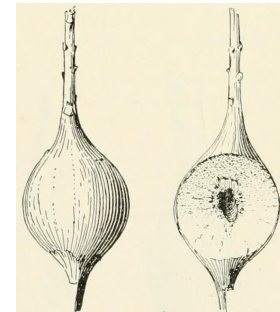


Figure 8.26: Fitness surface for gall diameter in goldenrod ball gallmakers. The dots are the measured survival probabilities of bins of different sized galls. The solid line is a fitted individual fitness surface ($w()$). Dotted line is \bar{w} plotted as a function of the population mean assuming a normal distribution with a standard deviation of 2mm. Data from WEIS and GORMAN (1990), Code here.

9

The Response of Multiple Traits to Selection.

The fitness of an organism depends on the outcome of many different organismal processes and phenotypes. Thus natural selection is often acting on many phenotypes in concert. In some cases the various directions that selection tries to pull the population phenotypes may not all be possible to satisfy all at once. Such fitness tradeoffs occur when selection acts on genetic correlated phenotypes in contradictory ways.

To understand the short-term consequence of selection on multiple phenotypes we can generalize the Breeder's equation to multiple traits¹. Considering two traits we can write our responses in both traits as

$$\begin{aligned} R_1 &= V_{A,1}\beta_1 + V_{A,1,2}\beta_2 \\ R_2 &= V_{A,2}\beta_2 + V_{A,1,2}\beta_1 \end{aligned} \tag{9.1}$$

¹ LANDE, R., 1979 Quantitative genetic analysis of multivariate evolution, applied to brain: body size allometry. Evolution 33(1Part2): 402–416

where the 1 and 2 index our two different traits. Here $V_{A,1}$ and $V_{A,2}$ are the additive genetic variance for trait 1 and 2 respectively, while $V_{A,1,2}$ is our additive covariance between our traits. Our selection gradient for trait 1, β_1 , represents the change in fitness as you change trait 1 alone holding other traits constant constant. These β can be estimated by multivariate regression, see below. The multivariate breeders equation is a statement that our response in any one phenotype is modified by selection on other traits that genetically covary with that trait.

We can also write this equivalently in matrix form, for an arbitrary number of traits. Writing our change in the mean of our multiple phenotypes within a generation as the vector \mathbf{S} and our response across multiple generations as the vector \mathbf{R} . These two quantities are related by

$$\mathbf{R} = \mathbf{G}\mathbf{V}^{-1}\mathbf{S} = \mathbf{G}\boldsymbol{\beta} \tag{9.2}$$

where \mathbf{V} and \mathbf{G} are our matrices of the variance-covariance of pheno-

types and additive genetic values (eqn. (7.20) (7.19)) and β is a vector of selection gradients (i.e. the change within a generation as a fraction of the total phenotypic variance). Note that $\beta = \mathbf{V}^{-1}\mathbf{S}$, such that each β represents the selection gradient on a trait accounting for its phenotypic covariances with other traits.

An example of the outcome of selection on multiple phenotypes consider the bout of selection measured by GRANT and GRANT (1995) in medium ground Darwin's finch (*Geospiza fortis*). They measured 634 birds in '76, of which only 15% survived to 1977. The birds who survived were heavier and had longer, deeper bills than average.

Trait	Mean before Selection (1976)	S	β	Mean next gen. (1978)
Weight	16.06	0.74	0.477	17.13
Bill Length	10.63	0.54	-0.144	10.95
Bill Depth	9.21	0.36	0.528	9.70

Accounting for the phenotypic covariances among the traits (\mathbf{V}^{-1}), they found that both weight and bill depth showed direct directional selection towards larger values (positive β s). However, bill length showed weak selection towards shorter beaks (negative β), reflecting the fact that bill length shows positive phenotypic correlation with bill depth and weight, and most of the direct selection was on weight and bill depth dragging bill length along. Looking at the next generation all three traits have all significantly increased. Thus despite selection possibly favouring shorter bill lengths, and certainly not favouring long bills, bill length increased in the next generation due to its positive genetic covariance with two traits that selection was acting to increase.

Question 1. You collect observations of red deer within a generation, recording an individual's number of offspring and phenotypes for a number of traits which are known to have additive genetic variation. Using your data, you construct the plots shown in Figure 9.1 (standardizing the phenotypes). Answer the following questions by choosing one of the bold options. Briefly justify each of your answers with reference to the breeder's equation and multi-trait breeder's equation.

A) Looking just at figure 9.1 A, in what direction do you expect male antler size to evolve?

Insufficient information, increase, decrease.

B) Looking just at figures 9.1 B and C, in what direction do you expect male antler size to evolve?

Insufficient information, increase, decrease.

C) Looking at figures 9.1 A, B, and C, in what direction do you expect male antler size to evolve?

Table 9.1: Trait means and selection differentials and gradients from an episode of selection in *Geospiza fortis*. Numbers from table 2 & 3 of GRANT and GRANT (1995).

Insufficient information, increase, decrease.

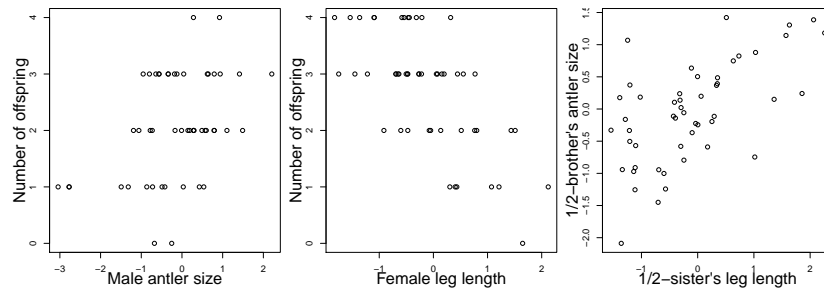


Figure 9.1: Observations of red deer within a generation; recording an individual's number of offspring and phenotypes (simulated data), which are known to have additive genetic variation. The figures left to right are A-C. (Data are simulated. Code here.)

As an example of correlated responses to selection, consider the WILKINSON (1993) selection experiment on Stalk-eyed flies (*Cryptodiopsis dalmanni*). Stalk-eyed flies have evolved amazingly long eye-stalks. In the lab, WILKINSON established six populations of wild-caught flies and selected up and down on males eye-stalk to body size ratio for 10 generations (left plot in Figure 9.2). Despite the fact that he did not select on females, he saw a correlated response in the females from each of the lines (right plot), because of the genetic correlation between male and female body proportions.

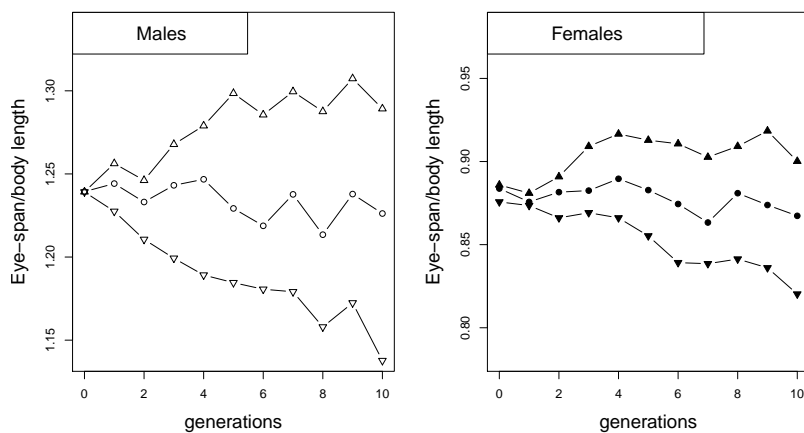
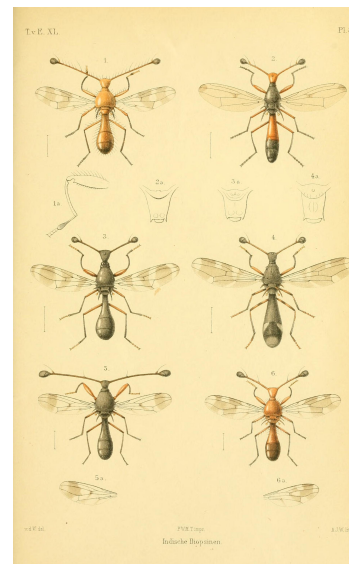


Figure 9.2: WILKINSON selected two populations of flies for increased eye-stalk to body length ratio in males (mean shown as up triangles), and two for a decreased ratio (down triangles), by taking the top 10 males with the highest (lowest) ratio out of 50 measures. He also established two control populations (circles). He constructed each generation of females by sampling 10 at random from each population. Data from WILKINSON (1993). Code here.



Question 2.

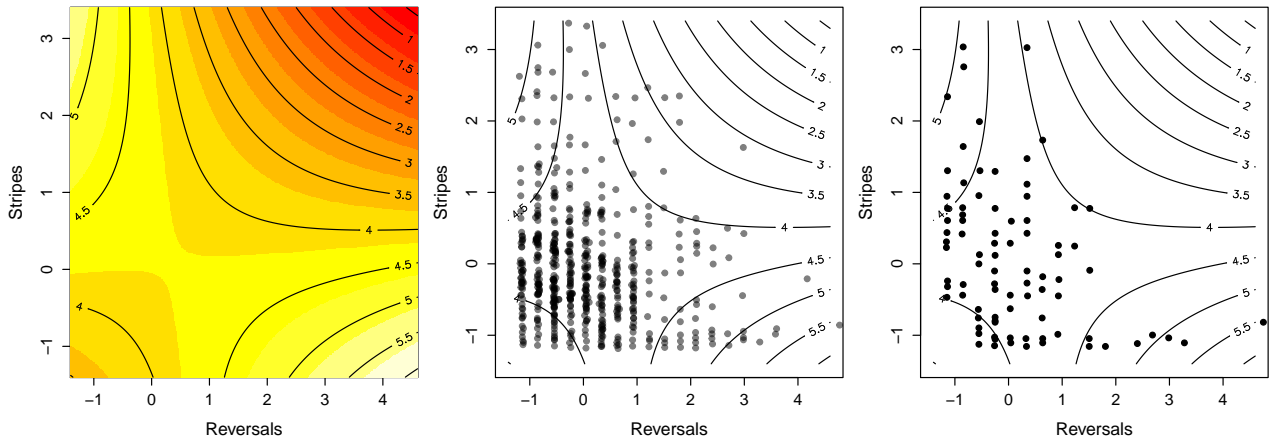
At the end of ten generations in WILKINSON's experiment (Figure 9.2), the males from the up- and down-selected lines had mean eye-stalk to body ratios of 1.29 and 1.14 respectively, while the females from the up- and down-selected lines had means of 0.9 and 0.82.

A) WILKINSON estimated that by selecting the top/bottom 10 males, he had on average shifted the mean body ratio by 0.024 within

Figure 9.3: Stalk-eyed Flies (*Diopsidae*). Diptera. van der Wulp. 1898. Image from the Biodiversity Heritage Library. Contributed by Smithsonian Libraries. Not in copyright.

each generation. What is the male heritability of eye-stalk to body-length ratio?

B) Assume that the additive genetic variance of male and female phenotypes are equal and that there is no direct selection on female body-proportion in this experiment, i.e. that all of the response in females is due to correlated selection. Can you estimate the male-female genetic correlation of the eye-stalk ratio?



Estimating multivariate selection gradients We can estimate multivariate directional (β) and quadratic selection gradients (γ) just as we did for a single traits (x_1 and x_2), using linear and quadratic models (in eqn (8.14) and (8.20)). For example, for two traits we can write

$$w_i \sim \beta_1 x_{1,i} + 1/2\gamma_1 x_{1,i}^2 + \beta_2 x_{2,i} + 1/2\gamma_2 x_{2,i}^2 + \gamma_{1,2} x_{1,i} x_{2,i} + \bar{w} \quad (9.3)$$

where β_1 and γ_1 are the directional and quadratic selection gradients for trait one, and similarly for trait two (LANDE and ARNOLD, 1983). The covariance selection gradient between traits is given by $\gamma_{1,2}$. This technique for measuring multivariate selection is sometimes called ‘Lande-Arnold regression’.

BRODIE III (1992)’s work provides a nice example of selection on multiple predation-avoidance traits in northwestern garter snakes (*Thamnophis ordinoides*). BRODIE III released hundreds of snakes born in the lab into the wild, and then performed mark-recapture observations to monitor their fate.

Before releasing them he measured how stripy they were, and their behavioural tendency to reversals of direction during simulated flight from a predator. His quadratic fitness surface is shown in Figure 9.4, based on fitting the regression given by eqn (9.3) to juvenile survival. He found that neither single trait directional or quadratic gradients

Figure 9.4: **Left)** The garter snake fitness surface estimated by BRODIE III (1992) lighter colours indicate higher relative fitness. **Middle)** The phenotypes of all of the snakes released by Brodie, each dot is an individual. **Right)** The phenotypes of surviving snakes. Note how snakes in the top left and bottom right corner are over represented in the survivors. Data from BRODIE III (1992) Code here..

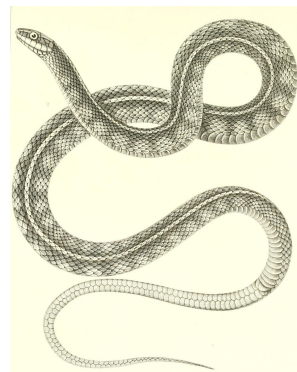


Figure 9.5: Northwestern garter snake (*Eutaenia cooperi*, now *Thamnophis ordinoides*)

The natural history of Washington territory, with much relating to Minnesota, Nebraska, Kansas, Oregon, and California (1859). Cooper J.G. and Suckley, G. Image from the Biodiversity Heritage Library. Contributed by Smithsonian Libraries. Not in copyright.

were significant, i.e. there was no apparent selection on one trait ignoring the other. However, there was a significant negative covariance ($\gamma_{1,2} < 0$). The individuals with the highest chance of survival are *either* highly striped and perform few reversals (top left corner), *or* have little striping but reverse course frequently (bottom right corner).

9.1 Some applications of the multivariate trait breeder's equation

The multivariate breeders equation has a lot of different uses in understanding the response of multiple traits to selection. It also offers strong insights into the mechanistic underpinnings of kin selection and sexual selection. We'll discuss these next.

9.1.1 Hamilton's Rule and the evolution of altruistic and selfish behaviours

“ ‘The only reason for making a buzzing-noise that I know of is because you’re a bee.’ Then [Pooh] thought another long time, and said: ‘The only reason for being a bee that I know of is to make honey...And the only reason for making honey is so as I can eat it.’ ”
—Winnie-the-Pooh, MILNE and SHEPARD (1926).

One of the seismic shifts caused by Darwin's work was the realisation that organisms don't exist for the benefit of other individuals or other species. Bees didn't evolve to pollinate flowers, any more than they evolved to make honey for bears. If we can say that there is a 'reason' why an organism exists it is only to leave offspring to the next generation. Pooh can be forgiven for straying from Darwinian thought, as he exists for the benefit of Christopher Robin and other childrens' bedtime stories.

However, there's a wrinkle to this Darwinian view. Worker bees don't make honey to benefit their offspring, they are sterile and are working for the benefit of the Queen bee and her offspring. Individuals frequently behave in ways that sacrifice their own fitness for the benefit of others. That selection favours such apparent acts of altruism is puzzling at first sight. HAMILTON (1964a,b) supplied the first general evolutionary explanation of such altruism. His intuition was that while an individual is losing out of some reproductive output, the alleles underlying an altruistic behaviour can still spread in the population if this cost is outweighed by benefits gained through the transmission of these alleles through a related individual. Note that this means that the allele is not acting in an self-sacrificing manner, even though individuals may act as a result.

Altruism reflects social interactions. So as a simple model let's imagine that individuals interact in pairs, with our focal individual i

MAYNARD SMITH (1964) coined the name kin selection to describe Hamilton's approach to this problem. It's also sometimes called the inclusive fitness approach, as we need to include not just one individual's fitness but the weighted sum of all the fitness of all their relatives.

being paired with an individual j . Imagine that individuals have two possible phenotypes $X = 1$ or 0 , corresponding to providing or withholding some small act of ‘altruism’ (we could just as easily flip these labels and call them an unselfish act and a selfish act respectively). Our pairs of individuals interacting could, for example, be siblings sharing a nest. The altruistic trait could be as simple as growing at a slightly slower rate so as to reducing sibling-competition for food from parents, or more complicated acts of altruism such as children foregoing their own reproduction so as to help their parents raise their siblings.

Providing the altruistic act has a cost C to the fitness of our individual and failing to provide this act has no cost. Receiving this altruistic act confers a fitness benefit B over individuals who did not receive this act. HAMILTON’s rule states that such a trait will spread through the population if

$$2FB > C \quad (9.4)$$

where F is the average kinship coefficient between the interacting individuals (i and j). In the usual formulation of Hamilton’s Rule our $2F$ is replaced by the ‘Coefficient of relationship’, which is the proportion of alleles shared between the individuals. Here we use two times the kinship coefficient to keep things inline with our notation for these chapters. Note that if our individuals are themselves inbred we need to do a little more careful to reconcile these two measures. So the altruistic behaviour will spread even if it is costly to the individual if its cost is paid off by the benefit to sufficiently related individuals.

As one example of kin-selection consider KRAKAUER (2005)’s work on co-operative courtship in wild turkeys (*Meleagris gallopavo*). Male turkeys often form display partnerships, with a subordinate male helping a dominant male with displaying to females and defending the females from other groups of males.

These pairs are often full brothers ($F = 0.25$), with the subordinate male often being the younger of the two. The subordinate male often loses out on mating opportunities over their entire lifetime by acting as a wingman for their older brothers. KRAKAUER (2005) estimated that dominant males gained an extra 6.1 offspring when they display with a partner than males who display alone. While the subordinate males lose out on fathering 0.9 offspring compared to solitary males. Thus the costs of helping by subordinate males is more than compensated by the fitness gains of their brothers ($(2 \times 0.25) \times 6.1 > 0.9$), and so the evolution of this altruistic helping in co-operative courtship is potentially well explained by kin-selection (see AKÇAY and VAN CLEVE, 2016, for more analysis).

Question 3. How would this answer be changed if the male



Figure 9.6: Turkey (*Meleagris gallopavo*).
Bilder-atlas zur Wissenschaftlich-populären
Naturgeschichte der Vögel in ihren sämtlichen
Hauptformen (1864). Wien, K.K. Hof Image
from the Biodiversity Heritage Library.
Contributed by Smithsonian Libraries. Not in
copyright.

Turkey partnerships were only 1/2 sibs, or first cousins?

Where does this result come from? Well, we can use our quantitative genetics framework to gain some intuition by deriving a simple version of Hamilton's Rule by thinking about the phenotypes of an individual's kin as genetically correlated phenotypes. To sketch a proof of this result, let's assume that our focal i individual's fitness can be written as

$$W(i, j) = W_0 + W_i + W_j \quad (9.5)$$

where W_i is the contribution of the fitness of the individual i due to their own phenotype, and W_j is the contribution to our individual i 's fitness due to the interacting individual j 's behaviour (i.e. j 's phenotype). With the benefit B and cost C , our $W(i, j)$ are depicted in Figure 9.7.

Following our multivariate breeder's equation, we can write the expected change of our behavioural phenotype as

$$R = \beta_i V_A + \beta_j V_{A,i,j}, \quad (9.6)$$

Our altruistic phenotype is increasing in the population if $R > 0$, i.e. if

$$\beta_i V_A + \beta_j V_{A,i,j} > 0 \quad (9.7)$$

The slope β_i of the regression of our focal individual's behavioural phenotype on fitness is proportional to $-C$. The slope β_j of the regression of our interacting partner's phenotype on our focal individual's fitness is proportional to B (with the same constant of proportionality). Therefore, our altruistic phenotype is increasing in the population if

$$\begin{aligned} \beta_i V_A + \beta_j V_{A,i,j} &> 0 \\ B \frac{V_{A,i,j}}{V_A} &> C \end{aligned} \quad (9.8)$$

So what's the average genetic covariance between individual i and j 's altruistic phenotype? Well it's the same behavioural phenotype in both individuals, so the phenotypes are genetically correlated if our individuals are related to each other. The covariance of the same phenotype between two individuals is just $2F_{i,j}V_A$ (see (7.15)). So our altruistic phenotype is increasing in the population if

$$\begin{aligned} B \frac{2F_{i,j}V_A}{V_A} &> C \\ 2F_{i,j}B &> C \end{aligned} \quad (9.9)$$

Seen from this perspective, HAMILTON's rule is simply a statement that altruistic behaviours can spread via kin-selection, if the average

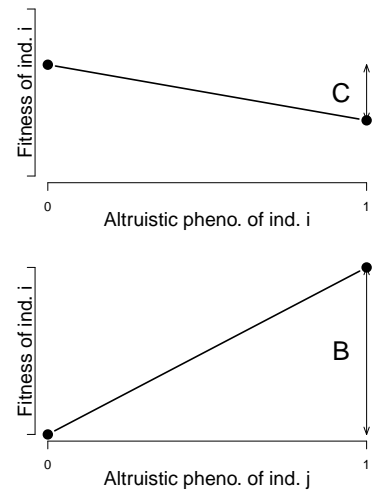


Figure 9.7: **Top)** The fitness of individual i as a function of their behavioural phenotype, where altruistic/non-altruistic behavioural phenotypes are encoded as 1 and 0 respectively. The direct fitness cost of behaving altruistically is C . **Bottom)** The fitness of our focal individual i as a function of the behavioural phenotype of their interacting partner (j). Our focal individual gets an increase B in fitness if their partner behaves altruistically. Code here.

Here we've following a simplified version of QUELLER (1992)'s treatment, to re-derive Hamilton's rule in a quantitative genetics framework (Hamilton's original papers did this in a population genetics framework).

cost to an individual of displaying an altruistic phenotype, i.e. carrying altruistic alleles, is paid back through the average benefit of interacting with altruistic relatives (kin).



Under the kin-selection, relatedness and the breeding structure of the populations are hypothesized to be a key factor in determining the evolution of altruistic behaviours. One most impressive example of the evolution of altruism is the repeated evolution of eusociality, where sterile castes have evolved to help to rear their siblings rather than their own offspring. Eusociality has evolved at least eight independent times in Hymenoptera (bees, wasps, and ants). There's huge variation in mating systems in Hymenoptera from high levels of multiple mating to monandry. HUGHES *et al.* (2008) conducted a comparative phylogenetic analysis of mating system across hundreds of Hymenoptera species. They found that each of the eight of eusocial clades had monandry, females mating with a single male, as an ancestral state. Thus, eusociality initially evolved in populations where relatedness was maximized among siblings.

9.1.2 Sexual selection and the evolution of mate preference by indirect benefits.

Organisms often put an enormous effort into finding and attracting mates, sometimes at a considerable cost to their chances of survival. Why are individuals so choosy about who they mate with, particularly when their choice seems to be based on elaborate characters and arbitrary displays that surely lower the viability of their mates?

One major reason why individuals evolve to be choosy about who they mate with is that it can directly impact their fitness. By choosing a mate with particular characteristics, individuals can gain more parental care for their offspring, avoid parasites, or be choosing a mate

Figure 9.8: A selection of the huge diversity of Hymenoptera.

Naturgeschichte, Klassification und Nomenclatur der Insekten vom Bienen, Wespen und Ameisen. Christ, JL Image from the Biodiversity Heritage Library. Contributed by University of Illinois Urbana Champaign. Not in copyright.

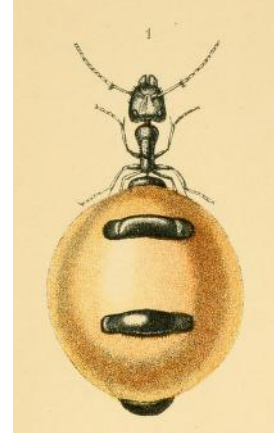


Figure 9.9: Australian Honey-pot Ant (*Camponotus inflatus*). Honey ants are gorged with honeydew collected by their nest mates, till they swell to the size of grapes, and are used as a food storage device.

Ants, bees, and wasps: a record of observations on the habits of the social Hymenoptera (1897) Lubbock, J. Image from the Biodiversity Heritage Library. Contributed by Smithsonian Libraries. Not in copyright.

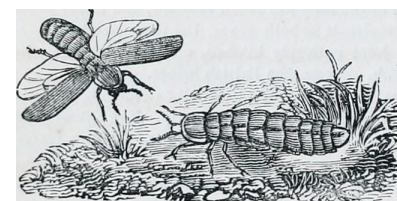


Figure 9.10: Male (left) and female (right) common glow worm (*Lampyris noctiluca*).

The animal kingdom : arranged after its organization; forming a natural history of animals, and an introduction to comparative anatomy. (1863) Cuvier, G. Image from the Biodiversity Heritage Library. Contributed by University of Toronto - Gerstein Science Information Centre. Not in copyright.

with higher fertility. For example, female glow-worms flash at night to attract males flying by. Females with larger, brighter lanterns have higher fecundity, so males with a preference for brighter flashes will gain a direct benefit to their own fitness. (Note that males will benefit even if these differences in female fecundity are entirely driven by differences in environment, and thus non-heritable.) Indeed male glow worms have evolved to be attracted to brighter flashing lures.

However, even in the absence of direct benefits of choice, selection can still indirectly favour the evolution of choosiness. These indirect benefits occur because individuals can have higher fitness offspring by choosing a mate whose phenotype indicates high viability (the so-called ‘good genes’ hypothesis), or by choosing a mate whose phenotype is simply attractive, and likely to produce similarly attractive offspring (the ‘runaway’ or ‘sexy sons’ hypothesis).

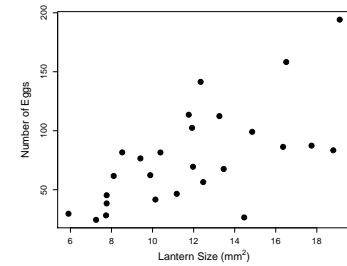
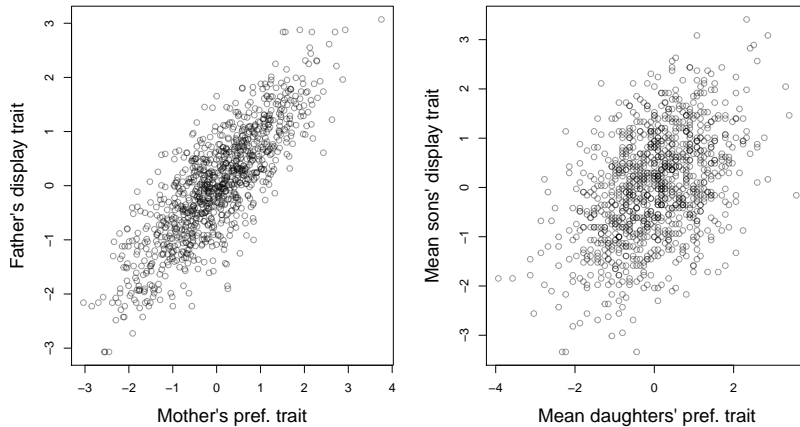


Figure 9.11: Female Glow worms who have the largest, and therefore brightest, lanterns have the highest fecundity. Data from HOPKINS *et al.* (2015). [Code here](#).

Figure 9.12: **Left**) Assortative mating between males and females. Males vary in a display trait (e.g. tail length), females vary in their preference for this trait. We see evidence of assortative mating as females with a preference for a particular value of the male trait tend to mate with those males. **Right**) As both male trait and female preference are genetic this establishes a genetic correlation in the next generation. This is simulated data. [Code here](#).

We'll denote a display trait, e.g. tail length, in males by σ and a preference trait in females by φ . Our display trait is under direct selection in males, such that its response to selection can be written as

$$R_\sigma = \beta_\sigma V_{A,\sigma} \quad (9.10)$$

Let's assume that the female preference trait, the degree to which females are attracted to long tails, is not under direct selection $\beta_\varphi = 0$. Then the response to selection of the preference trait can be written as

$$R_\varphi = \beta_\varphi V_{A,\varphi} + \beta_\sigma V_{A,\varphi\sigma} = \beta_\sigma V_{A,\varphi\sigma} \quad (9.11)$$

So the female preference will respond to selection if it is genetically correlated with the male trait, i.e. if $V_{A,\varphi\sigma}$ is not zero. There's a number of different ways this genetic correlation could arise; the simplest is that the loci underlying the male trait may have a pleiotropic

effect on female preference. However, female preference may often have quite a distinct genetic basis from male display traits.

A more general way in which trait-preference genetic correlations may arise is through assortative mating. As females vary in their tail-length preference, the ones with a preference for longer tails will mate with long-tailed males and the opposite for females with a preference for shorter tails. Therefore, a genetic correlation between display and preference traits will become established (see Figure 9.12).

The males with the longer tails will also carry the alleles associated with the preference for longer tails, as their long-tailed dads tended to mate with females with a genetic preference for long tails. Similarly, the males with shorter tails will carry alleles associated with the preference for shorter tails. Thus if there is direct selection for males with longer tails, then the female preference for longer tails will increase too, as it is genetically correlated via assortative mating.

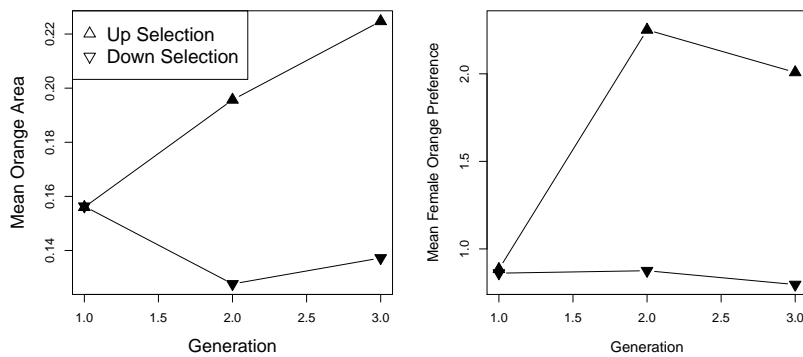


Figure 9.13: Mean phenotypes for the two up- and two down-selected populations of Guppies. Left panel: A response to selection was seen due to the direct selection on male colouration. Right panel: An indirect, correlated response was also seen in female preference. Data from HOUDE (1994). Code here.

As an example of how direct selection on display traits can drive the evolution of preference traits, let's consider some data from guppies. Guppies (*Poecilia reticulata*) are a classic system for studying the interplay of natural and sexual selection. In some populations of guppies, females show a preference for males with more orange colouration.

HOUDE (1994) established four replicate population pairs of guppies and selected one of each pair for an increased or decreased orange coloration in males, selecting the top/bottom 20 out of 50 males. She randomly chose females from each population to form the next generation, and so did not exert direct selection on females. She measured the response to selection on male colouration and on female preference for orange (left and right panels of Figure 9.13 respectively). In the lines that were selected for more orange males, females showed an increased preference for orange. While in those lines selected for



Figure 9.14: Guppy (*Poecilia reticulata*).
From a set of 1962 stamps of Hungary.
Contributed to wikimedia by Darjac, not
covered by copyright

less orange in male displays, females showed a decreased preference for orange. This is consistent with indirect selection on female orange preference as a response to selection on male colouration, due to a genetic correlation between female preference and male trait. It is *a priori* unlikely that pleiotropy is the source of the genetic correlation between these traits, rather it is likely caused by females assortatively mating with males that match their colour preference.

Returning to our bird tail example, what could drive the direct selection on male tail length? The selection for longer tails in males could come about because longer tails are genetically correlated with higher male viability, for example perhaps only males who gather an excess of food have the resources to invest in growing long tail, i.e. a long tail is an honest signal of fitness. This would correspond to a ‘good genes’ explanation of female mate choice evolution.

There’s another subtler way that selection could favour our male trait. Imagine that the variation in female preference trait is because some females have no strong preference for male tail length, but some females have a strong preference for males with longer tails.

Males with longer tails would then have higher fecundity than the short-tailed males as there’s a subset of females who are strongly attracted to long tails, and these males also get to mate with the other females. Thus selection favours long-tailed males, and so indirectly favours female preference for longer tails; females with a preference for longer-tails have sons who in turn are more attractive. This model is sometimes called the sexy-son model. It is also called the Fisherian runaway model (FISHER, 1915), as female preference and male trait can coevolve in an escalating fashion driving more and more extreme preferences for arbitrary traits. Thus many extravagant display traits in males and females may exist purely because individuals find them beautiful and are attracted to them.

“The case of the male Argus Pheasant is eminently interesting, because it affords good evidence that the most refined beauty may serve as a sexual charm, and for no other purpose.” – DARWIN (1888)

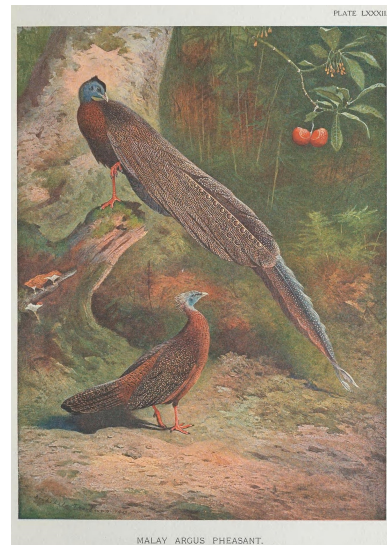


Figure 9.15: Argus Pheasant.
A monograph of the pheasants. (1918). Beebe, W Image from the Biodiversity Heritage Library. Contributed by Smithsonian Institution Libraries. Licensed under CC BY-2.0.

10

One-Locus Models of Selection

“Socrates consisted of the genes his parents gave him, the experiences they and his environment later provided, and a growth and development mediated by numerous meals. For all I know, he may have been very successful in the evolutionary sense of leaving numerous offspring. His phenotype, nevertheless, was utterly destroyed by the hemlock and has never since been duplicated. The same argument holds also for genotypes. With Socrates’ death, not only did his phenotype disappear, but also his genotype.[...] The loss of Socrates’ genotype is not assuaged by any consideration of how prolifically he may have reproduced. Socrates’ genes may be with us yet, but not his genotype, because meiosis and recombination destroy genotypes as surely as death.” –WILLIAMS (1966)

Individuals are temporary, their phenotypes are temporary, and their genotypes are temporary. However, the alleles that individuals transmit across generations have permanence. Sustained phenotypic evolutionary change due to natural selection occurs because of changes in the allelic composition of the population. To understand these changes, we need to understand how the frequency of alleles (genes) changes over time due to natural selection. We’ll also see that the because an individual’s genotype is just a ephemeral collection of alleles that genetic conflicts can arise that actually lower the fitness of individuals.

As we have seen, natural selection occurs when there are differences between individuals in fitness. We may define fitness in various ways. Most commonly, it is defined with respect to the contribution of a phenotype or genotype to the next generation. Differences in fitness can arise at any point during the life cycle. For instance, different genotypes or phenotypes may have different survival probabilities from one stage in their life to the stage of reproduction (viability), or they may differ in the number of offspring produced (fertility), or both. Here, we define the absolute fitness of a genotype as the expected number of offspring of an individual of that genotype. Differences in fitness among genotypes drive allele frequency change. In this chapter

we'll study the dynamics of alleles at a single locus. In this chapter we'll ignore the effects of genetic drift, and just study the deterministic dynamics of selection. We'll return to discuss the interaction of selection and drift in a couple of chapters.

10.0.1 Haploid selection model

We start out by modeling selection in a haploid model, as this is mathematically relatively simple. Let the number of individuals carrying alleles A_1 and A_2 in generation t be P_t and Q_t . Then, the relative frequencies at time t of alleles A_1 and A_2 are $p_t = P_t/(P_t + Q_t)$ and $q_t = Q_t/(P_t + Q_t) = 1 - p_t$. Further, assume that individuals of type A_1 and A_2 on average produce W_1 and W_2 offspring individuals, respectively. We call W_i the absolute fitness.

Therefore, in the next generation, the absolute number of carriers of A_1 and A_2 are $P_{t+1} = W_1 P_t$ and $Q_{t+1} = W_2 Q_t$, respectively. The mean absolute fitness of the population at time t is

$$\overline{W}_t = W_1 \frac{P_t}{P_t + Q_t} + W_2 \frac{Q_t}{P_t + Q_t} = W_1 p_t + W_2 q_t, \quad (10.1)$$

i.e. the sum of the fitness of the two types weighted by their relative frequencies. Note that the mean fitness depends on time, as it is a function of the allele frequencies, which are themselves time dependent.

As an example of a rapid response to selection on an allele in a haploid population, we can consider some data on the evolution of drug resistant viruses. FEDER *et al.* (2017) studied viral dynamics in a macaque infected with a strain of simian immunodeficiency virus (SHIV) that carries the HIV-1 reverse transcriptase coding region. The viral load of the macaque's blood plasma is shown as a black line in Figure 10.1. Twelve weeks after infection, the macaque was treated with an anti-retroviral drug that targeted the the virus' reverse transcriptase protein. Note how the viral load initially starts to drop once the drug is administered, suggesting that the absolute fitness of the original strain is less than one ($W_2 < 1$) in the presence of the drug (as their numbers are decreasing). However, the viral population rebounds as a mutation that confers drug resistance to the anti-retroviral drug arises in the SHIV and starts to spread. Viruses carrying this mutation (let's call them allele 1) likely have absolute fitness $W_1 > 1$. The frequency of the drug-resistant allele is shown in red; it quickly spreads from being undetectable in week 13, to being fixed in the SHIV population in week 20.

The rapid spread of this drug-resistant allele through the population is driven by the much greater relative fitness of the drug-resistant allele over the original strain in the presence of the anti-retroviral

The main focus of FEDER *et al.*'s work was modeling the complicated spatial dynamics of drug-resistant SHIV adaptation in different organ systems.

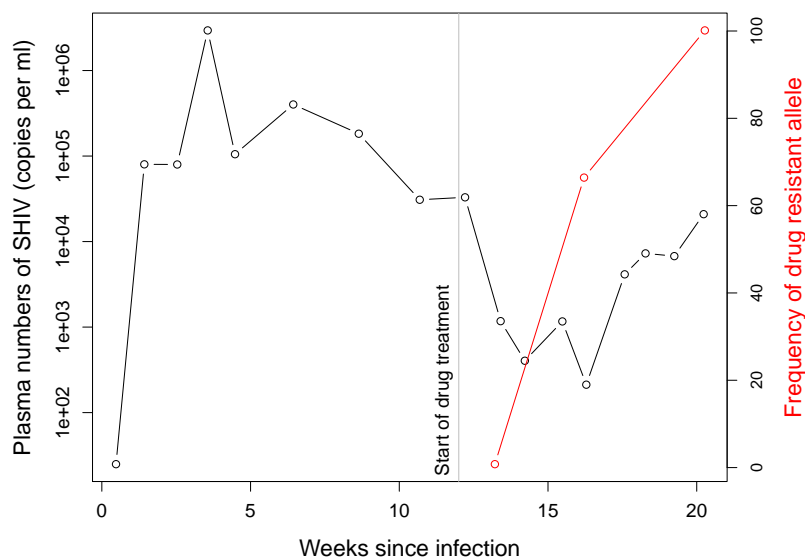


Figure 10.1: The rapid evolution of drug-resistant SHIV. The viral load of SHIV in the blood of a macaque (black line), the frequency of a drug resistance mutation (red line). Data from FEDER *et al.* (2017). Code here.

drug.

The frequency of allele A_1 in the next generation is given by

$$p_{t+1} = \frac{P_{t+1}}{P_{t+1} + Q_{t+1}} = \frac{W_1 P_t}{W_1 P_t + W_2 Q_t} = \frac{W_1 p_t}{W_1 p_t + W_2 q_t} = \frac{W_1}{\bar{W}_t} p_t. \quad (10.2)$$

Importantly, eqn. (10.2) tells us that the change in p only depends on a ratio of fitnesses. Therefore, we need to specify fitness only up to an arbitrary constant. As long as we multiply all fitnesses by the same value, that constant will cancel out and eqn. (10.2) will hold. Based on this argument, it is very common to scale absolute fitnesses by the absolute fitness of one of the genotypes, e.g. the most or the least fit genotype, to obtain relative fitnesses. Here, we will use w_i for the relative fitness of genotype i . If we choose to scale by the absolute fitness of genotype A_1 , we obtain the relative fitnesses $w_1 = W_1/W_1 = 1$ and $w_2 = W_2/W_1$.

Without loss of generality, we can therefore rewrite eqn. (10.2) as

$$p_{t+1} = \frac{w_1}{\bar{w}} p_t, \quad (10.3)$$

dropping the subscript t for the dependence of the mean fitness on time in our notation, but remembering it. The change in frequency from one generation to the next is then given by

$$\Delta p_t = p_{t+1} - p_t = \frac{w_1 p_t}{\bar{w}} - p_t = \frac{w_1 p_t - \bar{w} p_t}{\bar{w}} = \frac{w_1 p_t - (w_1 p_t + w_2 q_t) p_t}{\bar{w}} = \frac{w_1 - w_2}{\bar{w}} p_t q_t, \quad (10.4)$$

recalling that $q_t = 1 - p_t$.

Assuming that the fitnesses of the two alleles are constant over time, the number of the two allelic types τ generations after time 0 are $P_\tau = (W_1)^\tau P_0$ and $Q_\tau = (W_2)^\tau Q_0$, respectively. Therefore, the relative frequency of allele A_1 after τ generations past t is

$$p_\tau = \frac{(W_1)^\tau P_0}{(W_1)^\tau P_0 + (W_2)^\tau Q_0} = \frac{(w_1)^\tau P_0}{(w_1)^\tau P_0 + (w_2)^\tau Q_0} = \frac{p_0}{p_0 + (w_2/w_1)^\tau q_0}, \quad (10.5)$$

where the last step includes dividing the whole term by $(w_1)^\tau$ and switching from absolute to relative allele frequencies. Rearrange this to obtain

$$\frac{p_\tau}{q_\tau} = \frac{p_0}{q_0} \left(\frac{w_1}{w_2} \right)^\tau. \quad (10.6)$$

Solving this for τ yields

$$\tau = \log \left(\frac{p_\tau q_0}{q_\tau p_0} \right) / \log \left(\frac{w_1}{w_2} \right). \quad (10.7)$$

In practice, it is often helpful to parametrize the relative fitnesses w_i in a specific way. For example, we may set $w_1 = 1$ and $w_2 = 1 - s$, where s is called the selection coefficient. Using this parametrization, s is simply the difference in relative fitnesses between the two alleles. Equation (10.5) becomes

$$p_{t+\tau} = \frac{p_t}{p_t + q_t(1-s)^\tau}, \quad (10.8)$$

as $w_2/w_1 = 1 - s$. Then, if $s \ll 1$, we can approximate $(1 - s)^\tau$ in the denominator by $\exp(-s\tau)$ to obtain

$$p_{t+\tau} \approx \frac{p_t}{p_t + q_t e^{-s\tau}}. \quad (10.9)$$

This equation takes the form of a logistic function. That is because we are looking at the relative frequencies of two ‘populations’ (of alleles A_1 and A_2) that are growing (or declining) exponentially, under the constraint that p and q always sum to 1.

Moreover, eqn. (10.6) for the number of generations τ it takes for a certain change in frequency to occur becomes

$$\tau = -\log \left(\frac{p_\tau q_0}{q_\tau p_0} \right) / \log(1 - s). \quad (10.10)$$

Assuming again that $s \ll 1$, this simplifies to

$$\tau \approx \frac{1}{s} \log \left(\frac{p_\tau q_0}{q_\tau p_0} \right). \quad (10.11)$$

One particular case of interest is the time it takes to go from an absolute frequency of 1 to near fixation in a population of size N . In this case, we have $p_0 = 1/N$, and we may set $p_\tau = 1 - 1/N$, which

is very close to fixation. Then, plugging these values into eqn. (10.11), we obtain

$$\begin{aligned}\tau &= \frac{1}{s} \log \left(\frac{1 - 2/N + 1/N^2}{1/N^2} \right) \\ &\approx \frac{1}{s} (\log(N) + \log(N - 2)) \\ &\approx \frac{2}{s} \log(N)\end{aligned}\quad (10.12)$$

where we make the approximations $N^2 - 2N + 1 \approx N^2 - 2N$ and later $N - 2 \approx N$.

Question 1. In our example of the evolution of drug resistance, the drug-resistant SHIV virus spread from undetectable frequencies to $\sim 65\%$ frequency by 16 weeks post infection. An estimated effective population size of SHIV is 1.5×10^5 , and its generation time is ~ 1 day. Assuming that the mutation arose as a single copy allele very shortly the start of drug treatment at 12 weeks, what is the selection coefficient favouring the drug resistance allele?

Haploid model with fluctuating selection Selection pressures may change while a polymorphism persists in the population due to environmental changes. We can use our haploid model to consider this case where the fitnesses depend on time (DEMPSTER, 1955), and say that $w_{1,t}$ and $w_{2,t}$ are the fitnesses of the two types in generation t . The frequency of allele A_1 in generation $t + 1$ is

$$p_{t+1} = \frac{w_{1,t}}{\bar{w}_t} p_t, \quad (10.13)$$

which simply follows from eqn. (10.3). The ratio of the frequency of allele A_1 to that of allele A_2 in generation $t + 1$ is

$$\frac{p_{t+1}}{q_{t+1}} = \frac{w_{1,t}}{w_{2,t}} \frac{p_t}{q_t}. \quad (10.14)$$

Therefore, if we think of the two alleles starting in generation 1 at frequencies p_1 and q_1 , then τ generations later,

$$\frac{p_\tau}{q_\tau} = \left(\prod_{i=1}^{\tau} \frac{w_{1,i}}{w_{2,i}} \right) \frac{p_1}{q_1}. \quad (10.15)$$

The question of which allele is increasing or decreasing in frequency comes down to whether $(\prod_{i=1}^{\tau} w_{1,i}/w_{2,i})$ is > 1 or < 1 . As it is a little hard to think about this ratio, we can instead take the τ^{th} root of it and consider

$$\sqrt[\tau]{\left(\prod_{i=1}^{\tau} \frac{w_{1,i}}{w_{2,i}} \right)} = \frac{\sqrt[\tau]{\prod_{i=1}^{\tau} w_{1,i}}}{\sqrt[\tau]{\prod_{i=1}^{\tau} w_{2,i}}}. \quad (10.16)$$

The term

$$\sqrt{\prod_{i=1}^{\tau} w_{1,i}} \quad (10.17)$$

is the geometric mean fitness of allele A_1 over the τ generations past generation t . Therefore, allele A_1 will only increase in frequency if it has a higher geometric mean fitness than allele A_2 (at least in our simple deterministic model). This implies that an allele with higher geometric mean fitness can even invade and spread to fixation if its (arithmetic) mean fitness is lower than the dominant type. To see this consider two alleles that experience the fitnesses given in Table 10.1. The allele A_1 does much better in dry years, but suffers in wet years; while the A_2 is generalist and is not affected by the variable environment. If there is an equal chance of a year being wet or dry, the A_1 allele has higher (arithmetic) mean fitness, but it will be replaced by the A_2 allele as the A_2 allele has higher geometric mean fitness (See Figure 10.2).

	A_1	A_2
Dry	2	1.57
Wet	1.16	1.57
Arithmetic Mean	1.58	1.57
Geometric Mean	1.52	1.57

Table 10.1: Fitnesses of two alleles in wet and dry years. Means calculated assuming equal chances of wet and dry years. The geometric mean is calculated as $\sqrt{w_{\text{wet}} w_{\text{dry}}}$. Example numbers taken from SEGER and BROCKMANN (1987).

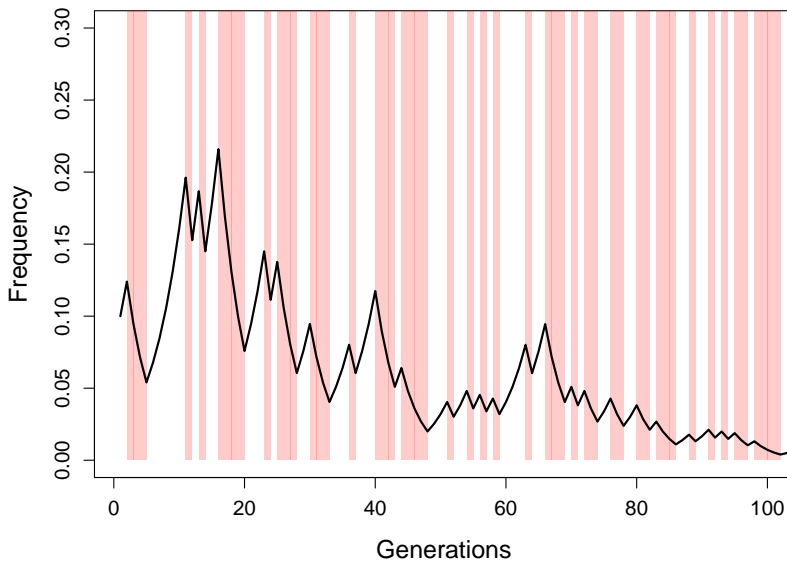


Figure 10.2: An example frequency trajectory of the A_1 allele under variable environments (using the fitnesses from Table 10.1). Wet years (generations) are shown in red, dry years in white. The environment flips at random each year. Note how the A_1 allele increases in frequency in the dry years as it has higher fitness, and yet the A_2 allele still wins out. [Code here.](#)

Evolution of bet hedging Don't put your eggs in one basket, it makes a lot of sense to spread your bets. Financial advisors often advise you to diversify your portfolio, rather than placing all your investments in one stock. Even if that stock looks very strong, you can come a cropper that $1/20$ times some particular part of the market crashes. Likewise, evolution can result in risk averse strategies. Some species of

bird lay multiple nests of eggs; some plants don't put all of their energy into seeds that will germinate next year. It can even make sense to hedge your bets even if that comes at an average cost (SEGER and BROCKMANN, 1987).

To see this lets think more about geometric fitness. We can write the relative fitness of an allele in a given generation i as $w_i = 1 + s_i$, such that we can write your geometric fitness as

$$\bar{g} = \sqrt[\tau]{\prod_{i=1}^{\tau-1} 1 + s_i} \quad (10.18)$$

when we think about products it's often natural to take the log to turn it into a sum

$$\begin{aligned} \log(\bar{g}) &= \frac{1}{\tau} \sum_{i=1}^{\tau-1} \log(1 + s_i) \\ &= \mathbb{E}[\log(1 + s_i)] \end{aligned} \quad (10.19)$$

equating the mean and the expectation. Assuming that s_i is small $\log(1 + s_i) \approx s_i - s_i^2/2$, ignoring terms s_i^3 and higher¹ then this is

$$\begin{aligned} \log(\bar{g}) &\approx \mathbb{E}\left[s_i - s_i^2/2\right] \\ &= \mathbb{E}[s_i] - \text{var}(s_i)/2 \end{aligned} \quad (10.20)$$

So genotypes with high arithmetic mean fitness can be selected against, i.e. have low geometric mean fitness against, if their fitness has too high a variance across generations (GILLESPIE, 1973, 1977). See our example above, Table 10.1 and Figure 10.2).

A classic example of bet-hedging is in delayed seed germination in plants (COHEN, 1966). In variable environments, such as deserts, it may make sense to spread your bets over years by having only a proportion of your seeds germinate in the first year. However, delaying germination can come at a cost due to seed mortality. GREMER and VENABLE (2014), using data from a long-term study various species of Sonoran Desert winter showed that annual plants were indeed pursuing adaptive bet-hedging strategies. The plant species with the highest variation in among-year yield had the lowest germination fraction per year. Further, GREMER and VENABLE showed through modeling life that by having per-year germination proportions < 1 all of the species were achieving higher geometric fitness at the expense of arithmetic fitness in the variable desert environment. See Figure 10.4 for an example of bet hedging in Woolly plantain.

¹ Here we're using a 2nd order Taylor approximation, see math appendix eqn (A.7).

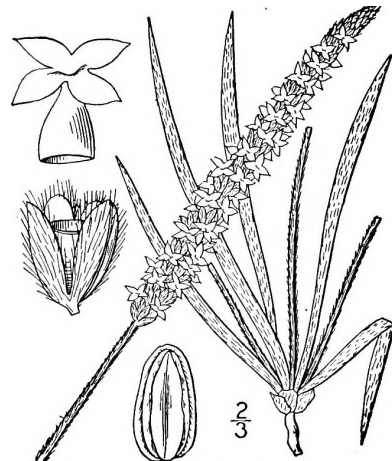


Figure 10.3: Woolly plantain (*Plantago patagonica*). One of the desert annuals shown to have a bet-hedging germination strategy by GREMER and VENABLE (2014).

An illustrated flora of the northern United States, Canada and the British possessions, from Newfoundland to the parallel of the southern boundary of Virginia, and from the Atlantic Ocean westward to the 102d meridian (1913) Britton, N.L. Image from the Biodiversity Heritage Library. Contributed by Cornell University Library. Not in copyright.

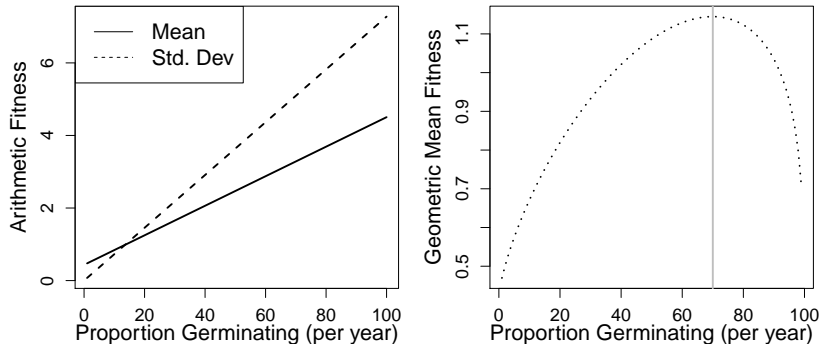


Figure 10.4: *Plantago patagonica*'s arithmetic fitness is an increasing function of the proportion of seeds germinating, due to seeds not surviving a germination delay. However, the standard deviation of fitness also increases with this proportion as they are more likely to have all of their seeds germinate in a bad year. Thus *Plantago patagonica* can achieve higher geometric fitness by only having a proportion of their seeds germinate. Thanks to Jenny Gremer for sharing these data from GREMER and VENABLE (2014). Code here.

Delayed reproduction is also a common example of bet-hedging in micro-organisms. For example, the Chicken Pox virus, varicella zoster virus, has a very long latent phase. After it causes chicken pox it enters a latent phase, residing inactive in neurons in the spinal cord, only to emerge 5–40 years later to cause the disease shingles. It is hypothesized that the virus actively suppresses itself as a strategy to allow it to emerge at a later time point as insurance against there being no further susceptible hosts at the time of its first infection (STUMPF *et al.*, 2002).

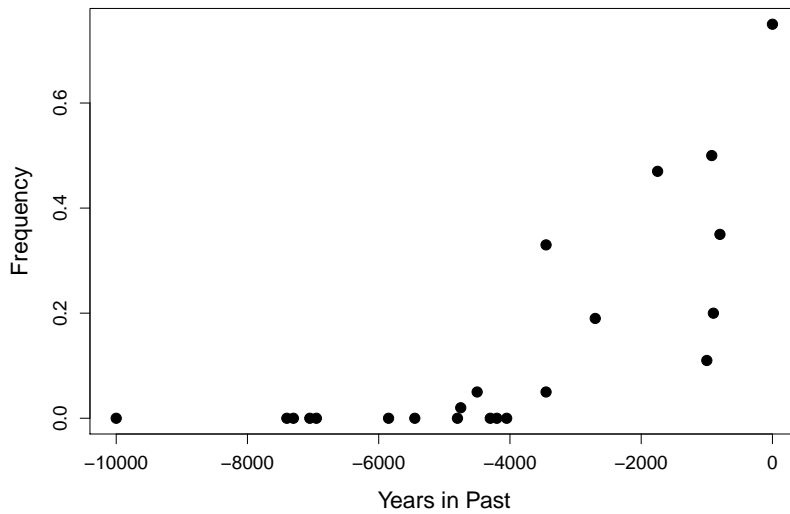


Figure 10.5: Frequency of the Lactase persistence allele in ancient and modern samples from Central Europe. Data compiled by MARCINIAK and PERRY (2017) from various sources. Thanks to Stephanie Marciniak for sharing these data. Code here.

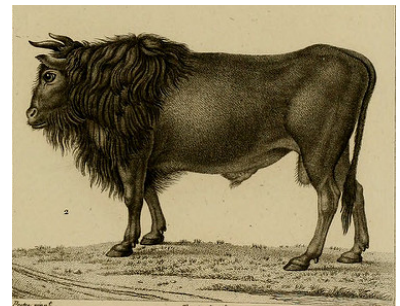


Figure 10.6: Auroch (*Bos primigenius*). Aurochs are an extinct species of large wild cattle that cows were domesticated from. Dictionnaire des sciences naturelles. 1816 Cuvier, F.G. Image from the Internet Archive. Contributed by NCSU Libraries. No known copyright restrictions.

10.0.2 Diploid model

We will now move on to a diploid model of a single locus with two segregating alleles. As an example of the change in the frequency of an

allele driven by selection, let's consider the evolution of Lactase persistence. A number of different human populations that historically have raised cattle have convergently evolved to maintain the expression of the protein Lactase into adulthood (in most mammals the protein is switched off after childhood), with different lactase-persistence mutations having arisen and spread in different pastoral human populations. This continued expression of Lactase allows adults to break down Lactose, the main carbohydrate in milk, and so benefit nutritionally from milk-drinking. This seems to have offered a strong fitness benefit to individuals in pastoral populations.

With the advent of techniques to sequence ancient human DNA, researchers can now potentially track the frequency of selected mutations over thousands of years. The frequency of a Lactase persistence allele in ancient Central European populations is shown in Figure 10.5. The allele is absent more than 5,000 years ago, but now found at frequency of upward of 70% in many European populations.

We will assume that the difference in fitness between the three genotypes comes from differences in viability, i.e. differential survival of individuals from the formation of zygotes to reproduction. We denote the absolute fitnesses of genotypes A_1A_1 , A_1A_2 , and A_2A_2 by W_{11} , W_{12} , and W_{22} . Specifically, W_{ij} is the probability that a zygote of genotype A_iA_j survives to reproduction. Assuming that individuals mate at random, the number of zygotes that are of the three genotypes and form generation t are

$$Np_t^2, \quad N2p_tq_t, \quad Nq_t^2. \quad (10.21)$$

The mean fitness of the population of zygotes is then

$$\overline{W}_t = W_{11}p_t^2 + W_{12}2p_tq_t + W_{22}q_t^2. \quad (10.22)$$

Again, this is simply the weighted mean of the genotypic fitnesses.

How many zygotes of each of the three genotypes survive to reproduce? An individual of genotype A_1A_1 has a probability of W_{11} of surviving to reproduce, and similarly for other genotypes. Therefore, the expected number of A_1A_1 , A_1A_2 , and A_2A_2 individuals who survive to reproduce is

$$NW_{11}p_t^2, \quad NW_{12}2p_tq_t, \quad NW_{22}q_t^2. \quad (10.23)$$

It then follows that the total number of individuals who survive to reproduce is

$$N(W_{11}p_t^2 + W_{12}2p_tq_t + W_{22}q_t^2). \quad (10.24)$$

This is simply the mean fitness of the population multiplied by the population size (i.e. $N\overline{w}$).

The relative frequency of A_1A_1 individuals at reproduction is simply the number of A_1A_1 genotype individuals at reproduction ($NW_{11}p_t^2$) divided by the total number of individuals who survive to reproduce (\bar{N}), and likewise for the other two genotypes. Therefore, the relative frequency of individuals with the three different genotypes at reproduction is

$$\frac{NW_{11}p_t^2}{\bar{N}}, \quad \frac{NW_{12}2p_tq_t}{\bar{N}}, \quad \frac{NW_{22}q_t^2}{\bar{N}} \quad (10.25)$$

(see Table 10.2).

	A_1A_1	A_1A_2	A_2A_2
Absolute no. at birth	Np_t^2	$N2p_tq_t$	Nq_t^2
Fitnesses	W_{11}	W_{12}	W_{22}
Absolute no. at reproduction	$NW_{11}p_t^2$	$NW_{12}2p_tq_t$	$NW_{22}q_t^2$
Relative freq. at reproduction	$\frac{W_{11}}{\bar{N}}p_t^2$	$\frac{W_{12}}{\bar{N}}2p_tq_t$	$\frac{W_{22}}{\bar{N}}q_t^2$

As there is no difference in the fecundity of the three genotypes, the allele frequencies in the zygotes forming the next generation are simply the allele frequency among the reproducing individuals of the previous generation. Hence, the frequency of A_1 in generation $t + 1$ is

$$p_{t+1} = \frac{W_{11}p_t^2 + W_{12}2p_tq_t}{\bar{N}}. \quad (10.26)$$

Note that, again, the absolute value of the fitnesses is irrelevant to the frequency of the allele. Therefore, we can just as easily replace the absolute fitnesses with the relative fitnesses. That is, we may replace W_{ij} by $w_{ij} = W_{ij}/W_{11}$, for instance.

Each of our genotype frequencies is responding to selection in a manner that depends just on its fitness compared to the mean fitness of the population. For example, the frequency of the A_1A_1 homozygotes increases from birth to adulthood in proportion to W_{11}/\bar{N} . In fact, we can estimate this fitness ratio for each genotype by comparing the frequency at birth compared to adults. As an example of this calculation, we'll look at some data from sticklebacks.

Marine threespine stickleback (*Gasterosteus aculeatus*) independently colonized and adapted to many freshwater lakes as glaciers receded following the last ice age, making sticklebacks a wonderful system for studying the genetics of adaptation. In marine habitats, most of the stickleback have armour plates to protect them from predation, but freshwater populations repeatedly evolve the loss of armour plates due to selection on an allele at the Ectodysplasin gene (EDA). This allele is found as a standing variant at very low frequency in marine populations; BARRETT *et al.* (2008) took advantage of this fact and collected and bred a population of marine individuals carrying

Table 10.2: Relative genotype frequencies after one episode of viability selection.

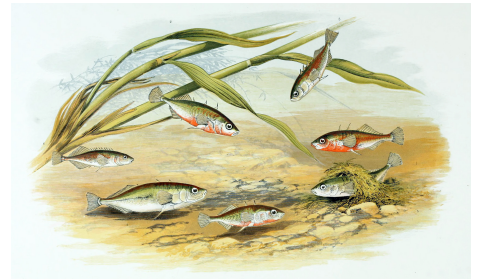


Figure 10.7: Freshwater threespine Stickleback (*G. aculeatus*). British fresh-water fishes. Houghton W 1879. Image from the Biodiversity Heritage Library. Contributed by Ernst Mayr Library, Harvard.. Not in copyright.

both the low- (L) and completely- plated (C) alleles. They introduced the offspring of this cross into four freshwater ponds and monitored genotype frequencies ² over their life courses:

	CC	LC	LL
Juveniles	0.55	0.23	0.22
Adults	0.21	0.53	0.26
Adults/Juv. (W_{\bullet}/\bar{W})	0.4	2.3	1.2
rel. fitness (W_{\bullet}/W_{12})	0.17	1.0	0.54

² The actual dynamics observed by BARRETT *et al.* are more complicated as in the very young fish selection reverses direction.

The heterozygotes have increased in frequency dramatically in the population as their fitness is more than double the mean fitness of the population. We can also calculate the relative fitness of each genotype by dividing through by the fitness of the fittest genotype, the heterozygote in this case (doing this cancels through \bar{W}). The relative fitness of the CC is $\sim 1/5$ of the heterozygote. Note that this calculation does not rely on the genotype frequencies being at their HWE in the juveniles.

- Question 2.** **A)** What is the frequency of the low-plated EDA allele (L) at the start of the stickleback experiment?
B) What is the frequency in the adults? **C)** Also calculate the frequency in adults using the relative fitnesses.

The change in frequency from generation t to $t + 1$ is

$$\Delta p_t = p_{t+1} - p_t = \frac{w_{11}p_t^2 + w_{12}p_tq_t}{\bar{w}} - p_t. \quad (10.27)$$

To simplify this equation, we will first define two variables \bar{w}_1 and \bar{w}_2 as

$$\bar{w}_1 = w_{11}p_t + w_{12}q_t, \quad (10.28)$$

$$\bar{w}_2 = w_{12}p_t + w_{22}q_t. \quad (10.29)$$

These are called the marginal fitnesses of allele A_1 and A_2 , respectively. They are so called as \bar{w}_1 is the average fitness of an allele A_1 , i.e. the fitness of A_1 in a homozygote weighted by the probability it is in a homozygote (p_t) plus the fitness of A_1 in a heterozygote weighted by the probability it is in a heterozygote (q_t). We further note that the mean relative fitness can be expressed in terms of the marginal fitnesses as

$$\bar{w} = \bar{w}_1p_t + \bar{w}_2q_t, \quad (10.30)$$

where, for notational simplicity, we have omitted subscript t for the dependence of mean and marginal fitnesses on time.

We can then rewrite eqn. (10.27) using \bar{w}_1 and \bar{w}_2 as

$$\Delta p_t = \frac{(\bar{w}_1 - \bar{w}_2)}{\bar{w}} p_t q_t. \quad (10.31)$$

The sign of Δp_t , i.e. whether allele A_1 increases or decreases in frequency, depends only on the sign of $(\bar{w}_1 - \bar{w}_2)$. The frequency of A_1 will keep increasing over the generations so long as its marginal fitness is higher than that of A_2 , i.e. $\bar{w}_1 > \bar{w}_2$, while if $\bar{w}_1 < \bar{w}_2$, the frequency of A_1 will decrease. Note the similarity between eqn. (10.31) and the respective expression for the haploid model in eqn. (10.4). (We will return to the special case where $\bar{w}_1 = \bar{w}_2$ shortly).

We can also rewrite (10.27) as

$$\Delta p_t = \frac{1}{2} \frac{p_t q_t}{\bar{w}} \frac{d\bar{w}}{dp}, \quad (10.32)$$

This form shows that the frequency of A_1 will increase ($\Delta p_t > 0$) if the mean fitness is an increasing function of the frequency of A_1 (i.e. if $\frac{d\bar{w}}{dp} > 0$). On the other hand, the frequency of A_1 will decrease ($\Delta p_t < 0$) if the mean fitness is a decreasing function of the frequency of A_1 (i.e. if $\frac{d\bar{w}}{dp} < 0$). Thus, although selection acts on individuals, under this simple model, selection is acting to increase the mean fitness of the population. The rate of this increase is proportional to the variance in allele frequencies within the population ($p_t q_t$). This formulation suggested to WRIGHT (1932) the view of natural selection as moving populations up local fitness peaks, as we encountered in Section 8.1.2 in discussing phenotypic fitness peaks. Again this view of selection as maximizing mean fitness only holds true if the genotypic fitnesses are frequency independent, later in this chapter we'll discuss some important cases where that doesn't hold.

Question 3. For many generations you have been studying an annual wildflower that has two color morphs, orange and white. You have discovered that a single bi-allelic locus controls flower color, with the white allele being recessive. The pollinator of these plants is an almost blind bat, so individuals are pollinated at random with respect to flower color. Your population census of 200 individuals showed that the population consisted of 168 orange-flowered individuals, and 32 white-flowered individuals.

Heavy February rainfall creates optimal growing conditions for an exotic herbivorous beetle with a preference for orange-flowered individuals. This year it arrives at your study site with a ravenous appetite. Only 50% of orange-flowered individuals survive its wrath, while 90% of white-flowered individuals survive until the end of the growing season.

A) What is the initial frequency of the white allele, and what do you have to assume to obtain this?

B) What is the frequency of the white allele in the seeds forming the next generation?

To see this we can write

$$\begin{aligned} \frac{d\bar{w}}{dp} &= \frac{d}{dp} (W_{11}p^2 + 2W_{12}p \\ &\quad - 2W_{12}p^2 + W_{22} - 2W_{22}p + W_{22}p^2) \\ &= 2(w_{11}p + w_{12} - 2pw_{12} - w_{22} - w_{22} + w_{22}p) \end{aligned}$$

On expansion of $\bar{w}_1 - \bar{w}_2$, we see that it matched the terms in the parentheses in the expression above. Thus, we see that we can replace $\bar{w}_1 - \bar{w}_2$ with $1/2 \frac{d\bar{w}}{dp}$.

10.0.3 Diploid directional selection

So far, our treatment of the diploid model of selection has been in terms of generic fitnesses w_{ij} . In the following, we will use particular parameterizations to gain insight about two specific modes of selection: directional selection and heterozygote advantage.

Directional selection means that one of the two alleles always has higher marginal fitness than the other one. Let us assume that A_1 is the fitter allele, so that $w_{11} \geq w_{12} \geq w_{22}$, and hence $\bar{w}_1 > \bar{w}_2$. As we are interested in changes in allele frequencies, we may use relative fitnesses. We parameterize the reduction in relative fitness in terms of a selection coefficient, similar to the one we met in the haploid selection section, as follows:

genotype	A_1A_1	A_1A_2	A_2A_2
absolute fitness	W_{11}	$\geq W_{12} \geq$	W_{22}
relative fitness (generic)	$w_{11} = W_{11}/\bar{w}$	$w_{12} = W_{12}/\bar{w}$	$w_{22} = W_{22}/\bar{w}$
relative fitness (specific)	1	$1 - sh$	$1 - s$.

Here, the selection coefficient s is the difference in relative fitness between the two homozygotes, and h is the dominance coefficient. For selection to be directional, we require that $0 \leq h \leq 1$ holds. The dominance coefficient allows us to move between two extremes. One is when $h = 0$, such that allele A_1 is fully dominant and A_2 fully recessive. In this case, the heterozygote A_1A_2 is as fit as the A_1A_1 homozygote genotype. The inverse holds when $h = 1$, such that allele A_1 is fully recessive and A_2 fully dominant.

We can then rewrite eqn. (10.31) as

$$\Delta p_t = \frac{p_t h s + q_t s(1-h)}{\bar{w}} p_t q_t, \quad (10.33)$$

where

$$\bar{w} = 1 - 2p_t q_t s h - q_t^2 s. \quad (10.34)$$

Question 4. Throughout the Californian foothills are old copper and gold-mines, which have dumped out soils that are polluted with heavy metals. While these toxic mine tailing are often depauperate of plants, *Mimulus guttatus* and a number of other plant species have managed to adapt to these harsh soils. WRIGHT *et al.* (2015) have mapped one of the major loci contributing to the adaptation to soils at two mines near Copperopolis, CA. WRIGHT *et al.* planted homozygote seedlings out in the mine tailings and found that only 10% of the homozygotes for the non-copper-tolerant allele survived to flower, while 40% of the copper-tolerant seedlings survived to flower.

A) What is the selection coefficient acting against the non-copper-tolerant allele on the mine tailing?

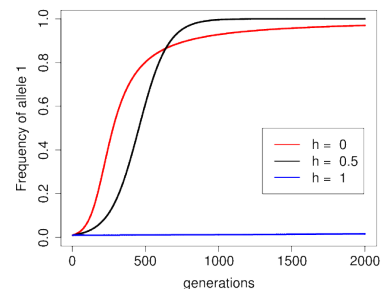


Figure 10.8: The trajectory of the frequency of allele A_1 , starting from $p_0 = 0.01$, for a selection coefficient $s = 0.01$ and three different dominance coefficients. The recessive beneficial allele ($h = 1$) will eventually fix in the population, but it takes a long time. Code here.

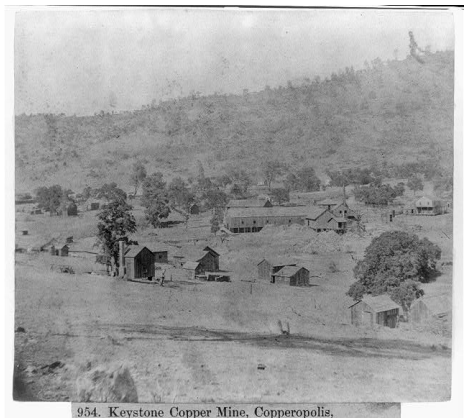


Figure 10.9: Keystone Copper Mine 1866, Copperopolis, Calaveras County. Image from picryl. Source Library of Congress, Public Domain.

B) The copper-tolerant allele is fairly dominant in its action on fitness. If we assume that $h = 0.1$, what percentage of heterozygotes should survive to flower?

Question 5. Comparing the red ($h = 0$) and black ($h = 0.5$) trajectories in Figure 10.8, provide an explanation for why A_1 increases faster initially if $h = 0$, but then approaches fixation more slowly compared to the case of $h = 0.5$.

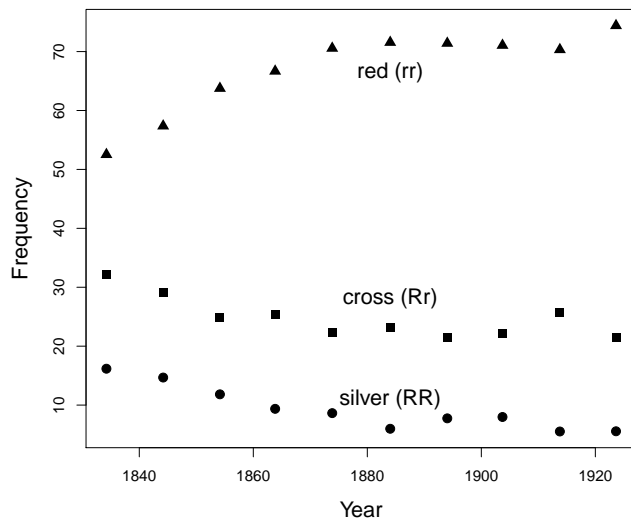


Figure 10.10: The frequency of red, cross, and silver fox morphs over the decades in Eastern Canada. These data are well described by recessive selection acting against the silver fox morph. Data from ELTON (1942), compiled by ALLENDORF and HARD (2009). Code here.



To see how dominance affects the trajectory of a real polymorphism, we'll consider an example from a colour polymorphism in red foxes (*Vulpes vulpes*).

There are three colour morphs of red foxes: silver, cross, and red (see Figure 10.11), with this difference primarily controlled by a single polymorphism with genotypes RR, Rr, and rr respectively. The fur pelts of the silver morph fetched three times the price for hunters compared to cross (a smoky red) and red pelts, the latter two being seen as roughly equivalent in worth. Thus the desirability of the pelts acts as a recessive trait, with much stronger selection against the silver homozygotes. As a result of this price difference, silver foxes were hunted more intensely and declined as a proportion of the population in Eastern Canada, see Figure 10.10, as documented by ELTON, from 16% to 5% from 1834 to 1937. HALDANE reanalyzed these data and showed that they were consistent with recessive selection acting against the silver morph alone. Note how the heterozygotes (cross) decline somewhat as a result of selection on the silver homozygotes, but overall the

Figure 10.11: Three colour morphs in red fox *V. vulpes*, cross, red, and silver foxes from left to right.
"The larger North American mammals" Nelson, E.W., Fuertes, L.A. 1916. Image from the Biodiversity Heritage Library. Contributed by Cornell University Library. No known copyright restrictions.

R allele is slow to respond to selection as it is ‘hidden’ from selection in the heterozygote state.

Directional selection on an additive allele. A special case is when $h = 0.5$. This case is the case of no dominance, as the interaction among alleles with respect to fitness is strictly additive. Then, eqn. (10.33) simplifies to

$$\Delta p_t = \frac{1}{2} \frac{s}{\bar{w}} p_t q_t. \quad (10.35)$$

If selection is very weak, i.e. $s \ll 1$, the denominator (\bar{w}) is close to 1 and we have

$$\Delta p_t = \frac{1}{2} s p_t q_t. \quad (10.36)$$

It is instructive to compare eqn. (10.36) to the respective expression under the haploid model. To this purpose, start from the generic term for Δp_t under the haploid model in eqn. (10.4) and set $w_1 = 1$ and $w_2 = 1 - s$. Again, assume that s is small, so that eqn. (10.4) becomes $\Delta p_t = s p_t q_t$. Hence, if s is small, the diploid model of directional selection without dominance is identical to the haploid model, up to a factor of 1/2. That factor is due to the choice of the parametrisation; we could have set $w_{11} = 1$, $w_{12} = 1 - s$, and $w_{22} = 1 - 2s$ in our diploid model instead, in which case the agreement with the haploid model would be perfect.

From this analogy, we can borrow some insight we gained from the haploid model. Specifically, the trajectory of the frequency of allele A_1 in the diploid model without dominance follows a logistic growth curve similar to eqn. (10.9). From this similarity, we can extrapolate from Equation (10.11) to find the time it takes for our diploid, beneficial, additive allele (A_1) to move from frequency p_0 to p_τ :

$$\tau \approx \frac{2}{s} \log \left(\frac{p_\tau q_0}{q_\tau p_0} \right) \quad (10.37)$$

generations; this just differs by a factor of 2 from our haploid model. Using this result we can find the time it takes for our favourable, additive allele (A_1) to transit from its entry into the population ($p_0 = 1/(2N)$) to close to fixation ($p_\tau = 1 - 1/(2N)$):

$$\tau \approx \frac{4}{s} \log(2N) \quad (10.38)$$

generations. Note the similarity to eqn. 10.12 for the haploid model, with a difference by a factor of 2 due to the choice of parametrization (and that the number of alleles is $2N$ in the diploid model, rather than N). Doubling our selection coefficient halves the time it takes for our allele to move through the population.

Question 6. Gulf killifish (*Fundulus grandis*) have rapidly adapted to the very high pollution levels in the Houston shipping canal since

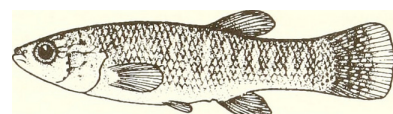


Figure 10.12: Gulf killifish (*Fundulus grandis*).

Distribution and abundance of fishes and invertebrates in Gulf of Mexico estuaries. Nelson D M and Pattillo M E Image from the Biodiversity Heritage Library. Contributed by MBLWHOI Library. No known copyright restrictions.

the 1950s. One of the ways that they've adapted is through the deletion of their aryl hydrocarbon receptor (AHR) gene. OZIOLOR *et al.* (2019) estimated that individuals who were homozygote for the intact AHR gene had a relative fitness of 20% of that of homozygotes for the deletion. Assuming an effective population size of 200 thousand individuals, how long would it take for the deletion to reach fixation, starting as a single copy in this population?

10.1 Balancing selection and the selective maintenance of polymorphism.

Directional selection on genotypes is expected to remove variation from populations, yet we see plentiful phenotypic and genetic variation in every natural population. Why is this? Three broad explanations for the maintenance of polymorphisms are

1. Variation is maintained by a balance of genetic drift and mutation (we discussed this explanation in Chapter 4).
2. Selection can sometimes act to maintain variation in populations (balancing selection).
3. Deleterious variation can be maintained in the population as a balance between selection removing variation and mutation constantly introducing new variation into the population.

We'll turn to these latter two explanations through this chapter and the next. Note that these explanations are not mutually exclusive. Each explanation will explain some proportion of the variation, and these proportions will differ over species and classes of polymorphism. A central challenge in population genomics is how we can do this in a systematic way.

10.1.1 Heterozygote advantage

One form of balancing selection occurs when the heterozygotes are fitter than either of the homozygotes. In this case, it is useful to parameterize the relative fitnesses as follows:

genotype	A_1A_1	A_1A_2	A_2A_2
absolute fitness	w_{11}	$< w_{12} >$	w_{22}
relative fitness (generic)	$w_{11} = W_{11}/W_{12}$	$w_{12} = W_{12}/W_{12}$	$w_{22} = W_{22}/W_{12}$
relative fitness (specific)	$1 - s_1$	1	$1 - s_2$

Here, s_1 and s_2 are the differences between the relative fitnesses of the two homozygotes and the heterozygote. Note that to obtain

relative fitnesses we have divided absolute fitness by the heterozygote fitness. We could use the same parameterization as in the model of directional selection, but the reparameterization we have chosen here makes the math easier.

In this case, when allele A_1 is rare, it is often found in a heterozygous state, while the A_2 allele is usually in the homozygous state, and so A_1 is more fit and increases in frequency. However, when the allele A_1 is common, it is often found in a less fit homozygous state, while the allele A_2 is often found in a heterozygous state; thus it is now allele A_2 that increases in frequency at the expense of allele A_1 . Thus, at least in the deterministic model, neither allele can reach fixation and both alleles will be maintained at an equilibrium frequency as a balanced polymorphism in the population.

We can solve for this equilibrium frequency by setting $\Delta p_t = 0$ in eqn. (10.31), i.e. $p_t q_t (\bar{w}_1 - \bar{w}_2) = 0$. Doing so, we find that there are three equilibria. Two of them are not very interesting ($p = 0$ or $q = 0$), but the third one is a stable polymorphic equilibrium, where $\bar{w}_1 - \bar{w}_2 = 0$ holds. Using our s_1 and s_2 parametrization above, we see that the marginal fitnesses of the two alleles are equal when

$$p_e = \frac{s_2}{s_1 + s_2} \quad (10.39)$$

for the equilibrium frequency of interest. This is also the frequency of A_1 at which the mean fitness of the population is maximized. The highest possible fitness of the population would be achieved if every individual was a heterozygote. However, Mendelian segregation of alleles in the gametes of heterozygotes means that a sexual population can never achieve a completely heterozygote population. This equilibrium frequency represents an evolutionary compromise between the advantages of the heterozygote and the comparative costs of the two homozygotes.

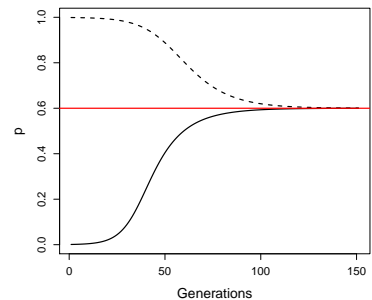
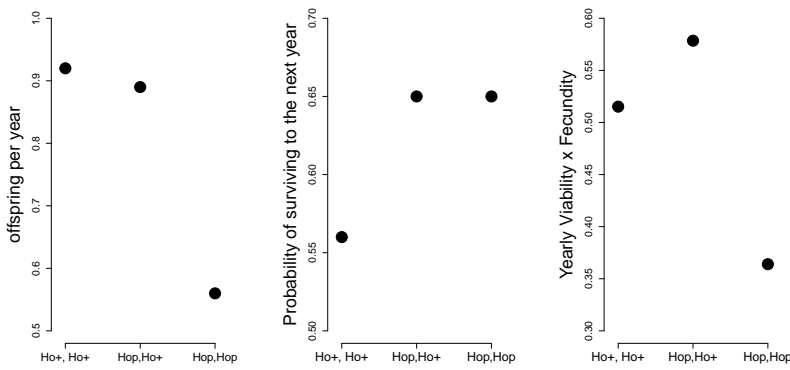


Figure 10.13: Two allele frequency trajectories of the A_1 allele subject to heterozygote advantage ($w_{11} = 0.9$, $w_{12} = 1$, and $w_{22} = 0.85$). In one simulation the allele is started from being rare in the population ($p = 1/1000$, solid line) and increases in frequency. In the other simulation the allele is almost fixed ($p = 999/1000$, dashed line). In both cases the frequency moves toward the equilibrium frequency. The red line shows the equilibrium frequency (p_e). Code here.

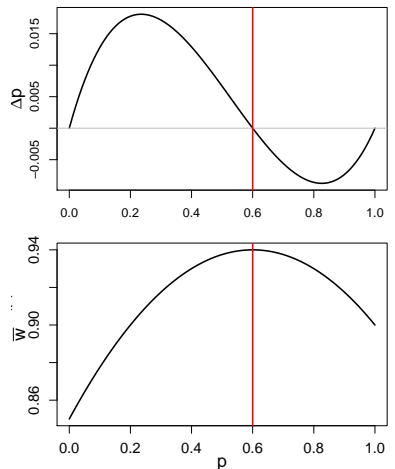


Figure 10.14: **Top**) The change in frequency of an allele with heterozygote advantage within a generation (Δp) as a function of the allele frequency. Fitnesses as in Figure 10.13. Note how the frequency change is positive below the equilibrium frequency (p_e) and negative above. **Bottom**) Mean fitness (\bar{w}) as a function of the allele frequency. The red line shows the equilibrium frequency (p_e). Code here.

Figure 10.15: For the three Soay sheep genotypes: the offspring per year (left), the probability of surviving a year (middle), and the product of the two (right). Thanks to Susan Johnston for supplying these simplified numbers from JOHNSTON *et al.* (2013). Code here.

One example of a polymorphism maintained by heterozygote advantage is a horn-size polymorphism found in Soay sheep, a population of feral sheep on the island of Soay (about 40 miles off the coast of Scotland). The horns of the soay sheep resemble those of the wild Mouflon sheep, and the male Soay sheep use their horns to defend females during the rut. JOHNSTON *et al.* (2013) found a large-effect locus, at the RXFP2 gene, that controls much of the genetic variation for horn size. Two alleles Ho^p and Ho^+ segregate at this locus. The Ho^+ allele is associated with growing larger horns, while the Ho^p allele is associated with smaller horns, with a reasonable proportion of Ho^p homozygotes developing no horns at all. JOHNSTON *et al.* (2013) found that the Ho locus had substantial effects on male, but not female, fitness (see Figure 10.15).

The Ho^p allele has a mostly recessive effect on male fecundity, with the Ho^p homozygotes having lower yearly reproductive success presumably due to the fact that they perform poorly in male-male competition (left plot Figure 10.15). Conversely, the Ho^+ has a mostly recessive effect on viability, with Ho^+ homozygotes having lower yearly survival (middle plot Figure 10.15), likely because they spend little time feeding during the rut and so lose substantial body weight. Thus both of the homozygotes suffer from trade-offs between viability and fecundity. As a result, the Ho^pHo^+ heterozygotes have the highest fitness (right plot Figure 10.15). The allele is thus balanced at intermediate frequency (50%) in the population due to this trade off between fitness at different life history stages.

Question 7. Assume that the frequency of the Ho^P allele is 10%, that there are 1000 males at birth, and that individual adults mate at random.

A) What is the expected number of males with each of the three genotypes in the population at birth?

B) Assume that a typical male individual of each genotype has the following probability of surviving to adulthood:

$Ho^+ Ho^+$	$Ho^+ Ho^p$	$Ho^p Ho^p$
0.5	0.8	0.8

Making the assumptions from above, how many males of each genotype survive to reproduce? **C)** Of the males who survive to reproduce, let's say that males with the Ho^+Ho^+ and Ho^+Ho^p genotype have on average 2.5 offspring, while Ho^pHo^p males have on average 1 offspring. Taking into account both survival and reproduction, how many offspring do you expect each of the three genotypes to contribute to the total population in the next generation?

D) What is the frequency of the Ho^+ allele in the sperm that will form this next generation?

E) How would your answers to B-D change if the Ho^p allele was at

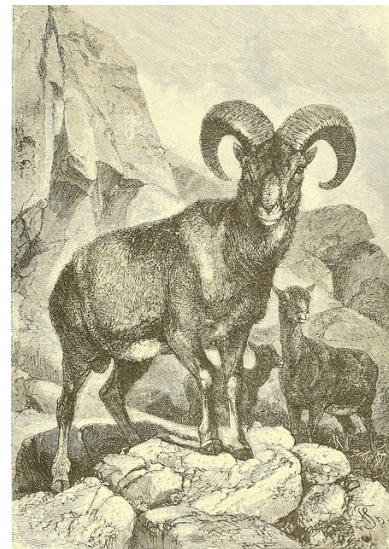


Figure 10.16: Mouflon (*Ovis orientalis orientalis*).

Animate creation. (1898). Wood, J. G. Image from the Biodiversity Heritage Library. Contributed by Smithsonian Libraries. Not in copyright.

The fitnesses here are chosen to roughly match those of the real Soay sheep example, as a full model would require us to more carefully model the life-histories of the sheep.

90% frequency?

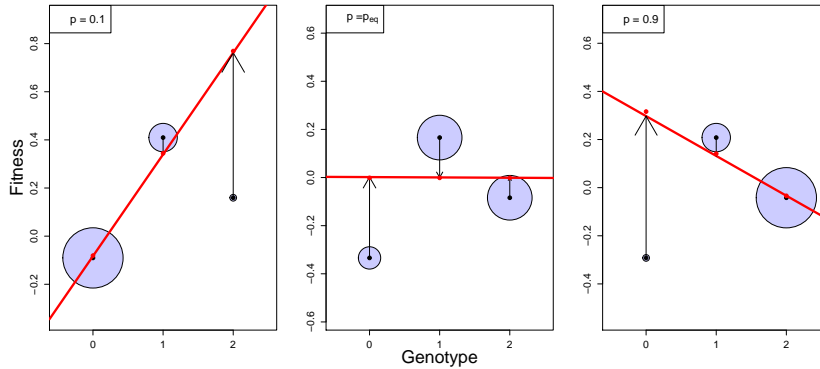


Figure 10.17: The deviation of the fitness of each genotype away from the mean population fitness (0) is shown as black dots. The area of each circle is proportion to the fraction of the population in each genotypic class (p^2 , $2pq$, and q^2). The additive genetic fitness of each genotype is shown as a red dot. The linear regression between fitness and additive genotype is shown as a red line. The black vertical arrows show the difference between the average mean-centered phenotype and additive genetic value for each genotype. The left panel shows $p = 0.1$ and the right panel shows $p = 0.9$; in the middle panel the frequency is set to the equilibrium frequency. [Code here.](#)

To push our understanding of heterozygote advantage a little further, note that the marginal fitnesses of our alleles are equivalent to the additive effects of our alleles on fitness. Recall from our discussion of non-additive variation (Section 7.1.1) that the difference in the additive effects of the two alleles gives the slope of the regression of additive genotypes on fitness, and that there is additive variance in fitness when this slope is non-zero. So what's happening here in our heterozygote advantage model is that the marginal fitness of the A_1 allele, the additive effect of allele A_1 on fitness, is greater than the marginal fitness of the A_2 allele ($\bar{w}_1 > \bar{w}_2$) when A_1 is at low frequency in the population. In this case, the regression of fitness on the number of A_1 alleles in a genotype has a positive slope. This is true when the frequency of the A_1 allele is below the equilibrium frequency. If the frequency of A_1 is above the equilibrium frequency, then the marginal fitness of allele A_2 is higher than the marginal fitness of allele A_1 ($\bar{w}_1 < \bar{w}_2$) and the regression of fitness on the number of copies of allele A_1 that individuals carry is negative. In both cases there is additive genetic variance for fitness ($V_A > 0$) and the population has a directional response. Only when the population is at its equilibrium frequency, i.e. when $\bar{w}_1 = \bar{w}_2$, is there no additive genetic variance ($V_A = 0$), as the linear regression of fitness on genotype is zero.

Underdominance. Another case that is of potential interest is the case of fitness underdominance, where the heterozygote is less fit than either of the two homozygotes. Underdominance can be parametrized as follows:

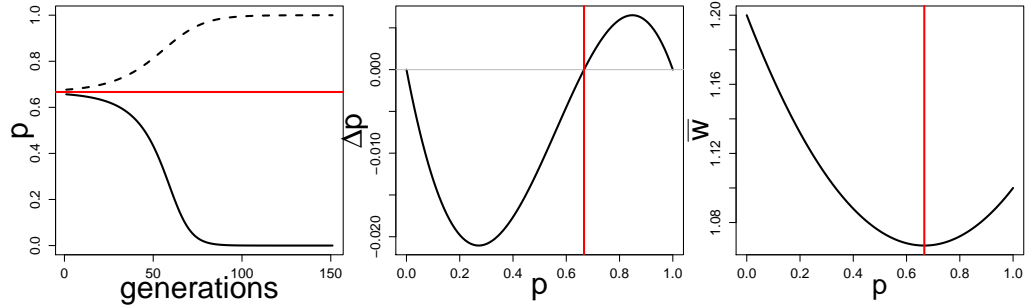
genotype	A_1A_1	A_1A_2	A_2A_2
absolute fitness	w_{11}	$> w_{12} <$	w_{22}
relative fitness (generic)	$w_{11} = W_{11}/W_{12}$	$w_{12} = W_{12}/W_{12}$	$w_{22} = W_{22}/W_{12}$
relative fitness (specific)	$1 + s_1$	1	$1 + s_2$

Underdominance also permits three equilibria: $p = 0$, $p = 1$, and a polymorphic equilibrium $p = p_U$. However, now only the first two equilibria are stable, while the polymorphic equilibrium is unstable. If $p < p_U$, then Δp_t is negative and allele A_1 will be lost, while if $p > p_U$, allele A_1 will become fixed.

While strongly-selected, underdominant alleles might not spread within populations (if $p_U \gg 0$), they are of special interest in the study of speciation and hybrid zones. That is because alleles A_1 and A_2 may have arisen in a stepwise fashion, i.e. not by a single mutation, but in separate subpopulations. In this case, heterozygote disadvantage will play a potential role in species maintenance.



Figure 10.18: In *Pseudacraea eurytus* there are two homozygotes morphs that mimic a different blue and orange butterfly; the heterozygote fails to mimic either successfully and so suffers a high rate of predation (OWEN and CHANTER, 1972). Illustrations of new species of exotic butterflies (1868) Hewitson. Image from the Biodiversity Heritage Library. Contributed by Smithsonian Libraries. Not in copyright.



Question 8. You are studying the polymorphism that affects flight speed in butterflies. The polymorphism does not appear to affect fecundity. Homozygotes for the B allele are slow in flight and so only 40% of them survive to have offspring. Heterozygotes for the polymorphism (Bb) fly quickly and have a 70% probability of surviving to reproduce. The homozygotes for the alternative allele (bb) fly very quickly indeed, but often die of exhaustion, with only 10% of them making it to reproduction.

- A)** What is the equilibrium frequency of the B allele?
- B)** Calculate the marginal absolute fitnesses of the B and the b allele at the equilibrium frequency.

Diploid fluctuating fitness Selection pressures fluctuate over time and can potentially maintain polymorphisms in the population. Two examples of polymorphisms fluctuating in frequency in response to temporally-varying selection are shown in Figure 10.20; thanks to the

Figure 10.19: **Left)** Two allele frequency trajectories of an A_1 allele subject to heterozygote disadvantage ($w_{11} = 1.1$, $w_{12} = 1$, and $w_{22} = 1.2$). The allele is started from just above and below the equilibrium frequency, in both cases the frequency move away the equilibrium frequency. The red line shows the unstable equilibrium frequency (p_e). **Middle)** The change in frequency of an allele with heterozygote disadvantage within a generation (Δp) as a function of the allele frequency. Fitnesses as in Figure 10.13. Note how the frequency change is negative below the equilibrium frequency (p_e) and positive above. **Right)** Mean fitness (\bar{w}) as a function of the allele frequency. Code here.

short lifespan of *Drosophila* we can see seasonally-varying selection. The first example is an inversion allele in *Drosophila pseudoobscura* populations. Throughout western North America, two orientations of the chromosome, two ‘inversion alleles’, exist: the Chiricahua and Standard alleles. DOBZHANSKY (1943) and WRIGHT and DOBZHANSKY (1946) investigated the frequency of these inversion alleles over four years at a number of locations and found that their frequency fluctuated systematically over the seasons in response to selection (left side of 10.20). If you’re still reading these notes send Prof. Coop a picture of Dobzhansky; Dobzhansky was one of the most important evolutionary geneticists of the past century and spent a bunch of time at UC Davis in his later years. Our second example is an insertion-deletion polymorphism in the Insulin-like Receptor gene in *Drosophila melanogaster*. PAABY *et al.* (2014) tracked the frequency of this allele over time and found it oscillated with the seasons (right side of 10.20). She and her coauthors also determined that these alleles had large effects on traits such as developmental time and fecundity, which could mediate the maintenance of this polymorphism through life-history trade-offs.

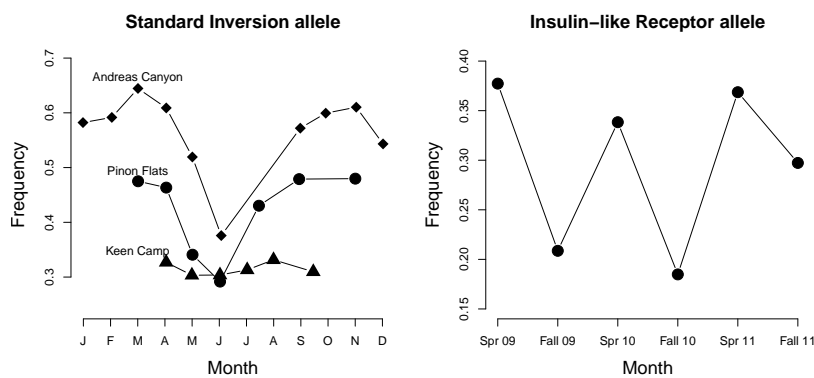


Figure 10.20: **Left)** Seasonal variation in the frequency of the ‘Standard’ inversion allele in *Drosophila pseudoobscura* for three populations from Mount San Jacinto, CA. These frequencies are an average over four years. Data from WRIGHT and DOBZHANSKY (1946). **Right)** The frequency of an allele at the Insulin-like Receptor gene over three years in *Drosophila melanogaster* samples from an Orchard in Pennsylvania. Data from PAABY *et al.* (2014). Code here.

To explore temporal fluctuations in fitness, we’ll need to think about the diploid absolute fitnesses being time-dependent, where the three genotypes have fitnesses $w_{11,t}$, $w_{12,t}$, and $w_{22,t}$ in generation t . Modeling the diploid case with time-dependent fitness is much less tractable than the haploid case, as segregation makes it tricky to keep track of the genotype frequencies. However, we can make some progress and gain some intuition by thinking about how the frequency of allele A_1 changes when it is rare (following the work of HALDANE and JAYAKAR, 1963).

When A_1 is rare, i.e. $p_t \ll 1$, the frequency of A_1 in the next gener-

ation (10.26) can be approximated as

$$p_{t+1} \approx \frac{w_{12}}{\bar{w}} p_t. \quad (10.40)$$

To obtain this equation, we have ignored the p_t^2 term (because it is very small when p_t is small) and we have assumed that $q_t \approx 1$ in the numerator. Following a similar argument to approximate q_{t+1} , we can write

$$\frac{p_{t+1}}{q_{t+1}} = \frac{w_{12,t} p_t}{w_{22,t} q_t}. \quad (10.41)$$

Starting from out from p_0 and q_0 in generation 0, then $t+1$ generations later we have

$$\frac{p_{t+1}}{q_{t+1}} = \left(\prod_{i=0}^t \frac{w_{12,i}}{w_{22,i}} \right) \frac{p_0}{q_0}. \quad (10.42)$$

From this we can see, following our haploid argument from above, that the frequency of allele A_1 will increase when rare only if

$$\frac{\sqrt[t]{\prod_{i=0}^t w_{12,i}}}{\sqrt[t]{\prod_{i=0}^t w_{22,i}}} > 1, \quad (10.43)$$

i.e. if the heterozygote has higher geometric mean fitness than the $A_2 A_2$ homozygote.

The question now is whether allele A_1 will approach fixation in the population, or whether there are cases in which we can obtain a balanced polymorphism. To investigate that, we can simply repeat our analysis for $q \ll 1$, and see that in that case

$$\frac{p_{t+1}}{q_{t+1}} = \left(\prod_{i=0}^t \frac{w_{11,i}}{w_{12,i}} \right) \frac{p_0}{q_0}. \quad (10.44)$$

Now, for allele A_1 to carry on increasing in frequency and to approach fixation, the $A_1 A_1$ genotype has to be out-competing the heterozygotes. For allele A_1 to approach fixation, we need the geometric mean of $w_{11,i}$ to be greater than the geometric mean fitness of heterozygotes ($w_{12,i}$). If instead heterozygotes have higher geometric mean fitness than the $A_1 A_1$ homozygotes, then the A_2 allele will increase in frequency when it is rare.

Intriguingly, we can thus have a balanced polymorphism even if the heterozygote is never the fittest genotype in any generation, as long as the heterozygote has a higher geometric mean fitness than either of the homozygotes. In this case, the heterozygote comes out ahead when we think about long-term fitness across heterogeneous environmental conditions, despite never being the fittest genotype in any particular environment.

As a toy example of this type of balanced polymorphism, consider a plant population found in one of two different environments each generation. These occur randomly; $1/2$ of time the population experiences

the dry environment and with probability $1/2$ it experiences the wet environment. The absolute fitnesses of the genotypes in the different environments are as follows:

Environment	AA	Aa	aa
Wet	6.25	5.0	3.75
Dry	3.85	5.0	6.15
arithmetic mean	5.05	5.0	4.95

Let's write $w_{AA,\text{dry}}$ and $w_{AA,\text{wet}}$ for the fitnesses of the AA homozygote in the two environments. Then, if the two environments are equally common, $\prod_{i=0}^t w_{AA,i} \approx w_{AA,\text{dry}}^{t/2} w_{AA,\text{wet}}^{t/2}$ for large values of t . To obtain an estimate of this product normalized over the t generations, we can take the t^{th} root to obtain the geometric mean fitness. Taking the t^{th} root, we find the geometric mean fitness of the AA allele is $w_{AA,\text{dry}}^{1/2} w_{AA,\text{wet}}^{1/2}$. Doing this for each of our genotypes, we find the geometric mean fitnesses of our alleles to be:

	AA	Aa	aa
Geometric mean	4.91	5.0	4.80

i.e. the heterozygote has higher geometric mean fitnesses than either of the homozygotes, despite not being the fittest genotype in either environment (nor having the highest arithmetic mean fitness). So the A_1 allele can invade the population when it is rare as it spread thanks to the higher fitness of the heterozygotes. Similarly the A_2 allele can invade the population when it is rare. Thus both alleles will persist in the population due to the environmental fluctuations, and the higher geometric mean fitness of the heterozygotes.

Negative frequency-dependent selection. In the models and examples above, heterozygote advantage maintains multiple alleles in the population because the common allele has a disadvantage compared to the other rarer allele. In the case of heterozygote advantage, the relative fitnesses of our three genotypes are not a function of the other genotypes present in the population. However, there's a broader set of models where the relative fitness of a genotype depends on the genotypic composition of the population; this broad family of models is called frequency-dependent selection. Negative frequency-dependent selection, where the fitness of an allele (or phenotype) decreases as it becomes more common in the population, can act to maintain genetic and phenotypic diversity within populations. While cases of long-term heterozygote advantage may be somewhat rare in nature, negative frequency-dependent selection is likely a common form of balancing selection.

One common mechanism that may create negative frequency-dependent selection is the interaction between individuals within or

This example is loosely based on the work of SCHEMSKE and BIERZY-CHUDEK (2001) on *Linanthus parryae*, a desert annual, endemic to California. There are blue- and a white-flowered colour morphs polymorphic many populations, with this polymorphism being controlled by a single dominant allele. The blue-flowered plants produce more seeds in dry years, i.e. they have higher fitness in these years, while the white-flowered plants have higher seed production in wet years. Thus both morphs can potentially be maintained in the population. See TURELLI *et al.* (2001) for a more detailed analysis.

among species. For example, negative frequency-dependent dynamics can arise in predator-prey or pathogen-host dynamics, where alleles conferring common phenotypes are at a disadvantage because predators or pathogens learn or evolve to counter the phenotypic effects of common alleles.

As one example of negative frequency-dependent selection, consider the two flower colour morphs in the deceptive Elderflower orchid (*Dactylorhiza sambucina*). Throughout Europe, there are populations of these orchids polymorphic for yellow- and purple-flowered individuals, with the yellow flower corresponding to a recessive allele. Neither of these morphs provide any nectar or pollen reward to their bumblebee pollinators. Thus these plants are typically pollinated by newly emerged bumblebees who are learning about which plants offer food rewards, with the bees alternating to try a different coloured flower if they find no food associated with a particular flower-colour morph (SMITHSON and MACNAIR, 1997). GIGORD *et al.* (2001) explored whether this behaviour by bees could result in negative frequency-dependent selection; out in the field, the researchers set up experimental orchid plots in which they varied the frequency of the two colour morphs. Figure 10.22 shows their measurements of the relative male and female reproductive success of the yellow morph across these experimental plots. When the yellow morph is rare, it has higher reproductive success than the purple morph, as it receives a disproportionate number of visits from bumblebees that are dissatisfied with the purple flowers. This situation is reversed when the yellow morph becomes common in the population; now the purple morph outperforms the yellow morph. Therefore, both colour morphs are maintained in this population, and presumably Europe-wide, due to this negative frequency-dependent selection.



Figure 10.21: Elderflower orchid (*Dactylorhiza sambucina*). Abbildungen der in Deutschland und den angrenzenden gebieten vorkommenden grundformen der orchideenarten (1904). Müller, W. Image from the Biodiversity Heritage Library. Contributed by New York Botanical Garden. Not in copyright.

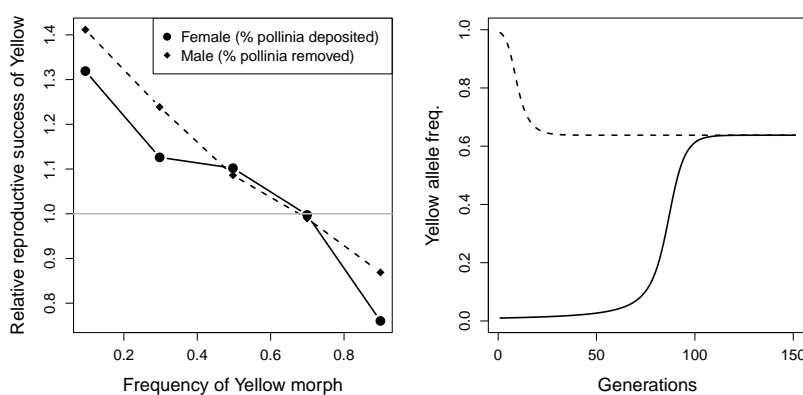


Figure 10.22: **Left**) Measures of the relative male- and female- reproductive success of the yellow Elderflower orchid morph as a function of the yellow morph in experimental plots. **Right**) Two allele frequency trajectories of the Yellow allele subject to negative frequency scheme given in the left plot (for an initial frequency of 0.01 and 0.99, solid and dotted line respectively). Note that the yellow Male reproductive success is measured in terms of the % of pollinia removed front a plant and female reproductive success is measured in terms of the % of stigmas receiving pollinia on a plant. These measures are made relative by dividing the reproductive success of the yellow morph by the mean of the yellow and purple morphs. Pollinia are the pollen masses of orchids, and other plants, where individual pollinium are transferred as a single unit by pollinators. Data from GIGORD *et al.* (2001). Code here.

Negative frequency-dependent selection can also maintain different breeding strategies due to interactions amongst individuals within a population. One dramatic example of this occurs in ruffs (*Philomachus pugnax*), a marsh-wading sandpiper that summers in Northern Eurasia. The males of this species lek, with the males gathering on open ground to display and attract females. There are three different male morphs differing in their breeding strategy. The large majority of males are ‘Independent’, with black or chestnut ruff plumage, and try to defend and display on small territories. ‘Satellite’ males, with white ruff plumage, make up ~ 16% of males and do not defend territories, but rather join in displays with Independent males and opportunistically mate with females visiting the lek. Finally, the rare ‘Faeder’ morph was only discovered in 2006 (JUKEMA and PIERSMA, 2006) and makes up less than 1% of males. These Faeder males are female mimics who hang around the territories of Independents and try to ‘sneak’ in matings with females. Faeder males have plumage closely resembling that of females and a smaller body size than other males, but with larger testicles (presumably to take advantage of rare mating opportunities). All three of these morphs, with their complex behavioural and morphological differences, are controlled by three alleles at a single autosomal locus, with the Satellite and Faeder alleles being genetically dominant over the high frequency Independent allele. The



Figure 10.23: Lekking Ruffs (*Philomachus pugnax*). Three Independent males, one Satellite male, and one female (or Faeder male?).

Painting by Johann Friedrich Naumann (1780–1857). Public Domain, wikimedia.

genetic variation for these three morphs is potential maintained by negative frequency-dependent selection, as all three male strategies are likely at an advantage when they are rare in the population. For example, while the Satellites mostly lose out on mating opportunities to Independents, they may have longer life-spans and so may have equal life-time reproductive success (WIDEMO, 1998). However, Satellite and Faeder males are totally reliant on the lekking Independent males, and so both of these alternative strategies cannot become overly com-

mon in the population. The locus controlling these differences has been mapped, and the underlying alleles have persisted for roughly four million years (KÜPPER *et al.*, 2016; LAMICHHANEY *et al.*, 2016). While this mating system is bizarre, the frequency dependent dynamics mean that it has been around longer than we've been using stone tools.

While these examples may seem somewhat involved, they must be simple compared to the complex dynamics that maintain the hundreds of alleles present at the genes in the Major histocompatibility complex (MHC). MHC genes are key to the coordination of the vertebrate immune system in response to pathogens, and are likely caught in an endless arms race with pathogens adapting to common MHC alleles, allowing rare MHC alleles to be favoured. Balancing selection at the MHC locus has maintained some polymorphisms for tens of millions of years, such that some of your MHC alleles may be genetically more closely related to MHC alleles in other primates than they are to alleles in your close human friends.

10.2 Sex ratios, sex ratio distorters, and other selfish elements.

We have seen that when selection acts on phenotypes and genotypes in a frequency-independent manner it can act to increase the mean fitness of the population, consist with our notation of selection driving our population to become better adapted to the environment (eqn. (8.19) and (10.32)). However, when the absolute fitnesses of individuals are frequency dependent, e.g. depend on the strategies deployed by others in the population, natural selection is not guaranteed to increase mean fitness. Nothing about the strategies pursued by the Ruffs discussed above seems well suited to maximizing the future growth rate of the population. One place where it is particularly apparent that frequency dependence drives non-optimal solutions from the perspective of the population is in the evolution of a 50/50 sex ratio. In fact as we'll see, selection can drive the evolution of traits that are actively harmful to the fitness of an individual when selection acts below the level of an individual.

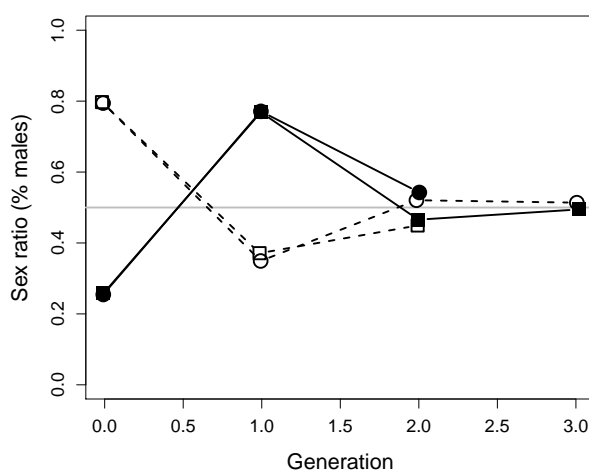


Figure 10.24: BASOLO (1994) explored sex ratio dynamics in platyfish (*Xiphophorus maculatus*), which has manipulable sex ratio due to its three factor sex determination. She started two replicates with a strong female bias (black) and two replicates with strong male bias (white). In all four cases the sex ratio quickly oscillated to a 50/50 sex ratio. Data from BASOLO (1994), Code here.

In many species, regardless of the mechanism of sex determination, the sex ratio is close to 50/50. Yet this is far from the optimum sex ratio from the perspective of the population viability. In many species females are the limiting sex, investing more in gametes and (sometimes) more in parental care. Thus a population having many females and few males would offer the fastest rate of population growth (i.e. the highest mean fitness). Why then is the sex ratio so often close to 50/50? Imagine if the population sex ratio was strongly skewed towards females. A rare autosomal allele that caused a mother to produced sons would have high fitness, as the mother's sons would have high reproductive success in this population of most females. Thus our initially rare allele would increase in frequency. Conversely if the sex ratio was strongly skewed towards males, a rare autosomal allele that causes a mother to produce daughters would spread. So selection on autosomal alleles favours the production of the rare sex, a form of negative frequency dependence, and this pushes the sex ratio away from being too skewed. Only the 50/50 sex ratio is evolutionarily stable as there is no rarer sex, and so no (autosomal) sex-ratio-altering mutation can invade a population with a 50/50. The 50/50 sex ratio is an example of an Evolutionary stable strategy (ESS), described in more detail in Section 10.2.2.

Adaptive adjustments to sex ratio in response to local mate competition. There are, however, situations where we see strong deviations away from a 50/50 sex ratio. This can represent an adaptive strategy to situations where individuals compete against relatives for access

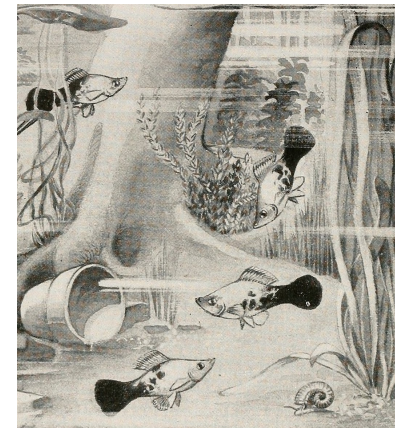


Figure 10.25: Poecilid Hybrid, *Xiphophorus helleri* × *Platypoecilus maculatus*.

Aquatic life, chapter by Curtis F.S. (1915)
Image from the Biodiversity Heritage Library.
Contributed by Harvard University, Museum of Comparative Zoology, Ernst Mayr Library. Not in copyright.

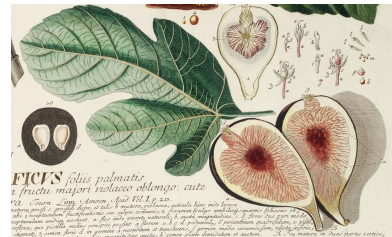
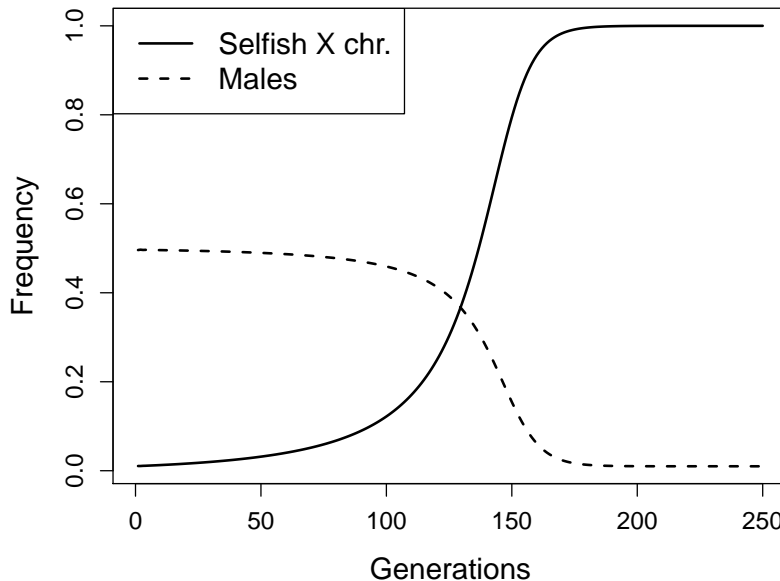
"An ESS is a strategy such that, if all the members of a population adopt it, then no mutant strategy could invade the population under the influence of natural selection" SMITH (1982), pg 10.

A version of this sex ratio argument was first put forward by DÜsing in 1884 and popularized by FISHER (1930), see EDWARDS (1998).

to resources or mating opportunities. To see this consider fig wasps. There are many species of fig wasp, which form a tight pollination symbiosis with many species of fig. Wasp females enter the inverted fig flower structure (top right Figure 10.26) pollinating the flowers.

They lay their eggs in some of the flowers, which form galls in response. The young, wingless, male wasps emerge from their galls first (Figure 10.27f) but they never leave the fig. Their only role in this is to fertilize the female wasps (Figure 10.27d) in the fig and then die. The female offspring (Figure 10.27a & e) emerge in the fig just as the male fig flowers are emerging. The female wasps burrow out and take the fig pollen with them as they fly off.

Female wasps have control over the sex of their offspring but what is their optimal strategy? Females have this degree of control as sex determination in wasps is haplo-diploid, with fertilized eggs developing as diploid females and unfertilized as males; by choosing to lay fertilized eggs they can control their number of daughters. If a female wasp lays her eggs into a fig with no other eggs, her sons will mate with her daughters and then die. Thus a lone female can maximize her contribution to the next generation by having many daughters, and just enough sons to fertilize them. And that's exactly what female wasps do, in many species of fig wasp 95% of individuals born are female.



10.2.1 Selfish genetic elements and selection below the level of the individual.

These ideas about individuals pursuing selfish strategies, which can lower the population's fitness, extends below the level of the individual. The alleles within an individual can sometimes pursue selfish strategies that actively harm the individuals that carry them. Here we'll take a tour of the rogues gallery of some the various genetic conflicts that occur and selfish genetic elements that exploit them. They're included in this chapter in part because much of their biology can be understood from the perspective of the ideas developed here. But the main reason for talking about them is that they're an amazing slice of biology.

Selfish sex chromosomes and sex ratio distortion From the perspective of the autosomes a 50/50 sex ratio normally represents a stable strategy, but all is not always harmonious in the genome. In systems with XY sex determination, male fertilization by Y-bearing sperm leads to sons, while male fertilization by X-bearing sperm leads to daughters. From the viewpoint of the X chromosome the Y-bearing sperm, and a male's sons, are an evolutionary deadend. We can imagine a mutation arising on the X chromosome that causes a poison to be released during gametogenesis that kills Y-bearing sperm. This would cause much of the ejaculate of the males carrying this mutation to be X-bearing sperm, and so these males would have mostly daughters. Such an allele would potentially spread in the population as it is over transmitted through males, even if it somewhat reduces the fitness of the individuals who carry it. The spread of this allele would strongly bias the population sex ratio towards females. Such 'selfish' X alleles turn out to be relatively common, and they can often substantially low the fitness of the bearer. They do not spread because they are good for the individual but rather because they are favoured due to selection below the level of the individual.

One example of a selfish X chromosome allele is the *Winters sex-ratio* system found in *Drosophila simulans*, so named as it was found in flies collected around Winters, California (just a few miles down the road from Davis). In crosses males carrying the selfish X chromosome have > 80% daughters. The gene responsible, *Dox* (*Distorter on the X*), is a gene duplicated by transposition and produces a transcript which targets a region on the Y chromosome preventing the Y-bearing sperm from developing TAO *et al.* (see Figure 10.29 from 2007).

The spread of such selfish sex chromosomes, distorting the sex ratio strongly away from 50/50, can have profound effects for population growth rates.³ However, the other sex chromosome and autosomes are

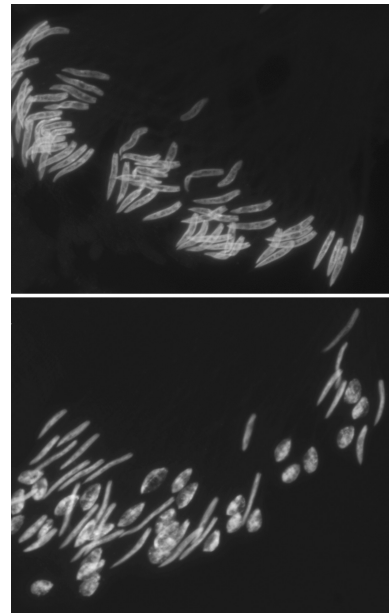


Figure 10.29: **Top)** Normally developing spermatids in *D. simulans*. **Bottom)** Abnormally developing spermatids in a male expressing *dox*. The spermatids that look like rice Krispies carry the Y chromosome, the normal, slender spermatids are X-bearing spermatids. Figure from TAO *et al.* (2007), cropped, licensed under CC BY 4.0.

³ Indeed people have long discussed using selfish Y chromosomes, driving an over production of sons, for population control of malaria-spreading mosquitos. Natural selfish systems on the Y appear rare, likely because of its low gene content.

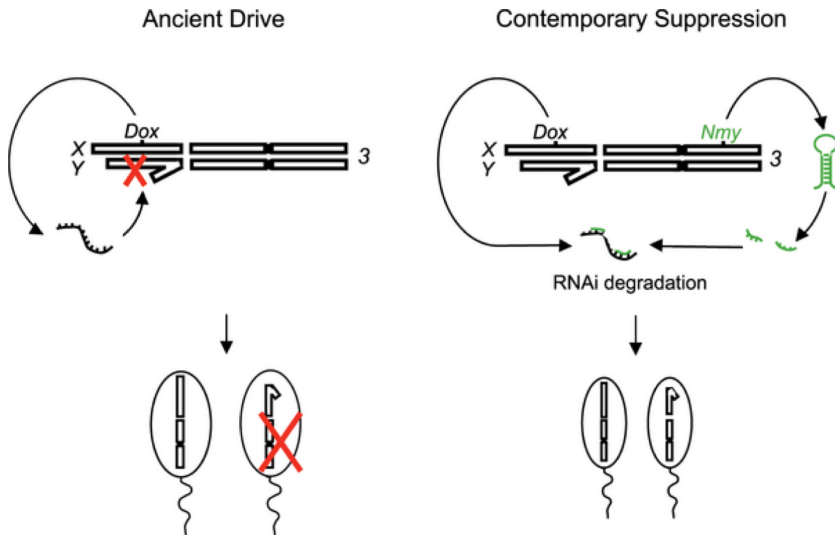


Figure 10.30: Mechanistic and Evolutionary Model for sex-ratio Distortion
Left) The X-linked Dox gene evolved to target the Y chromosome, blocking Y-bearing sperm from developing and so favouring its own transmission.
Right) Subsequently Dox was retrotransposed to an autosome forming the Nmy gene. Nmy was subsequently rearranged by a small duplication, and now blocks the action of dox by the formation of a hairpin small interfering RNA. Figure from FERREE and BARBASH (2007), licensed under CC BY 4.0. See LIN *et al.* (2018) for an update on the fascinating biology and further loci uncovered in this system.

not helpless against the spread of selfish sex chromosome elements. In the case of a selfish X chromosome that has achieved appreciable frequency in the population, there will be a strong excess of females in the population such that suppressors of drive can arise on the autosomes and spread due to the fact that they cause the male bearer to produce some sons and so spread due to Fisherian sex-ratio advantage. This has happened in the case of the Winters sex chromosome system. An autosomal allele has spread through the population that suppresses the selfish X chromosome, restoring the 50/50 sex ratio. Now the sex ratio distorter can only be found by crosses to naive populations, where the suppressor has not spread yet. The autosomal suppressor gene turns out to be a duplicate of the selfish dox gene, *NMY* (*Not Much Yang*), that moved to the autosome through retrotransposition and now blocks the action of dox through RNA-interference degradation of the dox transcript (TAO *et al.*, 2007, , see Figure 10.30).

Conflict due to maternally transmitted elements. Chromosomes transmitted maternally, i.e. only through mothers, also have divergent interests from the individual. Many plants are hermaphrodites producing both pollen and seeds. But from the perspective of the Mitochondria in an individual, pollen is a waste of energy as the Mitochondria won't be transmitted through it. Thus a mutation that arises on the Mitochondria abolishing male sexual function (pollen) and shunting energy into other processes can spread. The self spread of a Cytoplasmic Male Sterility (CMS) allele creates a population of females and hermaphrodite plants (a gynodioecious population). This

strong excess of female plants in turn can select for the spread of autosomal suppressors of CMS that are favoured by producing the rarer gamete (pollen), and so restore the population to hermaphroditism.

The spread of such CMS alleles, and subsequent autosomal suppression, is thought to be common in hermaphrodite species and often uncovered in crosses between diverged hermaphrodite populations. The discovery or deliberate creation of CMS alleles in agricultural plants is prized because it gives breeders more control over hybridization as they can more carefully control the pollen donor to the plants.

The maternal transmission of mtDNA also causes genetic conflicts in organisms with separate sexes. Males are an evolutionary dead end as far as mitochondria are concerned, and so mitochondrial mutations that lower a male's fitness are not removed from the population of mitochondria. Thus the Mitochondria genome may be a hotspot of alleles that are deleterious in males (an effect termed the "Mother's curse"). One example of a male-deleterious mitochondrial mutations



Figure 10.31: Bladder Campion (*Silene vulgaris*), on left, has both hermaphrodite and female plants due to CMS and nuclear restorer polymorphisms (CHARLESWORTH and LAPORTE, 1998). (*S. nutans* on right)

Billeder af nordens flora (1917). Mentz, A. Image from the Biodiversity Heritage Library. Contributed by The LuEsther T Mertz Library, the New York Botanical Garden. Not in copyright.



underlying Leber's 'hereditary optic neuropathy' (LHON) in humans. LHON causes degeneration of the optic nerve and loss of vision in teenage males (with much lower penetrance in women). One such LHON mutation is present at low frequency in the Quebec population. The Québécois population grew rapidly from a relatively small number of founders, leading to the prevalence of some disease mutations due to the founder effect. Thanks to the detailed genealogical records kept by French Canadians since the founding of Quebec, we know that nearly all the Québécois LHON alleles are descended from the mitochondria of a single woman, one of the *fille du roi*, who arrived in Quebec City in 1669 (LABERGE *et al.*, 2005). Using the genealogy,

Figure 10.32: Arrival of the fille du roi, the 'king's daughters' to Quebec city in 1667. Painting by Eleanor Fortescue-Brickdale. The fille du roi were some 800 women whose emigration to New France (Quebec) was paid for by a program established by King Louis XIV of France to address the strong gender imbalance of the new colony. You can read more in this Atlantic article by Sarah Zhang.

Painting from the Library and Archives Canada collection, Wikimedia, Public Domain.

Milot *et al.* (2017) tracked all of her mitochondrial descendants, individuals whose mothers were in her matrilineal line, and so identified all the individuals in the Québécois who carried this allele. There was no significant difference in the fitness of females who carried or didn't carry the mutation. In contrast, the fitness of male carriers of the mutation was only 65.3% that of male non-carriers. This mitochondria mutation has increased in frequency slightly over the past 290 years, despite its strong effects in males, due to the fact that its effects have no consequence for female fitness.

Question 9. The frequency of the LHON allele was roughly 1/2000 in 1669. If females suffered the same ill consequences as males what would be the frequency today? [assume there are ~29 years a generation]

Question 10. Kin selection has been proposed as a way that the male deleterious mitochondrial mutations could be removed from the population. Can you explain this idea?

It's not just chromosomes that get in on the act of the battle of the sexes. Numerous arthropods, including a high proportion of insects, are infected with the intracellular bacteria *Wolbachia*, which are passed to offspring through the maternal cytoplasm. As they are only transmitted by females, *Wolbachia* increase their transmission in a variety of selfish ways including feminization of males and killing male embryos. In one dramatic case, a male-killing *Wolbachia* strain forced a sex ratio of 100 females to every 1 male in *Hypolimnas bolina* (eggspot butterflies) throughout Southeast Asia. This extreme sex ratio persisted for many decades, according to the analysis of museum collections from the late 19C, before the sex ratio was rapidly restored to 50/50 by the spread of an autosomal suppressing allele. The autosomal suppressor allele spread very rapidly within populations taking just 5 years to spread through the population from 2001 to 2006.

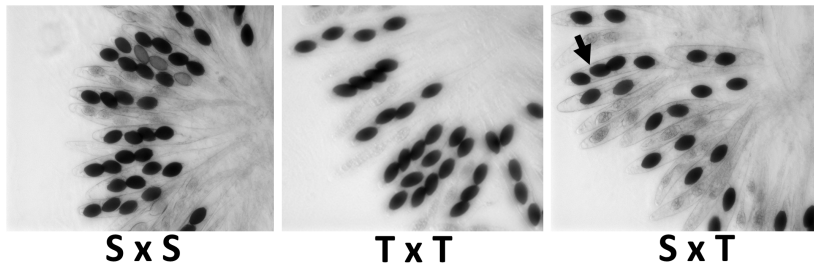
Selfish Autosomal Systems Self genetic systems can also arise and cause genetic conflicts on the autosomes. The interests of autosomal alleles are usually relatively well aligned with promoting the fitness of the individual who carries them. However, these interests can diverge during meiosis and gametogenesis. After all, there are two alleles at each autosomal locus but only one of them will get passed to a child, therefore there can be competition to be in gamete transmitted to the next generation.

The four products of meiosis in the fungus *Podospora anserina* are arrayed in the ascus⁴ of the spores for the next generation. There is a polymorphism S/T at the Spok gene in this species. In spores from



Figure 10.33: male Eggspot butterfly (*Hypolimnas bolina*).
P. Cramer's Uitlandsche kapellen (1780)
Image from the Biodiversity Heritage Library.
Contributed by Smithsonian Libraries. Not in copyright.

⁴ from the Greek word askos meaning wineskin.



SxS and TxT individuals all four products are present. However, only two out of four spores are present in the ~ 90% of asci from SxT individuals (GROGNET *et al.*, 2014). The T allele is releasing a toxin that poisons off the S carrying spores. The jury is still out on whether the T allele spread due to the advantage created by sabotaging its rival product of meiosis (SWEIGART *et al.*, 2019). However, in other systems it is clear that alleles have spread due to their selfish actions.

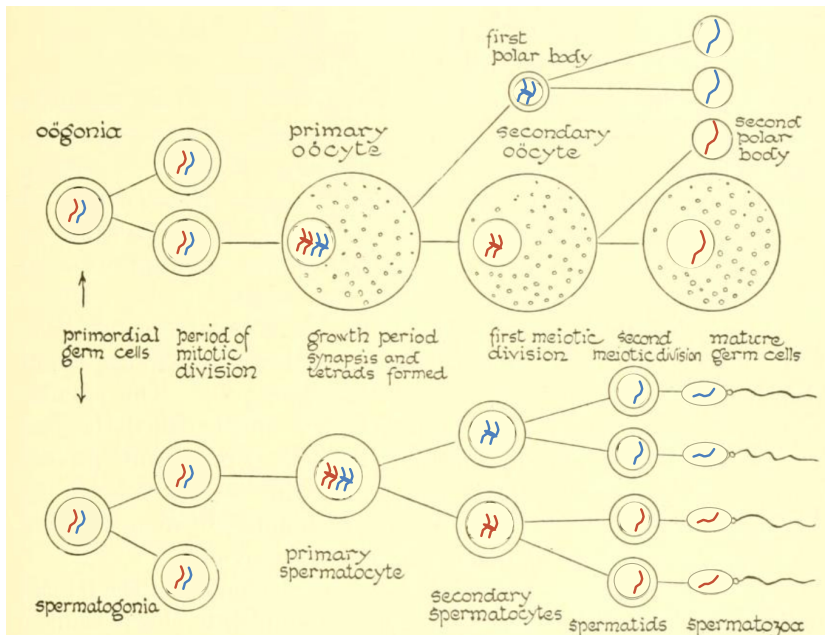


Figure 10.34: Pictures of *P. anserina* asci from various crosses. The arrow in the SxT picture shows a rare ascus carrying all four products of meiosis. Figure from GROGNET *et al.* (2014), licensed under CC BY 4.0.

Figure 10.35: The two copies of a chromosome are shown in red and blue through the process of female and male meiosis and gametogenesis. Crossovers are omitted to keep things simpler. Modified from original to include chromosomes transmitted. Biology: the story of living things (1937). Hunter, G.W., Walter H.E. Image from the Biodiversity Heritage Library. Contributed by MBLWHOI Library. No known copyright restrictions.

A number of well-established genetics systems illustrate in animals and plants how male and female gametogenesis offer different opportunities for selfish alleles (Figure 10.35). Just as how selfish X chromosome systems can spread by targeting sperm that carry the Y chromosome, selfish autosomal alleles can spread by targeting sperm carrying the other chromosome in heterozygotes. Both the Drosophila Segregation Distortion allele and the mouse T-allele are selfish autosomal systems that game transmission in heterozygotes by killing off

sperm that don't carry the allele in heterozygotes.

In females meiosis there is a unique opportunity for cheating. In male meiosis all four products of meiosis become gametes. However, only 1 of the four products of female meiosis becomes the egg, the other 3 products are fated to become the polar bodies. Thus alleles can cheat in female meiosis by preferentially getting transmitted into the egg rather than the polar body. If an allele on a red chromosome (in top panel of Figure 10.35) can manipulate any asymmetry of meioses so that it can be present in the egg > 50% of the time it will have a transmission advantage in female heterozygotes.

To see how such drivers can spread through the population lets consider the case of a population where an allele drives in both male and female gametogenesis. (Most selfish alleles will be sex-specific, but that makes the math a little more tricky.) Imagine a randomly-mating population of hermaphrodites. In this population, a derived allele (D) segregates that distorts transmission in its favour over the ancestral allele (d) in the production of all the gametes of heterozygotes. The drive leads to a fraction α of the gametes of heterozygotes (D/d) to carry the D allele ($\alpha \geq 0.5$). The D allele causes viability problems such that the relative fitnesses are $w_{dd} = 1$, $1 > w_{Dd} \geq w_{DD}$. If the D allele is currently at frequency p in the population at birth, its frequency at birth in the next generation will be

$$p' = \frac{w_{DD}p^2 + w_{Dd}\alpha 2pq}{\bar{w}} \quad (10.45)$$

when $\alpha = 1/2$, i.e. fair Mendelian transmission this is exactly the same as our directional selection, which results in our D allele being selected out of the population (blue line, Figure 10.36). However, if $\alpha > 1/2$, i.e. our deleterious allele cheats, it can potentially increase in the population when it is rare (red and black lines, Figure 10.36)). However, the allele can become trapped in the population at a polymorphic equilibrium if its cost is sufficient in homozygotes. This is akin to the case of heterozygote advantage, but now our allele offers no advantage to heterozygote but has a self advantage in heterozygotes.

Question 11. (Tricker question) Thinking of our autosomal driver from equation 10.45. **B)** Imagine the cost of the driver were additive, i.e. $w_{dd} = 1$, $w_{Dd} = 1 - e$, $w_{DD} = 1 - 2e$. Under what conditions can the driver invade the population? Can a polymorphic equilibrium be maintained?

A) Imagine the allele is completely recessive, i.e. $w_{dd} = w_{Dd} = 1$. What conditions do you need for a polymorphic equilibrium to be maintained? What is the equilibrium frequency of this balanced polymorphism?

Many of the known autosomal drive systems are polymorphic in

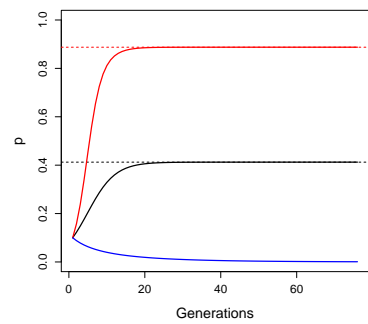


Figure 10.36: The fate of an unfit transmission distorter allele. If transmission is fair ($\alpha = 1/2$, blue curve) the allele is lost, but the stronger its drive in heterozygotes the faster its spread and the higher its final frequency in the population (black and red curves, $\alpha = 0.7$ & 0.9 respectively). With fitnesses $w_{dd} = 1$, $w_{Dd} = 0.95$, and $w_{DD} = 0.1$. The dotted lines show the predicted equilibrium. Code here.

populations, unable to reach fixation in the population due to their costs in homozygotes. It seems likely that this represents an ascertainment bias, and that many other selfish systems that had lower selective costs have swept to fixation.

10.2.2 Appendix: ESS for the sex ratio

Let R be the resources available to an individuals and C_σ and C_φ be the cost of producing a son and daughter respectively. If our focal mother directs s of her effort towards sons and $(1-s)$ of her effort towards daughters, she'll produce $\frac{Rs}{C_\sigma}$ sons and $\frac{R(1-s)}{C_\varphi}$ daughters. Let's assume that the mean reproductive value of daughters is 1. Given this, the average reproductive value of sons is the average number of matings that a male will have, i.e. the ratio # females/# males. So if the population has a sex ratio s_p , the fitness of our focal female is

$$W(s, s_p) = \left(\frac{R(1-s)}{C_\varphi} \times 1 \right) + \left(\frac{Rs}{C_\sigma} \times \frac{R(1-s_p)/C_\varphi}{Rs_p/C_\sigma} \right) \quad (10.46)$$

expressing fitness in terms the number of grandkids our focal female is expected to have.

To find the ESS we want a sex ratio s^* for the population such that no mutant has higher fitness. We can write this as as the population having strategy $s_p = s^*$, and then seeing what choice of s^* leads to $W(s^*, s^*) > W(s, s^*)$ for $s \neq s^*$, i.e. that no new strategy (s) has higher fitness than the ESS strategy s^* . We can find this ESS s^* by

$$\frac{\partial W(s, s_p)}{\partial s} \Big|_{s^* = s = s_p} = 0 \quad (10.47)$$

taking the derivative of Eqn 10.46 we obtain

$$\frac{\partial W(s, s_p)}{\partial s} = -\frac{R}{C_\varphi} + \frac{R}{C_\sigma} \left(\frac{R(1-s_p)/C_\varphi}{Rs_p/C_\sigma} \right) \quad (10.48)$$

setting $s^* = s = s_p$ and rearranging

$$\frac{R}{C_\varphi} = \frac{R}{C_\sigma} \left(\frac{R(1-s^*)/C_\varphi}{Rs^*/C_\sigma} \right) \quad (10.49)$$

which is satisfied when $s^* = 1/2$, i.e. devoting equal resources to male and female offspring is the ESS, which corresponds to a 50/50 sex ratio if male and female offspring are equally costly.

11

The Interaction of Selection, Mutation, and Migration.

Genetic variation is the raw fuel of evolution. Without variation, natural selection would have nothing to act on to shape adaptive traits. However, variation can be deleterious.

Mutation, broadly defined, is the ultimate source of all genetic variation and is constantly introducing new variation into all populations. However, mutation is random and so mutations that affect function are often damaging. Thus mutation will, in the absence of sufficiently strong selection, degrade pre-existing adaptations and undo the work of selection that has built up functional regions of DNA over time.

Migration, the movement of individuals into a population, can also increase variation to the population as the individuals bring new alleles in from surrounding populations. Thus migration can be an important source of adaptive alleles, aiding their spread amongst populations within a species. Adaptive alleles can introgress between species if low levels of interbreeding occur. They can sometimes spread between very diverged clades of species, indeed sometimes different domains of life, thanks to horizontal gene transfer. However, again, just like mutation, migration can disrupt adaptations. When populations are locally adapted migration amongst populations can introduce maladaptive alleles into well adapted populations. If this migration pressure is sufficiently strong, it can lead to the collapse of local adaptations, or even the collapse of species.

In this chapter we'll study some of the interplay between selection, migration, and mutation.

11.0.1 Mutation-Selection Balance

Mutation is constantly introducing new alleles into the population. Therefore, variation can be maintained within a population not only if selection is balancing (e.g. through heterozygote advantage or fluc-

tuating selection over time, as we have seen in the previous section), but also due to a balance between mutation introducing deleterious alleles and selection acting to purge these alleles from the population (HALDANE, 1937). To study mutation-selection balance, we return to the model of directional selection, where allele A_1 is advantageous, i.e.

genotype	A_1A_1	A_1A_2	A_2A_2
absolute fitness	W_{11}	$\geq W_{12} \geq$	W_{22}
relative fitness	$w_{11} = 1$	$w_{12} = 1 - sh$	$w_{22} = 1 - s$

We'll begin by considering the case where allele A_2 is not completely recessive ($h > 0$), so that the heterozygotes suffer at least some disadvantage. We denote by $\mu = \mu_{1 \rightarrow 2}$ the mutation rate per generation from A_1 to the deleterious allele A_2 , and assume that there is no reverse mutation ($\mu_{2 \rightarrow 1} = 0$). Let us assume that selection against A_2 is relatively strong compared to the mutation rate, so that it is justified to assume that A_2 is always rare, i.e. $q_t = 1 - p_t \ll 1$. Compared to previous sections, for mathematical clarity, we also switch from following the frequency p_t of A_1 to following the frequency q_t of A_2 . Of course, this is without loss of generality. The change in frequency of A_2 due to selection can be written as

$$\Delta_S q_t = \frac{\bar{w}_2 - \bar{w}_1}{\bar{w}} p_t q_t \approx -hsq_t. \quad (11.1)$$

This approximation can be found by assuming that $q^2 \approx 0$, $p \approx 1$, and that $\bar{w} \approx w_1$. All of these assumptions make sense if $q \ll 1$. From eqn. (11.1) we see that selection acts to reduce the frequency of A_2 (as both h and s are positive), and it does so geometrically across the generations. That is, if the initial frequency of A_2 is q_0 , then its frequency at time t is approximately

$$q_t = q_0(1 - hs)^t. \quad (11.2)$$

We will now consider the change in frequency induced by mutation. Recalling that μ is the mutation rate from A_1 to A_2 per generation, the frequency of A_2 after mutation is

$$q' = \mu p_t + q_t = \mu(1 - q_t) + q_t. \quad (11.3)$$

Assuming that $\mu \ll 1$ and that $q \ll 1$, the change in the frequency of allele A_2 due to mutation ($\Delta_M q_t$) can be approximated by

$$\Delta_M q_t = q' - q_t = \mu. \quad (11.4)$$

Hence, when A_2 is rare and the mutation rate is low, mutation acts to linearly increase the frequency of the deleterious allele A_2 .

If selection is to balance deleterious mutation, their combined effect over one generation has to be zero. Therefore, to find the mutation-selection equilibrium, we set

$$\Delta_M q_t + \Delta_S q_t = 0, \quad (11.5)$$

insert eqns. (11.1) and (11.4), and solve for q to obtain

$$q_e = q_t = \frac{\mu}{hs}. \quad (11.6)$$

We see that the frequency of the deleterious allele A_2 is balanced at a frequency equal to the mutation rate (μ) divided by the reduction in relative fitness in the heterozygote (hs).

It is worth pointing out that the fitness of the A_2A_2 homozygote has not entered this calculation, as A_2 is so rare that it is hardly ever found in the homozygous state. Therefore, if A_2 has any deleterious effect in a heterozygous state (i.e. if $h > 0$), it is this effect that determines the frequency at which A_2 is maintained in the population. Also, note that by writing the total change in allele frequency as $\Delta_M q_t + \Delta_S q_t$ we have implicitly assumed that we can ignore terms of order $\mu \times s$. That is, we have assumed that mutation and selection are both relatively weak. This assumption is valid under our prior assumption that both μ and s are small.

If an allele is truly recessive (although few likely are), we have $h = 0$, and so eqn. (11.6) is not valid. However, we can make an argument similar to the one above to show that, for truly recessive alleles,

$$q_e = \sqrt{\frac{\mu}{s}}. \quad (11.7)$$

Question 1. Oblong-winged katydids (*Amblycorypha oblongifolia*) are usually green. However, some are bright pink, thanks to an erythrism mutation (a nice example of early Mendelian reasoning in a wonderfully titled paper¹). This pink condition is thought to be due to a dominant mutation (Crew, 2013). Assume that roughly one in ten thousand katydids is bright pink and that the mutation rate at the gene underlying this condition is 10^{-5} . What is the relative fitness of heterozygotes for the pink mutation?

The genetic load of deleterious alleles What effect do such deleterious mutations at mutation-selection balance have on the population? It is common to quantify the effect of deleterious alleles in terms of a reduction of the mean relative fitness of the population. For a single site at which a deleterious mutation is segregating at frequency $q_e = \mu/(hs)$, the population mean relative fitness is reduced to

$$\bar{w} = 1 - 2p_e q_e h s - q_e^2 s \approx 1 - 2\mu. \quad (11.8)$$

Somewhat remarkably, the drop in mean fitness due to a site segregating at mutation-selection balance is independent of the selection coefficient against the heterozygote; it depends only on the mutation



Figure 11.1: Oblong-winged katydid. Field book of insects (1918). Lutz, F.E. : Illustrations by Edna L. Beutemüller. Image from the Biodiversity Heritage Library. Contributed by MBLWHOI Library. Not in copyright.

¹ WHEELER, W. M., 1907 Pink Insect Mutants. The American Naturalist 41(492): 773–780

rate. Intuitively this is because, given a fixed mutation rate, less deleterious alleles can rise to a higher equilibrium frequency, and thus contribute the same total load as more deleterious (rarer) alleles, but this load is spread across more individuals in the population. Note that this result applies only if the mutation is not totally recessive, i.e. if $h > 0$.

A fitness reduction of 2μ is very small, given that the mutation rate of a gene is likely $< 10^{-5}$. However, if there are many loci segregating at mutation-selection balance, small fitness reductions can accumulate to a substantial so-called genetic load, a major cause of variation in fitness-related traits among individuals. For example, the human genome contains over twenty thousand genes, and many other functional regions, the vast majority of which will be subject to purifying selection against mutations that disrupt their function. In humans, most loss of function (LOF) variants, which severely disrupt a protein-coding gene, are found at low frequencies. However, each human genome typically carries over a hundred LOF variants (MACARTHUR *et al.*, 2012; LEK *et al.*, 2016). Not every LOF allele will be deleterious; some could even be advantageous. However, the combined load of these LOF alleles must on average lower our fitness, otherwise selection wouldn't be removing them from the population. Each one of us carries a unique set of these LOF alleles, usually in a heterozygous state. We differ slightly in how many of these alleles we carry. For example, the left side of Figure 11.2 shows the distribution of the number of LOF alleles carried by 769 individuals of Dutch ancestry. The individuals who carry fewer of these LOF alleles will on average have higher fitness than those individuals with more.

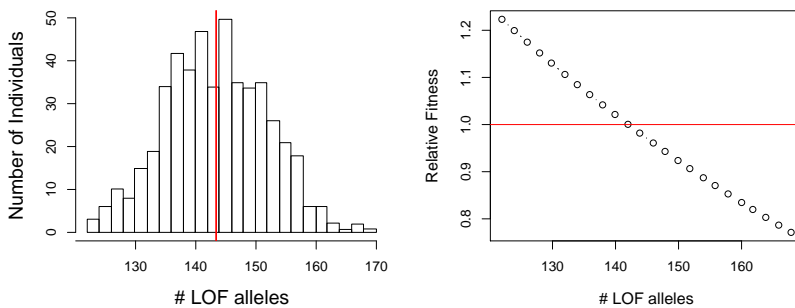


Figure 11.2: **Left)** The distribution of LOF alleles in 769 individuals from the Genome of the Netherlands project. Data from FRANCIOLI *et al.*. The average individual (red line) carries 144 LOF alleles. **Right).** The relative fitness of individuals carrying these varying numbers of LOF alleles, assuming multiplicative selection and a selection coefficient of $sh = 10^{-2}$ acting against these alleles (CASSA *et al.*, 2017). Code here.

How do these differences across individuals in total LOF mutations mount up? Well, if we are willing to assume that the fitness costs of deleterious alleles interact multiplicatively, we can make some progress. If an individual who carries one LOF mutation has a fitness

$1 - hs$, then an individual who's heterozygote for two LOF mutations would have fitness $(1 - hs)^2$, and an individual who is heterozygote for L LOF alleles would have fitness $(1 - hs)^L$. The right-hand side of Figure 11.2 shows the predicted fitness of individuals carrying varying number of LOF alleles, relative to the mean fitness of the sample, using this multiplicative model. We don't yet know how much lower the fitness of these individuals really is, nor do we know how most of these LOF alleles manifest their fitness consequences through disease and other mechanisms. However, it's a reasonable guess that this variation in LOF alleles, presumably maintained by mutation-selection balance, is a major source of variation in fitness.

11.0.2 Inbreeding depression

All else being equal, eqn. (11.6) suggests that mutations that have a smaller effect in the heterozygote can segregate at higher frequency under mutation-selection balance. As a consequence, alleles that have strongly deleterious effects in the homozygous state can still segregate at low frequencies in the population, as long as they do not have too strong a deleterious effect in heterozygotes. Thus, outbred populations may have many alleles with recessive deleterious effects segregating within them.

Question 2. Assume that a deleterious allele has a relative fitness .99 in heterozygotes and a relative fitness 0.2 when present in the homozygote state. Assume that the deleterious allele is at a frequency 10^{-3} at birth and the genotype frequencies follow from HWE. Only considering the fitness effects of this locus, and measuring fitness relative to the most fit genotype, answer the following questions:

- A) What is the average fitness of an individual in the population?
- B) What is the average fitness of the child of a full-sib mating?

One consequence of segregating for low-frequency recessive deleterious alleles is that inbreeding can reduce fitness. In typically outbred populations, the mean fitness of individuals decreases with the inbreeding coefficient, i.e. so-called 'inbreeding depression' is a common observation. This wide-spread observation dates back to systematic surveys of inbreeding depression by DARWIN (1876). Inbreeding depression is likely primarily a consequence of being homozygous at many loci for alleles with recessive deleterious effects.

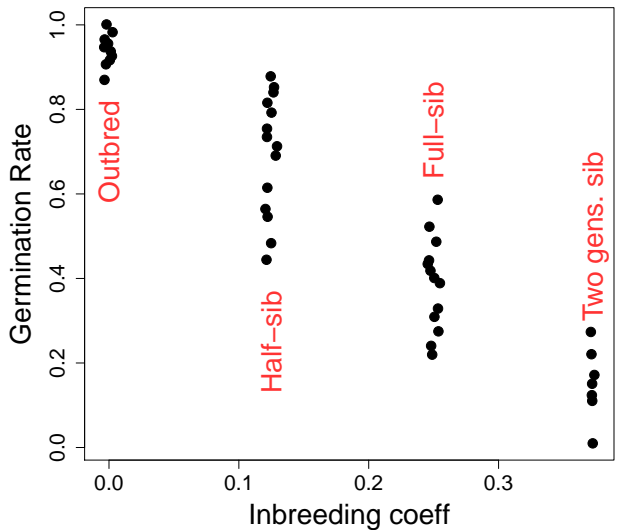


Figure 11.3: Data showing inbreeding depression over different degrees of inbreeding in *S. latifolia*. Each point is the mean seed germination rates for different family crosses. Data from RICHARDS. Code here.

One example of inbreeding depression is shown in Figure 11.3. White campion (*Silene latifolia*) is a dioecious flowering plant; dioecious means that the males and females are separate individuals. RICHARDS performed crosses to create offspring who were outbred, the offspring of half-sibs, full-sibs, and of two generations of full-sib mating. He measured their germination success, which is plotted in Figure 11.3. Note how the fitness of individuals declines with increased inbreeding.

Purging the inbreeding load. Populations that regularly inbreed over sustained periods of time are expected to partially purge this load of deleterious alleles. This is because such populations have exposed many of these alleles in a homozygous state, and so selection can more readily remove these alleles from the population.

If the population has sustained inbreeding, such that individuals in the population have an inbreeding coefficient F , deleterious alleles at each locus will find a new equilibrium frequency. Assuming the mutation-selection model, now with inbreeding, the equilibrium frequency is

$$q_e = \frac{\mu}{(h(1-F) + F)s} \quad (11.9)$$

The frequency of the deleterious allele is decreased due to the allele now being expressed in homozygotes, and therefore exposed to selection, more often due to inbreeding. Thus, all else being equal, populations with a high degree of inbreeding will purge their load.

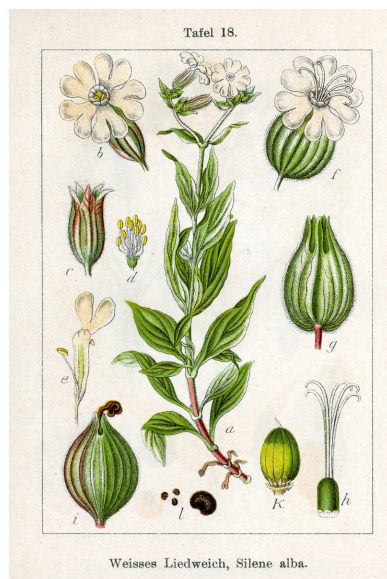


Figure 11.4: White campion (*S. latifolia*).
 Deutschlands Flora in Abbildungen (1796).
 Johann Georg Sturm (Painter: Jacob Sturm).
 Public Domain, wikipedia.

11.0.3 Migration-selection balance

Another reason for the persistence of deleterious alleles in a population is that there is a constant influx of maladaptive alleles from other populations where these alleles are locally adaptive. Migration-selection balance seems unlikely to be as broad an explanation for the persistence of deleterious alleles genome-wide as mutation-selection balance. However, a brief discussion of such alleles is worthwhile, as it helps to inform our ideas about local adaptation.

Local adaptation can occur over a range of geographic scales. Local adaptation is relatively unimpeded by migration at broad geographically scales, where selection pressures change more slowly than distances over which individuals typically migrate over a number of generations. Adaptation can, however, potentially occur on much finer geographic scales, from kilometers down to meters in some species. On such small scales, dispersal is surely rapidly moving alleles between environments, but local adaptation is maintained by the continued action of selection. An example of adaptation at fine-scales is shown in Figure 11.6 . JAIN and BRADSHAW (1966) studied the patterns of heavy-metal resistance in plants on mine tailings and in nearby meadows, a set of classic studies of population differences maintained by local adaptation to different soils. Even at these very short geograph-



Figure 11.5: Sweet vernal grass (*Anthoxanthum odoratum*).
Billeder af nordens flora (1917). Mentz, A & Ostenfeld, C H. Image from the Biodiversity Heritage Library. Contributed by New York Botanical Garden. Not in copyright.

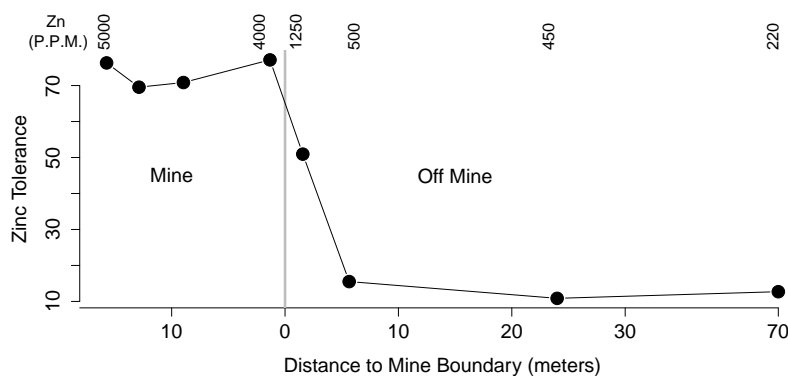


Figure 11.6: Data showing the Zinc tolerance of *Anthoxanthum odoratum* on and off of the Trelogan Mine, Flintshire, North Wales. The numbers along the top give the soil contamination of Zinc in parts per million. Data from JAIN and BRADSHAW (1966). Code here.

ically scales, over which seed and pollen will definitely move, we see strong local adaptation. Zinc-intolerant alleles are nearly absent from the mine tailings because they prevent plants from growing on these zinc-heavy soils; conversely, zinc-tolerant alleles do not spread into the meadow populations, likely due to some trade-off or fitness cost of zinc-tolerance.

As a first pass at developing a model of local adaptation, let's consider a haploid two-allele model with two different populations, see Figure 11.7, where the relative fitnesses of our alleles are as follows

allele	1	2
population 1	1	1-s
population 2	1-s	1

As a simple model of migration, let's suppose within a population a fraction of m individuals are migrants from the other population, and $1 - m$ individuals are from the same population.

To quickly sketch an equilibrium solution to this scenario, we'll take an approach analogous to our mutation-selection balance model. To do this, let's assume that selection is strong compared to migration ($s \gg m$), such that allele 1 will be almost fixed in population 1 and allele 2 will be almost fixed in population 2. If that is the case, migration changes the frequency of allele 2 in population 1 (q_1) by

$$\Delta_{Mig.} q_1 \approx m \quad (11.10)$$

while as noted above $\Delta_S q_1 = -sq_1$, so that migration and selection are at an equilibrium when $0 = \Delta_S q_1 + \Delta_{Mig.} q_1$, i.e. an equilibrium frequency of allele 2 in population 1 of

$$q_{e,1} = \frac{m}{s} \quad (11.11)$$

Here, migration is playing the role of mutation and so migration-selection balance (at least under strong selection) is analogous to mutation-selection balance.

We can use this same model by analogy for the case of migration-selection balance in a diploid model. For the diploid case, we replace our haploid s by the cost to heterozygotes hs from our directional selection model, resulting in a diploid migration-selection balance equilibrium frequency of

$$q_{e,1} = \frac{m}{hs} \quad (11.12)$$

As an example of fine-scale local adaptation due to a single locus, consider the case of the rock pocket mice adapting to lava flows. Throughout the deserts of the American Southwest there are old lava flows, where the rocks and soils are much dark than the surrounding desert.

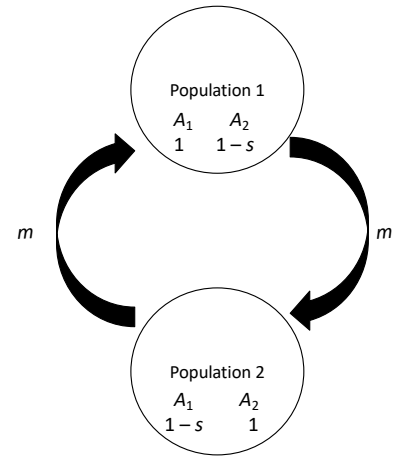


Figure 11.7: Setup of a two-population haploid model of local adaptation.

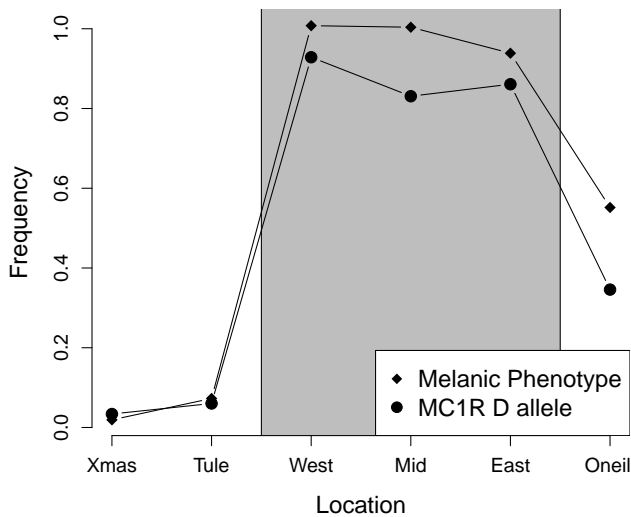


Figure 11.8: Frequency of melanic mice on the lava flow, and at nearby locations (diamonds). Frequency of MC1R melanic allele at same locations. Data from HOEKSTRA *et al.* (2004). Code here.

Many populations of small animals that live on these flows have evolved darker pigmentation to be cryptic against this dark substrate and better avoid visual predators. One example of such a locally adapted population are the rock pocket mice (*Chaetodipus intermedius*) who live on the Pinacate lava flow on the Arizona-Mexico border, studied by HOEKSTRA *et al.* (2004). These mice have much darker, more melanic pelts than the mice who live on nearby rocky outcrops (see Figure 11.8). NACHMAN *et al.* (2003) determined that a dominant allele (*D*) at MC1R is the primary determinant of this melanic phenotype. The frequency of this allele across study sites is shown in Figure 11.8. HOEKSTRA *et al.* (2004) found that other, unlinked markers showed little differentiation over these populations, suggesting that the migration rate is high.

Question 3. HOEKSTRA *et al.* (2004) found that the dark *D* allele was at 3% frequency at the Tule Mountains study site. Using F_{ST} -based approaches, for unlinked markers, they estimated that the per individual migration rate was $m = 7.0 \times 10^{-4}$ per generation between this site and the Pinacate lava flow. What is the selection coefficient acting against the dark *D* allele at the Tule Mountains site?

The width of a genetic cline. We can also extend these ideas beyond our discrete model to a model of a population spread out on a land-



Figure 11.9: Two species from the genus *Chaetodipus*, pocket mice, formerly known as *Perognathus*. Wild animals of North America, intimate studies of big and little creatures of the mammal kingdom (1918), Nelson, E. W. Image from the Biodiversity Heritage Library. Contributed by American Museum of Natural History Library. Not in copyright.

scape where individuals migrate in a more continuous fashion. For simplicity, let's assume a one dimensional habitat, where the habitat makes a sharp transition in the middle of our region. You could imagine this to be a set of populations sampled along a transect through some environmental transition. Our individuals disperse to live on average σ miles away from where they were born (we can think of this as our individuals migrating a random distance drawn from a normal distribution, with mean zero, and σ being the standard deviation of this distribution). . We'll think of a bi-allelic model where the homozygotes for allele 1 have an additive selective advantage s over allele 2 homozygotes to the east of our habitat transition (left of zero in Figure 11.10). This flips to allele 2 having the same advantage s west of the transition (right of zero). If you've read this send Prof Coop a picture of the East and West Beast.

"Upon an island hard to reach, the East Beast sits upon his beach. Upon the west beach sits the West Beast. Each beach beast thinks he's the best beast." – Theodor Seuss Geisel

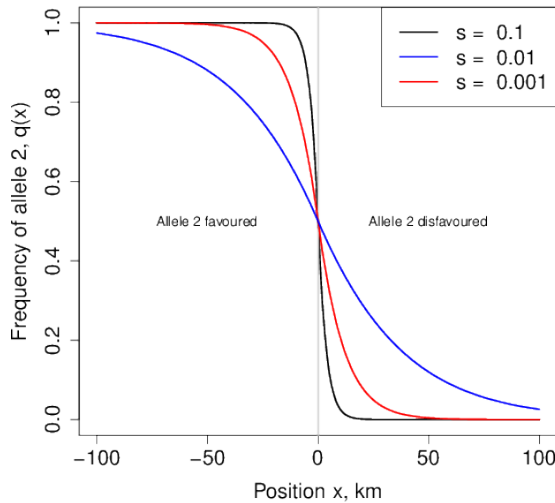


Figure 11.10: An equilibrium cline in allele frequency (the frequency of allele 2, $q(\cdot)$) is shown). Our individuals disperse an average distance of $\sigma = 1$ miles per generation, and our allele 2 has a relative fitness of $1 + s$ and $1 - s$ on either side of the environmental change at $x = 0$. Code here.

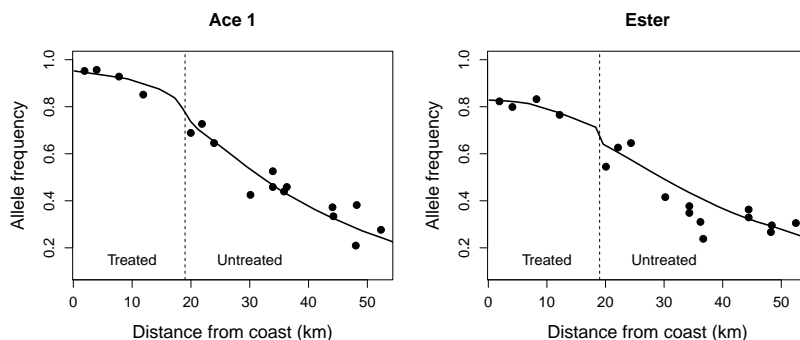
With this setup, we get an equilibrium distribution of our two alleles, where to the left of zero our allele 2 is at higher frequency, while to the right of zero allele 1 predominates. As we cross from the left to the right side of our range, the frequency of our allele 2 decreases in a smooth cline. The frequency of allele 2, $q(\cdot)$, is shown as a function of location along the cline for a variety of selection coefficients (s) in Figure 11.10. The width of this cline, i.e. the geographic distance over which the allele frequency changes, depends on the relative strengths of dispersal and selection. If selection is strong compared to dispersal, then selection acts to remove maladaptive alleles much faster than migration acts to move alleles across the environmental transition. Thus the allele frequency transition would be very rapid, and the cline

narrow, as we move across the environmental transition. In contrast, if individuals disperse long distances and selection is weak, many alleles are being moved back and forth over the environmental transition much faster than selection can act against these alleles and so the cline would be very wide.

The width of our cline, i.e. the distance over which we make this shift from allele 2 to allele 1 predominating, can be defined in a number of different ways. One way to define the cline width, which is simple to define but perhaps hard to measure accurately, is via the slope (i.e. the tangent) of $q(x)$ at $x = 0$. See Figure 11.11. Under this definition, the cline width is approximately

$$0.6\sigma/\sqrt{s} \text{ miles}, \quad (11.13)$$

note that the units are miles here just because we defined the average dispersal distance (σ) in miles above. Thus the cline will be wider if individuals disperse further, higher σ , and if selection is weaker, smaller s . The appendix below talks through the math underlying these ideas in more detail.



LENORMAND *et al.* (1999) collected mosquitoes (*Culex pipiens*) in a north-south transect moving away from the Southern French coast. Areas near the coast were treated with pesticides, and the mosquitos have evolved resistance, but areas just a few tens of kilometers from the coast were untreated. LENORMAND *et al.* estimated the frequency of two unlinked, pesticide-resistance alleles, and found them at high frequency near the coast but found that their frequencies declined rapidly moving inland. LENORMAND *et al.* fit migration-selection cline models to their data, similar to those in Figure 11.10, with the pesticide-resistance alleles having an selection advantage (s) in treated areas an a cost (c) in untreated areas (they didn't enforce the selective advantage and cost being symmetric).

They estimated that a higher selective advantage for the Ace 1 allele than Ester allele ($s = 0.33$ and $s = 0.19$ respectively) and a

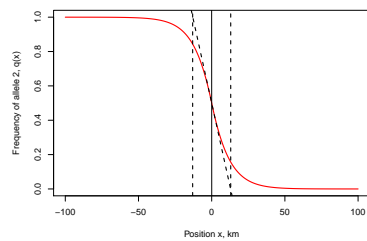


Figure 11.11: An equilibrium cline in allele frequency from Figure 11.10, $s = 0.01$. Vertical lines show the cline width. The diagonal line show the tangent to the cline at its midpoint. Code here.

Figure 11.12: Allele frequency clines of two pesticide resistance alleles, at the Ace 1 and Ester genes, in the mosquito *Culex pipiens*. The dotted line shows where we move from pesticide-treated to untreated areas as we move away from the French coast. The dots show observed allele frequencies, the solid lines clines fit under a migration-selection balance model of a cline. These allele frequencies represent collections over two summers, the frequencies of the alleles are substantially reduced in the winter due to the reduced use of pesticides. Data from LENORMAND *et al.* (1999). Code here.

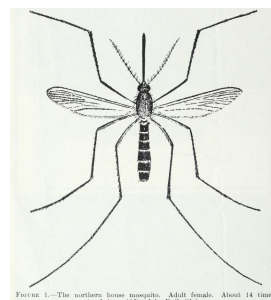


Figure 11.13: mosquito (*Culex pipiens*). Domestic mosquitoes (1939). Bishopp, F. C. Image from the Biodiversity Heritage Library. Contributed by U.S. Department of Agriculture, National Agricultural Library. Not in copyright.

higher cost to the Ace 1 allele than Ester allele in untreated areas ($c = 0.11$ and $c = 0.7$ respectively) potentially explaining the less extreme cline for Ester allele than the Ace 1 allele. Despite these strong selection pressures we still see a cline over tens of kilometers because dispersal is relatively high ($\sigma = 6.6\text{km per generation}$).

Hybrid zones Local adaptation isn't the only way that selection can generate strong spatial patterns. We can also see strong selection-driven clines when partially-reproductively isolated species spread back in to secondary contact they can hybridize bringing alleles together that may not work well with each other. One simple model of is to think about an under-dominant polymorphism, i.e. where the heterozygote has lower fitness. The two ancestral populations are alternatively fixed for the two fitter homozygote states, e.g. ancestral population 1 fixed A_1A_1 and ancestral population two the A_2A_2 . The hybrid population forming at the mating edge between the two ancestral populations has a high frequency of the less fit heterozygotes. Thus hybrids are at a disadvantage, potentially acting to keep the two populations from collapsing into each other.

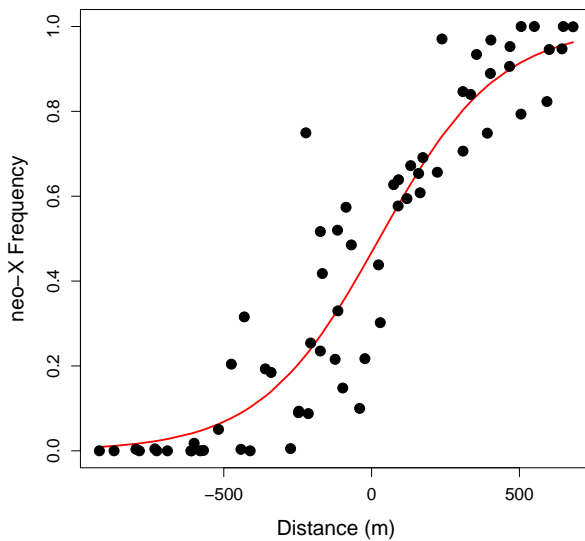
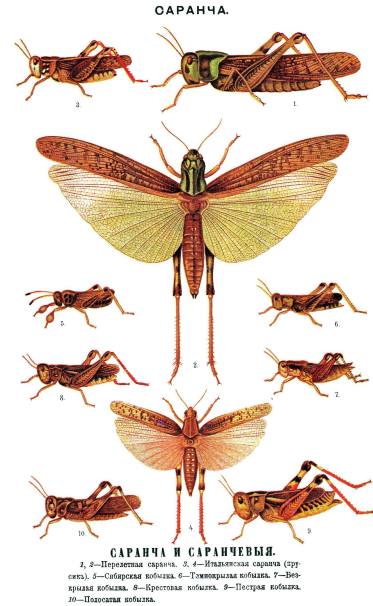


Figure 11.14: The frequency of the southern neo-X chromosome moving along a valley transect (more southern locations to the right of the graph). This represents data from four different valleys in the French Alps over less than a kilometer, each point represents a sample of 20 males. The red curve is the fitted cline under a model of heterozygote disadvantage (BAZIKIN, 1969). Data from BARTON and HEWITT (1981), Code here.



Two previously isolated populations of the short-horned grasshopper *Podisma pedestris* have spread into secondary contact in the French Alps, probably after the last ice age. The population that has spread into the Alps from the south has a large section of novel X chromosome, due to a chromosomal fusion. This 'neo-X' is absent in the populations that spread from the North into the Alps. The two

Figure 11.15: 7. *Podisma pedestris*, a species of short-horned grasshoppers; from a page illustrating *Orthoptera*. Illustration from Brockhaus and Efron Encyclopedic Dictionary (1890) Image wikipedia, public domain.

populations meet in many valleys running through the Alps, and repeat form a narrow hybrid zone, with the frequency of the neo-X chromosome forming a very steep cline transitioning in frequency over a few hundred meters (BARTON and HEWITT, 1981). One potential reason for this steep cline is that females who are heterozygous for the neo-X (neo-X/old-X) may have reduced fitness, consistent with an underdominant polymorphism. The neo-X allele cannot spread into the northern population as it cannot increase in frequency when rare. Conversely the northern population cannot displace the neo-X, as the old-X is at a disadvantage. This spatial distribution at this locus is a tension zone between the two populations, where neither population can make ground on the other due to the low fitness of the hybrid.

We can use our same continuous model of migration and selection to study this setup. Assuming that the homozygotes are equally fit, and that the heterozygotes relative fitness is reduced by a selection coefficient s_h , the width of the cline is

$$\frac{\sigma}{\sqrt{s_h}} \quad (11.14)$$

The stronger the selection the more abrupt the transition between the populations. These wingless grasshoppers move $\sigma \sim 20$ meters a generation. Thus a reduction in the relative fitness of the hybrid would be needed to explain this hybrid zone with a width of ~ 800 m.

More generally we can see tension zones arise when hybrids have reduced fitness compared to either species. For example, this can occur due to be due to bad epistatic interactions between alleles from each species. If selection is strong enough on hybrids, often because many loci are involved in incompatibilities between the species, the entire genome can be tied up in a tension zone between the two species.

Appendix: Some theory of the spatial distribution of allele frequencies under deterministic models of selection

Imagine a continuous haploid population spread out along a line. Each individual disperses a random distance Δx from its birthplace to the location where it reproduces, where Δx is drawn from the probability density $g(\cdot)$. To make life simple, we will assume that $g(\Delta x)$ is normally distributed with mean zero and standard deviation σ , i.e. migration is unbiased and individuals migrate an average distance of σ .

The frequency of allele 2 at time t in the population at spatial location x is $q(x, t)$. Assuming that only dispersal occurs, how does our allele frequency change in the next generation? Our allele frequency in the next generation at location x reflects the migration from different locations in the proceeding generation. Our population at location x

receives a contribution $g(\Delta x)q(x + \Delta x, t)$ of allele 2 from the population at location $x + \Delta x$, such that the frequency of our allele at x in the next generation is

$$q(x, t + 1) = \int_{-\infty}^{\infty} g(\Delta x)q(x + \Delta x, t)d\Delta x. \quad (11.15)$$

To obtain $q(x + \Delta x, t)$, let's take a Taylor series expansion of $q(x, t)$:

$$q(x + \Delta x, t) = q(x, t) + \Delta x \frac{dq(x, t)}{dx} + \frac{1}{2}(\Delta x)^2 \frac{d^2q(x, t)}{dx^2} + \dots \quad (11.16)$$

then

$$q(x, t+1) = q(x, t) + \left(\int_{-\infty}^{\infty} \Delta x g(\Delta x) d\Delta x \right) \frac{dq(x, t)}{dx} + \frac{1}{2} \left(\int_{-\infty}^{\infty} (\Delta x)^2 g(\Delta x) d\Delta x \right) \frac{d^2q(x, t)}{dx^2} + \dots \quad (11.17)$$

Because $g(\)$ has a mean of zero, $\int_{-\infty}^{\infty} \Delta x g(\Delta x) d\Delta x = 0$, and has because $g(\)$ has variance σ^2 , $\int_{-\infty}^{\infty} (\Delta x)^2 g(\Delta x) d\Delta x = \sigma^2$. All higher order terms in our Taylor series expansion cancel out (as all high moments of the normal distribution are zero). Looking at the change in allele frequency, $\Delta q(x, t) = q(x, t + 1) - q(x, t)$, so

$$\Delta q(x, t) = \frac{\sigma^2}{2} \frac{d^2q(x, t)}{dx^2} \quad (11.18)$$

This is a diffusion equation, so that migration is acting to smooth out allele frequency differences with a diffusion constant of $\frac{\sigma^2}{2}$. This is exactly analogous to the equation describing how a gas diffuses out to equal density, as both particles in a gas and our individuals of type 2 are performing Brownian motion (blurring our eyes and seeing time as continuous).

We will now introduce fitness differences into our model and set the relative fitnesses of allele 1 and 2 at location x to be 1 and $1 + s\gamma(x)$. To make progress in this model, we'll have to assume that selection isn't too strong, i.e. $s\gamma(x) \ll 1$ for all x . The change in frequency of allele 2 obtained within a generation due to selection is

$$q'(x, t) - q(x, t) \approx s\gamma(x)q(x, t)(1 - q(x, t)) \quad (11.19)$$

i.e. logistic growth of our favoured allele at location x . Putting our selection and migration terms together, we find the total change in allele frequency at location x in one generation is

$$q(x, t + 1) - q(x, t) = s\gamma(x)q(x, t)(1 - q(x, t)) + \frac{\sigma^2}{2} \frac{d^2q(x, t)}{dx^2} \quad (11.20)$$

In deriving this result, we have essentially assumed that migration acted upon our original allele frequencies before selection, and in doing so have ignored terms of the order of σs .

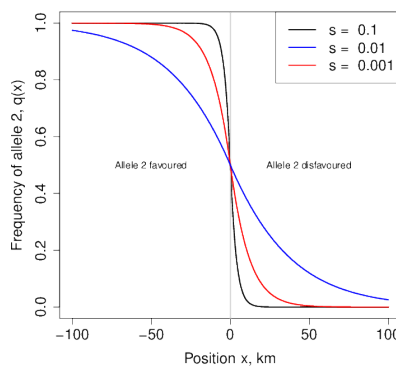


Figure 11.16: An equilibrium cline in allele frequency. Our individuals disperse an average distance of $\sigma = 1\text{km}$ per generation, and our allele 2 has a relative fitness of $1 + s$ and $1 - s$ on either side of the environmental change at $x = 0$.

The cline in allele frequency associated with a sharp environmental transition. To make progress, let's consider a simple model of local adaptation where the environment abruptly changes. Specifically, we assume that $\gamma(x) = 1$ for $x < 0$ and $\gamma(x) = -1$ for $x \geq 0$, i.e. our allele 2 has a selective advantage at locations to the left of zero, while this allele is at a disadvantage to the right of zero. In this case we can get an equilibrium distribution of our two alleles, where to the left of zero our allele 2 is at higher frequency, while to the right of zero allele 1 predominates. As we cross from the left to the right side of our range, the frequency of our allele 2 decreases in a smooth cline.

Our equilibrium spatial distribution of allele frequencies can be found by setting the left-hand side of eqn. (11.20) to zero to arrive at

$$s\gamma(x)q(x)(1-q(x)) = -\frac{\sigma^2}{2} \frac{d^2q(x)}{dx^2} \quad (11.21)$$

We then could solve this differential equation with appropriate boundary conditions ($q(-\infty) = 1$ and $q(\infty) = 0$) to arrive at the appropriate functional form for our cline. While we won't go into the solution of this equation here, we can note that by dividing our distance x by $\ell = \sigma/\sqrt{s}$, we can remove the effect of our parameters from the above equation. This compound parameter ℓ is the characteristic length of our cline, and it is this parameter which determines over what geographic scale we change from allele 2 predominating to allele 1 predominating as we move across our environmental shift.

12

The Impact of Genetic Drift on Selected Alleles

“Natural selection is a mechanism for generating an exceedingly high degree of improbability.” –R.A. Fisher

In the previous chapter we assumed that the selection acting on our alleles was strong enough that we could ignore the action of genetic drift in shaping allele frequencies. However, genetic drift affects all alleles, and so in this chapter we explore the interaction of selection and drift. Strongly selected alleles can be lost from the population via drift when they are rare in the population, while both weakly beneficial and weakly deleterious alleles are subject to the random whims of genetic drift throughout their entire time in the population. Understanding the interaction of selection and genetic drift is key to understanding the extent to which small populations may be mutation-limited in their rates of adaptation, and how rates of molecular and genome evolution may differ across taxa.

12.1 Stochastic loss of strongly selected alleles

Even strongly beneficial alleles can be lost from the population when they are sufficiently rare. This is because the number of offspring left by individuals to the next generation is fundamentally stochastic. A selection coefficient of $s=1\%$ is a strong selection coefficient, which can drive an allele through the population in a few hundred generations once the allele is established. However, if individuals have on average a small number of offspring per generation, the first individual to carry our beneficial allele, who has on average 1% more children than their peers, could easily have zero offspring, leading to the loss of our allele before it ever gets a chance to spread.

To take a first stab at this problem, let’s think of a very large haploid population in which a single individual starts with the selected allele, and ask about the probability of eventual loss of our selected allele starting from this single copy. To derive this probability of loss (p_L), we’ll make use of a simple argument (derived from branching

processes FISHER, 1923; HALDANE, 1927). Our selected allele will be eventually lost from the population if every individual with the allele fails to leave descendants. Well we can think about different cases:

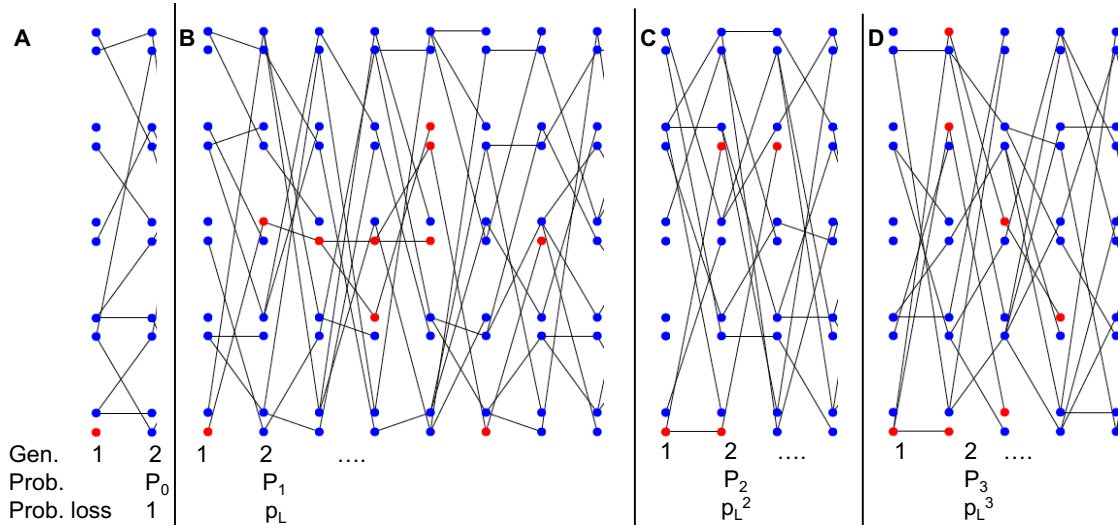


Figure 12.1: Four different outcomes of a selected allele present as a single copy in the population, leaving zero, one, two, three offspring in the next generation.

1. In our first generation, with probability P_0 our individual allele leaves no copies of itself to the next generation, in which case our allele is lost (Figure 12.1A).
2. Alternatively, our allele could leave one copy of itself to the next generation (with probability P_1), in which case with probability p_L this copy eventually goes extinct (Figure 12.1B).
3. Our allele could leave two copies of itself to the next generation (with probability P_2), in which case with probability p_L^2 both of these copies eventually go extinct (Figure 12.1C).
4. More generally, our allele could leave k copies ($k > 0$) of itself to the next generation (with probability P_k), in which case with probability p_L^k all of these copies eventually go extinct (e.g. Figure 12.1D).

Summing over these probabilities, we see that

$$p_L = \sum_{k=0}^{\infty} P_k p_L^k \quad (12.1)$$

We'll now need to specify P_k , the probability that an individual carrying our selected allele has k offspring. In order for this population to stay constant in size, we'll assume that individuals without the selected mutation have on average one offspring per generation, while

individuals with our selected allele have on average $1 + s$ offspring per generation. We'll assume that the number of offspring an individual has is Poisson distributed with mean given by 1 or $1 + s$, i.e. the probability that an individual with the selected allele has i children is

$$P_i = \frac{(1+s)^i e^{-(1+s)}}{i!} \quad (12.2)$$

Substituting P_k into the equation above, we see

$$\begin{aligned} p_L &= \sum_{k=0}^{\infty} \frac{(1+s)^k e^{-(1+s)}}{k!} p_L^k \\ &= e^{-(1+s)} \left(\sum_{k=0}^{\infty} \frac{(p_L(1+s))^k}{k!} \right) \end{aligned} \quad (12.3)$$

The term in the brackets is itself an exponential expansion, so we can rewrite this equation as

$$p_L = e^{(1+s)(p_L - 1)} \quad (12.4)$$

Solving for p_L would give us our probability of loss for any selection coefficient. Let's rewrite our result in terms of the probability of escaping loss, $p_F = 1 - p_L$. We can rewrite eqn. (12.4) as

$$1 - p_F = e^{-p_F(1+s)} \quad (12.5)$$

To gain an approximate solution for this result, let's consider a small selection coefficient $s \ll 1$ such that $p_F \ll 1$ and then use a Taylor series to expand out the exponential on the right hand side (ignoring terms of higher order than s^2 and p_F^2):

$$1 - p_F \approx 1 - p_F(1 + s) + p_F^2(1 + s)^2/2 \quad (12.6)$$

Solving this we find that

$$p_F = 2s. \quad (12.7)$$

Thus even an allele with a 1% selection coefficient has a 98% probability of being lost when it is first introduced into the population by mutation.

If the mutation rate towards our advantageous allele is μ , and there are N individuals in our haploid population, then $N\mu$ advantageous mutations arise per generation. Each of these new beneficial mutations has a probability p_F of fixing. Thus the number of advantageous mutations arising per generation that will eventually fix in the population is $N\mu p_F$, and the waiting time for a mutation that will fix to arise is the reciprocal of this: $1/N\mu p_F$. Thus, in adapting to a novel selection pressure via new mutations, the population size, the mutational target size, and the selective advantage of new mutations all matter. One

reason why combinations of drugs are used against viruses like HIV and malaria is that, even if the viruses adapt to one of the drugs, the viral load (N) of the patient is greatly reduced, making it very unlikely that the population will manage to fix a second drug-resistant allele.

Diploid model of stochastic loss of strongly selected alleles. We can also adapt this result to a diploid setting. Assuming that heterozygotes for the 1 allele have on average $1 + hs$ children, the probability allele 1 is not lost, starting from a single copy in the population, is

$$p_F = 2hs \quad (12.8)$$

for $h > 0$. Note this is a slightly different parameterization from our diploid model in the previous chapter; here h is the dominance of our positively selected allele, with $h = 1$ corresponding to the full selective advantage expressed in an individual with only a single copy. Thus the probability that a beneficial allele is not lost depends just on the relative fitness advantage of the heterozygote; this is because when the allele is rare it is usually present in heterozygotes and so its probability of escaping loss just depends on the fitness of these individuals compared to homozygotes for the ancestral allele (assuming an outbred population).

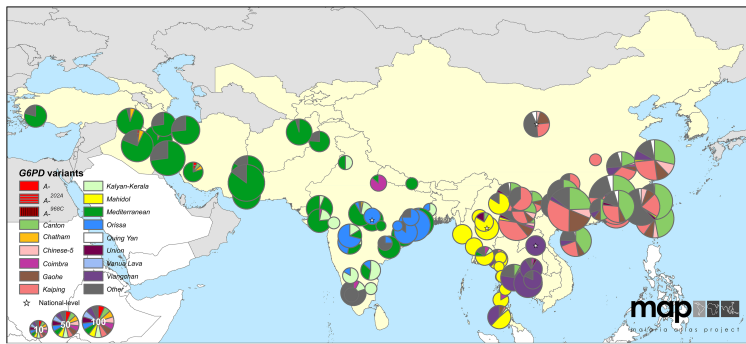


Figure 12.2: Map of G6PD-deficiency allele frequencies across Asia. The pie chart shows the frequency of G6PD-deficiency alleles. The size of the pie chart indicates the number of G6PD-deficient individuals sampled. Countries with endemic malaria are colored yellow. Figure from HOWES *et al.* (2013), licensed under CC BY 4.0.

Over roughly the past ten thousand years, adaptive alleles conferring resistance to malaria have arisen in a number of genes and spread through human populations in areas where malaria is endemic (KWIATKOWSKI, 2005). One particularly impressive case of convergent evolution in response to selection pressures imposed by malaria are the numerous changes throughout the G6PD gene, which include at least 15 common variants in Central and Eastern Asia alone that lower the activity of the enzyme (HOWES *et al.*, 2013). These alleles are now found at a combined frequency of around 8% frequency in malaria endemic areas, rarely exceeding 20% (HOWES

et al., 2012). Whether these variants *all* confer resistance to malaria is unknown, but a number of these alleles have demonstrated effects against malaria and are thought to have a selective advantage to heterozygotes $sh > 5\%$ where malaria is endemic (RUWENDE *et al.*, 1995; TISHKOFF *et al.*, 2001; LOUICHAROEN *et al.*, 2009).

With a 5% advantage in heterozygotes, a G6PD allele present as a single copy would only have a 10% probability of fixing in the population. If that's so, how come malaria adaptation has repeatedly occurred via changes at G6PD? Well, maybe adaptation didn't start from a single copy of the selected allele. How many copies of the G6PD-deficiency alleles do we expect were segregating in the population before selection pressures changed?

In the absence of malaria, these G6PD alleles are deleterious with carriers suffering from G6PD deficiency, leading to hemolytic anemia when individuals are exposed to a variety of different compounds, notably those present in fava beans. There's upward of one hundred bases where G6PD-deficiency alleles can arise, so assuming a mutation rate of $\approx 10^{-8}$ per base pair per generation, we can roughly estimate the rate of mutations arising that affect the G6PD gene as $\mu \approx 10^{-6}$ per generation. In the absence of malaria, the selective cost of being a heterozygote carrier of a G6PD-deficient allele must have been on the order of 5% or more, and thus the frequency of the allele under mutation-selection balance would have been $\approx 10^{-6}/0.05 = 2 \times 10^{-5}$.

Assuming an effective population size of 2 – 20 million individuals, roughly five to ten thousand years ago that means that there would have been forty to four hundred copies of the G6PD-deficiency allele present in the population when selection pressures shifted at the introduction of malaria. The chance that one of these newly adaptive alleles is lost is 90% but the chance that they're all lost is $< (0.9)^{40} \approx 0.02$, i.e. there would have been a greater than 98% chance that adaptation would occur via one or more alleles at G6PD. How many alleles would escape drift? Well with 40 – 400 copies of the allele pre-malaria, and each of them having a 10% probability of escaping drift, we expect between 4 and 40 G6PD alleles to escape drift and contribute to adaptation. We see 15 common G6PD alleles in Eurasia, so our simple model of adaptation from mutation-selection balance seems reasonable.

Question 1. ‘Haldane’s sieve’ is the name for the idea that the mutations that contribute to adaptation are likely to be dominant or at least co-dominant.

A) Briefly explain this argument with a verbal model relating to the results we've developed in the last two chapters.

B) Haldane’s sieve is thought to be less important for adaptation from previously deleterious standing variation, than adaptation from



Figure 12.3: Pythagoras’s “just say no to fava beans” campaign. Pythagoras prohibited the consumption of fava beans by his followers; perhaps because favism, the anemia induced in G6PD-deficient individuals by fava beans, is relatively common in the Mediterranean due to adaptation to endemic malaria. French early 16th Century. Woodner Collection, National Gallery of Art. Public Domain, wikimedia.

A full analysis of this case requires modeling of G6PD’s X chromosome inheritance, and the randomness in the number of copies of the allele present at mutation-selection balance (RALPH and COOP, 2015).



Figure 12.4: Haldane’s sieve. To our knowledge Haldane never wore a sieve, but we assume he owned one. Sieve, Flickr licensed under CC BY 2.0. Haldane, Public Domain, wikimedia.

new mutation. Can you explain the intuition behind of this idea?

C) Haldane's sieve is likely to be less important in inbred, e.g. selfing, populations. Why is this?

Question 2. Melanic squirrels suffer a higher rate of predation (due to hawks) than normally pigmented squirrels. Melanism is due to a dominant, autosomal mutation. The frequency of melanic squirrels at birth is 4×10^{-5} .

A) If the mutation rate to new melanic alleles is 10^{-6} , assuming the melanic allele is at mutation-selection equilibrium, what is the reduction in fitness of the heterozygote?

Suddenly levels of pollution increase dramatically in our population, and predation by hawks now offers an equal (and opposite) advantage to the dark individuals as it once offered to the normally pigmented individuals.

B) What is the probability that a single copy of this allele (present just once in the population) is lost?

C) If the population size of our squirrels is a million individuals, and is at mutation-selection balance, what is the probability that the population adapts from one or more allele(s) from the standing pool of melanic alleles?

12.2 The interaction between genetic drift and weak selection.

For strongly selected alleles, once the allele has escaped initial loss at low frequencies, its path will be determined deterministically by its selection coefficients. However, if selection is weak compared to genetic drift, the stochasticity of reproduction can play a role in the trajectory an allele takes even when it is common in the population. If selection is sufficiently weak compared to genetic drift, then genetic drift will dominate the dynamics of alleles and they will behave like they're effectively neutral. Thus, the extent to which selection can shape patterns of molecular evolution will depend on the relative strengths of selection and genetic drift. But how weak must selection on an allele be for drift to overpower selection? And do these interactions between selection and drift have longterm consequences for genome-wide patterns evolution?

To model selection and drift each generation, we can first calculate the deterministic change in our allele frequency due to selection using our deterministic formula. Then, using our newly calculated expected allele frequency, we can binomially sample two alleles for each of our offspring to construct the next generation. This approach to jointly modeling genetic drift and selection is called the Wright-Fisher model.

Under the Wright-Fisher model, we will calculate the expected



Figure 12.5: cress bug (*Asellus aquaticus*) in the isopod family *Asellidae*. Brehms Tierleben. Allgemeine kunde des Tierreichs (1911). Brehm A.E. Image from the Biodiversity Heritage Library. Contributed by Smithsonian Libraries. Not in copyright.

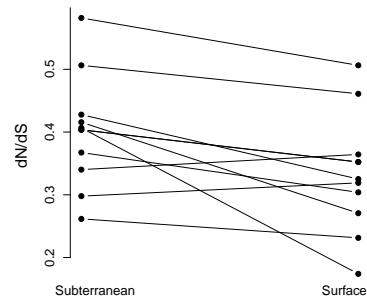


Figure 12.6: Asellid isopods have repeatedly invaded subterranean, ground-water habitats from surface-water habitats, and leading to a genome-wide increase in d_N/d_S and larger genomes (Data from LEFÉBURE *et al.*, 2017, comparing independent isopod species pairs). One possible explanation of this is that the longterm effective population sizes of the subterranean species are lower and so these species are less able to prevent mildly deleterious alleles fixing, and also less able to prevent genome expansion from the accumulation of weakly deleterious, extraneous genomic DNA. Code here.

change in allele frequency due to selection and the variance around this expectation due to drift. To make our calculations simpler, let's assume an additive model, i.e. $h = 1/2$, and that $s \ll 1$ so that $\bar{w} \approx 1$. Using our directional selection deterministic model, from Chapter 10, and these approximations gives us our deterministic change due to selection

$$\Delta_{sp} = \mathbb{E}(\Delta p) = \frac{s}{2}p(1-p) \quad (12.9)$$

To obtain our new frequency in the next generation, p_1 , we binomially sample from our new deterministic frequency $p' = p + \Delta_{sp}$, so the variance in our allele frequency change from one generation to the next is given by

$$Var(\Delta p) = Var(p_1 - p) = Var(p_1) = \frac{p'(1-p')}{2N} \approx \frac{p(1-p)}{2N}. \quad (12.10)$$

where the previous allele frequency p drops out because it is a constant and the variance in our new allele frequency follows from the fact that we are binomially sampling $2N$ new alleles from a frequency p' to form the next generation.

To get our first look at the relative effects of selection vs. drift we can simply look at when our change in allele frequency caused by selection within a generation is reasonably faithfully passed down through the generations. In particular, if our expected change in allele frequency is much greater than the variance around this change, genetic drift will play little role in the fate of our selected allele (once the allele is not at low copy number within the population). When does selection dominant genetic drift? This will happen if $\mathbb{E}(\Delta p) \gg Var(\Delta p)$, i.e. when $|Ns| \gg 1$. Conversely, any hope of our selected allele following its deterministic path will be quickly undone if our change in allele frequencies due to selection is much less than the variance induced by drift. So if the absolute value of our population-size-scaled selection coefficient $|Ns| \ll 1$, then drift will dominate the fate of our allele.

To make further progress on understanding the fate of alleles with selection coefficients of the order $1/N$ requires more careful modeling. However, under our diploid model, with an additive selection coefficient s , we can obtain the probability that allele 1 fixes within the population, starting from a frequency p :

$$p_F(p) = \frac{1 - e^{-2Ns}}{1 - e^{-2Ns}} \quad (12.11)$$

The proof of this result is sketched out below (see Section 12.2.1). A new allele that arrives in the population at frequency $p = 1/(2N)$ has a probability of reaching fixation of

$$p_F\left(\frac{1}{2N}\right) = \frac{1 - e^{-s}}{1 - e^{-2Ns}} \quad (12.12)$$

To see this denote our new count of allele 1 by i , then

$$\begin{aligned} Var(p_1 - p) &= Var\left(\frac{i}{2N} - p\right) = Var\left(\frac{i}{2N}\right) \\ &= \frac{Var(i)}{(2N)^2} \end{aligned}$$

and from binomial sampling $Var(i) = 2Np'(1-p')$ and so we arrive at our answer. Assuming that $s \ll 1$, $p' \approx p$, then in practice we can use

$$Var(\Delta p) = Var(p' - p) \approx p(1-p)/2N.$$

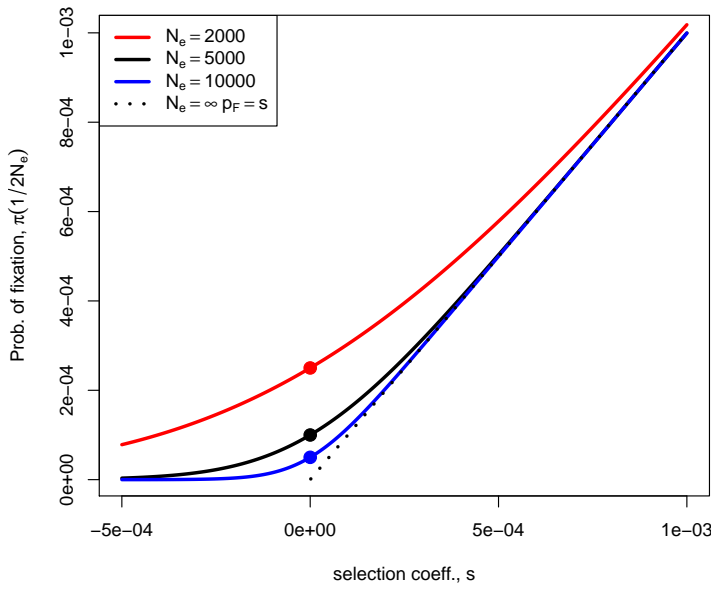


Figure 12.7: The probability of the fixation of a new mutation with selection coefficient s ($h = 1/2$) in a diploid population of effective size N_e . The dashed line gives the infinite population solution. The dots give the solution for $s \rightarrow 0$, i.e. the neutral case, where the probability of fixation is $1/(2N_e)$. Code here.

If $s \ll 1$ but $Ns \gg 1$ then $p_F(\frac{1}{2N}) \approx s$, which nicely gives us back the result that we obtained above for an allele under strong selection (eqn. (12.8)). Our probability of fixation (eqn. (12.12)) is plotted as a function of s and N in Figure 12.7. To recover our neutral result, we can take the limit $s \rightarrow 0$ to obtain our neutral fixation probability, $1/(2N)$.

In the case where Ns is close to 1, then

$$p_F\left(\frac{1}{2N}\right) \approx \frac{s}{1 - e^{-2Ns}} \quad (12.13)$$

This is greater than our earlier result $p_F = s$ from the branching process argument (using our additive model of $h = 1/2$), increasingly so for smaller N . Why is this? The reason why is that p_F is really the probability of "never being lost" in an infinitely large population. So to persist indefinitely, the allele has to escape loss permanently, by never being absorbed by the zero state. When the population size is finite, to fix we only need to reach a size $2N$ individuals. Weakly beneficial mutations ($Ns \sim 1$) are slightly more likely to fix than the s probability, as they only have to reach $2N$ to never be lost.

If, for selection to operate on an allele, we need the selection coefficient to satisfy $|Ns| \gg 1$, then that holds if $|s| \gg 1/N$. Well, effective population sizes are often reasonably large, on the order of hundreds of thousands or millions of individuals, thus selection coefficients on the order of 10^{-5} to 10^{-6} can be effectively selected upon, i.e. se-

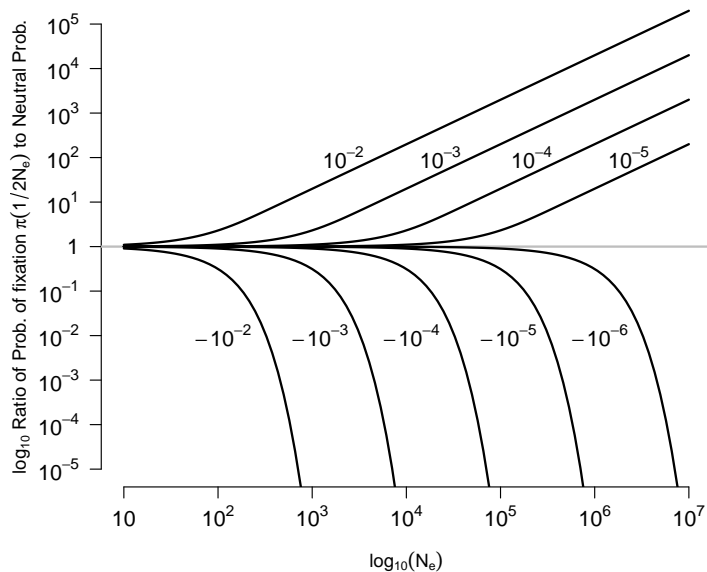


Figure 12.8: The probability of the fixation of a new mutation with selection coefficient s relative to the neutral fixation probability ($1/2N_e$) as a function of the effective size N_e . The selection coefficient is shown next to the line. Note how quickly the probabilities move away from the neutral expectation as $N_e s$ moves passed 1. [Code here.](#)

lection equivalent to individuals have incredibly slight advantages in terms of the number of offspring they leave to the next generation (see Figure 12.8). While we are incapable of detecting measuring all but the large fitness effect sizes, except in some elegant experiments (e.g. in microbes), such small effects are visible to selection in large populations. Thus, if consistent selection pressures are exerted over long time periods, natural selection can potentially finely tune various aspects of an organism.

As one example of this fine-tuning, consider how carefully crafted and optimized the sequence of codons is for translation. Due to the degeneracy of the protein code, multiple codons code for the same amino-acid. For example, there are six different codons that can code leucine. While these synonymous codons are equivalent at the protein level, cells do differ in the number of tRNA molecules that bind these codons and so the efficacy and accuracy with which proteins can be formed through translation and folding. These slight differences in translation rates likely often correspond to tiny differences in fitness, but do they matter?

In many organisms there is a strong bias in the codons to encode particular amino-acids, see Figure 12.9, with the most abundant codon matching the most abundant tRNA in cells. This 'codon bias' likely reflects the combined action of weak selection and mutational pressure, pushing the codon composition of the genome and tRNA abundances

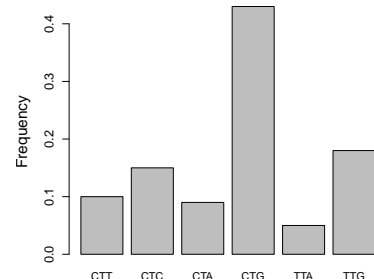


Figure 12.9: Data from *Drosophila melanogaster* on the frequency of different codons for Leucine. Data from Genscript. [Code here.](#)

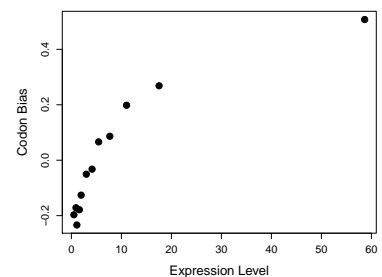


Figure 12.10: A measure of unequal codon frequencies (F) plotted in bins of gene expression (E) for genes across the *Drosophila melanogaster* genome. Data from HEY and KLIMAN (2002). [Code here.](#)

towards an adaptive compromise. These selection pressures have acted over long time periods, as codon usage patterns are often very similar for species that diverged over many tens of millions of years ago. Compared to other genes, highly expressed genes show a strong bias towards using codons matching abundant tRNAs, consistent with the idea that the synonymous codon content of highly expressed genes is evolving to optimize their translation (see Figure 12.10 for an early example). These patterns likely represent the action of selection pressures that are incredibly weak on average, but that have played out over vast time-periods.

The fixation of slightly deleterious alleles. From Figure 12.7 we can see that weakly deleterious alleles can also fix, especially in small populations. To understand how likely it is that deleterious alleles by chance reach fixation by genetic drift, let's assume a diploid model with additive selection (with a selection coefficient of $-s$ against our allele 2).

If $Ns \gg 1$ then our deleterious allele (allele 2) cannot possibly reach fixation. However, if Ns is not large, then the probability of fixation

$$p_F \left(\frac{1}{2N} \right) \approx \frac{s}{e^{2Ns} - 1} \quad (12.14)$$

for our single-copy deleterious allele. So deleterious alleles can fix within populations (albeit at a low rate) if Ns is not too large. As above, this is because while deleterious mutations will never escape loss in infinite populations, they can become fixed in finite population by reaching $2N$ copies.

Question 3. An additive mutation arises that lowers the relative fitness of heterozygotes by 10^{-5} . What is the probability that this mutation fixes in a diploid population with effective size of 10^4 ? What is the probability it fixes in a population of effective size 10^6 ? By comparing both to their neutral probability describe the intuition behind this result.

OHTA proposed the ‘nearly-neutral’ theory of molecular evolution in a series of papers¹. She suggested that a reasonable fraction of newly arising functional mutations may have very weak selection coefficients, such that species with smaller effective population sizes may have higher rates of fixation of these very weakly deleterious alleles. In effect, her suggestion is that the constraint parameter C of a functional region is not a fixed property, but rather depends on the ability of the population to resist the influx of very weakly deleterious mutations.

¹ OHTA, T., 1972 Population size and rate of evolution. *Journal of Molecular Evolution* 1(4): 305–314; OHTA, T., 1973 Slightly deleterious mutant substitutions in evolution. *Nature* 246(5428): 96; and OHTA, T., 1987 Very slightly deleterious mutations and the molecular clock. *Journal of Molecular Evolution* 26(1–2): 1–6

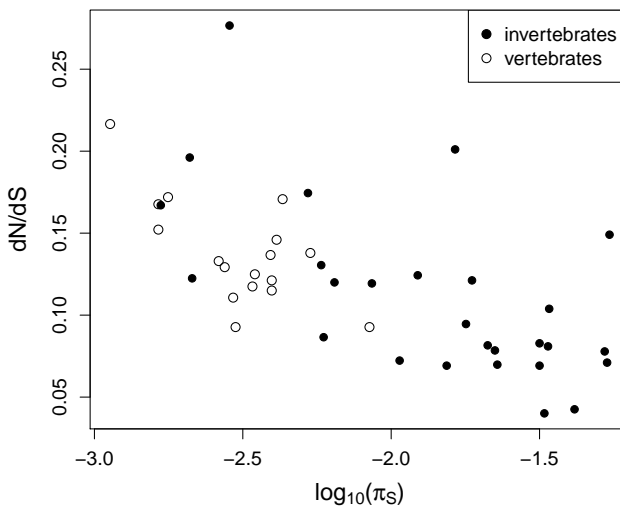


Figure 12.11: Data from 44 metazoan species from Cuttlefish to Sifakas. Each dot represents the average of over many genes plotting d_N/d_S against synonymous diversity (π_S). Data from GALTIER (2016). Code here.

Across species, genome-wide averages of d_N/d_S do seem to be correlated with measures of the effective population size (such as synonymous diversity), see Figure 12.11. This evidence supports the idea that in species with smaller effective population sizes (lower π_S), proteins may be subject to lower degrees of constraint, as very weakly deleterious mutations are able to fix. Thus, some reasonable proportion of functional substitutions in populations with small effective population sizes, such as humans, may be mildly deleterious.

12.2.1 Appendix: The fixation probability of weakly selected alleles

What is the probability a weakly beneficial or deleterious additive allele fixes in our population? We'll let $P(\Delta p)$ be the probability that our allele frequency shifts by Δp in the next generation. Using this, we can write our probability $p_F(p)$ in terms of the probability of achieving fixation averaged over the frequency in the next generation

$$p_F(p) = \int p_F(p + \Delta p)P(\Delta p)d(\Delta p) \quad (12.15)$$

This is very similar to the technique that we used when deriving our probability of escaping loss in a very large population above.

So we need an expression for $p_F(p + \Delta p)$. To obtain this, we'll do a Taylor series expansion of $p_F(p)$, assuming that Δp is small:

$$p_F(p + \Delta p) \approx p_F(p) + \Delta p \frac{dp_F(p)}{dp} + (\Delta p)^2 \frac{d^2 p_F(p)}{dp^2}(p) \quad (12.16)$$



Figure 12.12: Common Cuttlefish (*Sepia officinalis*).
Cefalopodi viventi nel Golfo di Napoli (1896).
Jatta G. Image from the Biodiversity Heritage Library. Contributed by Smithsonian Libraries. Licensed under CC BY-2.0.

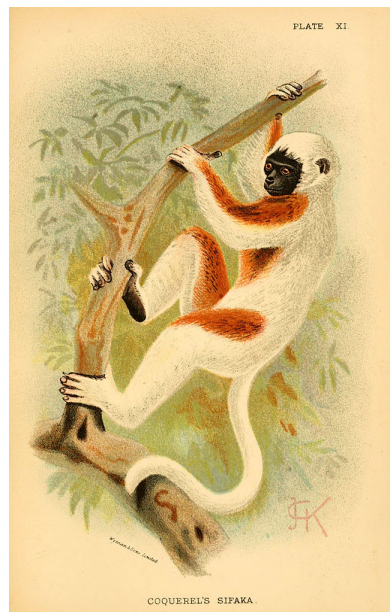


Figure 12.13: Coquerel's Sifaka (*Propithecus coquereli*).
A hand-book to the primates (1894). Forbes, H. O. Image from the Biodiversity Heritage Library. Contributed by Smithsonian Libraries. Licensed under CC BY-2.0.

ignoring higher order terms.

Taking the expectation over Δp on both sides, as in eqn. 12.15, we obtain

$$p_F(p) = p_F(p) + \mathbb{E}(\Delta p) \frac{dp_F(p)}{dp} + \mathbb{E}((\Delta p)^2) \frac{d^2p_F(p)}{dp^2} \quad (12.17)$$

Well, $\mathbb{E}(\Delta p) = \frac{s}{2}p(1-p)$ and $Var(\Delta p) = \mathbb{E}((\Delta p)^2) - \mathbb{E}^2(\Delta p)$, so if $s \ll 1$ then $\mathbb{E}^2(\Delta p) \approx 0$, and $\mathbb{E}((\Delta p)^2) = \frac{p(1-p)}{2N}$. Substituting in these values and subtracting p from both sides of our equation, this leaves us with

$$0 = \frac{s}{2}p(1-p) \frac{dp_F(p)}{dp} + \frac{p(1-p)}{2N} \frac{d^2p_F(p)}{dp^2} \quad (12.18)$$

and we can specify the boundary conditions to be $p_F(1) = 1$ and $p_F(0) = 0$. Solving this differential equation is a somewhat involved process, but in doing so we find that

$$p_F(p) = \frac{1 - e^{-2Ns p}}{1 - e^{-2Ns}} \quad (12.19)$$

This proof can be extended to alleles with arbitrary dominance, however, this does not lead to a analytically tractable expression so we do not pursue this here.

13

The Effects of Linked Selection.

GENETIC DRIFT IS NOT THE ONLY SOURCE OF RANDOMNESS in the dynamics of alleles. Alleles also experience random fluctuations in frequency due to the fact that they present on a set of random genetic backgrounds with different fitnesses. For example, when a beneficial allele arises via a single mutation, it arises on a particular genetic background, i.e. a particular haplotype (Figure 13.1A). Imagine this mutation arising in a region with no recombination, or in an organism where genetic exchange is rare. If our beneficial allele becomes established in the population, i.e. escapes loss by genetic drift in those first few generations, it will start to increase in frequency rapidly. As it rises in frequency, so will the alleles that happened to be present on the haplotype that the mutation arose on (if those other alleles are neutral or at least not too deleterious). These other alleles are getting to 'hitchhiking' along. The alleles that are not on that particular background are swept out of the population, so the net effect of this selective sweep is to remove genetic diversity from the population. Diversity will eventually recover, as new mutations arise and some slowly drift up in frequency. But in the short-term, selective sweeps remove genetic variation from populations.

WILLIAMS and PENNINGS (2019) have visualized selective sweeps in HIV. In Figure 13.1B) we see a set of HIV haplotypes sampled from a patient before and after of a selective sweep of a drug-resistant mutation. The patient is taking a retrotransposase inhibitor (Efavirenz), but sadly within 161 days a drug-resistant mutation that changes the HIV retrotransposase protein has arisen and spread. Note how a particular haplotype is now fixed in the sample, and little genetic diversity remains, due to the hitchhiking effect of the strong selective sweep of this allele.

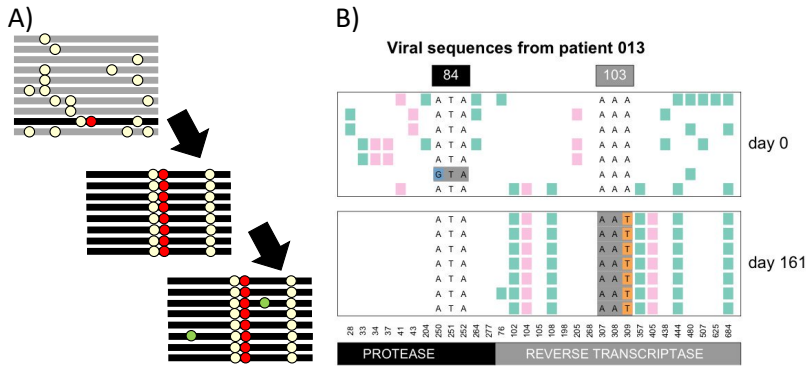


Figure 13.1: **A)** In the top panel, a selected mutation (red dot) arises on a particular haplotype in the population. It sweeps to fixation, carrying with it the haplotype on which it arose, middle panel, erasing the standing genetic diversity in the region. The bottom panel is some time after the selective sweep when some new neutral alleles (green dots) have started to drift up in frequency. **B)** Top panel: HIV sequences from a patient at the start of drug treatment in the protease and retrotransposase coding regions. Bottom panel: A sample 161 days later, after a drug resistant mutation has spread, the $A \rightarrow T$ in the 103rd codon of retrotransposase. Each row is a haplotype, with the alleles present shown as coloured blocks. Figure B from WILLIAMS and PENNINGS (2019), licensed under CC BY 4.0.

To better understand hitchhiking, first let's imagine examining variation at a locus fully linked to our selected locus, just after our sweep reached fixation. Neutral alleles sampled at this locus must trace their ancestral lineages back to the neutral allele on whose background the selected allele initially arose (Figure 13.2). This is because that background neutral allele, which existed τ generations ago, is the ancestor of the entire population at this fully linked locus. Our individuals who carry the beneficial allele are, from the perspective of these alleles, experiencing a rapidly expanding population. Therefore, a pair of neutral alleles sampled at our linked neutral locus will be forced to coalesce $\approx \tau$ generations ago. A newly derived allele with an additive selection coefficient s will take a time $\tau = 4 \log(2N)/s$ generations to reach fixation within our population (see eqn. (10.38)). This is a very short-time scale compared to the average neutral coalescent time of $2N$ generations for a pair of alleles. Thus we expect little variation, as few mutations will have arisen on these very short branches, and those that have done will likely be singletons in our sample.

Now let's think about a sweep in a recombining region. Again the selected mutation arises on a particular haplotype, and it and its haplotype starts to increase in frequency in the population. However, now recombination events can occur between haplotypes carrying and not carrying the selected allele, in individuals who are heterozygote for the selected allele. These recombination events allow alleles that were not present on the original selected haplotype to avoid being swept out of the population, and also decouple the selected allele somewhat from hitchhiking alleles, preventing many of them from hitchhiking all the way to fixation. Far out from the selected site, the recombination rate is high enough that alleles that were present on the original background barely get to hitchhike along at all, as recombination breaks up their association with the selected allele very

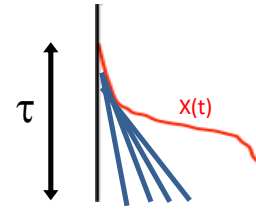


Figure 13.2: The coalescent of 4 lineages, marked in blue, at a locus completely linked to our selected allele. The frequency trajectory of the selected allele $X(t)$ is shown in red.

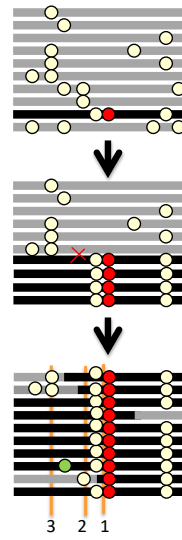


Figure 13.3: A cartoon depiction of a sweep of a red beneficial allele over three time points. The haplotype that the beneficial arose on by mutation is shown in black. The three vertical orange lines mark the loci shown in Figure 13.4. Neutral alleles segregating prior to the sweep appear as white circles, new mutations after the sweep as green circles.

rapidly.

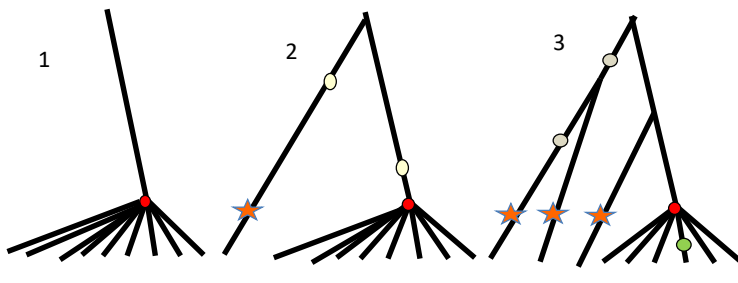


Figure 13.4: Coalescent genealogies at three loci different distances along the genome from a selective sweep. The locations of these three loci along the genome are marked in Figure 13.3. The selected mutation is shown in red. Lineages descended from recombination events during the sweep are marked in stars. Neutral mutations close to each of the loci are shown on the genealogy.

What do the coalescent genealogies look like at loci various distances away from the selected site? Well, close to the selected site all our alleles in the present day trace back to a most recent common ancestral allele present on that selected haplotype, and so are all forced to coalesce around τ generations ago (locus 1). Slightly further out from the selected site (locus 2), we have lineages that don't trace their ancestry back to the original selected haplotype, but instead are descended from recombinant haplotypes that recombined onto the sweep (the haplotype 2 from the bottom). These lineages can coalesce neutrally with the other ancestral lineages over far deeper time scales and mutations on these deeper lineages correspond to the standing diversity present in our population prior to the sweep. As we move even further out from the selected site (locus 3), we encounter more and more lineages descended from recombinant haplotypes that coalesce neutrally much deeper in time than τ , allowing diversity to recover to background levels as we move away from the selected site.

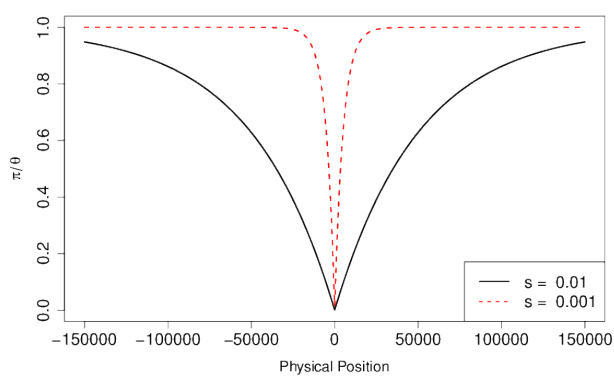


Figure 13.5: The expected reduction in diversity compared to its neutral expectation as a function of the distance away from a site where a selected allele has just gone to fixation. The sweeps associated with two different strengths of selection are shown, corresponding to a short timescale (τ) for the sweep and long one. The recombination rate is $r_{BP} = 1 \times 10^{-8}$. Code here.

To model the expected pattern of diversity surrounding a selected site, we can think about a pair of alleles sampled at a neutral locus a recombination distance r away from our selected site. Our pair of

alleles will be forced to coalesce $\approx \tau$ generations if neither of them of are descended from recombinant haplotypes (Left side of Figure 13.6).

We know that in the present day our neutral lineage is linked to the selected allele. The probability that our lineage, in some generation t back in time, is in a heterozygote is $1 - X(t)$, and the probability that a recombination occurs in that individual is r . So the probability that our neutral lineage is descended from a recombinant haplotype t generations back is

$$r(1 - X(t)) \quad (13.1)$$

So the probability (p_{NR}) that our lineage is not descended from a recombinant haplotype from a recombination event in the τ generations it takes our selected allele to move through the population is

$$p_{NR} = \prod_{t=1}^{\tau} (1 - r(1 - X(t))) \quad (13.2)$$

Assuming that r is small, then $(1 - r(1 - X(t))) \approx e^{-r(1-X(t))}$, such that

$$p_{NR} = \prod_{t=1}^{\tau} (1 - r(1 - X(t))) \approx \exp\left(-r \sum_{t=1}^{\tau} 1 - X(t)\right) = \exp\left(-r\tau(1 - \hat{X})\right) \quad (13.3)$$

where \hat{X} is the average frequency of the derived beneficial allele across its trajectory as it sweeps up in frequency, $\hat{X} = \frac{1}{\tau} \sum_{t=1}^{\tau} X(t)$. As our allele is additive, its trajectory for frequencies < 0.5 is the mirror image of its trajectory for frequencies > 0.5 , therefore its average frequency $\hat{X} = 0.5$. This simplifies our expression to

$$p_{NR} = e^{-r\tau/2}. \quad (13.4)$$

The probability that neither of our lineages is descended from a recombinant haplotype, and hence are forced to coalesce, is p_{NR}^2 (assuming that they coalesce at a time close to τ so that they recombine independently of each other for times $< \tau$).

If one or other of our lineages is descended from a recombinant haplotype, it will take them on average $\approx 2N$ generations to find a common ancestor, as we are back to our neutral coalescent probabilities (Right side of Figure 13.10). Thus, the expected time till our pair of lineages find a common ancestor is

$$\mathbb{E}(T_2) = \tau \times p_{NR}^2 + (1 - p_{NR}^2)(\tau + 2N) \approx (1 - p_{NR}^2) 2N \quad (13.5)$$

where this last approximation assumes that $\tau \ll 2N$. So the expected pairwise diversity for neutral alleles at a recombination distance r away from the selected sweep (π_r) is

$$\mathbb{E}(\pi_r) = 2\mu\mathbb{E}(T_2) \approx \pi_0 (1 - e^{-r\tau}) \quad (13.6)$$

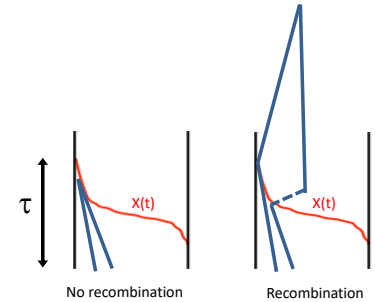
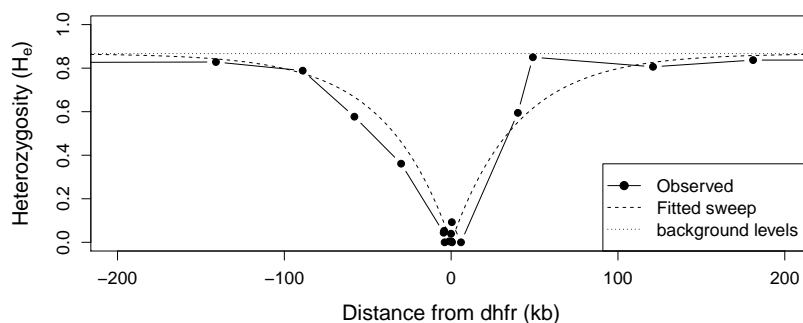


Figure 13.6: **Left**) two lineages coalesce roughly τ generations ago as they are both descended from the selected haplotypes. **Right**) One of our two lineages is descended from the selected haplotype but the other is descended from a recombinant on to the sweep. The pair on the right coalesce much deeper back in time.

So diversity increases as we move away from the selected site, slowly and exponentially plateauing to its neutral expectation π_0 .

The malaria pathogen (*Plasmodium falciparum*) has evolved drug resistance to anti-malaria drugs, often by changes at the dhfr gene. Figure 13.8 shows levels of genetic diversity (heterozygosity) at a set of markers moving out from the dhfr gene in a set of drug resistant malaria sequences collected in Thailand (NASH *et al.*, 2005). We see the characteristic dip in diversity around the gene, with zero diversity at a number of the loci very close to the gene, suggesting a strong selective sweep. Fitting our simple model of a sweep to this data, we estimate that $\tau \approx 40$ generations, corresponding to the drug-resistance allele fixing in very short time period.



To get a sense of the physical scale over which diversity is reduced, consider a region where recombination occurs at a rate r_{BP} per base pair per generation, and a locus ℓ base pairs away from the selected site, such that $r = r_{BP}\ell$ (where $r_{BP}\ell \ll 1$ so we don't need to worry about more than one recombination event occurring per generation). Typical recombination rates are on the order of $r_{BP} = 10^{-8}$. In Figure 13.5 we show the reduction in diversity, given by eqn. (13.6), for two different selection coefficients.

For our expected diversity level to recover to 50% of its neutral expectation $\mathbb{E}(\pi_r)/\theta = 0.5$, requires a physical distance ℓ^* such that $\log(0.5) = -r_{BP}\ell^*\tau$, and by re-arrangement,

$$\ell^* = \frac{-\log(0.5)}{r_{BP}\tau}. \quad (13.7)$$

As τ depends inversely on the selection s (eqn. (10.38)), the width of our trough of reduced diversity depends on s/r_{BP} . All else being equal, we expect stronger sweeps or sweeps in regions of low recombination to have a larger hitchhiking effect. For example, in a genomic region with a recombination rate $r_{BP} = 10^{-8}\text{bp}^{01}$ a selection coefficient of $s = 0.1\%$ would reduce diversity over 10's of kb, while a sweep of $s = 1\%$ would affect $\sim 100\text{kb}$.

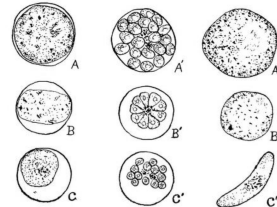


FIG. 47. Comparison of three species of malaria parasites $\times 2000$ (figures selected largely from Manson). A, A' and A'', *Plasmodium vivax*; B, B' and B'', *Plasmodium vivax*; C and C'', *Plasmodium falciparum*. A, B and C, mature parasites in red corpuscles. A', B' and C', segmented parasites ready to leave corpuscles. A'', B'' and C'', mature gametocytes.

Figure 13.7: Three species of malaria parasites (*Plasmodium*) in red blood cells.

Animal parasites and human disease (1918). Chandler, A.C. Image from the Biodiversity Heritage Library. Contributed by Cornell University Library. Not in copyright.

Figure 13.8: Levels of heterozygosity at a set of microsatellite markers surrounding the dhfr gene in samples of drug-resistant malaria (*Plasmodium falciparum*) from Thailand. The dotted horizontal line gives the average level of heterozygosity found at these markers in a set of drug-resistant malaria; we take this background as our π_0 . The dashed line shows our fitted hitchhiking model from equation 13.6 with $\tau \approx 40$, fitted by non-linear least squares. The recombination rate in *P. falciparum* is $r_{BP} \approx 10^{-6}\text{bp}^{-1}$. Data from NASH *et al.* (2005). Code here.

Question 1. VAN'T HOF *et al.* (2011) identified the genetic basis of melanism in the peppered moth (*Biston betularia*). This allele swept to fixation in northern parts of the UK; a classic case of adaptation to industrial pollution (made famous by the work of KETTLEWELL, see MAJERUS (2009) and COOK *et al.* (2012)). The genetic basis of melanism is a transposable element (TE) inserted into a pigmentation gene. VAN'T HOF *et al.* found that diversity is suppressed in a broad region around the TE. Specifically, on the background of the TE, it takes roughly 200 kb in either direction for diversity levels to recover to 50% of genome-wide levels.

Random facts: In all moths and butterflies only males recombine; chromosomes are transmitted without recombination in females. The recombination rate in males is 2.9 cM/Mb. Peppered moths have an effective population size of roughly a hundred thousand individuals. Kettlewell used to eat moths when out collecting them in the field (personal communication, Art. Shapiro).

A) Briefly explain how this pattern offers further evidence that the melanistic allele was favoured by selection.

B) Using this information, and assuming the allele's effects on fitness are additive, what is your estimate of the age of the allele?

C) What is your estimate of the selection coefficient favouring this melanistic allele?

Other signals of selective sweeps The primary signal of a recently completed selective sweep is the characteristic reduction in diversity surrounding the selected site. However, sweeps do leave other signals and these have also often been used to identify loci undergoing selection. For example, neutral alleles further away from the selected site may hitchhiking only part of the way to fixation if recombination occurs during the sweep, which can lead to an excess of high-frequency derived alleles at intermediate distances away from the selected site, a pattern lasting for a short time after a sweep (FAY and WU, 2000; PRZEWORSKI, 2002; KIM, 2006). Also, as neutral diversity levels slowly recover through an influx of new mutations after a sweep, there is a strong skew towards low frequency derived alleles, a pattern that persists for many generations (BRAVERMAN *et al.*, 1995; PRZEWORSKI, 2002; KIM, 2006). The excess of rare alleles, compared to a neutral model, can be captured by statistics such as Tajima's D (which we encountered back in our discussion of the neutral site frequency eqn 4.43). Thus one way to look for loci that have undergone selective sweeps is to calculate Tajima's D from data in windows along the genome and look for strong departures from the null distribution.



Figure 13.9: peppered moth (*Biston betularia*), non-melanistic morph
Les papillons dans la nature (1934). Robert, P.-A. Image from the Biodiversity Heritage Library. Contributed by University of Illinois Urbana-Champaign. Not in copyright.

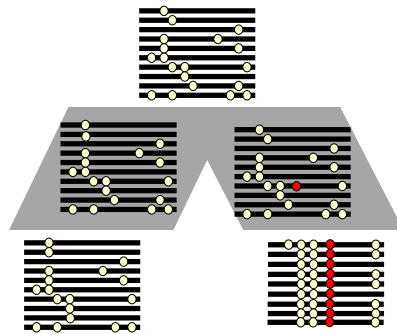


Figure 13.10: Two populations descended from a common ancestral population. A beneficial mutation has occurred in population and swept to fixation.

We can also use comparisons among multiple populations to look for evidence of sweeps occurring in one of the populations, for example to identify alleles involved in local adaptation (see 13.10). A selective sweep will decrease the within-population diversity (H_S) surrounding the selected site, without affecting the diversity between different populations. Thus local sweeps create peaks of F_{ST} between weakly differentiated populations.

HOHENLOHE *et al.* (2010) studied genome-wide patterns of F_{ST} between marine and freshwater populations of threespine stickleback (*Gasterosteus aculeatus*), plotted in Figure 13.11. Between different marine populations, they found no strong peaks of F_{ST} ; however, between the marine and freshwater comparisons they found a number of high F_{ST} peaks that were replicated over a number of freshwater-marine comparisons. They identified a number of novel regions responsible for the adaptation of sticklebacks to freshwater environments and also a number of loci previously identified in crosses between marine and freshwater populations. For example, the first peak of Linkage Group IV includes Ectodysplasin A (Eda), a gene involved in the adaptive loss of armour plating in freshwater environments.

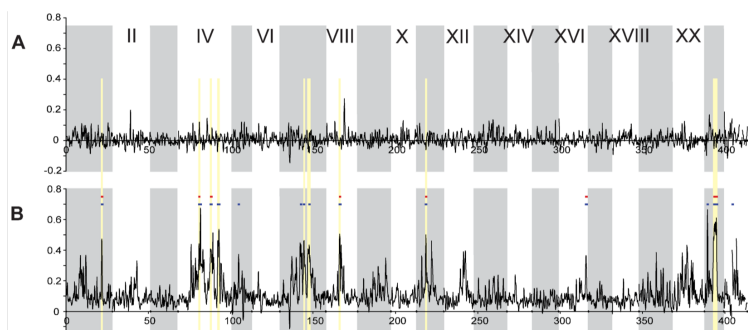


Figure 13.11: F_{ST} across the stickleback genome, with colored bars indicating significantly elevated ($p \leq 10^{-5}$, blue; $p \leq 10^{-7}$, red) and reduced ($p \leq 10^{-5}$, green) values. The alternating white and grey panels indicate different linkage groups. **A)** F_{ST} between two oceanic populations **B)** Average F_{ST} between a freshwater population and the two marine populations. Figure and caption text from HOHENLOHE *et al.* (2010), licensed under CC BY 4.0.

Soft Sweeps from multiple mutations and standing variation. In our sweep model above, we assumed that selection favoured a beneficial allele from the moment it entered the population as a single copy mutation (left panel, Figure 13.12). However, when a novel selection pressure switches on, multiple mutations at the same gene may start to sweep, such that no one of these alleles sweeps to fixation (middle panel, Figure 13.12). These sweeps involving multiple mutations significantly soften the impact of selection on genomic diversity, and so are called 'soft sweeps'.

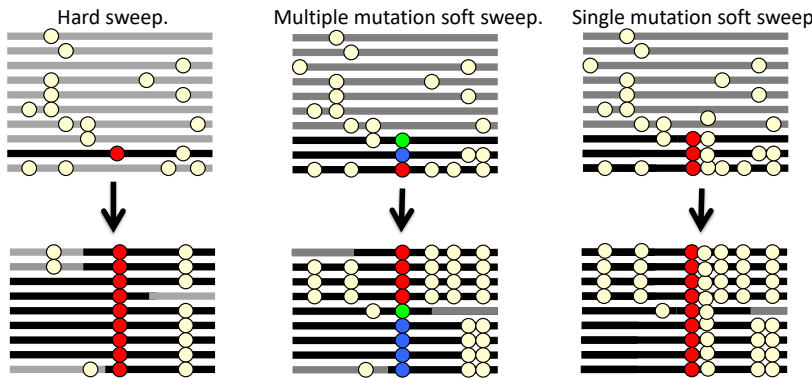


Figure 13.12: Three types of sweeps.

Another way that the impact of a sweep can be softened is if our allele was segregating in the population for some time before it became beneficial. That additional time means that our allele can have recombined onto various haplotype backgrounds, such that when selection pressures switch, the selected allele sweeps up in frequency on multiple different haplotypes (right panel, Figure 13.12). Detecting and differentiating these different types of sweeps is an active area of empirical research and theory in population genomics (see HERMISSON and PENNINGS (2017) for an overview of developments in this area).

13.1 The genome-wide effects of linked selection.

To what extent are patterns of variation along the genome and among species shaped by linked selection, such as selective sweeps? We can hope to identify individual cases of strong selective sweeps along the genome, but how do they contribute to broader patterns of variation?

Two observations have puzzled population geneticists since the inception of molecular population genetics. The first is the relatively high level of genetic variation observed in most obligately sexual species. The neutral theory of molecular evolution was developed in part to explain these high levels of diversity. As we saw in Chapter 4, under a simple neutral model, with constant population size, we

should expect the amount of neutral genetic diversity to scale with the product of the population size and mutation rate. The second observation, however, is the relatively narrow range of polymorphism across species with vastly different census sizes (see Figure 2.3 and LEFFLER *et al.* (2012) for a recent review). As highlighted by LEWONTIN (1974) in his discussion of the paradox of variation, this observation seemingly contradicts the prediction of the neutral theory that genetic diversity should scale with the census population size. There are a number of explanations for the discrepancy between genetic diversity levels and census population sizes. The first is that the effective size of the population (N_e) is often much lower than the census size, due to high variance in reproductive success and frequent bottlenecks (as discussed in Chapter 4). The second major explanation, put forward by MAYNARD SMITH and HAIGH (1974), is that neutral levels of diversity are also systematically reduced by the effects of linked selection. In large populations, selective sweeps and other forms of linked selection may come to dominate over genetic drift as a source of stochasticity in allele frequencies, potentially establishing an upper limit to levels of diversity (KAPLAN *et al.*, 1989; GILLESPIE, 2000).

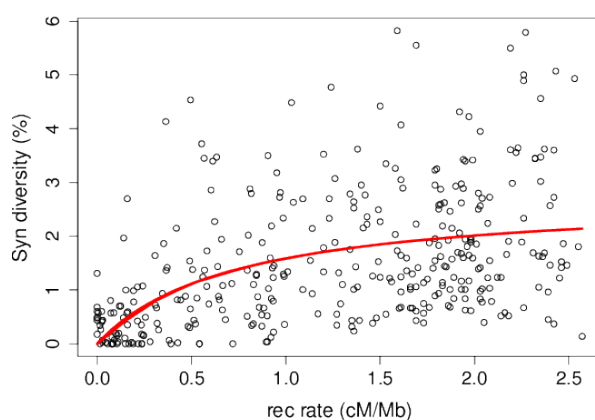


Figure 13.13: The relationship between (sex-averaged) recombination rate and synonymous site pairwise diversity (π) in *Drosophila melanogaster*. The curve is the predicted relationship between π and recombination rate, obtained by fitting the recurrent hitchhiking equation (13.13) to this data using non-linear least squares via the `nls()` function in R. Data from (SHAPIRO *et al.*, 2007), kindly provided by Peter Andolfatto, see SELLA *et al.* (2009) for details. Code here.

One strong line of evidence for the action of linked selection in reducing levels of polymorphism is the positive correlation between putatively neutral diversity and recombination seen in a number of species, as, all else being equal, linked selection should remove diversity more quickly in regions of low recombination (AGUADÉ *et al.*, 1989; BEGUN and AQUADRO, 1992; WIEHE and STEPHAN, 1993b; CUTTER and CHOI, 2010; CAI *et al.*, 2009). For example, *Drosophila melanogaster* diversity levels are much lower in genomic regions of low recombination (see Figure 13.13). This pattern can not

be explained by differences in mutation rate between low and high recombination regions as this pattern is not seen strongly in divergence data among species.

These patterns could reflect the action of selective sweeps happening recurrently along the genome. In the next section we'll present a model for how levels of genetic diversity should depend on recombination and the density of functional sites under a model of recurrent selective sweeps. However, other forms of linked selection can impact genetic diversity in similar ways. For example, linked genetic diversity is continuously lost from natural populations due to the removal of haplotypes that carry deleterious alleles (CHARLESWORTH *et al.*, 1995; HUDSON and KAPLAN, 1995b); this is called the 'background selection' model. Below we'll discuss the background selection model and its basic predictions.

More generally, a wide range of models of selection predict the removal of neutral diversity linked to selected sites. This is because the diversity-reducing effects of high variance in reproductive success are compounded over the generations when there is heritable variance in fitness (ROBERTSON, 1961; SANTIAGO and CABALLERO, 1995, 1998; BARTON, 2000). Many different modes of linked selection likely contribute to these genome-wide patterns of diversity; the present challenge is how to differentiate among these different modes.

13.1.1 A simple recurrent model of selective sweeps

To explain how a constant influx of sweeps could impact levels of diversity, here we will develop a model of recurrent selective sweeps.

Imagine we sample a pair of neutral alleles at a locus a genetic distance r away from a locus where sweeps are initiated within the population at some very low rate ν per generation. The waiting time between sweeps at our locus is exponentially distributed $\sim \text{Exp}(\nu)$. Each sweep rapidly transits through the population in τ generations, such that each sweep is finished long before the next sweep ($\tau \ll 1/\nu$).

As before, the chance that our neutral lineage fails to recombine off the sweep is p_{NR} , such that the probability that our pair of lineages are forced to coalesce by a sweep is $e^{-r\tau}$. Our lineages therefore have a very low probability

$$\nu e^{-r\tau} \tag{13.8}$$

of being forced to coalesce by a sweep per generation. If our lineages do not coalesce due to a sweep, they coalesce at a neutral rate of $1/2N$ per generation. Thus the average waiting time till a coalescent event between our neutral pair of lineages due to either a sweep or a neutral coalescent event is

$$\mathbb{E}(T_2) = \frac{1}{\nu e^{-r\tau} + 1/2N} \tag{13.9}$$

Now imagine that the sweeps don't occur at a fixed location with respect to our locus of interest, but now occur uniformly at random across our genome. The sweeps are initiated at a very low rate of ν_{BP} per basepair per generation. The rate of coalescence due to sweeps at a locus ℓ basepairs away from our neutral loci is $\nu_{BP}e^{-r_{BP}\ell\tau}$. If our neutral locus is in the middle of a chromosome that stretches L basepairs in either direction, the total rate of sweeps per generation that could force our pair of lineages to coalesce is

$$2 \int_0^L \nu_{BP} e^{-r_{BP}\ell\tau} d\ell = \frac{2\nu_{BP}}{r_{BP}\tau} (1 - e^{-r_{BP}\tau L}) \quad (13.10)$$

so that if L is very large ($r_{BP}\tau L \gg 1$), the rate of coalescence per generation due to sweeps is $2\nu_{BP}/r_{BP}\tau$. The total rate of coalescence for a pair of lineages per generation is then

$$\frac{2\nu_{BP}}{r_{BP}\tau} + \frac{1}{2N} \quad (13.11)$$

So our average time till a pair of lineages coalesce is

$$\mathbb{E}(T_2) = \frac{1}{\frac{2\nu_{BP}}{r_{BP}\tau} + 1/2N} = \frac{r_{BP}2N}{4N\nu_{BP}/\tau + r_{BP}} \quad (13.12)$$

such that our expected pairwise diversity ($\pi = 2\mu\mathbb{E}(T_2)$) in a region with recombination rate r_{BP} that experiences sweeps at rate ν_{BP} is

$$\mathbb{E}(\pi) = \pi_0 \frac{r_{BP}}{\frac{4N\nu_{BP}}{\tau} + r_{BP}} \quad (13.13)$$

where π_0 is our expected diversity without any selective sweeps, ($pi_0 = \theta = 4N\mu$). The expected diversity increases with r_{BP} , as higher recombination rates decrease the likelihood a neutral allele hitchhikes along with a sweep and is thus forced to coalesce by the sweep. Expected diversity decreases with ν_{BP} , as a greater density of functional sites experiencing sweeps increases the chance of being linked to a nearby sweep. As we move to high r_{BP} , assuming that ν_{BP} doesn't increase with r_{BP} , our level of diversity should plateau to θ , the level of genetic diversity of a neutral site completely unlinked to any selected loci. If we assume that our genome experiences a constant rate of sweeps of a given strength, i.e. that $4N\nu_{BP}/\tau$ is a constant, we can fit the variation in π across regions that vary in their recombination rate (r_{BP}) to estimate a population's rate of recurrent sweeps per basepair. An example of fitting this curve to data from *Drosophila melanogaster* is shown in Figure 13.13; see WIEHE and STEPHAN (1993a) for an early example of fitting a similar recurrent hitchhiking model to such data. The parameter giving us this best-fitting curve is $4N\nu_{BP}/\tau \approx 7 \times 10^{-9}$. With an effect population size of a million and assuming that the sweeps take a thousand generations to reach fixation,

we find this implies $\nu_{BP} \approx 10^{-12}$. Thus, a really low rate of moderately strong sweeps, roughly one every megabase every million generations, is all we need to explain the profound dip in diversity seen in regions of the genome with low recombination. However, sweeps from positively selected alleles are not the only cause of genome-wide signals of linked selection. Selection against deleterious alleles can also drive these patterns.

13.1.2 Background selection

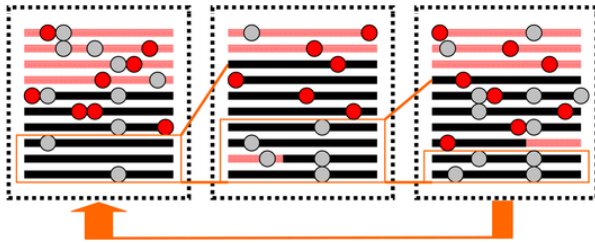
Populations experience a constant influx of deleterious mutations at functional loci while selection acts to purge them from the population, thus preventing deleterious substitutions and maintaining function at these loci. As we discussed in Chapter 10, this balance between mutation and selection results in a constant level of deleterious variation in the population. The constant selection against this deleterious variation has effects on diversity at linked sites. Each deleterious mutation arises at random on a haplotype in the population, and as selection purges this mutation, it removes with it any neutral alleles that were also on this haplotype. This constant removal of linked alleles from the population acts to reduce diversity in regions surrounding functional loci (HUDSON and KAPLAN, 1995a; NORDBORG *et al.*, 1996), an effect known as background selection (BGS).

What proportion of our haplotypes are free of deleterious mutations in any given generation, and so free to contribute to future generations? Well, under mutation-selection balance, a constrained locus with a mutation rate μ towards deleterious alleles that experience a selection coefficient sh against them in heterozygotes, will result in μ/sh chromosomes carrying the deleterious allele. Some of these haplotypes may be passed on to the next generation, but if they are fully linked to the deleterious locus they will all eventually be lost because they carry a deleterious mutation at a site under constraint. Thus, for a neutral polymorphism completely linked to a constrained locus, only $2N(1 - \mu/sh)$ alleles get to contribute to future generations. Therefore, the level of pairwise diversity in a constant population due to BGS at such a locus will be

$$\mathbb{E}[\pi] = 2\mu \times 2N(1 - \mu/sh) = \pi_0(1 - \mu/sh) \quad (13.14)$$

where $\pi_0 = 4N\mu$, the level of neutral pairwise diversity in the absence of linked selection.

The effects of background selection are more pronounced in regions of low recombination, where neutral alleles are less able to recombine off the background of deleterious alleles. Thus, under background selection, we also expect to see reduced diversity in regions of lower recombination.



For a neutral locus that is a recombination fraction r away from a locus subject to constraint, the level of diversity is

$$\mathbb{E}[\pi] = \pi_0 \left(1 - \frac{\mu sh}{2(r+sh)^2}\right) \quad (13.15)$$

As we move away from a locus experiencing purifying selection, we increase r , and diversity should recover. For example, moving away from genic regions in the maize genome we see the average level of diversity recover. This occurs in both maize and teosinte, the wild progenitor of maize. The dip in diversity around non-synonymous sites is stronger in teosinte, perhaps because the accelerated drift due to the bottleneck in maize may have somewhat released constraint on sites where very weakly deleterious alleles segregated previously at mutation-selection balance.

More generally, if a neutral locus is surrounded by L loci experiencing purifying selection at recombination distances r_1, \dots, r_L , then compounding equation (13.15) across these loci, the expected reduced diversity is approximately

$$\mathbb{E}[\pi] = \pi_0 \prod_{i=1}^L \left(1 - \frac{\mu sh}{2(r_i+sh)^2}\right) \approx \exp\left(\sum_{i=1}^L \frac{\mu sh}{2(r_i+sh)^2}\right) \quad (13.16)$$

To model an average neutral locus in a genomic region with a given recombination rate, we can imagine that our neutral locus is situated in the center of a large region with total recombination rate R and total deleterious mutation rate U , where $U = \mu L$. Then our expression for diversity, equation (13.16), simplifies to

$$\mathbb{E}[\pi] \approx \pi_0 \exp(-U/(sh+R)) \approx \pi_0 \exp(-U/R). \quad (13.17)$$

In this last approximation, we assume that we're looking at a large region, with $R \gg sh$. Note that much like genetic load, equation (11.8), this expression depends only on the total deleterious mutation rate. Any dependence on the selection coefficient drops out, as weakly selected mutations segregate in the population at higher frequencies, but are also removed from the population more slowly, allowing more of the genome to recombine off the deleterious background.

Figure 13.14: A cartoon depiction of a region for 10 haplotypes experiencing background selection. Neutral mutations are shown as gray circles, and deleterious mutations in red. Over time, chromosomes carrying deleterious mutations are removed from the population, such that most individuals are descended from a subset of chromosomes free of deleterious alleles (highlighted here by orange boxes). Mutation is constantly generating new deleterious alleles on the background of chromosomes previously free of deleterious alleles. Figure modified from SELLA *et al.* (2009), licensed under CC BY 4.0.

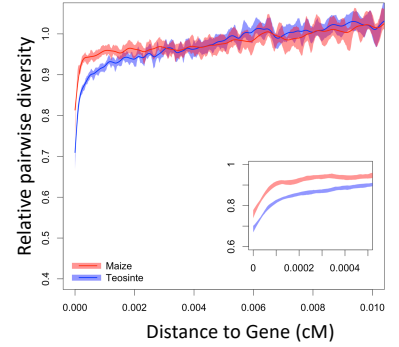


Figure 13.15: Relative diversity compared to the mean diversity in windows ≥ 0.01 cM as a function of the distance to the nearest gene. See (BEISSINGER *et al.*, 2016) for details. Figure licensed under CC BY 4.0 by Jeff Ross-Ibarra.

For a first go at fitting this to genome-wide data, we could look at diversity in windows of length W bp (as in Figure 13.16). If we assume that there is a constant rate of deleterious mutation per base pair, μ_{BP} , then $U = \mu_{BP}W$. Furthermore, if our genomic window has a recombination rate r_{BP} per base-pair, our total genetic length is $R = r_{BP}W$. Making these substitutions in equation (13.17), our window size cancels out to give

$$\mathbb{E}[\pi] \approx \pi_0 \exp(-\mu_{BP}/r_{bp}) \quad (13.18)$$

Looking across windows that vary in their recombination rate, i.e. r_{BP} , we can fit equation (13.18) to data to estimate μ_{BP} . An example of doing this to data from *D. melanogaster* is shown in Figure 13.16, yielding an estimate of the deleterious mutation rate of $\mu_{BP} \approx 3.2 \times 10^{-9}$. This is roughly on the same order as the mutation rate per base pair in *D. melanogaster*, and so this deleterious mutation rate estimate is somewhat high as it would require most of the genome to be constrained, but as a first approximation it's not terrible. Note how similar the fit is to a model of hitchhiking, suggesting that both BGS and hitchhiking are capable of explaining the broad relationship between diversity and recombination seen in *D. melanogaster* and other species.

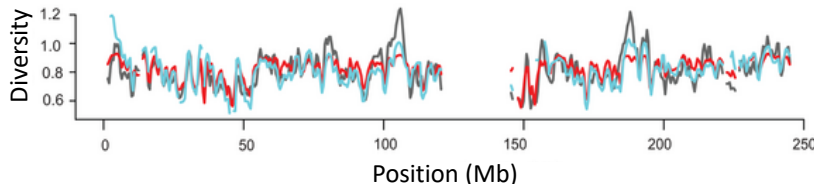


Figure 13.16: The relationship between recombination rate and synonymous site pairwise diversity (π) in *D. melanogaster*, as in Figure 13.13. The red curve is the predicted relationship between π and recombination rate, obtained by fitting the BGS equation (13.17) to this data using non-linear least squares via the `nls()` function in R. The blue line is the recurrent hitchhiking equation line from Figure 13.13. Code here.

As our annotations of functional regions of the genome have improved, so have our methods to infer background selection. A more rigorous version of this analysis today would incorporate variation in coding density among windows into the parameter μ_{BP} . With detailed genomic annotations showing coding regions and constrained non-coding regions, we can also move beyond just analyzing broad-scale patterns. For example, MCVICKER *et al.* (2009) fit a model of background selection to putatively neutral pairwise diversity along the human genome, using equation 13.16 to estimate the effect of BGS at each locus, weighing the genetic distance to all of the surrounding coding regions and constrained non-coding sites. This allowed MCVICKER *et al.* (2009) to estimate mutation rates and average selection coefficients acting against deleterious alleles in these regions of the genome. This best fitting model also allowed them to predict

Figure 13.17: Observed (black line) and predicted pairwise diversity across chromosome 1, from a background selection model that assumes a uniform mutation rate (red line) or a mutation rate that varies with local human/dog divergence (blue line). Figure from (MCVICKER *et al.*, 2009), licensed under CC BY 4.0.

diversity levels along the genome, a section of which is shown in figure 13.17. Thus, broad-scale features of polymorphism along the genome are well described by background selection (or by linked selection more generally).

The deleterious mutation rates estimated by MC VICKER *et al.* (2009) from fitting a model of BGS were again too high, as in the *Drosophila* example above, suggesting the BGS alone is not sufficient to explain all of the effect of linked selection. But how then do we go about distinguishing the impact of BGS from hitchhiking?

Distinguishing the impact of hitchhiking from background selection in genome-wide data A variety of approaches have been taken to start to separate the effects of hitchhiking from background selection. Much of the strongest evidence showing the effects of both comes from *Drosophila melanogaster* and we review some of that evidence here. Hitchhiking is expected to have systematic effects on the neutral site frequency spectrum, distorting it towards rare minor alleles, (reflecting the slow recovery of diversity following a sweep). Therefore, we should expect a distortion of summary statistics such as Tajima's D in regions of low recombination if hitchhiking is contributing to the reduction in diversity in these regions (BRAVERMAN *et al.*, 1995; PRZEWORSKI, 2002; KIM, 2006). In *D. melanogaster*, there is a greater skew towards rare alleles at putatively neutral sites in regions of low recombination (ANDOLFATTO and PRZEWORSKI, 2001; SHAPIRO *et al.*, 2007), see left panel of Figure 13.18. However, while this skew isn't expected under simple models of strong background selection, other models of background selection can lead to such patterns.

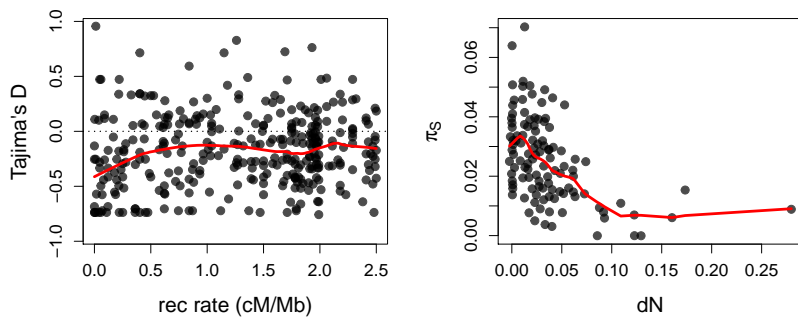


Figure 13.18: **Left)** Average Tajima's D in genomic windows plotted against their recombination rate in *D. melanogaster*. Data from SHAPIRO *et al.* (2007). **Right)** Synonymous pairwise diversity in genomic windows as a function of the density of non-synonymous substitutions in the window. Data from ANDOLFATTO (2007). Code here.

Another prediction of the hitchhiking model, where an allele sweeps to fixation, is that there should be a functional substitution associated with each sweep. Or, to flip that around, we might expect to see a greater impact of hitchhiking where there are more functional

substitutions. For example, regions surrounding non-synonymous substitutions should have lower levels of diversity, if a high fraction of non-synonymous substitutions are adaptive. Again, this pattern is seen in *D. melanogaster* (ANDOLFATTO, 2007; MACPHERSON *et al.*, 2007; SATTATH *et al.*, 2011b), right side of Figure 13.18.

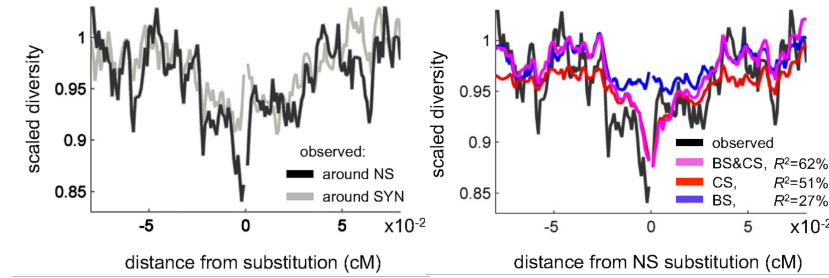


Figure 13.19: **Left)** Scaled synonymous pairwise diversity levels around non-synonymous (NS) and synonymous (SYN) substitutions in *D. melanogaster*. **Right)** Predicted scaled diversity levels around non-synonymous substitutions based on models including background selection (BS), classic sweeps (CS) and both (BS & CS). Figure from ELYASHIV *et al.* (2016), licensed under CC BY 4.0.

Pushing this idea further, we can look at the dip in diversity surrounding a non-synonymous substitution averaged across all the substitutions in the genome. ELYASHIV *et al.* (2016) found a stronger dip in diversity around non-synonymous substitutions than synonymous substitutions (see also SATTATH *et al.*, 2011a). Extending the model of MCVICKER *et al.* (2009) to fit a model of background selection and hitchhiking to putative neutral diversity along the genome, they found that the dip in diversity around synonymous substitutions comes mostly from BGS. But to fully explain the dip in diversity around non-synonymous substitutions, a reasonable proportion of these non-synonymous substitutions have to have been accompanied by a classic (hard) sweep. The majority of these sweeps are estimated to be due to very weak selection, with selection coefficients $< 10^{-4}$. Furthermore, ELYASHIV *et al.* (2016) estimated a 77 - 89% reduction in neutral diversity due to selection on linked sites, and concluded that no genomic window was entirely free of the effects of selection. Thus linked selection has a profound effect in some species such as *Drosophila melanogaster*.

14

Interaction of Multiple Selected Loci

Selection doesn't act on loci in isolation, and the fates of selected alleles in the genome are correlated. In the prior chapter we looked into how selected loci affected neutral loci. Here we'll explore the interaction of multiple selected loci. Throughout this chapter we'll see how multi-locus dynamics are key to understanding hypotheses about the evolutionary significance of sexual reproduction, after all the primary evolutionary costs and benefits of sex arise from the independent assortment of chromosomes and recombination. Multi-locus dynamics are also often key to understanding how new species arise and are maintained. From a population-genetic perspective, species are sets of traits and alleles held together by assortative mating and selection.

14.1 Why sex?

The vast majority of eukaryotic organisms reproduce sexually. Sexual reproduction, the fusion of two cells to form a zygote (*syngamy*) followed by meiosis, represents an ancient feature of eukaryotes. However, the ubiquity of sex is not just due to sex being a fixed ancestral state of eukaryotes. Many eukaryotic species are not obligately sexual and can reproduce clonally (i.e. asexually), e.g. vegetative growth in plants. However, they will reproduce clonally only for a short while before having sex again. There are even asexual vertebrate lineages. For example, there are a number of obligately parthenogenic species of whiptail lizard (*Aspidoscelis*), where every individual in the species is female and reproduce clonally. However, only a small fraction of eukaryote species are obligate asexuals, and these species appear to be short-lived twigs on the eukaryotic tree of life.

Sex reproduction is confined to eukaryotes but most non-eukaryotic species have some form of genetic exchange where genetic material is acquired and incorporation into their genomes via a range of mechanisms. These non-eukaryotic mechanisms often seem to have evolved in part because they facilitate genetic exchange

Thus, sex and genetic exchange are incredibly widespread. Yet sex has substantial short-term costs.

The costs of sex. Three broad costs of sex have often been hypothesized:

1. The cost of mating. Finding and attracting a mate are costly and may be impossible, and mating can be dangerous.
2. The cost of recombination. Why risk breaking it up a winning genotype? If you've managed to survive to reproduce you're genotype likely can't be a terrible fit to the environment. But if you engage in sexual reproduction, i.e. meiosis, you're shuffling up your genome with that of your partner. There's no guarantee that this new genotype will work well in the current environment.
3. The two-fold cost of sex (SMITH, 1971). The offspring of sexual organisms have two parents. Therefore, sexual parents only contribute half of their genome to their offspring. While asexual organisms contribute their entire genome to the next generation. Thus a sexual organism has to have twice as many children to leave the same number of copies of their genome to the next generation. That might be doable if both sexual parents were equally committed to contributing to those offspring. However, that is rarely the case. This cost is sometimes called the two-fold cost of males, as males often provide little in terms of resources to their children. Thus any allele that makes its host asexual should initially spread all else being equal.

Yet sex and other forms of genetic exchange persist, despite these short-term advantages to asexual reproduction. Indeed asexual lineages often arise and spread within some sexual populations due to these advantages.

The benefits of sex. Numerous benefits to sexual reproduction have been suggested. Throughout this chapter we'll encounter a range of models that touch on the advantages of sex. We'll see that selection allows beneficial alleles to shed their background of deleterious alleles as they sweep through the population. In the absence of sex and recombination, beneficial alleles can block each other's progression to fixation, so called 'clonal interference'. Another major advantage of sex is that beneficial alleles can be brought together on the same genetic background via recombination, allowing faster rates of adaptation.

14.2 A two locus model of selection and recombination.

Models involving many selected loci can be very challenging to analyze. Luckily for us many of the key insights of the interaction of selection and recombination can be understood in relatively intuitive terms, and demonstrated using two locus models.

Consider two biallelic loci segregating for A/a and B/b . There are four haplotypes, AB , Ab , aB , ab , which for simplicity we label 1-4. The frequency of our four haplotypes are x_1 , x_2 , x_3 , and x_4 . Each individual has a genotype consisting of two haplotypes; we label w_{ij} the fitness of an individual with the genotype made up of haplotype i and j (we assume that $w_{ij} = w_{ji}$, i.e. there are no parent of origin effects). Assuming that these fitnesses reflect differences due to viability selection, and that individuals mate at random, we can write the following table of our genotype proportions after selection:

	AB	Ab	aB	ab
AB	$w_{11}x_1^2$	$w_{12}2x_1x_2$	$w_{13}2x_1x_3$	$w_{14}2x_1x_4$
Ab	•	$w_{22}x_2^2$	$w_{23}2x_2x_3$	$w_{24}2x_2x_4$
aB	•	•	$w_{33}x_3^2$	$w_{34}2x_3x_4$
ab	•	•	•	$w_{44}x_4^2$

This follows from assuming that our haplotypes are brought together at random (HWE), then discounted by their fitnesses. Our mean fitness \bar{w} is the sum of all the entries in the table, so dividing by \bar{w} normalizes the complete table to sum to one. The frequency of the AB haplotype (1) in the next generation of gametes is

$$x'_1 = \frac{(w_{11}x_1^2 + \frac{1}{2}w_{12}2x_1x_2 + \frac{1}{2}w_{13}2x_1x_3 + \frac{1}{2}(1-r)w_{14}2x_1x_4 + \frac{1}{2}rw_{23}2x_2x_3)}{\bar{w}} \quad (14.1)$$

This is a bit of a mouthful, but each of the terms is easy to understand. Each of the HWE genotype frequencies (e.g. $2x_1x_2$) is weighted by its fitness relative to the mean fitness (w_{ij}/\bar{w}), and by its probability of transmitting the AB haplotype to the next generation. For example, AB/Ab individuals (1/2) transmit the AB haplotype only half the time. The final two terms include the recombination fraction (r). The first term involving recombination refers to the AB/ab genotype (1/4), who with probability $(1-r)/2$ transmits a non-recombinant AB haplotype to the gamete. Similarly, the second term refers to the Ab/aB genotype; a proportion $r/2$ of its gametes carry the recombinant AB haplotype.

In the single locus case, we defined the marginal fitness of an allele. Here it will help us to define the marginal fitness of the i^{th} haplotype:

$$\bar{w}_i = \sum_{j=1}^4 w_{ij}x_j \quad (14.2)$$

This is the fitness of the i^{th} haplotype averaged over all of the diploid genotypes it could occur in, weighted by their probability under random mating. Using this notation, and with some rearrangement of equation (14.1), we obtain

$$x'_1 = \frac{x_1 \bar{w}_1 - w_{14}rD}{\bar{w}} \quad (14.3)$$

Here we have assumed that $w_{23} = w_{14}$, i.e. that the fitness of AB/ab individuals is the same as Ab/aB individuals (i.e. that fitness depends only on the alleles carried by an individual, and not on which chromosome they are carried; this assumption is sometimes called no *cis*-epistasis).

We can then write the change in the frequency of our 1 haplotype as

$$\Delta x_1 = \frac{x_1(\bar{w}_1 - \bar{w}) - rw_{14}D}{\bar{w}} \quad (14.4)$$

Generalizing this result, we write the change in any haplotype i from our set of four haplotypes as

$$\Delta x_i = \frac{x_i(\bar{w}_i - \bar{w}) \pm rw_{14}D}{\bar{w}} \quad (14.5)$$

where the coupling haplotypes 1 and 4 use $+D$ and repulsion haplotypes 2 and 3 use $-D$. Note that the sum of these four Δx_i is zero, as our haplotype frequencies sum to one.

So the change in the frequency of a haplotype (e.g. AB, haplotype 1) is determined by the interplay of two factors: First, the extent to which the marginal fitness of our haplotype is higher (or lower) than the mean fitness of the population (the magnitude and sign of $(\bar{w}_1 - \bar{w})/\bar{w}$). Second, whether there is a deficit or any excess of our haplotype compared to linkage equilibrium (the magnitude and sign of D), modified by the strength of recombination. This tension between selection promoting particular haplotypic combinations, and recombination breaking up overly common haplotypes is the key to a lot of interesting dynamics and evolutionary processes.

14.3 Types of interaction between selection and recombination

Throughout the rest of the chapter we'll discuss some general forms to the interactions between selected loci and how recombination plays into either facilitating or hindering selection. To illustrate these ideas we make use of Muller diagrams (MULLER, 1932), where we visualize the allele dynamics in terms of a plot of the stack frequencies over time. All of our simulations use the same basic two locus dynamics given by eqn (14.5). To keep things simpler we just discuss through the qualitative dynamics of these models, but many of these models have been investigated in much more depth.

14.3.1 The hitchhiking of neutral alleles

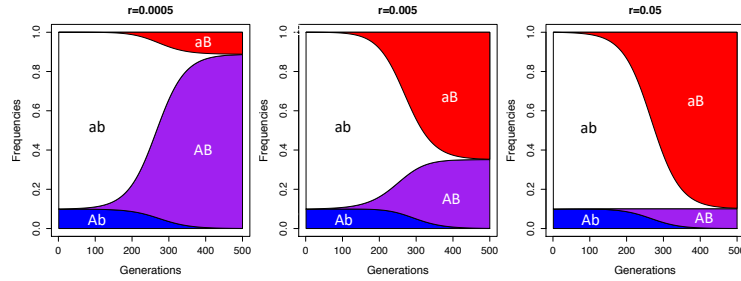


Figure 14.1: A beneficial mutation B arises on the background of a neutral allele whose initial frequency is $p_A = 10\%$. The beneficial allele has a strong, additive selection coefficient of $hs = 0.05$.

Let's start by revisiting our neutral hitchhiking in this two locus setting in the previous chapter we saw that neutral alleles can hitchhike along with our selected allele if they are tightly linked enough. Figure 14.1 shows the frequency trajectories of the various haplotypes for neutral allele (A) that is present at 10% frequency in the population when our beneficial allele (B) arises on its background. When the recombination rate (r) is low between the loci, A gets to hitchhike to high frequency, but for higher recombination rates it only gets dragged to intermediate frequencies. For the highest recombination rate shown ($r \approx s$) the neutral allele's dynamics ($p_{Ab} + p_{AB}$) are barely changed at all, as it recombines on and off the sweeping allele frequently and so barely perceives the sweep.

14.3.2 The hitchhiking of deleterious alleles

Deleterious alleles can also hitchhike along with beneficial mutations if they are not too deleterious compared to the benefits offered by the selected allele. Again our allele A is at 10% frequency in the population in Figure 14.2, but this time it is deleterious and so initially decreasing in frequency across the generations when the beneficial mutation (B) arises on its background. If the loci are tightly linked, and A were too deleterious, B would never get to take off in the population. However, if the benefits of B outweighs the cost of A , even in the case of no recombination between our loci, allele A gets to hitchhike to fixation and merely slows down B 's rate of increase and their combined fitness is reduced. With moderate amounts of recombination between the loci, our deleterious starts to hitchhike but before it can get to fixation the beneficial allele manages to recombine off its background. This recombinant aB haplotype, which has higher fitness as it lacks the deleterious allele can now sweep through the population displacing the AB haplotype. For higher recombination events we have to wait less long for a recombination to breakup the hitchhiking deleterious allele, so the adaptive allele easily escapes its background. For

the purposes of illustration here we've used a relatively common deleterious allele, but in reality these alleles will likely be often be rare in the population and at mutation selection balance. If they are rare it is likely that a beneficial mutation arises on a specific deleterious allele's background, but as we have seen there are likely going to be many rare deleterious alleles in the population so it is likely that a beneficial mutations may often have to contend with deleterious hitchhikers.

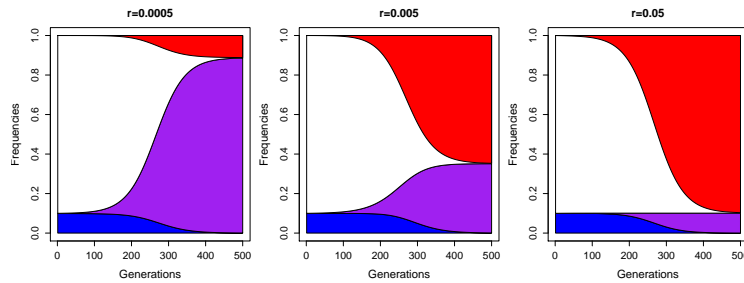


Figure 14.2: The hitchhiking of a deleterious allele. The beneficial allele B arises on the background of a deleterious allele A, and the extent to which the A allele gets to hitchhiking along depends on the recombination rate. [Code here.](#)

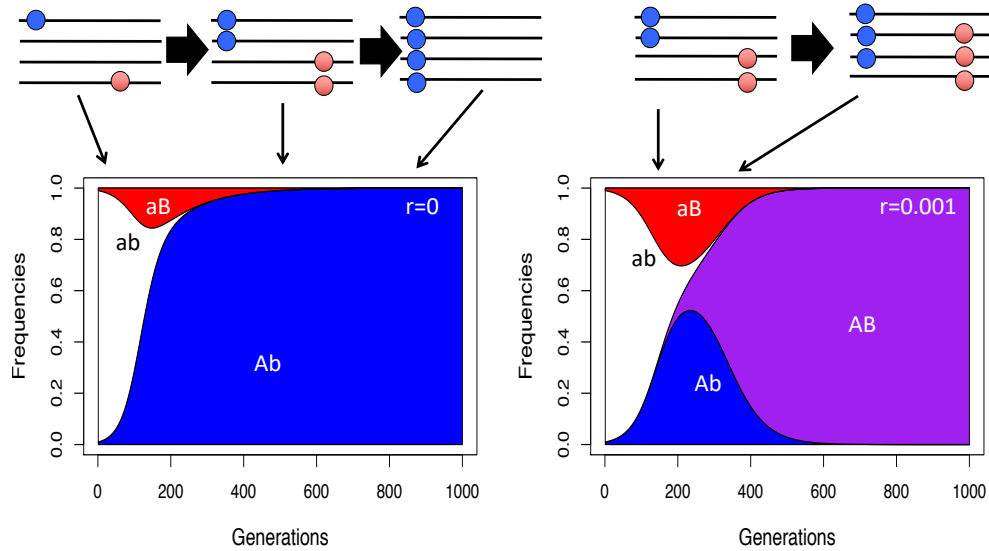


Figure 14.3: Interference between two positively selected alleles. **Left)** the red and blue (A and B) beneficial alleles arise on different haplotypes. They rise in frequency, but in the absence of recombination only one can fix. This is shown in a Muller diagram, where p_{AB} is initially set to zero. **Right)** In the presence of recombination the population can generate the recombinant (AB) haplotype, which can subsequently fix. [Code here.](#)

14.3.3 Clonal interference between favourable alleles.

When rates of sex and recombination are zero, or very low, positively selected alleles can prevent each other reach fixation and so the rate of adaptation can be slowed. In the absence of sex and recombination, when two positively selected alleles arise on different genetic backgrounds in the population they cannot both fix (left side of Figure 14.3). They can initially increase in frequency, but necessarily compete with each other when they become common. This is called selec-

tive interference, or sometime clonal interference. If one of the alleles has a much larger selection coefficient it will fix, forcing the other allele from the population, but when they are relatively equally matched it may take some time for this situation to resolve itself resulting in a traffic jam in the population. Thus in an asexual adaptive alleles necessarily have to fix sequentially. However, with even a small amount of recombination beneficial alleles can recombine on to each others background, allowing them to fix in parallel (right side of Figure 14.3).

Given the rapid evolution of HIV we can see interference taking place over very short time periods indeed. HIV uses its reverse transcriptase (RT) gene to write itself from an RNA virus into its host's DNA, allowing HIV to hijack the hosts regulatory machinery, a critical part of its life cycle. One of the early HIV drugs was Efavirenz, which inhibits HIV's RT protein. Sadly, mutations are common in the RT HIV gene, and these mutations, in the presence of the drug, confer a profound fitness advantage, allowing them to spread through the HIV population in patients undergoing anti-HIV treatment. In Figure 14.4 we see that by day 224 after the start of drug treatment two different drug-resistance amino-acid changes beginning to spread within a patient (also shown as a Muller diagram in Figure 14.5). Because these alleles occur on different genetic backgrounds, with little chance for genetic exchange between them, they interfere in each other progress as they compete to fix within the population. Eventually the amino acid change at site 188 wins out.

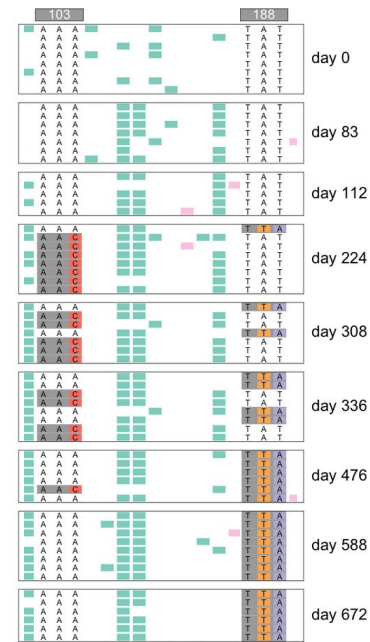


Figure 14.4: HIV sequences from a patient over the course of drug treatment in the retrotransposase coding region. Figure cropped from WILLIAMS and PENNINGS (2019), licensed under CC BY 4.0.

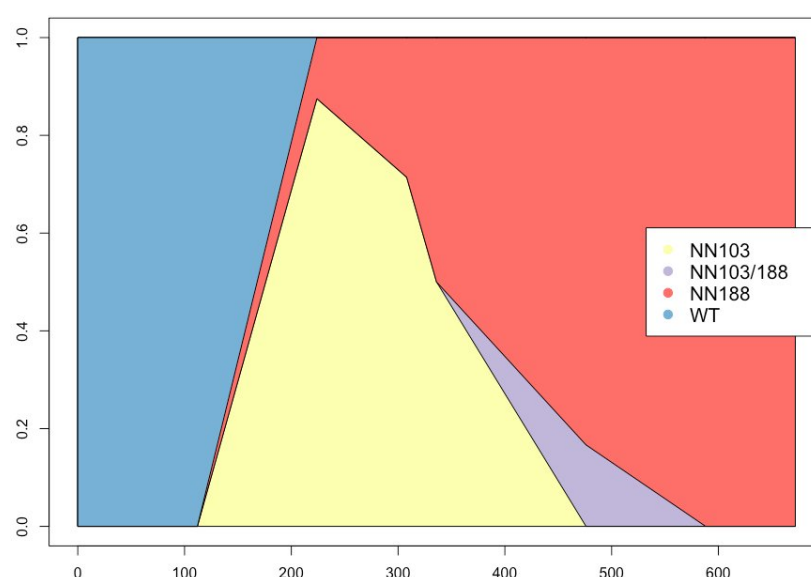
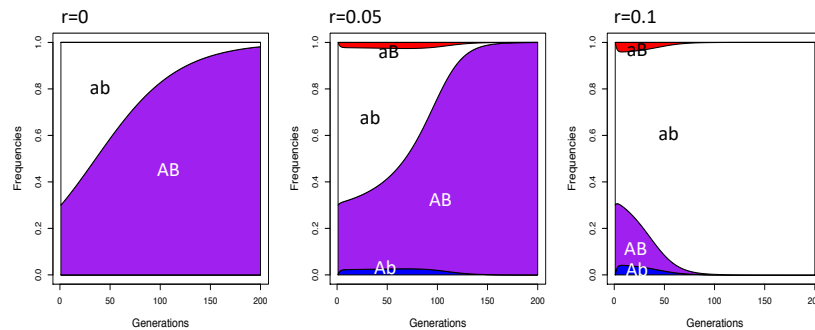


Figure 14.5: Muller plot of the drug resistance interference dynamics from Figure 14.4. Figure from WILLIAMS and PENNINGS (2019), licensed under CC BY 4.0.

14.3.4 Epistatic combinations of alleles and the cost of recombination.

Recombination comes at a cost. While recombination can bring beneficial combinations of alleles together, it will also tear them apart. To see this imagine a pair of alleles A and B at two loci that work very well together, and offer a fitness advantage over the ancestral combination of allele a and b. You could for example imagine that A and B are changes in a protein and its receptor, and that they offer a much more efficient signalling response. However, imagine that A doesn't work with b, nor does the allele a work well with B. Perhaps that the protein made by allele A gums up the receptor b, and similarly for the other the other combination.



“Love, love will tear us apart again” –Joy Division.

Figure 14.6: Code here.

The haplotype AB can spread from low frequency if recombination doesn't break it apart at too high a rate. When recombination rates are higher, recombination prevents either the A or the B allele from spreading because recombination swaps the A allele from the B background onto the b background, where it suffers low fitness (and similarly for the B allele). The ab haplotype doesn't suffer the same consequence because it is in the majority, so when recombination occurs the a allele is usually recombined back on to the b background with no consequence. Thus recombination can prevent the spread of beneficial epistatic combinations of alleles. We'll look into this more when we discuss the evolution of recombination suppressors in Section 14.3.7.

14.3.5 Muller's ratchet

There is a constant influx of deleterious mutations along any chromosome (red alleles in Figure 14.8). In asexual populations, or regions of the genome lacking recombination, this leads to nearly inevitable decrease in fitness due to the loss of high fitness haplotypes a process known as ‘Muller's ratchet’ (MULLER, 1964).

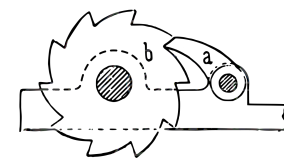


Figure 14.7: A Ratchet. A cog (b) with asymmetric teeth that can only turn one way as the pawl (a) prevents it turning the other way.
Original sketch from Brockhaus Konversations-Lexikon, Vol. 10, 1894, page 420. Georg Wiora (reworked by Dr. Schorsch). From wikipedia. Licensed under CC BY-2.0

Different haplotypes vary in the number of deleterious alleles they carry. The haplotypes carrying the most deleterious alleles can be lost by drift, and by selection acting against them, but haplotypes carrying high numbers of deleterious alleles are easily recreated by new mutations. The converse can also happen, if the selection against these each deleterious alleles is relatively weak, the population can accidentally lose the haplotype carrying the least number of deleterious alleles (middle panel of Figure 14.8).

Once we have lost this haplotype it is hard to recreate, as that would require unlikely back mutations to remove the deleterious mutations from the population. After the loss of the least deleterious haplotype, we have ratcheted up the mean deleterious mutations in the population and ratcheted down the mean fitness of the population. This will keep happening, by chance we can keep losing the haplotype with fewest deleterious alleles (bottom left panel of Figure 14.8). Thus number of deleterious alleles carried in our asexual population will gradually increase. This may eventually doom asexual population to extinction, as their mean fitness declines over time.

In a sexual population, the same process can start. We can lose by chance the haplotype with the fewest deleterious mutations (middle right panel of Figure 14.8). However, recombination among deleterious haplotypes can recreate this haplotype carrying few deleterious alleles. Such a crossover is shown as a red X in the middle right panel of Figure 14.8, and the resulting recombinant haplotype few of deleterious is shown in the lower right panel. Therefore, Muller's ratchet doesn't tick forward in sexual populations, as even a small amount of recombination is enough to stop its progression.

14.3.6 An example of the costs of asexuality.

In the Evening primrose genus (*Oenothera*), there are a number of young, independently-derived, asexual species. In each species this asexuality is due to a complicated series of reciprocal translocations, Figure 14.9 which prevent recombination and segregation and ensure that every plant is permanently-heterozygote for these rearrangements due to lethality. This system is quite complicated, and super cool. We don't need to worry about the details but importantly each species is functionally asexual. HOLLISTER *et al.* (2014) sampled transcriptome data from across the Evening primrose clade, and took advantage of 7 independent, asexual-sexual sister pairs of species to examine the impact of the evolution of asexuality for molecular evolution.

The d_N/d_S for the sexual and asexual species for each of the seven pairs (C1-C7) is shown in Figure 14.10. In every pair d_N/d_S is higher in the asexual species. The genomes of the asexual species are evolving in

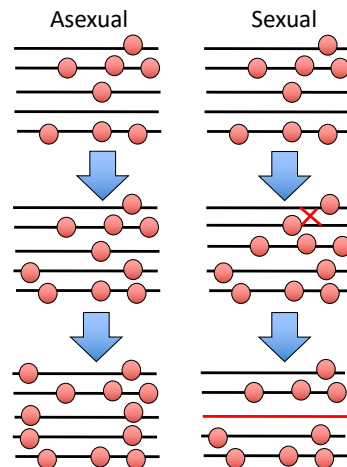


Figure 14.8: A cartoon of haplotypes at three time points showing the action of Muller's ratchet in an asexual population.

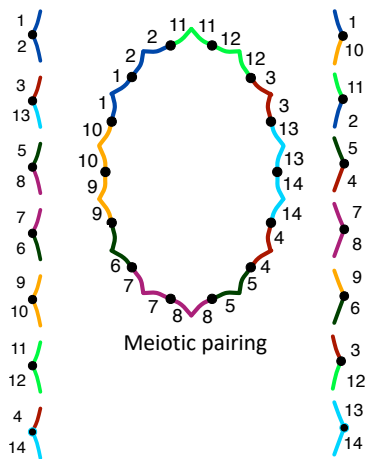


Figure 14.9: A schematic diagram of the karyotype of an evening primrose. The two columns show a heterozygote individual's diploid chromosomal complement. Each chromosome is heterozygote for two different translocations. For example both the top-most chromosomes has one arm from chromosome 1, but the other arm is heterozygote for a large translocation from the ancestral chromosome 2 and 10. Due to these translocations the meiotic pairing form a complete ring of chromosomes, which prevent crossing over and independent segregation. Thanks to Jesse Hollister for this image.

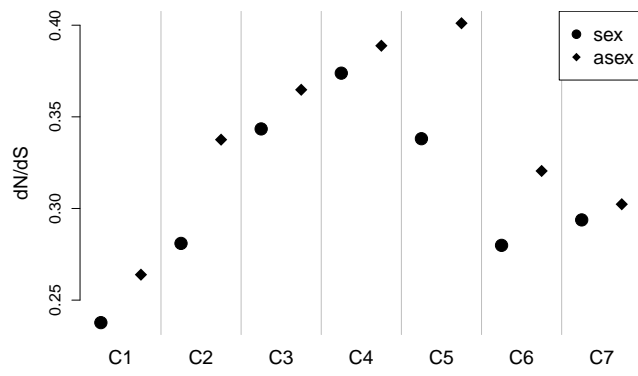


Figure 14.10: d_N/d_S calculated on sexual (circles) and asexual (diamonds) lineages of each of seven sister pairs of species. Data from HOLLISTER *et al.* (2014). Code here. |

a less constrained fashion, likely due to weakly deleterious mutations accumulating due to hitchhiking with beneficial alleles and the slow crank of Muller's ratchet.

14.3.7 The maintenance of combinations of alleles in the face of recombination.

In some cases balancing selection may be attempting to maintain multiple combinations of alleles in the population that work well together. However, recombination may be constantly ripping those alleles away from each other making it difficult to maintain these alleles. This can select for the suppression of recombination. Some of the most dramatic demonstrations of this tension involve the evolution of so-called super genes. We'll first consider the evolution of a mimicry supergene in *Heliconius numata* as an example of these dynamics.

Some of the most spectacular examples of Müllerian mimicry in the world are found in *Heliconius* butterflies. These butterflies are unpalatable to predators, and different species mimic each other so benefiting from not being eaten by predators, which rapidly learn to avoid all these species. In many of these species multiple mimicry morphs are found as we move across geographic space. In *Heliconius numata* a number of different morphs mimic morphs from a distantly related *Melinaea* species, see Figure 14.12.

To keep things relatively simple lets focus on two differences between *silvana* and *bicoloratus*, the yellow stripe on the top wing of *silvana* and the black bottom wing of *bicoloratus*. Lets imagine that these two differences are due to a simple two locus system (see left column of Figure 14.13). The first locus segregates for Y/y, where the Y allele encodes for a top-wing yellow band, and y encodes for the ab-



Figure 14.11: Showy evening primrose (*Oenothera speciosa*), the sexual species in the clade C2 from Figure 14.10.

Favourite flowers of garden and greenhouse (1896). Step, E. Image from the Biodiversity Heritage Library. Contributed by Missouri Botanical Garden. Licensed under CC BY-2.0.



Figure 14.12: Five sympatric forms of *H. numata* from northern Peru, and their distantly related mimetic *Melinaea* species. First row: *M. menophilus* ssp. nov., *M. ludovica ludovica*, *M. marsaeus rileyi*, *M. marsaeus mothone*, and *M. marsaeus phasiana*. Second row, *H. n. f. tarapotensis*, *H. n. f. silvana*, *H. n.f. aurora*, *H. n.f. bicoloratus*, and *H. n. f. arcuella*. Figure and caption from JORON et al. (2006) cropped, licensed under CC BY 4.0.

sence of the yellow band. The second locus segregates for B/b where B encodes for the bottom-wing being black, and b for the absence of black on the bottom wing. If Y is recessive and B is dominant, then the silvana phenotype corresponds to a YY bb genotype. Due to the dominance of the y and B alleles the bicoloratus phenotype can be achieved by various genotypes (Yy Bb, yy BB, Yy BB, yy Bb). Lets assume that both of these phenotypes offer an advantage as they mimic a *M. menophilus* model. But there are also genotypes that don't do as well; YY BB individuals have a yellow band and a black bottom and so don't do a great job mimicking anything and so will be eaten. Thinking about the four possible haplotypes, y-B has high marginal fitness as due to its combo of dominant alleles it'll always produce a bicoloratus phenotype. Likewise the Y-b haplotype has high marginal fitness, as it does well in the homozygous state (*silvana* phenotype), and when it is paired with the y-B allele. However, the Y-B and y-b haplotypes fair less well as they carry two alleles that don't work well with each other and so are often individuals who suffer high rates of predation.

If no recombination occurs between these loci ($r = 0$, Figure 14.13), then the Y-B and y-b are selected out of the population, and the y-B and Y-b can be stably maintained. However, when there's too much recombination between our loci (e.g. $r = 0.4$, Figure 14.13) the high-fitness haplotypes keep getting ripped apart by recombination and the Y-b is lost from the population as it's recessive advantage is lost as it's too often being broken up by recombination in heterozygotes.

14.3.8 Supergenes to the rescue!

So our polymorphisms can only be maintained if they are tightly linked, i.e if these alleles arose at loci that are genetically close to each other. But how is it possible that these alleles arose close to

"coadapted combinations of several or many genes locked in inverted sections of chromosomes and therefore inherited as single units." DOBZHANSKY (1970) on supergenes.

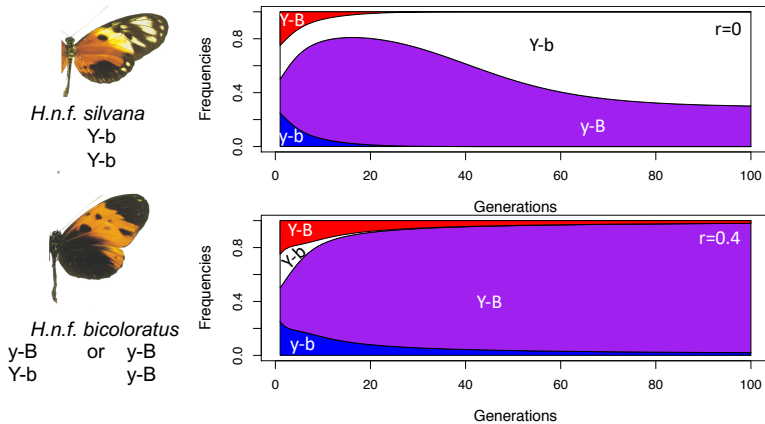
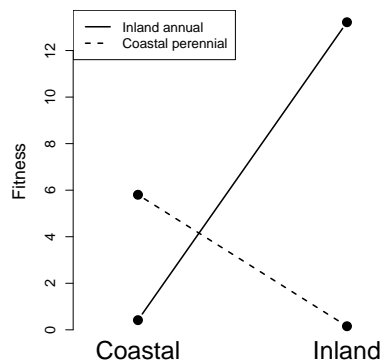


Figure 14.13: Left column a hypothetical two locus model to describe the *H. numata silvana* and *bicoloratus* morphs.. Right column the frequency dynamics of the four haplotypes under two different recombination regimes. The model has negative frequency dependent selection acting to increase the frequency of the mimicry morph that is rarer in the population. While all individuals with genotypes corresponding to a mixed phenotype, e.g. *YY BB*, have very low fitness as they mimic no Melinaea and so are quickly eaten. Butterflies cropped from JORON *et al.* (2006) cropped, licensed under CC BY 4.0, Code here.

each other? Well the trick is that they don't necessarily have to arise very close to each other. If such a system is polymorphic but being regularly broken up by recombination, a chromosomal inversion—the flipping around of a whole section of chromosome—can arise and will suppress recombination. Imagine that our two loci are far apart genetically, and a chromosomal inversion arises on the *Y-b* background forming the *b-Y* haplotype. This inverted haplotype will not recombine with the *y-B* haplotype when it is present in a heterozygote, thus it is not broken down by recombination. This inverted haplotype, which enjoys the fitness benefits of the *Y-b*, can therefore replace the *Y-b* haplotype in the population. The two other low fitness haplotypes will disappear as they are no longer being generated by recombination, leaving just the *y-B* and *b-Y*. The polymorphism system now behaves like alleles at a single locus, a super gene (e.g. like $r = 0$ in Figure 14.13).

Now the *H. numata* system is vastly more complicated than our toy two locus system, presumably involving many changes and refinements, but the same principle holds (JORON *et al.*, 2011). The differences between the different *H. numata* mimicry morphs is found on a single chromosome, and the inheritance behaves as if controlled by a single locus (albeit with many alleles). The *H. n. f. silvana* individuals carry a recessive haplotype of alleles that is known to be locked together by a $\sim 400\text{kb}$ inversion, that is a different chromosomal orientation from the *bicoloratus* allele (haplotype) which acts as

a dominant allele. Other alleles at this same chromosomal region provide the genetic basis of the other morphs, and sometimes correspond to further inversions with a range of dominance relationships.



Local Adaptation, Speciation, and Inversions. Inversions have long been thought to play an important role in local adaptation and speciation. One example of an inversion underlying local adaptation occurs in *Mimulus guttatus*, in Western North America, where there are annual and perennial ecomorphs with very different life history strategies (see Figure 14.14). The perennial form grows in many places along the Pacific coast, and in other places with year around moisture; it invests a lot of resources in achieving large size and laying down resources for the next year, and as a result flowers late. The annual form grows inland, e.g. the California central valley, where it has to invest all its effort in flowering rapidly before the long, hot, dry summer. Neither ecomorph does well in the other's environment. The perennials get crisped before they have a chance to flower, while the annuals suffer from high rates of herbivory and cannot tolerate the salt spray. LOWRY and WILLIS (2010) found that large inversion controlled a lot of the phenotypic variation in flowering time and a range of other morphological differences between these two morphs. They also showed that the inversion controlled a reasonable proportion of the differences in fitness in the field, consistent with it underlying the fitness tradeoffs involved in local adaptation.

Why would an inversion be involved in locking together local adapted alleles? The basic idea, like above, is an inversion can be selected for we have two (or more) loci segregating for locally adapted alleles (Figure 14.15). Locally advantageous haplotypes are in danger of being broken up by recombination with maladapted haplotypes, which are constantly being introduced into each population by migration from the other. If an inversion arises that locks these alleles

Figure 14.14: **Left)** A coastal perennial and an Inland annuals *Mimulus guttatus* LOWRY and WILLIS (2010), image from LOWRY and WILLIS (2010) licensed under CC BY 4.0.

Right) A reciprocal transplant experiment showing that coastal perennial and an Inland annuals are locally adapted to their respective habitats. Data from LOWRY and WILLIS (2010), Code here..

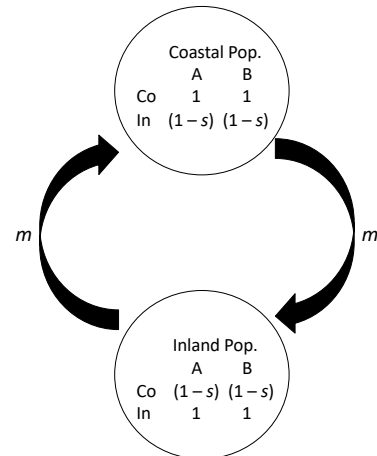


Figure 14.15: A two locus, two population migration-selection balance system. Two loci A and B segregate for an Inland and Coastal adapted alleles.

together in one population, it can be selected for as does not suffer the ill effects from recombination with migrating maladaptive haplotype.

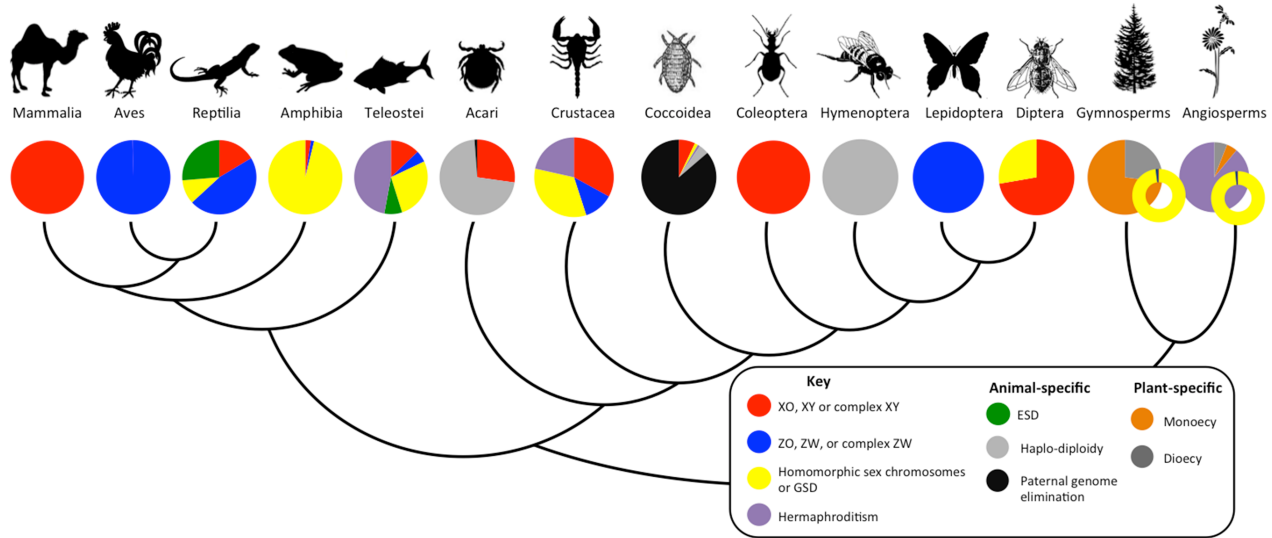


Figure 14.16: Diversity of sex determination systems for representative plant and animal clades. Figure and caption from BACHTROG *et al.* (2014), licensed under CC BY 4.0.

14.3.9 Sex Chromosomes and the dynamics of selection and recombination.

The evolution of sex chromosomes and new systems of genetic sex determination provide a beautiful demonstration of the interplay of selection and recombination. But first it's worth taking a step back and thinking the difference between an species being sexual, having male and female gametes, and having separate sexes (i.e. males and females), and the mechanisms for determining the sexes. Many species are sexual but with no separate sexes or even male or female gametes. The production of different sized gametes (anisogamy) has arisen a number of times in multi-cellular life, with male and female gametes are defined by their relative sizes. The smaller, and often more mobile, gametes are defined male gametes (e.g. sperm), while the larger, well provisioned, and often less mobile are defined as female gametes (e.g. egg cell). The evolution of anisogamy is thought to be due to disruptive selection due to a tradeoff pulling in opposite directions towards mobile gametes able to move further and in the opposite direction towards better provisioned gametes better able to build larger zygotes. In many organisms individuals can produce both male and female gametes, while some species have evolved separate sexes, likely in part as an inbreeding avoidance mechanism. There is huge diversity in sex determination mechanisms across the eukaryotic tree (Figure 14.16). This is all to say, that biology is wonderfully diverse and complicated.

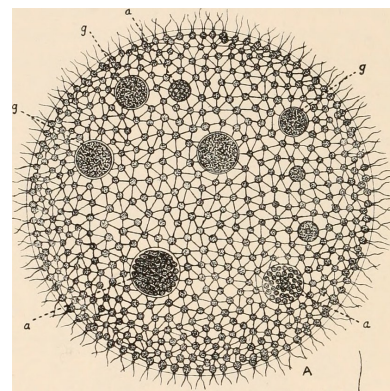


Figure 14.17: *Volvox aureus*, Volvox are spherical, multicellular green algae. The surface is made up of a single layer of somatic cells (up to 50k cells) beating their flagella. Some species of Volvox have individuals with both male and female gametes, being made here in the germ cells (a and g respectively) in the middle of the sphere. Some Volvox have separate sexes, where different individuals produce male and female gametes.

In mammals, and many other systems with genetic sex determination, the genes responsible for sex determination lie on a pair of heteromorphic sex chromosomes, i.e. pair of chromosomes that are quite different in size. In mammals where most males are XY and females XY. Where the male determining Y chromosome that has a very small gene content compared to the X chromosome. But in other groups such as birds, and some snakes, sex determination is a ZW system with females being ZW and males being ZZ. In those systems females carry a gene poor W with males being the homogametic sex, carrying two Zs. If you are still reading send Graham a picture of Nettie Stevens, she discovered sex chromosomes in 1905 (STEVENS, 1905). These examples of heteromorphic sex chromosomes, and many others like them, are thought to have arisen from an ancestral pair of autosomes? What then explains their evolution?

One broad explanation for the evolution of sex chromosome is illustrated in Figure 14.18 and goes as follows:

1. There are a pair of ancestral autosomes with sexually-antagonistic male-beneficial, female-detrimental alleles segregating on them (the converse can occur but aren't central to the evolution of Y chromosomes). These alleles can persist in the population for some time but are eventually lost due to their cost in females.
2. A dominant, male-determining allele arises on one of the chromosomes. Let's call this chromosome our proto-Y and the other our proto-X. All individuals who are heterozygous for the Proto-Y will be male, individuals who are homozygous for the proto-X. No individuals will be homozygous for the proto-Y, as individuals can receive at most one Proto-Y, that of their father.
3. Our sexually-antagonistic alleles benefit from being on the same chromosome as our male-determining allele as then they are guaranteed to be in males. However, if they recombine off the proto-Y onto the proto-X they are at a disadvantage.
4. If an inversion arises on the background of the proto-Y chromosome it can lock together the male-determining allele and some of our sexually-antagonistic alleles. This inversion can initially spread as it gains the benefit of the sexually-antagonistic alleles without the cost of recombination. This inversion can't spread to fixation as Fisherian selection on the sex ratio keeps it in check.
5. Further inversions can potentially cement additional sexually-antagonistic alleles into tight linkage with the male-determining allele.

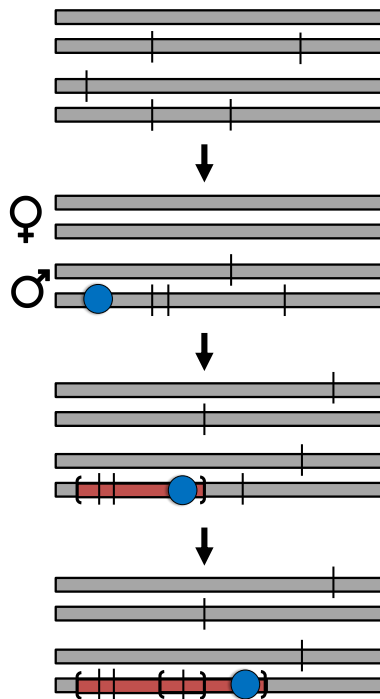


Figure 14.18: A cartoon of formation of a neo-Y chromosome and subsequent suppression of recombination. A pair of orthologous autosomes is shown in the top most panel. Sexually-antagonistic male-beneficial, female-detrimental alleles are shown as vertical lines. A newly arising dominant, male-determining allele is shown as a blue circle. The inversions are shown as brackets. The non-recombining region linked to the sex determining allele coloured red.

Sex chromosomes, under this hypothesis, are super genes locking together sex determination and sexually-antagonistic alleles. Our male-beneficial, female-detrimental alleles work well on the background of the male-determining allele and poorly off it, that's exactly the supergene setup we encountered in Section 14.3.8. This sketch can be flipped to describe the evolution of ZY systems.



Figure 14.19: The sex-specific effects of the OB allele.

Image credits: Blue mbuna Male *L. fuelleborni* by Chnee2; OB Male *L. fuelleborni* by Dorenko; Brown ob *Tropheops* female by Alexandra Tyers; Female *L. fuelleborni* orange morph, by Mikko Stenberg

A colourful example of the initial conditions for the evolution of a novel sex determination system is offered in lake Malawi there are many very closely related cichlids species (ROBERTS *et al.*, 2009). In many of these species the males are brightly coloured to attract females, while the females are often brown to help them avoid predators. In some of these species there is an alternative orange morph, called the marmalade cat morph, which are cryptic against the rocky bottom of the lake. This morph is due to a dominant mutation called OB at the pax7, and the allele appears to be shared across many of these species. This OB allele works well in females, however, in the males the OB allele disrupts their bright colouration. Thus the OB polymorphism is sexually antagonistic, i.e. it works well in females and poorly in males.

Males carrying the male-deleterious OB allele are rarely found, despite the allele being common in females. Why is that? Well because the OB allele is tightly linked to a newly emerged female-determining allele (W), with males carrying two copies of the Z allele. Males usually are homozygous for the ob-Z haplotype, while females can be either orange (OB-W/ob-Z) or brown (ob-W/ob-Z). Recombination between these two loci seems to be very rare, and so the sexually an-

tagonistic allele OB appears to be mainly female specific. Thus the spread of this sex determining allele has potentially helped resolve sexually-antagonism while it aided its own spread. An inversion on the Z background would lock together these two alleles, and spread.

The degradation of heterogametic sex chromosomes. Our inversions on the neo-Y chromosome have created a issue (or conversely the neo-W in ZW systems). The inverted block, containing the male-determining allele, is now inherited as a non-recombining haplotype. Why's that? Well the inversion doesn't recombine in heterozygotes, and the neo-Y inversion region is only ever found in heterozygote males.¹ Thus the region of chromosome tied up within inversions is effectively asexual and subject to many of the issues that come along with that. The hitchhiking of deleterious alleles will be common and Muller's Rachet will begin to tick. Many mildly deleterious alleles will be allowed to fix through these mechanisms, leading to the accumulation of premature stop codons and silencing mutations in non-essential genes within the neo-Y inversion. The X chromosome will maintain copies of these genes, and sometimes the expression of these genes will have to be up-regulated in males to accommodate for the degradation of the Y based copy leading to lower dosage of these genes.² Transposable elements can also accumulate on the non-recombining section of the Y chromosome, some times in huge numbers, as the purging of these transposable elements will be inefficient in this region. But there's little to stop the non-recombining section of neo-Y chromosome from expanding more due to the short-sighted selection for inversions that further tie up sexually-antagonistic alleles. Our non-recombining section of the Y chromosome maybe expanding to occupy more of the chromosome, as it is losing functional genes and bloating up with repetitive DNA. Eventually much of what remains may be genes that are essential to male function, as is the case with old Y chromosomes such as humans.

¹ This differs from the situation that most other non-sex chromosome inversions find themselves in as they homozygous some of the time and so experience recombination.

² Indeed in some heterogametic sex chromosome systems there are evolved dosage compensation systems that deal specifically with these issues.

A.

An Introduction to Mathematical Concepts

"Now, in the first place I deny that the mathematical theory of population genetics is at all impressive, [... We] made simplifying assumptions which allowed us to pose problems soluble by the elementary mathematics at our disposal, and even then did not always fully solve the simple problems we set ourselves. Our mathematics may impress zoologists but do not greatly impress mathematicians."—HALDANE

Throughout these notes we make use of mathematical concepts, many of which are based in probability theory and statistics. Here we briefly review some of these concepts. The wikipedia pages on statistics and math topics are often excellent introductions and worth consulting if you want to know more. Parts of this primer were originally written by Sebastian Schreiber and myself for our Fall quarter of the PBG core (although I take full credit for any errors subsequently introduced). Some of these concepts may go beyond what you have covered in previous courses. The notes do not rely on you knowing all of these results, but I'll refer to this appendix when these concepts first come up in the main body of the notes. To answer the questions in the first chapter you will need to know some basic rules of probability, so reviewing Sections A.2.2 and A.2.1 below would be a good place to start.

A.1 Calculus

In evolutionary genetics we're often interested in how quantities change over time, and so we're interested in the rate of change over time. This particular obsession is shared with much of science and so the concepts we make use of pop up in many other fields. The *derivative* $f'(a)$ of a function $f(x)$ at $x = a$ represents the instantaneous rate of change of the function, $\frac{df(x)}{dx}$, at $x = a$ or, equivalently, the slope of the graph of the function at $x = a$. A derivative of zero indicates a local maxima, minima, or saddle point of the function see Figure A.1.

To give a physical example, imagine that the derivative of position

From Haldane's entertaining response to Mayr's criticism of population genetics. .

HALDANE, J. B. S., 1964 A defense of beanbag genetics. Perspectives in Biology and Medicine 7(3): 343–360

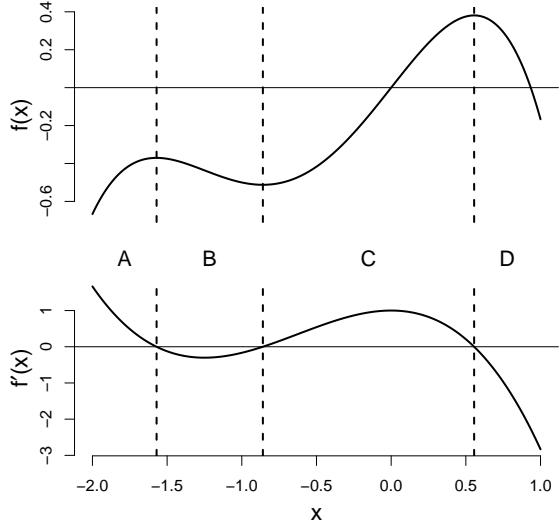


Figure A.1: **Top**) An example function, $f(x) = x - (5/6)x^3 - (1/3)x^4$, and **Bottom**) its derivative
 $f'(a) = 1 - 3(5/6)x^2 - 4(1/3)x^3$
Code here.

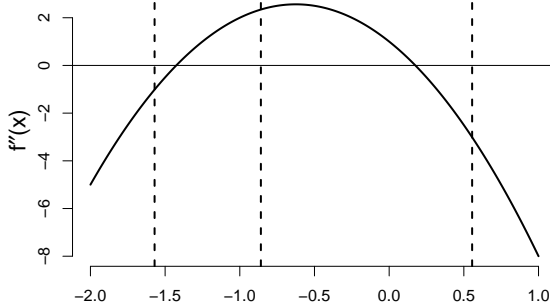
with respect to time gives the (instantaneous) speed of a car. Think of the top panel of Figure A.1 as showing a car driving up and down an alley, the page, with $f(x)$ giving the car's position at time x . The bottom panel shows the car's speed, with the sign (i.e. + or -) of the derivative giving the direction of movement. Moving from left along the x (time) axis, in time period A our car is moving up the alley (page), the speed is positive (i.e. $f'(a) > 0$). In the time period B, the car is reversing down the alley, its speed is negative ($f'(a) < 0$). As we move from A to B the car is beginning to slow down, i.e. the derivative gets small in magnitude, as it's going to reverse direction at time indicated by the first dotted line at the point. At the dotted line between A and B, we are at the moment when the car is changing direction, the car is stationary, its speed is zero (i.e. $f'(a) = 0$).

We'll sometimes want to know about the *second derivative* of f , denoted by $f''(a)$ or $\frac{d^2f(a)}{dx^2}$. The second derivative measures the rate at which the first derivative is changing i.e. the concavity/convexity of the function. See Figure A.2. In our physical example, the second derivative with respect to time is the (instantaneous) acceleration of the car, as it is the rate of change in the speed of the car (signed by whether it's accelerating in a positive or negative direction). One useful property of the second derivative is that it is positive at local maxima of the function, and negative for local minima of the function.

A.1.1 Approximating functions by Taylor Series.

A wonderful thing about derivatives is that they allow us to approximate complicated, nonlinear functions by linear functions (this is

Figure A.2: Code here.



called a first-order Taylor approximation). Namely, a *first order approximation* of $f(x)$ at $x = a$ is given by

$$f(x) \approx f(a) + f'(a)(x - a) \text{ for } x \text{ near } a \quad (\text{A.1})$$

Returning to our car example, this corresponds to trying to guess the position of the car extrapolating from its current location and speed. We'll do well when the car is traveling at a relatively constant speed, i.e. isn't accelerating or decelerating too fast.

Two common first-order Taylor approximations that we'll encounter throughout the notes are

$$\exp(x) \approx 1 + x \text{ for } x \text{ near } 0 \quad (\text{A.2})$$

$$(1 - x)^k \approx 1 - kx \text{ for } x \text{ near } 0 \quad (\text{A.3})$$

we'll also use the Taylor approximation given by eqn (A.2) as a trick to write

$$(1 + x)^L \approx \exp(Lx) \text{ for } x \text{ near } 0, \quad (\text{A.4})$$

which allows us to move from a geometric decay to an exponential decay. As a generalization of this, we'll approximate the product

$$\prod_{i=1}^L (1 + x_i) \approx \exp\left(\sum_{i=1}^L x_i\right) \text{ if all } x_i \text{ are near } 0, \quad (\text{A.5})$$

which is useful as it allows us move from a product to thinking about a sum (where averages are easier to think about).

We'll sometimes want more accuracy and so use a *second order approximation*, i.e. we will approximate the graph of a function with a parabola instead of a line (see Figure A.4). This is often useful when examining the effects of stochasticity on some process. These second-order Taylor approximations take the form:

$$f(x) \approx f(a) + f'(a)(x - a) + f''(a)(x - a)^2 / 2 \quad (\text{A.6})$$

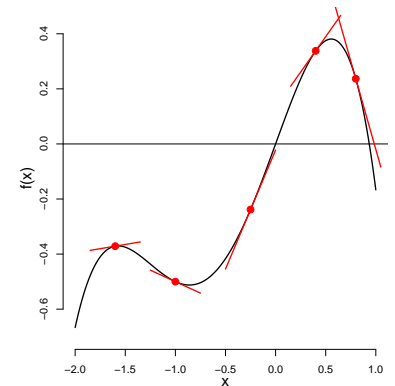


Figure A.3: Our function from the top panel of Figure A.1 approximated by first-order taylor approximations (red lines) at a variety of points a (solid dots). Note how the approximation breaks down away from the dot, I stop plotting the approximation a little away from the dot for ease of presentation. Code here.

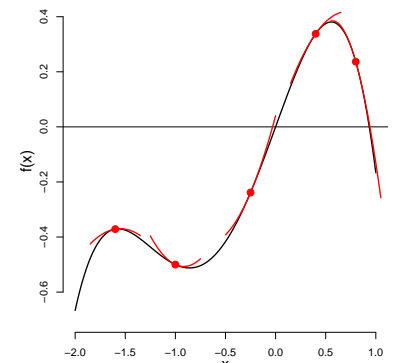


Figure A.4: Our function from the top panel of Figure A.1 approximated by second-order taylor approximations (red lines) at a variety of points a (solid dots). Code here.

where $f''(a)$ denotes the *second derivative* of f at $x = a$. In our car example, this is equivalent to predicting the location of the car from its speed *and* acceleration.

One place this second order approximation is useful is for the log function and yields

$$\log(1 + x) \approx x - x^2/2 \text{ for } x \text{ near 0.} \quad (\text{A.7})$$

A.1.2 Integrals

Regarding *integrals* $\int_a^b f(x) dx$, just remember that they represent the *signed area* “under” the graph of $y = f(x)$ over the interval $[a, b]$.

A.2 Probability

Evolution is fundamentally a random process. Which individuals live, die, and reproduce in any given moment is far from predictable. The randomness of Mendelian transmission, what genetic material is transmitted to the next generation, reflects randomness at the molecular and cellular level. While this makes it impossible to predict the outcome for a given individual we can speak of average outcomes and the statistical properties of evolutionary processes. Indeed evolution is a statistical process, evolution occurs because some types of individuals, and alleles, on average leave more offspring to subsequent generations. Thus to understand the details of models of evolutionary change we will have to understand something about probability and statistics.

A.2.1 Random Variables

A *random variable* X , roughly, is a variable that takes on values drawn randomly from some probability distribution. There are two major types of random variables, discrete and continuous. For a discrete random variable, think of it as a person calling out numbers by drawing them randomly out of a hat with some distribution of numbered slips of paper. We use uppercase X to think about the number that might be drawn (before it is drawn) and lowercase x to denote the number that is actually drawn. *Discrete random variables* take on a countable number of values, say x_1, x_2, \dots , with some probabilities p_1, p_2, \dots . We can denote this assumption as

$$\mathbb{P}[X = x_i] = p_i \text{ “the probability that } X \text{ equals } x_i \text{ is } p_i\text{”}$$

Continuous random variables, which can take on values in a continuum, are characterized by their *probability density function* $p(x)$ i.e. a function that satisfies $p(x) \geq 0$ for all x and $\int_{-\infty}^{\infty} p(x) dx = 1$. For

example, think about the precise time of day a baby is born in a hospital (not just the hour or the minute, where discrete random variables would suffice, but the precise moment). For these variables,

$$\mathbb{P}[a \leq X \leq b] = \int_a^b p(x) dx \text{ “the probability that } X \text{ is interval } [a, b] \text{ equals the area under the curve } p(x) \text{ from } a \text{ to } b”$$

for example, we could ask the probability that a baby was born somewhere between midnight and 12.18am.

A.2.2 Basic Rules of Probability

Imagine a fairground game where you reach into a box and pull out an egg. There are 100 eggs in the box, 57 of them are empty. Forty three have a toy in them. There are eggs with a stuffed dog toy, eggs with a cat toy, eggs with a lizard toy, eggs with both a dog and cat toy in them. The counts of each type of egg are shown in Figure A.5.

Question 1. You reach into the box and pull out one egg:

- i) For each egg type (dog alone, cat alone, lizard, dog+cat, and no prize), what is the probability that you get an egg of that type? What do these probabilities sum to?
- ii) What's the probability of getting an egg with a dog? What is the probability of getting an egg with a dog in it *or* an egg without a dog in it.
- iii) What's the probability of getting an egg with a dog in it *or* an egg with a lizard.

These questions above illustrate the principle that if events A & B are mutually exclusive then $\mathbb{P}(A \text{ or } B) = \mathbb{P}(A) + \mathbb{P}(B)$, following from these $\mathbb{P}(A \text{ or not } A) = \mathbb{P}(A) + \mathbb{P}(\text{not } A) = 1$. What is the probability of getting an egg with a dog *or* a cat? Well, for events that are not mutually exclusive we need to discount the sum of the probabilities by their overlap, giving

$$\mathbb{P}(A \text{ or } B) = \mathbb{P}(A) + \mathbb{P}(B) - \mathbb{P}(A \& B). \quad (\text{A.8})$$

We call $\mathbb{P}(A \& B)$ the joint probability of A & B.

Question 2. What is the probability $\mathbb{P}(\text{dog or cat})$?

Conditional probability We often want to know the *conditional probability*, the probability of an event conditional on some other particular event. For example, the conditional probability of getting a cat toy given that I've pulled out an egg containing a dog (recall that ten of the hundred eggs contain both a dog and a cat toy.). We write this as $\mathbb{P}(\text{cat}|\text{dog})$, where we read $|\text{dog}$ as ‘given dog’ or ‘conditional on dog’.

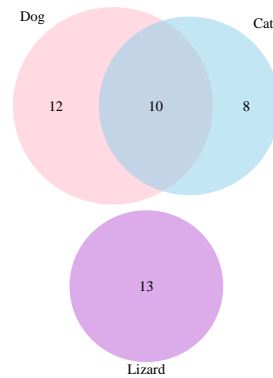


Figure A.5: Venn diagram of fair-ground game toys, there are a hundred eggs in total, including 57 eggs with no prize that are not shown. [Code here.](#)

The rule of conditional probabilities is that

$$\mathbb{P}(A|B) = \frac{\mathbb{P}(A \ \& \ B)}{P(B)} \quad (\text{A.9})$$

we can now answer

Question 3. What is $\mathbb{P}(\text{cat}|\text{dog})$?

Explain the underlying intuition of your answer?

By rearranging eqn (A.9), we obtain the rule that

$$\mathbb{P}(A \ \& \ B) = \mathbb{P}(A|B)\mathbb{P}(B). \quad (\text{A.10})$$

Thus we can always obtain the joint probability of A & B by multiplying the conditional probability by the probability of the event we are conditioning on. Equivalently, we could have computed the joint probability as

$$\mathbb{P}(A \ \& \ B) = \mathbb{P}(B|A)\mathbb{P}(A). \quad (\text{A.11})$$

these two ways of writing the same thing will come in useful in just a moment.

The total probability of an event can be obtained by summing over all of the L mutually exclusive ways that A can happen

$$\mathbb{P}(A) = \sum_{i=1}^L \mathbb{P}(A \ \& \ B_i) = \sum_{i=1}^L \mathbb{P}(A|B_i)\mathbb{P}(B_i) \quad (\text{A.12})$$

where B_1, \dots, B_L give the mutually exclusive events that can occur alongside our event B. This is the *law of total probability*. For example, we can write the probability of obtaining a cat as

$$\mathbb{P}(\text{cat}) = \mathbb{P}(\text{cat} \ \& \ \text{dog}) + \mathbb{P}(\text{cat} \ \& \ \text{not dog}). \quad (\text{A.13})$$

Independence Two events are *independent* of each other if

$$\mathbb{P}(A \ \& \ B) = \mathbb{P}(A)\mathbb{P}(B) \quad (\text{A.14})$$

this requirement implies independence because the conditional and unconditional probabilities are equal, $P(A) = P(A|B)$, i.e. I learn nothing about the event A from the event B having occurred. For example, if I draw two eggs with replacement from the box the probability of getting a lizard then a dog is $\mathbb{P}(\text{lizard then}\&\text{dog}) = \mathbb{P}(\text{lizard})\mathbb{P}(\text{dog})$.

Bayes Rule We often want to reverse of conditional probability statements, i.e. turn the statement of $P(B|A)$ into the statement of $P(A|B)$. We have two different ways of expressing the joint probability in terms of conditional probabilities. Because they each equal the joint probability, they are equal to each other, meaning

$$\mathbb{P}(B|A)\mathbb{P}(A) = \mathbb{P}(A|B)\mathbb{P}(B). \quad (\text{A.15})$$

Rearranging eqn (A.15) we obtain

$$\mathbb{P}(B|A) = \frac{\mathbb{P}(A|B)\mathbb{P}(B)}{\mathbb{P}(A)} \quad (\text{A.16})$$

Equation (A.16) is also called “*Bayes’ Rule*” or “*Bayes’ Theorem*,” and it which allows us to reverse the variable we condition on.

Question 4. Use Bayes’ rule to calculate $\mathbb{P}(\text{dog}|\text{cat})$ from the conditional probability you calculated in Question 3.

A.2.3 Expectation of a Random Variable

The *expectation of a random variable* is the point at which the distribution is “balanced”. For discrete random variables it is given by

$$\mu = \mathbb{E}[X] = p_1x_1 + p_2x_2 + \dots + \quad (\text{A.17})$$

The average outcome ¹ over a set of independent events is an estimate of the mean $\hat{\mu}$, where the hat denotes that it is an estimate. A more precise interpretation of the relationship between the average and the expectation is given by the law of large numbers described below. For a continuous random variable,

$$\mathbb{E}[X] = \int x p(x) dx. \quad (\text{A.19})$$

For any “reasonable” function, one can define $\mathbb{E}[f(X)]$ by

$$\mathbb{E}[f(X)] = p_1f(x_1) + p_2f(x_2) + \dots \quad (\text{A.20})$$

for discrete random variables and

$$\mathbb{E}[f(X)] = \int f(x)p(x) dx \quad (\text{A.21})$$

for continuous random variables.

A particularly important choice of f is $f(x) = (x - \mu)$. In this case,

$$\sigma^2 = \mathbb{E}[(X - \mu)^2] = \mathbb{E}[X^2] - \mu^2 \quad (\text{A.22})$$

is the *variance of X* which measures the mean deviation squared around the mean i.e. “the spread around the mean”. σ (i.e. the square root of the variance) is the standard deviation of X . We can compute the sample variance as

$$\widehat{\sigma^2} = \frac{1}{L-1} \sum_{i=1}^L (X_i - \bar{X})^2 \quad (\text{A.23})$$

Note that the units of our variance will be the units of X^2 , e.g. if X is height measurements in cm the variance will have units cm^2 .

According to Pascal, the expectation is the excitement a gambler feels when placing a bet i.e. each term in the sum equals the probability of winning times the amount won. Apparently Pascal knew some unusually rational gamblers.

¹ Recalling that we compute average, the sample mean, of a set of numbers X_1, \dots, X_L as

$$\bar{X} = \frac{1}{L} \sum_{i=1}^L X_i \quad (\text{A.18})$$

where the bar over the X denotes that it is the average value of X .

One reason that the standard deviation is a more intuitive than the variance is that its units are the same as X , e.g. cms.

Another important choice of f is $f(x) = \log x$. Provided that X is positive, $\exp(\mathbb{E}[\log X])$ corresponds to the *geometric mean of X* . Alternatively $1/\mathbb{E}[1/X]$ corresponds to the *harmonic mean of X* .

Question 5. Your friend offers you a wager on the outcome of one round of playing the fairground egg game. She'll give you: \$1 for a only dog, \$2 for a only cat \$5 for an egg with a cat and a dog, and \$4 for a lizard. However, she'll take \$1 from you if you get an empty egg. What is your expected payout?

Some Useful Properties of Expectations. One of most useful mathematical properties of the expectation is its linearity, in that the expectation of a linear function of random variables is the linear function applied to the expectation, i.e.

$$\mathbb{E}[aX + bY + c] = a\mathbb{E}[X] + b\mathbb{E}[Y] + c \quad (\text{A.24})$$

where X and Y are random variables, and a , b , and c are constants. This holds regardless of whether X and Y are independent. Note, that our multipliers (a & b) must be constant, as this does not hold for the expectation of products of random variables. One sensible property of the linearity is the units of the mean is the same as our observation, for example if we change our measure height of adult height from inches to cm, the unit our mean also changes from inches to cm (as this change just involves multiplying by a number).

Using our linearity of expectations, we can obtain an analogous result for the variance

$$\text{Var}[aX + bY + c] = a^2\text{Var}[X] + b^2\text{Var}[Y] \quad (\text{A.25})$$

this holds if X and Y are independent variables, if they are not we need to account for their covariance. Note that the constant c has disappeared as the variance is a statement about the spread of the points around the mean, and so it doesn't matter how we shift the mean.

We are often interested in the expectation of a random variable X conditional on some event $Y = y$, this *conditional expectation* is

$$\mathbb{E}[X|Y = y] = \sum_{i=1}^L x_i \mathbb{P}(X = x_i | Y = y) \quad (\text{A.26})$$

summing over the L possible values X could take. For example, we could ask the expected payoff of your friend's wager conditional on knowing that you have an egg with a dog in it. With the analogous

expression for continuous random variables replacing the sum with an integral.

We can recover our total expectation from the conditional expectations by taking the sum of our conditional expectation over the values that Y could take, weighting each by their probability

$$\mathbb{E}[X] = \sum_{j=1}^M \mathbb{E}[X|Y = y_j] \mathbb{P}(Y = y_j) \quad (\text{A.27})$$

this is the law of total expectation, the analog to the law of total probability (eqn (A.12)). We can write this law more generally as $\mathbb{E}[\mathbb{E}[X|Y]]$, i.e. we are taking the expectation of our conditional expectation over Y .

A.2.4 Discrete Random Variable Distributions.

Important discrete random variables include

Binomial random variables count the number X of heads when flipping a coin n times whose probability of being heads is p . In which case,

$$p_i = \frac{n!}{i!(n-i)!} p^i (1-p)^{n-i} \quad 0 \leq i \leq n. \quad (\text{A.28})$$

For a binomial random variable, $\mathbb{E}[X] = np$ and $\sigma^2 = np(1-p)$. Examples are shown in Figure A.6, Note how the mass of the distribution becomes more centered on the mean for larger sample sizes, as the standard deviation increases only as \sqrt{n} . Another way that we can write that our observation i is drawn from the binomial distribution is $i \sim \text{Binomial}(p, n)$, where $i \sim$ is read as “ i is distributed as” (we will use the notation as short hand for random variable in the notes).

Geometric random variables count the total number of flips X before seeing a heads on a coin with probability p of being heads. In which case,

$$p_i = p(1-p)^{i-1} \quad i = 1, 2, \dots \quad (\text{A.29})$$

For a geometric random variable $\mathbb{E}[X] = 1/p$; if our coin is fair $p = 1/2$ we wait two flips for a head on average while if the coin-flip is very biased against heads $p \ll 1$ we can be waiting a very long time. The variance of a geometric random variable is $\sigma^2 = 1-p/p^2$, which means that the mass of the distribution is much more spread out if we consider the waiting time for rare events. See Figure A.7 for examples of the distribution.

Poisson random variables count the i events that occur in a fixed interval of time or space (t), when these events occur independently

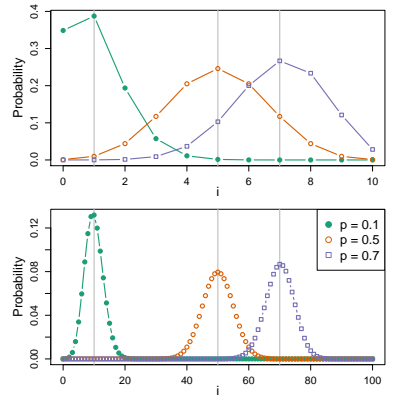


Figure A.6: Binomial distribution for a sample of $n = 10$ and $n = 100$, the vertical lines show the means np . Code here.

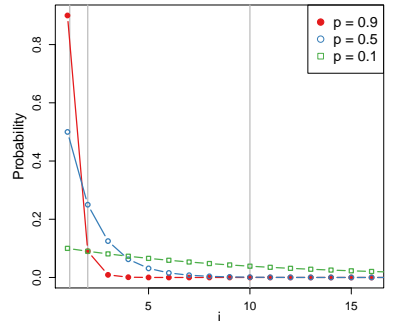


Figure A.7: Geometric distribution for different probabilities of success (p). The vertical lines show the means $1/p$. Code here.

of each other and of time. If λ events are expected to occur in this interval, then

$$p_i = \lambda^i e^{-\lambda} / i! \quad (\text{A.30})$$

For a random Poisson variable $\mathbb{E}[X] = \lambda$.

The form of this is less intuitive than that of the binomial. However, the Poisson is actually a limiting case of the binomial. Think of setting up a game of chance, where there's a very large number of coin flips ($n \rightarrow \infty$), but you've set the chance of heads on a single coin flip is very low ($p = \lambda/n \rightarrow 0$, where λ is a constant). Under these conditions you'd still expect some heads ($np = \lambda$), and the distribution of the number of heads is Poisson.² See Figure A.8 to see how well they match. Therefore, the Poisson represents a limit of the binomial for rare events.

A.2.5 Continuous Random Variable Distributions.

Important continuous random variables include

Uniform random variables correspond to “randomly” choosing a number in an interval, say $[a, b]$. The pdf for a uniform is

$$p(x) = \frac{1}{b-a} \text{ for } x \in [a, b] \text{ and 0 otherwise.} \quad (\text{A.32})$$

For a uniform random variable $\mathbb{E}[X] = (a+b)/2$.

Exponential random variables with rate parameter $\lambda > 0$ correspond to the waiting time for an event which occurs with probability $\lambda \Delta t$ over a time interval of length Δt . For these random variables

$$p(x) = \lambda \exp(-\lambda x) \text{ for } x \geq 0 \text{ and 0 otherwise.} \quad (\text{A.33})$$

For an exponential random variable $\mathbb{E}[X] = 1/\lambda$.

Normal random variables have the “bell-shaped” or “Gaussian” shaped distribution. They are characterized by two parameters, the mean μ and the standard deviation σ , and

$$p(x) = \frac{1}{\sigma\sqrt{2\pi}} \exp(-(x-\mu)^2/(2\sigma^2)). \quad (\text{A.34})$$

For a normal random variable $\mathbb{E}[X] = \mu$.

Multiple random variables

Covariance and Independence To fully specify multiple random variables, say X and Y , one needs to know their joint distribution. For

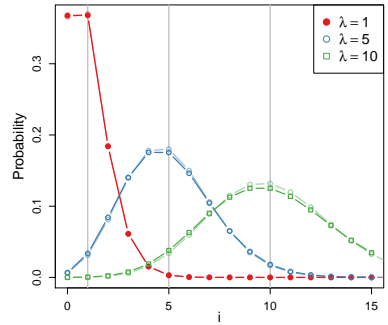


Figure A.8: Poisson distribution with different means (λ). The vertical lines show the means. The lighter coloured lines show a binomial with $n = 100$ and $p = \lambda/n$ to illustrate how well the Poisson approximates the binomial for rare events (it's hard to see them as they are close together!). Code here.

² To see this we substitute $p = \lambda/n$ into our binomial probability and take the limit as $n \rightarrow \infty$

$$\begin{aligned} p_i &= \frac{n!}{i!(n-i)!} p^i (1-p)^{n-i} \\ &= \lim_{n \rightarrow \infty} \frac{n(n-1)\dots(n-i+1)}{i!} \left(\frac{\lambda}{n}\right)^i \left(1 - \frac{\lambda}{n}\right)^{n-i} \\ &= \lim_{n \rightarrow \infty} \frac{n^i}{i!} \frac{\lambda^i}{n^i} \left(1 - \frac{\lambda}{n}\right)^n \\ &= \lim_{n \rightarrow \infty} \frac{\lambda^i}{i!} e^{-\lambda} \end{aligned} \quad (\text{A.31})$$

The third line assumes that $n - i \approx n$, which holds for $n \gg i$, and uses our exponential approximation given by eqn (A.4).

The Exponential distribution is the continuous-time version of the Geometric distribution. Informally this can be seen by considering the trials in the geometric distribution as corresponding to narrow time-intervals, where the probability of success is small. Then we can use our exponential approximation to the geometric probability (eqn (A.4)).

example, if X and Y are discrete random variables taking on the values x_1, x_2, x_3, \dots , then the joint distribution is given by

$$p_{i,j} = \mathbb{P}[X = x_i, Y = x_j] \text{ "the probability that } X \text{ equals } x_1 \text{ and } Y \text{ equals } x_2" \quad (\text{A.35})$$

for all i and j , see also our discussion around eqn. (A.14).

Alternatively, if X and Y are continuous random variables, then the joint distribution is a function of the form $p(x, y)$ which satisfies

$$\mathbb{P}[a \leq X \leq b, c \leq Y \leq d] = \int_a^b \int_c^d p(x, y) dx dy. \quad (\text{A.36})$$

where X and Y are said to be independent if we can write the joint density as a product of the probability density functions

$$p(x, y) = p(x)p(y). \quad (\text{A.37})$$

Given any function $f(x, y)$ of x and y , one can define the expectation $\mathbb{E}[f(X, Y)]$ by integrating with respect to the distribution.

Namely,

$$\mathbb{E}[f(X, Y)] = \int \int f(x, y)p(x, y) dx dy \text{ for continuous case and } \sum_i \sum_j f(x_i, x_j)p_{i,j} \text{ in discrete case} \quad (\text{A.38})$$

The covariance of X and Y is given by

$$\text{Cov}(X, Y) = \mathbb{E}[(X - \mu_X)(Y - \mu_Y)] = \mathbb{E}[XY] - \mu_X\mu_Y. \quad (\text{A.39})$$

X and Y are said to be *uncorrelated* if their covariance equals zero. If X and Y are independent, then they are guaranteed to be uncorrelated, but it is possible to construct X and Y to be uncorrelated but not independent.

Binary variable correlations One application of our covariance formula is to two binary variables, for example taking values A/a and B/b . Let's set $X = 1$ if A , and $X = 0$ otherwise, and $Y = 1$ if B . For example, you could imagine drawing a once from a deck of cards and A being the event of drawing an queen or a jack, with a being any other type of card, and B being that the card is a heart and b it being any other suit. So $XY = 1$ if our card is a Queen or Jack of Hearts, and zero otherwise. Then

$$\mathbb{E}[XY] - \mathbb{E}[X]\mathbb{E}[Y] = \mathbb{P}(X = A, Y = B) - \mathbb{P}(X = A)\mathbb{P}(Y = B) = p_{AB} - (p_A p_B) \quad (\text{A.40})$$

where p_{AB} is the frequency of AB , eg. the proportion of cards that are the Queen or Jack of hearts in our deck, and p_A is the (marginal) frequency of B , e.g. the proportion of Heart suite cards (and similarly for p_B).

Question 6. What is the covariance for A and B in our deck of cards example?

Sample Covariance and Correlation We can calculate the *sample covariance* for X and Y of a set of observations of X_1, \dots, X_L and Y_1, \dots, Y_L , where these observations are paired (X_i, Y_i) as

$$\widehat{\sigma_{XY}^2} = \frac{1}{L-1} \sum_{i=1}^L (X_i - \bar{X})(Y_i - \bar{Y}) \quad (\text{A.41})$$

this captures the extent to which two sets of numbers covary. For example, the running speeds of kids in a race at age 8 and 9 positively covary. Example datasets are shown in Figure A.9.

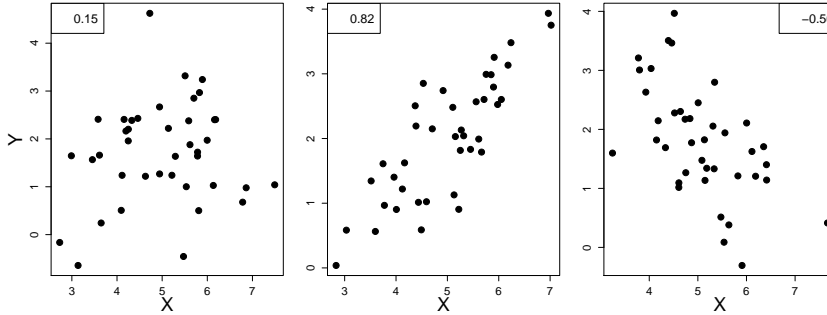


Figure A.9: Examples of datasets where pairs of variables show varying degrees of covariance, the sample correlation ($\widehat{\rho_{XY}}$) is shown in the top corner. [Code here.](#)

To move covariances to a more understandable scale we can divide through by the product of the standard deviations

$$\text{Cor}(X, Y) = \rho_{XY} = \frac{\sigma_{XY}}{\sigma_X \sigma_Y} \quad (\text{A.42})$$

this is the *correlation* of our variables X and Y , if we calculate it for our sample it is our *sample correlation*. A correlation can range between 1, perfectly correlated, to -1 perfectly negatively correlated. If $\rho_{XY} = 0$ the variables are said to be uncorrelated.

Fitting a linear regression using least squares. We often want to approximate the relationship between our two variables X and Y by the best fitting linear relationship predicting Y value from their observed X value. For example, think of a linear prediction of a child's weight from their height. See Figure A.10 for an example plot. To do this we can think of approximating the Y_i that accompanies the X_i value for the i^{th} pair of data points by

$$Y_i \approx a + bX_i \quad (\text{A.43})$$

where a and b are the intercept and slope of a line.

What is the best fitting line? Well one common definition of the optimal fit is the choice of a and b that minimize the squared error between the observed (Y) and their predicted values, i.e.

$$\sum_{i=1}^L (Y_i - a - bX_i)^2 \quad (\text{A.44})$$

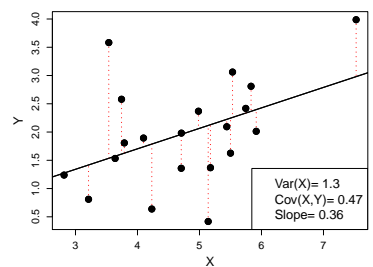


Figure A.10: An example of a linear regression with best fitting least-squares line. The sample variance and covariance are given, so that you can see for yourself that the best fitting slope is just the ratio of these two. [Code here.](#)

here $(Y_i - a - bX_i)^2$ is the squared residual error, the square of the length of the dotted lines in Figure A.10. The best fitting slope, i.e. that with least squared error, is

$$b = \widehat{\sigma_{XY}^2} / \widehat{\sigma_X^2} \quad (\text{A.45})$$

i.e. the sample covariance of X and Y divided by the sample variance of X . Thus the slope will be of the same sign as the covariance, and will be larger in magnitude when the covariance of X and Y is a large proportion of the variance of X .

This least squares fit is the solution to the linear regression

$$Y_i \sim a + bX_i + \epsilon_i \quad (\text{A.46})$$

where the errors (ϵ_i) are uncorrelated across data points with an expectation of zero and constant but unknown variance. These assumptions would hold for example if $\epsilon_i \sim \text{Normal}(0, \sigma)$.

We often want to include additional terms in our regression, or have more complicated error structures, but these extensions can usually be understood as simple extensions of this machinery. For example, least-squares can also be used to fit a non-linear function of X , $f(X, \Omega)$, where we minimize

$$\sum_{i=1}^L (Y_i - f(X_i; \Omega))^2 \quad (\text{A.47})$$

over our choices of parameters Ω . Often there is no analytical solution, i.e. no equivalent of eqn. A.45, and the answer must be found computationally exploring over choices of Ω (using tools available in R and other programming languages). Throughout the book we use non-linear least squares to fit various models to data.

Useful Properties of Covariances. Following from the linearity of expectation, eqn (A.24), if we rescale X to $mX + n$ and Y to $oY + p$ then

$$\text{Cov}(mX + n, oY + p) = (mo)\text{Cov}(X, Y) \quad (\text{A.48})$$

Such linear transforms leaves our correlation unaffected, as it cancels out of the top and bottom of eqn (A.42). While it multiplies the linear slope by m/o . Thus for our correlation it does not matter what units we measure X and Y . While our linear slope is always in the units of $\text{units}(X)/\text{units}(Y)$, for example m/s if we were predicting the distance (Y in meters) traveled by runners in time intervals (Y seconds).

Useful Limits.

Law of Large Numbers If X_1, X_2, \dots are a sequence of independent random variables (i.e. “the outcomes of a sequence of independent

experiments) with common expectation $\mu = \mathbb{E}[X_i]$, then

$$\frac{X_1 + \cdots + X_n}{n} \rightarrow \mu \text{ as } n \rightarrow \infty \text{ with probability one.} \quad (\text{A.49})$$

Hence, LLN implies that if you repeat a bunch of experiments and take the average outcome (\bar{X}) from the experiments, the value you get is likely to be close the expected outcome of the experiment.

Of course, in the real world, we can only perform a finite number of experiments in which case it is useful to have a sense of how much variation there will be in the average outcome. The central theorem is the key tool for understanding this variation.

Central Limit Theorem If X_1, X_2, \dots are a sequence of independent random variables (i.e. “the outcomes of a sequence of independent experiments) with common expectation $\mu = \mathbb{E}[X_i]$ and variance σ^2 , then

$$\frac{X_1 + \cdots + X_n - \mu n}{\sqrt{n}\sigma} \rightarrow \text{normal distribution with mean 0 and variance 1 as } n \rightarrow \infty \quad (\text{A.50})$$

Hence, for n large enough $X_1 + \cdots + X_n$ is approximately normally distributed with mean μn and variance $\sigma^2 n$. This is one of the reasons the normal distribution is so useful, many outcomes (e.g. phenotypes) have an approximately normal distribution as they are the combined outcome of many (somewhat) independent quantities.

Bibliography

- AGUADÉ, M., N. MIYASHITA, and C. H. LANGLEY, 1989 Reduced variation in the yellow-achaete-scute region in natural populations of *Drosophila melanogaster*. *Genetics* **122**: 607–615.
- AGUILLO, S. M., J. W. FITZPATRICK, R. BOWMAN, S. J. SCHOECH, A. G. CLARK, G. COOP, and N. CHEN, 2017, 08) Deconstructing isolation-by-distance: The genomic consequences of limited dispersal. *PLOS Genetics* **13**(8): 1–27.
- AKÇAY, E. and J. VAN CLEVE, 2016 There is no fitness but fitness, and the lineage is its bearer. *Phil. Trans. R. Soc. B* **371**(1687): 20150085.
- ALCAIDE, M., E. S. SCORDATO, T. D. PRICE, and D. E. IRWIN, 2014 Genomic divergence in a ring species complex. *Nature* **511**(7507): 83.
- ALEXANDER, D. H., J. NOVEMBRE, and K. LANGE, 2009 Fast model-based estimation of ancestry in unrelated individuals. *Genome research* **19**(9): 1655–1664.
- ALGEE-HEWITT, B. F., M. D. EDGE, J. KIM, J. Z. LI, and N. A. ROSENBERG, 2016 Individual identifiability predicts population identifiability in forensic microsatellite markers. *Current Biology* **26**(7): 935–942.
- ALLENDORF, F. W. and J. J. HARD, 2009 Human-induced evolution caused by unnatural selection through harvest of wild animals. *Proceedings of the National Academy of Sciences* **106**(Supplement 1): 9987–9994.
- ALVAREZ, G., F. C. CEBALLOS, and C. QUINTEIRO, 2009 The role of inbreeding in the extinction of a European royal dynasty. *PLoS One* **4**(4): e5174.

- ANDOLFATTO, P., 2007 Hitchhiking effects of recurrent beneficial amino acid substitutions in the *Drosophila melanogaster* genome. *Genome Res.* **17**: 1755–1762.
- ANDOLFATTO, P. and M. PRZEWORSKI, 2001 Regions of lower crossing over harbor more rare variants in African populations of *Drosophila melanogaster*. *Genetics* **158**: 657–665.
- AYLLON, F., E. KJÆRNER-SEMB, T. FURMANEK, V. WENNEVIK, M. F. SOLBERG, G. DAHLE, G. L. TARANGER, K. A. GLOVER, M. S. ALMÉN, C. J. RUBIN, and OTHERS, 2015 The vgl3 locus controls age at maturity in wild and domesticated Atlantic salmon (*Salmo salar* L.) males. *PLoS genetics* **11**(11): e1005628.
- BACHTROG, D., J. E. MANK, C. L. PEICHEL, M. KIRKPATRICK, S. P. OTTO, T.-L. ASHMAN, M. W. HAHN, J. KITANO, I. MAYROSE, R. MING, and OTHERS, 2014 Sex determination: why so many ways of doing it? *PLoS biology* **12**(7): e1001899.
- BARRETT, R. D. H., S. M. ROGERS, and D. SCHLUTER, 2008 Natural Selection on a Major Armor Gene in Threespine Stickleback. *Science* **322**(5899): 255–257.
- BARSON, N. J., T. AYKANAT, K. HINDAR, M. BARANSKI, G. H. BOLSTAD, P. FISKE, C. JACQ, A. J. JENSEN, S. E. JOHNSTON, S. KARLSSON, and OTHERS, 2015 Sex-dependent dominance at a single locus maintains variation in age at maturity in salmon. *Nature* **528**(7582): 405.
- BARTON, N. and G. HEWITT, 1981 A chromosomal cline in the grasshopper *Podisma pedestris*. *Evolution*: 1008–1018.
- BARTON, N. H., 2000 Genetic hitchhiking. *Philos. Trans. R. Soc. Lond., B, Biol. Sci.* **355**: 1553–1562.
- BASOLO, A. L., 1994 The dynamics of Fisherian sex-ratio evolution: theoretical and experimental investigations. *The American Naturalist* **144**(3): 473–490.
- BAZYKIN, A., 1969 Hypothetical mechanism of speciation. *Evolution* **23**(4): 685–687.
- BECQUET, C., N. PATTERSON, A. C. STONE, M. PRZEWORSKI, and D. REICH, 2007 Genetic structure of chimpanzee populations. *PLoS genetics* **3**(4): e66.

- BEGUN, D. J. and C. F. AQUADRO, 1992 Levels of naturally occurring DNA polymorphism correlate with recombination rates in *D. melanogaster*. *Nature* **356**: 519–520.
- BEISSINGER, T. M., L. WANG, K. CROSBY, A. DURVA-SULA, M. B. HUFFORD, and J. ROSS-IBARRA, 2016 Recent demography drives changes in linked selection across the maize genome. *Nature plants* **2**(7): 16084.
- BELL, M. A., M. P. TRAVIS, and D. M. BLOUW, 2006 Inferring natural selection in a fossil threespine stickleback. *Paleobiology* **32**(4): 562–577.
- BOX, G. E., 1979 Robustness in the strategy of scientific model building. In *Robustness in statistics*, pp. 201–236. Elsevier.
- BRADBURY, G. S., P. L. RALPH, and G. M. COOP, 2016 A spatial framework for understanding population structure and admixture. *PLoS genetics* **12**(1): e1005703.
- BRANDVAIN, Y., A. M. KENNEY, L. FLAGEL, G. COOP, and A. L. SWEIGART, 2014 Speciation and introgression between *Mimulus nasutus* and *Mimulus guttatus*. *PLoS Genetics* **10**(6): e1004410.
- BRAVERMAN, J. M., R. R. HUDSON, N. L. KAPLAN, C. H. LANGLEY, and W. STEPHAN, 1995 The hitchhiking effect on the site frequency spectrum of DNA polymorphisms. *Genetics* **140**: 783–796.
- BRODIE III, E. D., 1992 Correlational selection for color pattern and antipredator behavior in the garter snake *Thamnophis ordinoides*. *Evolution* **46**(5): 1284–1298.
- CAI, J. J., J. M. MACPHERSON, G. SELLA, and D. A. PETROV, 2009 Pervasive hitchhiking at coding and regulatory sites in humans. *PLoS Genet.* **5**: e1000336.
- CASSA, C. A., D. WEGHORN, D. J. BALICK, D. M. JORDAN, D. NUSINOW, K. E. SAMOCHA, A. O'DONNELL-LURIA, D. G. MACARTHUR, M. J. DALY, D. R. BEIER, and OTHERS, 2017 Estimating the selective effects of heterozygous protein-truncating variants from human exome data. *Nature genetics* **49**(5): 806.
- CHARLESWORTH, B., 2009 Effective population size and patterns of molecular evolution and variation. *Nature Reviews Genetics* **10**(3): 195.

- CHARLESWORTH, D., B. CHARLESWORTH, and M. T. MORGAN, 1995 The pattern of neutral molecular variation under the background selection model. *Genetics* **141**: 1619–1632.
- CHARLESWORTH, D. and V. LAPORTE, 1998 The male-sterility polymorphism of *Silene vulgaris*: analysis of genetic data from two populations and comparison with *Thymus vulgaris*. *Genetics* **150**(3): 1267–1282.
- CHEN, N., E. J. COSGROVE, R. BOWMAN, J. W. FITZ-PATRICK, and A. G. CLARK, 2016 Genomic Consequences of Population Decline in the Endangered Florida Scrub-Jay. *Current Biology* **26**(21): 2974 – 2979.
- COHEN, D., 1966 Optimizing reproduction in a randomly varying environment. *Journal of theoretical biology* **12**(1): 119–129.
- COLBERT, E. H., 1948 Evolution of the horned dinosaurs. *Evolution* **2**(2): 145–163.
- COOK, L. M., B. S. GRANT, I. J. SACCHERI, and J. MALLETT, 2012 Selective bird predation on the peppered moth: the last experiment of Michael Majerus. *Biology Letters* **8**(4): 609–612.
- COTTERMAN, C. W., 1940 A calculus for statistico-genetics. Ph. D. thesis, The Ohio State University.
- COUSMINER, D. L., D. J. BERRY, N. J. TIMPSON, W. ANG, E. THIERING, E. M. BYRNE, H. R. TAAL, V. HUIKARI, J. P. BRADFIELD, M. KERKHOF, and OTHERS, 2013 Genome-wide association and longitudinal analyses reveal genetic loci linking pubertal height growth, pubertal timing and childhood adiposity. *Human molecular genetics* **22**(13): 2735–2747.
- CUTTER, A. D. and J. Y. CHOI, 2010 Natural selection shapes nucleotide polymorphism across the genome of the nematode *Caenorhabditis briggsae*. *Genome Res.* **20**: 1103–1111.
- DARWIN, C., 1859 *On the Origin of Species by Means of Natural Selection*. London: Murray. or the Preservation of Favored Races in the Struggle for Life.
- DARWIN, C., 1876 The effect of cross and self fertilization in the vegetable kingdom: Murray. London, UK.
- DARWIN, C., 1888 *The descent of man and selection in relation to sex*, Volume 1. Murray.
- DEMPSTER, E., 1955 Maintenance of genetic heterogeneity. *Cold Spring Harb Symp Quant Biol* **20**: 25–32.

- DICKERSON, R. E., 1971 The structure of cytochrome c and the rates of molecular evolution. *Journal of Molecular Evolution* 1(1): 26–45.
- DOBZHANSKY, T., 1943 Genetics of natural populations IX. Temporal changes in the composition of populations of *Drosophila pseudoobscura*. *Genetics* 28(2): 162.
- DOBZHANSKY, T., 1951 *Genetics and the Origin of Species* (3rd Ed. ed.), pp. 16.
- DOBZHANSKY, T., 1970 *Genetics of the evolutionary process*, Volume 139. Columbia University Press.
- EDWARDS, A., 1961 The population genetics of “sex-ratio” in *Drosophila pseudoobscura*. *Heredity* 16(3): 291.
- EDWARDS, A. W., 1998 Natural selection and the sex ratio: Fisher’s sources. *The American Naturalist* 151(6): 564–569.
- ELTON, C., 1942 *Voles, mice and lemmings. Problems in population dynamics*. Oxford: Clarendon Press.
- ELYASHIV, E., S. SATTATH, T. T. HU, A. STRUTSOVSKY, G. MCVICKER, P. ANDOLFATTO, G. COOP, and G. SELLA, 2016 A genomic map of the effects of linked selection in *Drosophila*. *PLoS genetics* 12(8): e1006130.
- EWENS, W. J., 2010 What is the gene trying to do? *British Journal for the Philosophy of Science* 62(1): 155–176.
- EWENS, W. J., 2016 Motoo Kimura and James Crow on the Infinitely Many Alleles Model. *Genetics* 202(4): 1243–1245.
- FAITH, M. S., A. PIETROBELL, C. NUNEZ, M. HEO, S. B. HEYMSFIELD, and D. B. ALLISON, 1999 Evidence for independent genetic influences on fat mass and body mass index in a pediatric twin sample. *Pediatrics* 104(1): 61–67.
- FAY, J. C. and C. I. WU, 2000 Hitchhiking under positive Darwinian selection. *Genetics* 155: 1405–1413.
- FEDER, A. F., C. KLINE, P. POLACINO, M. COTTRELL, A. D. KASHUBA, B. F. KEELE, S.-L. HU, D. A. PETROV, P. S. PENNINGS, and Z. AMBROSE, 2017 A spatio-temporal assessment of simian/human immunodeficiency virus (SHIV) evolution reveals a highly dynamic process within the host. *PLoS pathogens* 13(5): e1006358.

- FERREE, P. M. and D. A. BARBASH, 2007 Distorted sex ratios: a window into RNAi-mediated silencing. *PLoS biology* **5**(11): e303.
- FISHER, R. A., 1915 The evolution of sexual preference. *The Eugenics Review* **7**(3): 184.
- FISHER, R. A., 1923 XXI.—on the dominance ratio. *Proceedings of the royal society of Edinburgh* **42**: 321–341.
- FISHER, R. A., 1930 *The genetical theory of natural selection: a complete variorum edition*. Oxford University Press.
- FRANCIOLI, L. C., A. MENELAOU, S. L. PULIT, F. VAN DIJK, P. F. PALAMARA, C. C. ELBERS, P. B. NEERINCX, K. YE, V. GURYEV, W. P. KLOOSTERMAN, and OTHERS, 2014 Whole-genome sequence variation, population structure and demographic history of the Dutch population. *Nature genetics* **46**(8): 818.
- FRENTIU, F. D., G. D. BERNARD, C. I. CUEVAS, M. P. SISON-MANGUS, K. L. PRUDIC, and A. D. BRISCOE, 2007 Adaptive evolution of color vision as seen through the eyes of butterflies. *Proceedings of the National Academy of Sciences* **104**(suppl 1): 8634–8640.
- GALEN, C., 1996 Rates of floral evolution: adaptation to bumblebee pollination in an alpine wildflower, *Polemonium viscosum*. *Evolution* **50**(1): 120–125.
- GALTIER, N., 2016 Adaptive protein evolution in animals and the effective population size hypothesis. *PLoS genetics* **12**(1): e1005774.
- GIGORD, L. D., M. R. MACNAIR, and A. SMITHSON, 2001 Negative frequency-dependent selection maintains a dramatic flower color polymorphism in the rewardless orchid *Dactylorhiza sambucina* (L.) Soo. *Proceedings of the National Academy of Sciences* **98**(11): 6253–6255.
- GILLESPIE, J. H., 1973 Natural selection with varying selection coefficients—a haploid model. *Genetics Research* **21**(2): 115–120.
- GILLESPIE, J. H., 1977 Natural selection for variances in offspring numbers: a new evolutionary principle. *The American Naturalist* **111**(981): 1010–1014.
- GILLESPIE, J. H., 2000 Genetic drift in an infinite population. The pseudohitchhiking model. *Genetics* **155**: 909–919.
- GINGERICH, P., 1983 Rates of evolution: effects of time and temporal scaling. *Science* **222**: 159–162.

- GRANT, P. R. and B. R. GRANT, 1995 Predicting microevolutionary responses to directional selection on heritable variation. *Evolution* 49(2): 241–251.
- GRANT, P. R. and B. R. GRANT, 2002 Unpredictable evolution in a 30-year study of Darwin's finches. *science* 296(5568): 707–711.
- GREMER, J. R. and D. L. VENABLE, 2014 Bet hedging in desert winter annual plants: optimal germination strategies in a variable environment. *Ecology Letters* 17(3): 380–387.
- GROGNET, P., H. LALUCQUE, F. MALAGNAC, and P. SILAR, 2014 Genes that bias Mendelian segregation. *PLoS genetics* 10(5): e1004387.
- HALDANE, J., 1942 The selective elimination of silver foxes in eastern Canada. *Journal of Genetics* 44(2-3): 296–304.
- HALDANE, J. and S. JAYAKAR, 1963 Polymorphism due to selection of varying direction. *Journal of Genetics* 58(2): 237–242.
- HALDANE, J. B. S., 1927 A mathematical theory of natural and artificial selection, part V: selection and mutation. In *Mathematical Proceedings of the Cambridge Philosophical Society*, Volume 23, pp. 838–844. Cambridge University Press.
- HALDANE, J. B. S., 1937 The Effect of Variation of Fitness. *The American Naturalist* 71(735): 337–349.
- HALDANE, J. B. S., 1949 Suggestions as to quantitative measurement of rates of evolution. *Evolution* 3(1): 51–56.
- HALDANE, J. B. S., 1964 A defense of beanbag genetics. *Perspectives in Biology and Medicine* 7(3): 343–360.
- HAMILTON, W. D., 1964a The genetical evolution of social behaviour. II. *Journal of theoretical biology* 7(1): 17–52.
- HAMILTON, W. D., 1964b The genetical evolution of social behaviour. II. *Journal of theoretical biology* 7(1): 17–52.
- HERMISSON, J. and P. S. PENNINGS, 2017 Soft sweeps and beyond: understanding the patterns and probabilities of selection footprints under rapid adaptation. *Methods in Ecology and Evolution* 8(6): 700–716.
- HEY, J. and R. M. KLIMAN, 2002 Interactions between natural selection, recombination and gene density in the genes of *Drosophila*. *Genetics* 160(2): 595–608.

- HOEKSTRA, H. E., K. E. DRUMM, and M. W. NACHMAN, 2004 Ecological genetics of adaptive color polymorphism in pocket mice: geographic variation in selected and neutral genes. *Evolution* **58**(6): 1329–1341.
- HOHENLOHE, P. A., S. BASSHAM, P. D. ETTER, N. STIFFLER, E. A. JOHNSON, and W. A. CRESKO, 2010 Population genomics of parallel adaptation in threespine stickleback using sequenced RAD tags. *PLoS genetics* **6**(2): e1000862.
- HOLLISTER, J. D., S. GREINER, W. WANG, J. WANG, Y. ZHANG, G. K.-S. WONG, S. I. WRIGHT, and M. T. JOHNSON, 2014 Recurrent loss of sex is associated with accumulation of deleterious mutations in *Oenothera*. *Molecular biology and evolution* **32**(4): 896–905.
- HOPKINS, J., G. BAUDRY, U. CANDOLIN, and A. KAITALA, 2015 I'm sexy and I glow it: female ornamentation in a nocturnal capital breeder. *Biology letters* **11**(10): 20150599.
- HOUDE, A. E., 1994 Effect of artificial selection on male colour patterns on mating preference of female guppies. *Proc. R. Soc. Lond. B* **256**(1346): 125–130.
- HOWES, R. E., M. DEWI, F. B. PIEL, W. M. MONTEIRO, K. E. BATTLE, J. P. MESSINA, A. SAKUNTABHAI, A. W. SATYAGRAHA, T. N. WILLIAMS, J. K. BAIRD, and S. I. HAY, 2013 Spatial distribution of G6PD deficiency variants across malaria-endemic regions. *Malar. J.* **12**: 418.
- HOWES, R. E., F. B. PIEL, A. P. PATIL, O. A. NYANGIRI, P. W. GETHING, M. DEWI, M. M. HOGG, K. E. BATTLE, C. D. PADILLA, J. K. BAIRD, and S. I. HAY, 2012 G6PD deficiency prevalence and estimates of affected populations in malaria endemic countries: a geostatistical model-based map. *PLoS Medicine* **9**(11): e1001339.
- HUDSON, R. R., 2015, 07)A New Proof of the Expected Frequency Spectrum under the Standard Neutral Model. *PLOS ONE* **10**(7): 1–5.
- HUDSON, R. R. and N. L. KAPLAN, 1995a Deleterious background selection with recombination. *Genetics* **141**: 1605–1617.
- HUDSON, R. R. and N. L. KAPLAN, 1995b The coalescent process and background selection. *Philos. Trans. R. Soc. Lond., B, Biol. Sci.* **349**: 19–23.

- HUDSON, R. R., M. KREITMAN, and M. AGUADÉ, 1987 A test of neutral molecular evolution based on nucleotide data. *Genetics* **116**(1): 153–159.
- HUGHES, W. O., B. P. OLDROYD, M. BEEKMAN, and F. L. RATNIEKS, 2008 Ancestral monogamy shows kin selection is key to the evolution of eusociality. *Science* **320**(5880): 1213–1216.
- HUNT, G., M. A. BELL, and M. P. TRAVIS, 2008 Evolution toward a new adaptive optimum: phenotypic evolution in a fossil stickleback lineage. *Evolution* **62**(3): 700–710.
- JAIN, S. and A. D. BRADSHAW, 1966 Evolutionary divergence among adjacent plant populations I. The evidence and its theoretical analysis. *Heredity* **21**(3): 407.
- JANICKE, T., I. K. HÄDERER, M. J. LAJEUNESSE, and N. ANTHES, 2016 Darwinian sex roles confirmed across the animal kingdom. *Science advances* **2**(2): e1500983.
- JENNINGS, W. B. and S. V. EDWARDS, 2005 Speciation history of Australian grass finches (*Poephila*) inferred from thirty gene trees. *Evolution* **59**(9): 2033–2047.
- JOHANNSEN, W., 1911 The Genotype Conception of Heredity. *The American Naturalist* **45**(531): 129–159.
- JOHNSTON, S. E., J. GRATTON, C. BERENOS, J. G. PILKINGTON, T. H. CLUTTON-BROCK, J. M. PEMBERTON, and J. SLATE, 2013 Life history trade-offs at a single locus maintain sexually selected genetic variation. *Nature* **502**(7469): 93.
- JORON, M., L. FREZAL, R. T. JONES, N. L. CHAMBERLAIN, S. F. LEE, C. R. HAAG, A. WHIBLEY, M. BECUWE, S. W. BAXTER, L. FERGUSON, and OTHERS, 2011 Chromosomal rearrangements maintain a polymorphic supergene controlling butterfly mimicry. *Nature* **477**(7363): 203.
- JORON, M., R. PAPA, M. BELTRÁN, N. CHAMBERLAIN, J. MAVÁREZ, S. BAXTER, M. ABANTO, E. BERMINGHAM, S. J. HUMPHRAY, J. ROGERS, and OTHERS, 2006 A conserved supergene locus controls colour pattern diversity in *Heliconius* butterflies. *PLoS biology* **4**(10): e303.
- JUKEMA, J. and T. PIERSMA, 2006 Permanent female mimics in a lekking shorebird. *Biology letters* **2**(2): 161–164.
- KAPLAN, N. L., R. R. HUDSON, and C. H. LANGLEY, 1989 The hitchhiking effect revisited. *Genetics* **123**: 887–899.

- KARN, M. N. and L. PENROSE, 1951 Birth weight and gestation time in relation to maternal age, parity and infant survival. *Annals of eugenics* **16**(1): 147–164.
- KETTLEWELL, H. B. D., 1955 Selection experiments on industrial melanism in the Lepidoptera. *Heredity* **9**(3): 323.
- KIM, Y., 2006 Allele frequency distribution under recurrent selective sweeps. *Genetics* **172**: 1967–1978.
- KIMURA, M., 1968 Evolutionary rate at the molecular level. *Nature* **217**(5129): 624–626.
- KIMURA, M., 1983 *The neutral theory of molecular evolution*. Cambridge University Press.
- KIMURA, M. and J. F. CROW, 1964 The number of alleles that can be maintained in a finite population. *Genetics* **49**(4): 725.
- KIMURA, M. and T. OHTA, 1974 On some principles governing molecular evolution. *Proceedings of the National Academy of Sciences* **71**(7): 2848–2852.
- KING, J. L. and T. H. JUKES, 1969 Non-darwinian evolution. *Science* **164**(3881): 788–798.
- KLINKA, D. R. and T. E. REIMCHEN, 2009 Adaptive coat colour polymorphism in the Kermode bear of coastal British Columbia. *Biological Journal of the Linnean Society* **98**(3): 479–488.
- KORNEGAY, J. R., J. W. SCHILLING, and A. C. WILSON, 1994 Molecular adaptation of a leaf-eating bird: stomach lysozyme of the hoatzin. *Molecular Biology and Evolution* **11**(6): 921–928.
- KRAKAUER, A. H., 2005 Kin selection and cooperative courtship in wild turkeys. *Nature* **434**(7029): 69.
- KRUUK, L. E., J. SLATE, J. M. PEMBERTON, S. BROTH-ERSTONE, F. GUINNESS, and T. CLUTTON-BROCK, 2002 Antler size in red deer: heritability and selection but no evolution. *Evolution* **56**(8): 1683–1695.
- KÜPPER, C., M. STOCKS, J. E. RISSE, N. DOS REMEDIOS, L. L. FARRELL, S. B. MCRAE, T. C. MORGAN, N. KARLIONOVA, P. PINCHUK, Y. I. VERKUIL, and OTHERS, 2016 A supergene determines highly divergent male reproductive morphs in the ruff. *Nature Genetics* **48**(1): 79.

KWIATKOWSKI, D. P., 2005, August)How malaria has affected the human genome and what human genetics can teach us about malaria. *Am. J. Hum. Genet.* 77(2): 171–192.

LABERGE, A.-M., M. JOMPHE, L. HOUDE, H. VÉZINA, M. TREMBLAY, B. DESJARDINS, D. LABUDA, M. ST-HILAIRE, C. MACMILLAN, E. A. SHOUBRIDGE, and OTHERS, 2005 A “Fille du Roy” introduced the T14484C Leber hereditary optic neuropathy mutation in French Canadians. *The American Journal of Human Genetics* 77(2): 313–317.

LAMICHHANEY, S., G. FAN, F. WIDEMO, U. GUNNARSSON, D. S. THALMANN, M. P. HOEPPNER, S. KERJE, U. GUSTAFSON, C. SHI, H. ZHANG, and OTHERS, 2016 Structural genomic changes underlie alternative reproductive strategies in the ruff (*Philomachus pugnax*). *Nature Genetics* 48(1): 84.

LANDE, R., 1976 Natural selection and random genetic drift in phenotypic evolution. *Evolution* 30(2): 314–334.

LANDE, R., 1979 Quantitative genetic analysis of multivariate evolution, applied to brain: body size allometry. *Evolution* 33(1Part2): 402–416.

LANDE, R. and S. J. ARNOLD, 1983 The measurement of selection on correlated characters. *Evolution* 37(6): 1210–1226.

LAURIE, C. C., D. A. NICKERSON, A. D. ANDERSON, B. S. WEIR, R. J. LIVINGSTON, M. D. DEAN, K. L. SMITH, E. E. SCHADT, and M. W. NACHMAN, 2007, 08)Linkage Disequilibrium in Wild Mice. *PLOS Genetics* 3(8): 1–9.

LAWSON, D. J., L. VAN DORP, and D. FALUSH, 2018 A tutorial on how not to over-interpret STRUCTURE and ADMIXTURE bar plots. *Nature communications* 9(1): 3258.

LEFÉBURE, T., C. MORVAN, F. MALARD, C. FRANÇOIS, L. KONECNY-DUPRÉ, L. GUÉGUEN, M. WEISS-GAYET, A. SEGUIN-ORLANDO, L. ERMINI, C. DER SARKISSIAN, and OTHERS, 2017 Less effective selection leads to larger genomes. *Genome research*: gr-212589.

LEFFLER, E. M., K. BULLAUGHEY, D. R. MATUTE, W. K. MEYER, L. SEGUREL, A. VENKAT, P. ANDOLFATTO, and M. PRZEWORSKI, 2012 Revisiting an old riddle: what determines genetic diversity levels within species? *PLoS biology* 10(9): e1001388.

- LEK, M., K. J. KARCZEWSKI, E. V. MINIKEL, K. E. SAMOCHA, E. BANKS, T. FENNELL, A. H. O'DONNELL-LURIA, J. S. WARE, A. J. HILL, B. B. CUMMINGS, and OTHERS, 2016 Analysis of protein-coding genetic variation in 60,706 humans. *Nature* 536(7616): 285.
- LENORMAND, T., D. BOURGUET, T. GUILLEMAUD, and M. RAYMOND, 1999 Tracking the evolution of insecticide resistance in the mosquito *Culex pipiens*. *Nature* 400(6747): 861.
- LEWONTIN, R. C., 1970 The units of selection. *Annual review of ecology and systematics* 1(1): 1–18.
- LEWONTIN, R. C., 1974 *The Genetic Basis of Evolutionary Change*. Columbia University Press, New York.
- LEWONTIN, R. C., 1994, 05)[DNA Fingerprinting: A Review of the Controversy]: Comment: The Use of DNA Profiles in Forensic Contexts. *Statist. Sci.* 9(2): 259–262.
- LEWONTIN, R. C., 2001 *Thinking about evolution: historical, philosophical, and political perspectives*, Chapter Natural History and Formalism in Evolutionary Genetics, pp. 7–20. Cambridge University Press.
- LI, J. Z., D. M. ABSHER, H. TANG, A. M. SOUTHWICK, A. M. CASTO, S. RAMACHANDRAN, H. M. CANN, G. S. BARSH, M. FELDMAN, L. L. CAVALLI-SFORZA, and OTHERS, 2008 Worldwide human relationships inferred from genome-wide patterns of variation. *science* 319(5866): 1100–1104.
- LIN, C.-J., F. HU, R. DUBRUILLE, J. VEDANAYAGAM, J. WEN, P. SMIBERT, B. LOPPIN, and E. C. LAI, 2018 The hpRNA/RNAi pathway is essential to resolve intragenomic conflict in the *Drosophila* male germline. *Developmental cell* 46(3): 316–326.
- LISTER, A., 1989 Rapid dwarfing of red deer on Jersey in the last interglacial. *Nature* 342(6249): 539.
- LOCKE, D. P., L. W. HILLIER, W. C. WARREN, K. C. WORLEY, L. V. NAZARETH, D. M. MUZNY, S.-P. YANG, Z. WANG, A. T. CHINWALLA, P. MINX, and OTHERS, 2011 Comparative and demographic analysis of orang-utan genomes. *Nature* 469(7331): 529.
- LOSOS, J. B., S. J. ARNOLD, G. BEJERANO, E. BRODIE III, D. HIBBETT, H. E. HOEKSTRA, D. P. MINDELL, A. MONTEIRO, C. MORITZ, H. A. ORR, and OTHERS, 2013 Evolutionary biology for the 21st century. *PLoS Biology* 11(1): e1001466.

- LOUICHAROEN, C., E. PATIN, R. PAUL, I. NUCHPRAY-OON, B. WITOONPANICH, C. PEERAPITTAYAMONGKOL, I. CASADEMONT, T. SURA, N. M. LAIRD, P. SINGHASIVANON, L. QUINTANA-MURCI, and A. SAKUNTABHAI, 2009, December)Positively selected G6PD-Mahidol mutation reduces *Plasmodium vivax* density in Southeast Asians. *Science* 326(5959): 1546–1549.
- LOWRY, D. B. and J. H. WILLIS, 2010 A widespread chromosomal inversion polymorphism contributes to a major life-history transition, local adaptation, and reproductive isolation. *PLoS biology* 8(9): e1000500.
- MACARTHUR, D. G., S. BALASUBRAMANIAN, A. FRANKISH, N. HUANG, J. MORRIS, K. WALTER, L. JOSTINS, L. HABEGGER, J. K. PICKRELL, S. B. MONTGOMERY, and OTHERS, 2012 A systematic survey of loss-of-function variants in human protein-coding genes. *Science* 335(6070): 823–828.
- MACPHERSON, J. M., G. SELLA, J. C. DAVIS, and D. A. PETROV, 2007 Genomewide spatial correspondence between non-synonymous divergence and neutral polymorphism reveals extensive adaptation in *Drosophila*. *Genetics* 177: 2083–2099.
- MAJERUS, M. E., 2009 Industrial melanism in the peppered moth, *Biston betularia*: an excellent teaching example of Darwinian evolution in action. *Evolution: Education and Outreach* 2(1): 63.
- MALÉCOT, G., 1948 Les mathématiques de l'hérédité.
- MALÉCOT, G., 1969 The Mathematics of Heredity (Revised, edited and translated by Yermanos, DM).
- MARCINIAK, S. and G. H. PERRY, 2017 Harnessing ancient genomes to study the history of human adaptation. *Nature Reviews Genetics* 18(11): 659.
- MAYNARD SMITH, J., 1964 Group selection and kin selection. *Nature* 201(4924): 1145.
- MAYNARD SMITH, J. and J. HAIGH, 1974 The hitch-hiking effect of a favourable gene. *Genet. Res.* 23: 23–35.
- MCDONALD, J. H. and M. KREITMAN, 1991 Adaptive protein evolution at the Adh locus in *Drosophila*. *Nature* 351(6328): 652.
- MCVICKER, G., D. GORDON, C. DAVIS, and P. GREEN, 2009 Widespread genomic signatures of natural selection in hominid evolution. *PLoS Genet.* 5: e1000471.

- MENOZZI, P., A. PIAZZA, and L. CAVALLI-SFORZA, 1978 Synthetic maps of human gene frequencies in Europeans. *Science* 201(4358): 786–792.
- MEREDITH, R. W., J. GATESY, W. J. MURPHY, O. A. RYDER, and M. S. SPRINGER, 2009, 09) Molecular Decay of the Tooth Gene Enamelin (ENAM) Mirrors the Loss of Enamel in the Fossil Record of Placental Mammals. *PLOS Genetics* 5(9): 1–12.
- MESSIER, W. and C.-B. STEWART, 1997 Episodic adaptive evolution of primate lysozymes. *Nature* 385(6612): 151.
- MILNE, A. A. and E. H. SHEPARD, 1926 *Winnie-the-Pooh*.
- MILLOT, E., C. MOREAU, A. GAGNON, A. A. COHEN, B. BRAIS, and D. LABUDA, 2017 Mother's curse neutralizes natural selection against a human genetic disease over three centuries. *Nature ecology & evolution* 1(9): 1400.
- MULLER, H. J., 1932 Some genetic aspects of sex. *The American Naturalist* 66(703): 118–138.
- MULLER, H. J., 1964 The relation of recombination to mutational advance. *Mutation Research/Fundamental and Molecular Mechanisms of Mutagenesis* 1(1): 2–9.
- NACHMAN, M. W., H. E. HOEKSTRA, and S. L. D'AGOSTINO, 2003 The genetic basis of adaptive melanism in pocket mice. *Proceedings of the National Academy of Sciences* 100(9): 5268–5273.
- NASH, D., S. NAIR, M. MAYXAY, P. N. NEWTON, J.-P. GUTHMANN, F. NOSTEN, and T. J. ANDERSON, 2005 Selection strength and hitchhiking around two anti-malarial resistance genes. *Proceedings of the Royal Society of London B: Biological Sciences* 272(1568): 1153–1161.
- NELSON, M. R., D. WEGMANN, M. G. EHM, D. KESSNER, P. S. JEAN, C. VERZILLI, J. SHEN, Z. TANG, S.-A. BACANU, D. FRASER, and OTHERS, 2012 An abundance of rare functional variants in 202 drug target genes sequenced in 14,002 people. *Science*: 1217876.
- NORDBORG, M., B. CHARLESWORTH, and D. CHARLESWORTH, 1996 The effect of recombination on background selection. *Genet. Res.* 67: 159–174.
- NOVEMBRE, J. and M. STEPHENS, 2008 Interpreting principal component analyses of spatial population genetic variation. *Nature genetics* 40(5): 646.

- OHTA, T., 1972 Population size and rate of evolution. *Journal of Molecular Evolution* **1**(4): 305–314.
- OHTA, T., 1973 Slightly deleterious mutant substitutions in evolution. *Nature* **246**(5428): 96.
- OHTA, T., 1987 Very slightly deleterious mutations and the molecular clock. *Journal of Molecular Evolution* **26**(1-2): 1–6.
- OHTA, T. and J. H. GILLESPIE, 1996 Development of neutral and nearly neutral theories. *Theoretical population biology* **49**(2): 128–142.
- OWEN, D. and D. CHANTER, 1972 Polymorphic mimicry in a population of the African butterfly, *Pseudacraea eurytus* (L.) (Lep. Nymphalidae). *Insect Systematics & Evolution* **3**(4): 258–266.
- OZIOLOR, E. M., N. M. REID, S. YAIR, K. M. LEE, S. G. VERPLOEG, P. C. BRUNS, J. R. SHAW, A. WHITEHEAD, and C. W. MATSON, 2019 Adaptive introgression enables evolutionary rescue from extreme environmental pollution. *Science* **364**(6439): 455–457.
- PAABY, A. B., A. O. BERGLAND, E. L. BEHRMAN, and P. S. SCHMIDT, 2014 A highly pleiotropic amino acid polymorphism in the *Drosophila* insulin receptor contributes to life-history adaptation. *Evolution* **68**(12): 3395–3409.
- PATTERSON, N., A. L. PRICE, and D. REICH, 2006 Population structure and eigenanalysis. *PLoS genetics* **2**(12): e190.
- PICKRELL, J. K., T. BERISA, J. Z. LIU, L. SÉGUREL, J. Y. TUNG, and D. A. HINDS, 2016 Detection and interpretation of shared genetic influences on 42 human traits. *Nature genetics* **48**(7): 709.
- POTTI, J. and D. CANAL, 2011 Heritability and genetic correlation between the sexes in a songbird sexual ornament. *Heredity* **106**(6): 945.
- PRITCHARD, J. K., M. STEPHENS, and P. DONNELLY, 2000 Inference of population structure using multilocus genotype data. *Genetics* **155**(2): 945–959.
- PROVINE, W. B., 2001 *The origins of theoretical population genetics: with a new afterword*. University of Chicago Press.
- PRZEWORSKI, M., 2002 The signature of positive selection at randomly chosen loci. *Genetics* **160**: 1179–1189.

- PTAK, S. E., A. D. ROEDER, M. STEPHENS, Y. GILAD,
S. PÄÄBO, and M. PRZEWORSKI, 2004 Absence of the TAP2
human recombination hotspot in chimpanzees. *PLoS biology* **2**(6):
e155.
- QUELLER, D. C., 1992 Quantitative genetics, inclusive fitness, and
group selection. *The American Naturalist* **139**(3): 540–558.
- R, 2018 R: A Language and Environment for Statistical Computing.
- RALPH, P. L. and G. COOP, 2015 The role of standing variation
in geographic convergent adaptation. *The American Naturalist* **186**(S1): S5–S23.
- RANDS, C. M., S. MEADER, C. P. PONTING, and
G. LUNTER, 2014 8.2% of the human genome is constrained:
variation in rates of turnover across functional element classes in the
human lineage. *PLoS genetics* **10**(7): e1004525.
- RICHARDS, C. M., 2000 Inbreeding depression and genetic rescue
in a plant metapopulation. *The American Naturalist* **155**(3): 383–
394.
- RITLAND, K., C. NEWTON, and H. MARSHALL, 2001 Inheritance
and population structure of the white-phased “Kermode”
black bear. *Current Biology* **11**(18): 1468 – 1472.
- ROBERTS, R. B., J. R. SER, and T. D. KOCHER, 2009 Sexual
conflict resolved by invasion of a novel sex determiner in Lake
Malawi cichlid fishes. *Science* **326**(5955): 998–1001.
- ROBERTSON, A., 1961 Inbreeding in artificial selection programmes.
Genet. Res. **2**: 189—194.
- ROBINSON, J. A., D. ORTEGA-DEL VECCHYO, Z. FAN,
B. Y. KIM, C. D. MARSDEN, K. E. LOHMUELLER, R. K.
WAYNE, and OTHERS, 2016 Genomic flatlining in the endangered
island fox. *Current Biology* **26**(9): 1183–1189.
- ROBINSON, L. M., J. R. BOLAND, and J. M. BRAVERMAN,
2016 Revisiting a Classic Study of the Molecular Clock. *Journal of
molecular evolution* **82**(2-3): 110–116.
- ROSENBERG, N. A., J. K. PRITCHARD, J. L. WEBER,
H. M. CANN, K. K. KIDD, L. A. ZHIVOTOVSKY, and
M. W. FELDMAN, 2002 Genetic structure of human populations.
science **298**(5602): 2381–2385.

- RUWENDE, C., S. C. KHOO, R. W. SNOW, S. N. YATES, D. KWIATKOWSKI, S. GUPTA, P. WARN, C. E. ALLSOPP, S. C. GILBERT, and N. PESCHU, 1995, July)Natural selection of hemi- and heterozygotes for G6PD deficiency in Africa by resistance to severe malaria. *Nature* **376**(6537): 246–249.
- SAMS, A. J. and A. R. BOYKO, 2018a Fine-scale resolution and analysis of runs of homozygosity in domestic dogs. *bioRxiv*.
- SAMS, A. J. and A. R. BOYKO, 2018b Fine-Scale Resolution of Runs of Homozygosity Reveal Patterns of Inbreeding and Substantial Overlap with Recessive Disease Genotypes in Domestic Dogs. *G3: Genes, Genomes, Genetics*: g3–200836.
- SANKARARAMAN, S., N. PATTERSON, H. LI, S. PÄÄBO, and D. REICH, 2012, 10)The Date of Interbreeding between Neandertals and Modern Humans. *PLOS Genetics* **8**(10): 1–9.
- SANTIAGO, E. and A. CABALLERO, 1995 Effective size of populations under selection. *Genetics* **139**: 1013–1030.
- SANTIAGO, E. and A. CABALLERO, 1998 Effective size and polymorphism of linked neutral loci in populations under directional selection. *Genetics* **149**: 2105–2117.
- SATTATH, S., E. ELYASHIV, O. KOLODNY, Y. RINOTT, and G. SELLA, 2011a Pervasive adaptive protein evolution apparent in diversity patterns around amino acid substitutions in *Drosophila simulans*. *PLoS genetics* **7**(2): e1001302.
- SATTATH, S., E. ELYASHIV, O. KOLODNY, Y. RINOTT, and G. SELLA, 2011b Pervasive adaptive protein evolution apparent in diversity patterns around amino acid substitutions in *Drosophila simulans*. *PLoS Genet.* **7**: e1001302.
- SCHEMSKE, D. W. and P. BIERZYCHUDEK, 2001 Perspective: evolution of flower color in the desert annual *Linanthus parryae*: Wright revisited. *Evolution* **55**(7): 1269–1282.
- SEGER, J. and H. BROCKMANN, 1987 *Oxford Surveys in Evolutionary Biology*, Volume 4, Chapter What is bet-hedging, pp. 182–211. Oxford University Press.
- SELLA, G., D. A. PETROV, M. PRZEWORSKI, and P. ANDOLFATTO, 2009 Pervasive natural selection in the *Drosophila* genome? *PLoS genetics* **5**(6): e1000495.
- SHAPIRO, J. A., W. HUANG, C. ZHANG, M. J. HUBISZ, J. LU, D. A. TURRISSINI, S. FANG, H. Y. WANG, R. R.

- HUDSON, R. NIELSEN, Z. CHEN, and C. I. WU, 2007 Adaptive genic evolution in the *Drosophila* genomes. *Proc. Natl. Acad. Sci. U.S.A.* **104**: 2271–2276.
- SMITH, J. M., 1971 The origin and maintenance of sex. In *Group selection*, pp. 163–175. Routledge.
- SMITH, J. M., 1982 *Evolution and the Theory of Games*. Cambridge university press.
- SMITH, J. N. and A. A. DHONDT, 1980 Experimental confirmation of heritable morphological variation in a natural population of song sparrows. *Evolution*: 1155–1158.
- SMITH, J. N. and R. ZACH, 1979 Heritability of some morphological characters in a song sparrow population. *Evolution* **33**(1Part2): 460–467.
- SMITH, T. B., 1993 Disruptive selection and the genetic basis of bill size polymorphism in the African finch Pyrenestes. *Nature* **363**(6430): 618.
- SMITHSON, A. and M. R. MACNAIR, 1997 Negative frequency-dependent selection by pollinators on artificial flowers without rewards. *Evolution* **51**(3): 715–723.
- STEVENS, N. M., 1905 *Studies in Spermatogenesis: With especial reference to the "accessory chromosome"*, Volume 36. Carnegie Institution of Washington.
- STUMPF, M. P., Z. LAIDLAW, and V. A. JANSEN, 2002 Herpes viruses hedge their bets. *Proceedings of the National Academy of Sciences* **99**(23): 15234–15237.
- STURTEVANT, A. H., 1915 The behavior of the chromosomes as studied through linkage. *Zeitschrift für induktive Abstammungs-und Vererbungslehre* **13**(1): 234–287.
- SWEIGART, A. L., Y. BRANDVAIN, and L. FISHMAN, 2019 Making a Murderer: The Evolutionary Framing of Hybrid Gamete-Killers. *Trends in Genetics*.
- TAJIMA, F., 1989 Statistical method for testing the neutral mutation hypothesis by DNA polymorphism. *Genetics* **123**(3): 585–595.
- TAO, Y., L. ARARIPE, S. B. KINGAN, Y. KE, H. XIAO, and D. L. HARTL, 2007 A sex-ratio meiotic drive system in *Drosophila simulans*. II: an X-linked distorter. *PLoS biology* **5**(11): e293.

- TAO, Y., J. P. MASLY, L. ARARIPE, Y. KE, and D. L. HARTL, 2007 A sex-ratio meiotic drive system in *Drosophila simulans*. I: an autosomal suppressor. *PLoS biology* 5(11): e292.
- TISHKOFF, S. A., R. VARKONYI, N. CAHINHINAN, S. ABBES, G. ARGYROPOULOS, G. DESTRO-BISOL, A. DROUSIOTOU, B. DANGERFIELD, G. LEFRANC, J. LOISELET, A. PIRO, M. STONEKING, A. TAGARELLI, G. TAGARELLI, E. H. TOUMA, S. M. WILLIAMS, and A. G. CLARK, 2001 Haplotype Diversity and Linkage Disequilibrium at Human G6PD: Recent Origin of Alleles That Confer Malarial Resistance. *Science* 293(5529): 455–462.
- TOEWS, D. P., S. A. TAYLOR, R. VALLENDER, A. BRELFORD, B. G. BUTCHER, P. W. MESSEY, and I. J. LOVETTE, 2016 Plumage Genes and Little Else Distinguish the Genomes of Hybridizing Warblers. *Current Biology* 26(17): 2313 – 2318.
- TURELLI, M., D. W. SCHEMSKE, and P. BIERZYCHUDEK, 2001 Stable two-allele polymorphisms maintained by fluctuating fitnesses and seed banks: protecting the blues in *Linanthus parryae*. *Evolution* 55(7): 1283–1298.
- ULIZZI, L. and L. TERRENATO, 1992 Natural selection associated with birth weight. VI. Towards the end of the stabilizing component. *Annals of human genetics* 56(2): 113–118.
- UYEDA, J. C., T. F. HANSEN, S. J. ARNOLD, and J. PIEN-AAR, 2011 The million-year wait for macroevolutionary bursts. *Proceedings of the National Academy of Sciences* 108(38): 15908–15913.
- VAN'T HOF, A. E., N. EDMONDS, M. DALÍKOVÁ, F. MAREC, and I. J. SACCHERI, 2011 Industrial melanism in British peppered moths has a singular and recent mutational origin. *Science* 332(6032): 958–960.
- VERMEIJ, G. J., 1982 Phenotypic evolution in a poorly dispersing snail after arrival of a predator. *Nature* 299(5881): 349.
- VOIGHT, B. F., A. M. ADAMS, L. A. FRISSE, Y. QIAN, R. R. HUDSON, and A. DI RIENZO, 2005 Interrogating multiple aspects of variation in a full resequencing data set to infer human population size changes. *Proceedings of the National Academy of Sciences* 102(51): 18508–18513.

- VONHOLDT, B. M., J. P. POLLINGER, D. A. EARL, J. C. KNOWLES, A. R. BOYKO, H. PARKER, E. GEFEN, M. PILOT, W. JEDRZEJEWSKI, B. JEDRZEJEWSKA, V. SIDOROVICH, C. GRECO, E. RANDI, M. MUSIANI, R. KAYS, C. D. BUSTAMANTE, E. A. OSTRANDER, J. NOVEMBRE, and R. K. WAYNE, 2011 A genome-wide perspective on the evolutionary history of enigmatic wolf-like canids. *Genome Research*.
- WANG, J., J. DING, B. TAN, K. M. ROBINSON, I. H. MICHELSON, A. JOHANSSON, B. NYSTEDT, D. G. SCOFIELD, O. NILSSON, S. JANSSON, and OTHERS, 2018 A major locus controls local adaptation and adaptive life history variation in a perennial plant. *Genome biology* *19*(1): 72.
- WATTERSON, G., 1975 On the number of segregating sites in genetical models without recombination. *Theoretical population biology* *7*(2): 256–276.
- WEIS, A. E. and W. L. GORMAN, 1990 Measuring selection on reaction norms: an exploration of the *Eurosta-Solidago* system. *Evolution* *44*(4): 820–831.
- WELCH, A. M., M. J. SMITH, and H. C. GERHARDT, 2014 A multivariate analysis of genetic variation in the advertisement call of the gray treefrog, *Hyla versicolor*. *Evolution* *68*(6): 1629–1639.
- WHEELER, W. M., 1907 Pink Insect Mutants. *The American Naturalist* *41*(492): 773–780.
- WIDEMO, F., 1998 Alternative reproductive strategies in the ruff, *Philomachus pugnax*: a mixed ESS? *Animal Behaviour* *56*(2): 329–336.
- WIEHE, T. and W. STEPHAN, 1993a Analysis of a genetic hitchhiking model, and its application to DNA polymorphism data from *Drosophila melanogaster*. *Molecular Biology and Evolution* *10*(4): 842–854.
- WIEHE, T. H. and W. STEPHAN, 1993b Analysis of a genetic hitchhiking model, and its application to DNA polymorphism data from *Drosophila melanogaster*. *Mol. Biol. Evol.* **10**: 842–854.
- WILKINSON, G. S., 1993 Artificial sexual selection alters allometry in the stalk-eyed fly *Cyrtodiopsis dalmanni* (Diptera: Diopsidae). *Genetics Research* *62*(3): 213–222.
- WILLIAMS, G. C., 1966 *Adaptation and Natural Selection*. Princeton.

WILLIAMS, K.-A. and P. S. PENNINGS, 2019 Drug resistance evolution in HIV in the late 1990s: hard sweeps, soft sweeps, clonal interference and the accumulation of drug resistance mutations. bioRxiv.

WISELY, S. M., S. W. BUSKIRK, M. A. FLEMING, D. B. McDONALD, and E. A. OSTRANDER, 2002 Genetic Diversity and Fitness in Black-Footed Ferrets Before and During a Bottleneck. *Journal of Heredity* 93(4): 231–237.

WRIGHT, K. M., U. HELLSTEN, C. XU, A. L. JEONG, A. SREEDASYAM, J. A. CHAPMAN, J. SCHMUTZ, G. COOP, D. S. ROKHSAR, and J. H. WILLIS, 2015 Adaptation to heavy-metal contaminated environments proceeds via selection on pre-existing genetic variation. bioRxiv: 029900.

WRIGHT, S., 1932 *The roles of mutation, inbreeding, crossbreeding, and selection in evolution*, Volume 1. na.

WRIGHT, S., 1943 Isolation by Distance. *Genetics* 28(2): 114–138.

WRIGHT, S., 1949 The Genetical Structure of Populations. *Annals of Eugenics* 15(1): 323–354.

WRIGHT, S. and T. DOBZHANSKY, 1946 Genetics of natural populations. XII. Experimental reproduction of some of the changes caused by natural selection in certain populations of *Drosophila pseudoobscura*. *Genetics* 31(2): 125.

WRIGHT, S. I., I. V. BI, S. G. SCHROEDER, M. YAMASAKI, J. F. DOEBLEY, M. D. McMULLEN, and B. S. GAUT, 2005 The Effects of Artificial Selection on the Maize Genome. *Science* 308(5726): 1310–1314.

YANG, Z., 1998 Likelihood ratio tests for detecting positive selection and application to primate lysozyme evolution. *Molecular Biology and Evolution* 15(5): 568–573.

ZUCKERKANDL, E. and L. PAULING, 1965 Evolutionary divergence and convergence in proteins. In *Evolving genes and proteins*, pp. 97–166. Elsevier.